

**Evaluation of the role of innate lymphoid cells
following viral vector vaccination**

Zheyi Li

A thesis submitted for the degree of Doctor of Philosophy of

The Australian National University

March 2018



The Molecular Mucosal Vaccine Immunology Group,


The John Curtin School of Medical Research,

The Australian National University,

Canberra, Australia

Statement

I declare that all the data presented in this thesis were obtained from my own experiments under the supervision of A/Prof. Charani Ranasinghe. This whole thesis is my own work, except otherwise stated. All the recombinant fowl pox virus vaccine stocks used in this thesis were constructed in Dr. David Boyle's laboratory at CSIRO or A/Prof. Ranasinghe's laboratory and were kindly provided to me. I certify that this work contains no material which has been accepted for the award of any other degree or diploma in any university.

 Zheyi Li

Zheyi Li

Acknowledgements

I would like to thank number of people who have supported and encouraged me throughout the journey of my PhD research. First and foremost, I express my deepest gratitude to my supervisor A/Prof. Charani Ranasinghe for her great support and guidance over the years. Without her encouragement, the work in this thesis would not have been possible. I am extremely lucky to have a supervisor who not only trained me to be a better researcher, but also has become my personal moral standard.

My sincere thanks go to past and present members in our laboratory. Special thanks to Dr. Danushka Wijesundara, Dr. Shubhanshi Trivedi and Ghamdan Al-Eryani, who helped me a lot when I just joined the laboratory. Thank you to Annette and Jay for taking care of everyone in the laboratory over the years. A huge thanks to Dr. Mayank Khanna and Sreeja Roy for their wise suggestions and helping me whenever needed; I treasure them like my brother and sister. Thanks also to other past and present students of the group, Matthew, Althea, Megat, Alice, David, Irwan, Mitch and Sally for all your friendship and support. I was lucky to have worked with such a great group of people.

I express my warm thanks to Michael Devoy and Dr. Harpreet Vohra at the MCRF/JCSMR ANU for their technical assistance with flow cytometry. I could not have come this far without their wise and professional support. Thanks to Barbara Burke at the APF animal facility, Pamela Wozniak and Andrew Talbot at the JCSMR store. Thanks also to JCSMR HDR coordinators and PhD convenors for their great support throughout my PhD project.

Finally, this journey would not have been possible without the support of my family. My deepest thank to my parents Fu Jun and Li Zheng and my grandmother for their unconditional love and support throughout these years. A special thank to the most important person in my life, my fiancée Angela Zhou who was always there supporting me and caring for me more than herself. I am sure spending the rest of my life with you would be the most beautiful thing that could ever happen. Thank you for everything.

Publications

- Roy S, Mahboob S, **Li Z**, Jaeson MI, Jackson RJ, Grubor-Bauk B, Wijesundara DK, Gowans EJ, Ranasinghe C. Innate lymphoid cell derived-cytokine balance plays a crucial role in DC recruitment following viral vector-based vaccination. (2018 submitted)
- [◇]**Li Z**, Jackson RJ, Ranasinghe C. Vaccination route can significantly alter the innate lymphoid cell subsets: a feedback between IL-13 and IFN- γ . *NPJ Vaccines*. 2018; 3:10. doi:10.1038/s41541-018-0048-6.
- Ranasinghe C, Roy S, **Li Z**, Khanna M, Jackson RJ. IL-4 and IL-13 receptors. *Encyclopedia of Signaling Molecules, 2nd Edition*. 2018. Springer.

[◇]*This work is presented in Chapter 3 of this thesis.*

Conference presentations

- **Li. Z**, Ng A, Trivedi S, Jackson RJ and Ranasinghe C. IL-4/IL-13 inhibitor mucosal vaccination strategies induce high quality T and B cell immunity by modulating innate lymphoid and antigen presenting cells at the vaccination site. ASI Annual conference 2015 (Poster presentation).
- **Li. Z**, Ng A, Trivedi S, Jackson RJ and Ranasinghe C. IL-4/IL-13 inhibitor mucosal vaccination strategies induce high quality T and B cell immunity by modulating innate lymphoid and antigen presenting cells at the vaccination site. ASI Annual conference 2015, mucosal immunology workshop (Oral presentation).
- Ranasinghe C*, **Li Z**, Ng A, Worley M, Trivedi S and Jackson R. Novel IL-4R antagonist and IL-13Ra2 adjuvanted HIV vaccines can induce excellent high-quality T and B cell immunity. Vaccines R&D 2015, USA (*Presented by supervisor),
- **Li Z**, Ng A, Trivedi S, Jackson RJ, Ranasinghe C*. IL-4/IL-13 inhibitor vaccines induce protective immunity by modulating innate lymphocytic, dendritic and macrophage cell subsets at the vaccination site. Australasian HIV&AIDS Conference 2015 (*Presented by supervisor).

Abstract

Over the past decade, studies in our laboratory have established that i) compared to systemic route of delivery, mucosal delivery of recombinant fowlpox virus (rFPV) prime can induce excellent high avidity mucosal/systemic HIV-specific CD8⁺ T cell immunity, ii) this was associated with IL-4/IL-13 cytokine milieu and iii) transient inhibition of IL-13 at the vaccination site can recruit unique lung dendritic cell (DC) subsets, responsible for the induction of high quality CD8⁺ T cell immunity. Therefore, to understand which cells at the vaccination site was the predominant source of IL-13 was assessed by evaluating the different cells at the vaccination site, specifically innate lymphoid cells (ILC) following rFPV vaccination with and without transient inhibition of IL-13. These studies for the first time revealed that ILC2 were the main source of IL-13 at the vaccination site (24 h post vaccination) responsible for inducing high quality T and B cells immune responses reported previously. Intranasal vaccination induced ST2/IL-33R⁺ ILC2 in lung, whilst intramuscular vaccination exclusively induced IL-25R⁺ ILC2 in muscle. Moreover, adjuvants that transiently inhibited IL-13 at the vaccination site significantly influenced the IFN- γ expression by ILC1/ILC3 indicating that ILC2-derived IL-13 at the vaccination site also modulated ILC1/ILC3 function/activity.

As intranasal and intramuscular vaccinations induced different ILC2 subsets, two rFPV vaccines co-expressing adjuvants that transiently sequestered IL-25 and IL-33 at the vaccination site (rFPV-IL-12BP and rFPV-IL-33BP) were used to further evaluate ILC development following vaccination. Unlike IL-13 inhibitor vaccination conditions, intranasal delivery of IL-25BP adjuvanted vaccine induced not only ST2/IL-33R⁺ ILC2 but also IL-25R⁺ and TSLPR⁺ ILC2 subsets that were able to express IL-13. Moreover

TSLPR⁺ ILC2 subset was also able to express IL-4. Interestingly, intranasal delivery of IL-25BP also induced significantly elevated number of NKp46^{+/-} ILC1/ILC3 expressing IL-17A compared to IFN- γ , unlike the unadjuvanted or IL-13 inhibitor conditions. Taken together, these inhibitor studies indicated that IL-25 play a fundamental role in early ILC development than IL-33, suggesting that there is a hierarchical regulation of ILC development, where IL-25 is most likely the master regulator of ILC.

Data also revealed that ILC and their cytokine expression profiles were vastly different during permanent versus transient blockage of IL-13, and STAT6 at the vaccination site. STAT6^{-/-} mice given the FPV-HIV vaccine showed elevated ST2/IL-33R⁺ ILC2-driven IL-13 expression whilst reduced IFN- γ expression by both NKp46^{+/-} ILC1/ILC3, unlike transient blockage of STAT6 which showed the opposing effect. When IL-13^{-/-} mice were vaccinated with FPV-HIV significantly elevated lung lineage⁻ ST2/IL-33R⁺ ILC2s were detected compared to BALB/c mice given the FPV-HIV-IL-13R α 2 adjuvanted vaccine (transient inhibition of IL-13), and their NKp46^{+/-} ILC1/ILC3-driven IFN- γ expression was significantly lower compared to transient inhibition of STAT6. In previous studies when IL-13 was inhibited, no or low antibody differentiation has been reported, unlike STAT6 inhibition. Thus, current data further corroborated that ST2/IL-33R⁺ ILC2-derived IL-13 play a crucial role in modulating downstream B cell immune outcomes. Specifically, co-regulation of ST2/IL-33R⁺ ILC2-derived IL-13 and NKp46^{+/-} ILC1/ILC3-derived IFN- γ may play an important role in modulating antibody differentiation process in a STAT6 independent manner via the IL-13R α 2 pathway.

When trying to understand the molecular mechanism involved in this process, data revealed that the expression of IL-13R α 2, type I and II IL-4Rs on ST2/IL-33R⁺ ILC2 and NKp46⁻ ILC1/ILC3 were co-regulated 24 h post intranasal rFPV vaccination.

Inhibition of STAT6 signalling significantly impacted the IL-13R α 2 expression on both ST2/IL-33R⁺ ILC2 and NKp46⁻ ILC1/ILC3, unlike IL-13 inhibition, suggesting that under STAT6 inhibition conditions, IL-13 could signal via IL-13R α 2 pathway. As elevated number of ST2/IL-33R⁺ ILC2 expressing IL-13R α 2 were detected in BALB/c mice given the FPV-HIV-IL-4R antagonist vaccine, this also indicated an autocrine regulation of IL-13 at the ILC2 via IL-13R α 2. The IL-4/IL-13 receptor expression profile on NKp46⁺ ILC1/ILC3 and NKp46⁻ ILC1/ILC3 were vastly different, suggesting that these cells may play different roles in downstream immune outcomes.

Collectively, findings in this thesis demonstrated that i) ILC activity is significantly modulated by route of vaccine delivery and vaccine adjuvants early as 24 h post vaccination, ii) When designing vaccines against chronic pathogens, understanding the fundamental roles of ILC at the vaccination site may help design better vaccines in the future, iii) IL-25 regulated initial development/differentiation of all ILCs and IL-33 most likely only play a role in ILC2 homing to the lung mucosae, iv) Post viral vector vaccination ILC-derived IL-13 and IFN- γ balance was crucial for shaping the downstream immune outcomes, v) The IL-13 regulation at the ILC level occurred via an STAT6 independent pathway, most likely IL-13R α 2 (due to low IL-13 conditions). In conclusion, this work has provided unique insights into ILC function and activity during viral vector vaccination, that could be used to tailor vaccine vectors to induce effective immune outcomes against target pathogens (for example TB verses an HIV vaccine).

Abbreviations

γ C	Common gamma chain
AIDS	Acquired immune deficiency syndrome
APC	Antigen presenting cells
BALT	Bronchus-associated lymphoid tissue
BFA	Brefeldin A
CD	Cluster of differentiation
CES	Chicken embryo skin cells
CHILP	Common helper innate lymphoid progenitor
CILP	Common innate lymphoid progenitor
CLP	Common lymphoid progenitor
CO ₂	Carbon dioxide
CTL	Cytotoxic T lymphocyte
DC	Dendritic cells
FACS	Fluorescence-activated cell sorting
FMO	Fluorescence minus one
GALT	Gut-associated lymphoid tissue
GATA3	Transcription factor GATA3
HCl	Hydrogen chloride
HIV	Human immunodeficiency virus
IC	Intracellular
ICOS	Inducible T - cell costimulator
Id2	Inhibitor of DNA binding 2
IFN- γ	Interferon γ
Ig	Immunoglobulin

IL	Interleukin
IL-13 ^{-/-}	Interleukin 13 knockout
IL-13R α 1	Interleukin 13 receptor α 1
IL-13R α 2	Interleukin 13 receptor α 2
IL-4 ^{-/-}	Interleukin 4 knockout
IL-4R α	Interleukin 4 receptor α
ILC	Innate lymphoid cells
IM	Intramuscular
IN	Intranasal
IRS	Insulin receptor substrate
JAK	Janus Kinase
KLRG1	Killer-cell lectin like receptor G1
KO	knockout
LPS	Lipopolysaccharides
LTi	Lymphoid tissue inducer
M cells	Microfold cells
MALT	Mucosa-associated lymphoid tissue
MEM	Minimum essential medium eagle
MVA	Modified vaccinia Ankara
NALT	Nasopharynx-associated lymphoid tissue
NF- κ B	Nuclear factor kappa-light-chain-enhancer of activated B cells
NH ₄ Cl	Ammonium chloride
NK cells	Nature killer cells
NKp46	Natural cytotoxicity receptor NKp46
nM	nanomolar
PAMPs	Pathogen Associated Molecular Patterns

PBS	Phosphate-buffered saline
PFA	Paraformaldehyde
PFU	Plaque forming unit
PI3-K	Phosphoinositide 3-kinase
PLZF	Promyeloid leukaemia zinc finger
pM	picomolar
RAG	Recombination activating gene
RBC	Red blood cells
rDNA	Recombinant DNA
rFPV	Recombinant fowlpox virus
ROR α	Retinoic acid receptor-related receptor α
ROR γ t	Retinoic-acid-receptor-related orphan nuclear receptor gamma
RPM	Revolutions per minute
RPMI	Roswell Park Memorial Institute medium
RT	Room temperature
rVV	Recombinant vaccinia virus
Sca-1	Stem cell antigen 1
SIV	Simian immunodeficiency virus
ST2	Suppression of tumorigenicity 2
STAT6	Signal transducer and activator of transcription 6
STAT6 ^{-/-}	Signal transducer and activator of transcription 6 knockout
TB	Tuberculosis
T-bet	T-box transcription factor
TGF- β	Transforming growth factor β
T _H cells	T helper cells
TLRs	Toll-Like Receptors

TNF- α	Tumor necrosis factor α
TSLP	Thymic stromal lymphopoietin
WT	Wild type

Table of Contents

Statement	iii
Acknowledgements	v
Publications	vii
Conference presentations	viii
Abstract	ix
Abbreviations	xiii
Chapter 1: General Introduction	1
1.1 The immune system overview diary.	3
1.1.1 Innate immune system.	3
1.1.2 Adaptive immune system.	6
1.2 The mucosal immune system.	10
1.3 Current state of HIV vaccines.	16
1.4 Mucosal HIV vaccines.	18
1.4.1 Vaccine vectors and routes of vaccine delivery.	18
1.4.2 Cytokine cell milieu.	22
1.5 IL-4 and IL-13 signalling pathway.	23
1.6 IL-4R antagonist and IL-13R α 2 adjuvanted mucosal HIV vaccines.	26
1.7 Innate lymphoid cells (ILCs).	32
1.7.1 ILC2.	32
1.7.2 ILC1 and ILC3.	35
1.7.3 ILC development.....	38

1.7.4 ILC in inflammation and asthma.	38
1.7.5 ILC in parasitic and helminth infections.....	41
1.7.6 ILC in viral infection.....	41
1.7.7 Plasticity of ILCs.	42
1.8 Scope of this PhD thesis.....	45
Chapter 2: General Materials and Methods.....	49
2.1 Materials.....	51
2.2 Methods.....	55
2.2.1 Mice.	55
2.2.2 Primary chicken embryo skin culture.	55
2.2.3 Recombinant virus stock preparation.....	56
2.2.4 Recombinant virus titration.....	56
2.2.5 Immunization.	57
2.2.6 Preparation of lung lymphocytes.	57
2.2.7 Preparation of muscle lymphocytes.	58
2.2.8 Surface and intracellular staining of ILC.....	59
2.2.9 General ILC gating strategy.....	60
2.2.10 Calculation of cell numbers.	70
2.2.11 Statistical analysis.....	70
Chapter 3: Vaccination route can significantly alter the innate lymphoid cell subsets: A feedback between IL-13 and IFN-γ.....	71
3.1 Abstract.....	73

3.2 Introduction.....	74
3.3 Materials and Methods.....	76
3.3.1 Mice and immunisation.....	76
3.3.2 Surface and intracellular staining.....	76
3.4 Results.....	78
3.4.1 Intranasal vaccination induces lineage ⁻ ST2/IL-33R ⁺ ILC2s expressing IL-13 at the lung mucosae and IL-4R antagonist/IL-13R α 2 adjuvanted vaccines inhibit this activity.....	78
3.4.2 Expression of IFN- γ and IL-22 by NKp46 ⁺ ILC subset is differentially regulated following FPV-HIV-IL-13R α 2 and FPV-HIV-IL-4R antagonist vaccination at the lung mucosae.....	88
3.4.3 FPV-HIV-IL-4R antagonist vaccine significantly increases IFN- γ production by NKp46 ⁻ ILC at the lung mucosae.....	91
3.4.4 Intramuscular vaccination induces exclusive lineage ⁻ IL-25R ⁺ ILC2 subset at the vaccination site.....	98
3.4.5 Intramuscular vaccination induces uniquely different lineage ⁻ NKp46 ⁻ and NKp46 ⁺ ILC subsets at the vaccination site.....	103
3.5 Discussion.....	110
Chapter 4: Transient inhibition of IL-25 at the lung mucosae can significantly modulate ILC2 development and function.....	115
4.1 Abstract.....	117
4.2 Introduction.....	117
4.3 Materials and Methods.....	122

4.3.1 Mice and immunisation.....	122
4.3.2 Surface and intracellular staining.....	122
4.4 Results.....	124
4.4.1 Following i.n. FPV-IL-25BP vaccination lineage ⁻ IL-33R/ST2 ⁻ IL-25R ⁺ and lineage ⁻ IL-33R/ST2 ⁻ TSLPR ⁺ ILC2 subsets were recruited to the lung mucosae.	124
4.4.2 Following FPV-IL-25BP vaccination distinctive IL-13 and IL-4 expression profiles were detected in the different lung ILC2 subsets.	127
4.4.3 Following FPV-HIV-IL-25BP vaccination lineage ⁻ IL-33R/ST2 ⁻ NKp46 ^{+/-} ILCs were found to express IFN- γ and IL-17A.	130
4.4.5 Following intranasal FPV-HIV-IL-25BP vaccination a novel lineage ⁻ IL-33R/ST2 ⁻ IL-25R ⁻ TSLPR ⁻ ILC2 cell subset expressing IL-13 and IL-4 was discovered.	135
4.5 Discussion.....	138
Chapter 5: Evaluation of ILC subsets in IL-4, IL-13 and STAT6 knockout mice following intranasal rFPV vaccination.	143
5.1 Abstract.....	145
5.2 Introduction.....	145
5.3 Materials and Methods.....	147
5.3.1 Mice and immunisation.....	147
5.3.2 Surface and intracellular staining.....	147
5.4 Results.....	148

5.4.1 Following i.n. rFPV vaccination lung lineage ⁻ IL-33R/ST2 ⁺ ILC2 in IL-4 ^{-/-} , IL-13 ^{-/-} and STAT6 ^{-/-} mice were significantly different compared to WT BALB/c mice.....	148
5.4.2 In KO mice the Sca-1 regulation on lung lineage ⁻ IL-33R/ST2 ⁺ ILC2 was mainly observed at 24 h post vaccination.	149
5.4.3 WT BALB/c and STAT6 ^{-/-} mice showed elevated numbers of lung lineage ⁻ IL-33R/ST2 ⁺ ILC2 expressing IL-13 compared to IL-4 ^{-/-} mice.....	154
5.4.4 Lung lineage ⁻ IL-33R/ST2 ⁻ NKp46 ^{+/-} ILC1/ILC3 numbers were regulated differently in IL-13 ^{-/-} , IL-4 ^{-/-} , and STAT6 ^{-/-} mice.	154
5.4.5 Following intranasal vaccination, STAT6 ^{-/-} mice showed extremely low lung lineage ⁻ IL-33R/ST2 ⁻ NKp46 ^{+/-} ILC1/ILC3 expressing IFN- γ and IL-22.....	159
5.4.6 Following viral vector vaccination, ILC2-driven IL-13 and ILC1/ILC3-driven IFN- γ expression were inversely correlated.....	162
5.5 Discussion.....	165
Chapter 6: Evaluation of IL-13Rα2, type I and II IL-4 receptor complexes on different ILC subsets following rFPV vaccination.....	175
6.1 Abstract.....	177
6.2 Introduction.....	177
6.3 Materials and Methods.....	179
6.3.1 Mice and immunisation.....	179
6.3.2 Surface staining.....	179
6.4 Results.....	183

6.4.1 Elevated number of ST2/IL-33R ⁺ ILC2 and NKp46 ⁻ ILC1/ILC3 were found to express IL-13Rα2 following FPV-HIV-IL-4R antagonist vaccination.....	183
6.4.2 Following FPV-HIV-IL-13Rα2 adjuvanted vaccination, IL-13Ra2 was not regulated on ST2/IL-33R ⁺ ILC2 or NKp46 ⁻ ILC1/ILC3.	195
6.4.3 Following transient or permanent inhibition of IL-4/IL-13, IL-13Rα2 were not regulated on NKp46 ⁺ ILC1/ILC3 unlike NKp46 ⁻ ILC1/ILC3.....	202
6.5 Discussion	209
Chapter 7: General Discussion.	215
7.1 General discussion.	217
7.2 Future directions.	222
Refences.....	224

Chapter 1.

General Introduction.

1.1 The immune system overview diary.

Humans and animals are continually exposed to microbes and harmful substances that are inhaled, swallowed, or inhabit the skin and mucous membranes. Whether these microbes and substances threaten normal homeostasis depends on their pathogenicity and the host defence mechanisms, which forms the immune system. The immune system is divided into two compartments determined by the speed and specificity of the responses. The innate immune system induces responses that are rapid but non-specific whilst the adaptive immune system is slow and induce pathogen-specific responses¹ (**Fig. 1.1**).

1.1.1 Innate immune system.

The physical, chemical, and microbiological barriers are the crucial first line of defence against pathogen invasion² (**Fig 1.2**). For example, the skin, gastrointestinal, respiratory, and urogenital tracts contain epithelial cells which are joined by tight junctions and form an effective seal against the external environment. The internal epithelia are also known as mucosal epithelia because of their ability to secrete mucus^{3, 4}, comprised of antimicrobial peptides, fatty acids, enzymes (specifically, lysozymes), α -defensins and β -defensins. Moreover, healthy epithelial surfaces also contain a large number of non-pathogenic bacteria, known as the microbiota^{5, 6}. Microbiota also helps strengthen the barrier functions of the epithelia by producing antimicrobial substances, such as lactic acid. There are also cells in the innate immune compartment, which express different sensing receptors, such as macrophages that express Toll-Like Receptors (TLRs). TLRs can recognise pathogens by binding their Pathogen Associated Molecular Patterns (PAMPs)⁷ to initiate defence against microbial pathogens. Moreover, antiviral activity induced by type I interferons (IFN) also play a crucial role in the innate immune system^{8, 9, 10}.

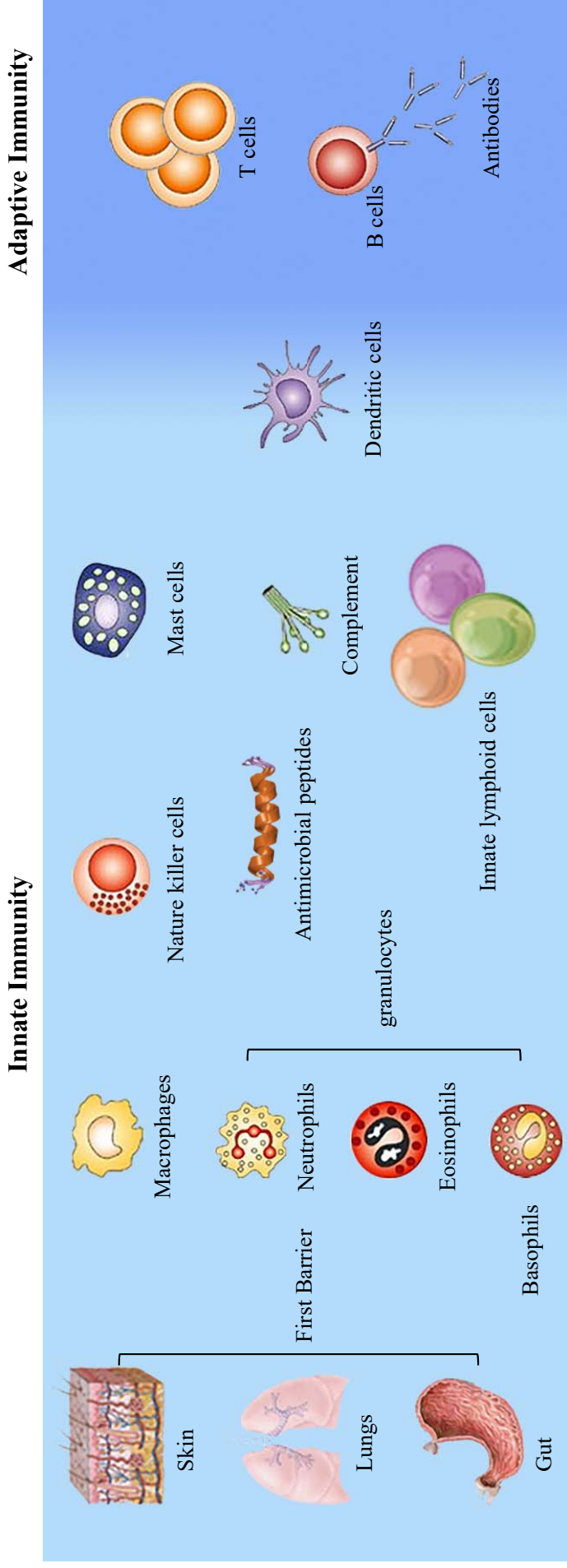


Fig. 1.1. The immune system overview.

The immune system is comprised of two compartments, the innate immune system which acts rapidly in a non-specific manner and the adaptive immune system which develops slowly and acts in a specific manner. The innate immune system consists of physical, chemical, and microbiological barriers as well as various cells. The adaptive immune system mainly consists of T cells, B cells.

	Skin	Gut	Lungs	Eyes/nose/oral
Physical		Epithelial cells		
	Longitudinal flow of air or fluid		Cilia	Tears/cilia
Chemical	Fatty acids	Low PH	Pulmonary surfactant	Enzymes
	β -defensins	Enzymes		
	Lamellar bodies	α -defensins	α -defensins	Histatins
	Cathelicidin	Cathelicidin	Cathelicidin	β -defensins
Microbiological		Normal microbiota		

Fig 1.2. The first line of defense in innate immune system.

Surface epithelia provide physical, chemical, and microbiological barriers to infection.

The innate immune system is comprised of a large number of cellular and humoral elements (**Table 1.1**). Most of these elements in the innate system are present before the onset of an infection, however these protective mechanisms are not pathogen specific. Key cells that are involved in this process include mast cells, macrophages, natural killer cells (NK cells), dendritic cells, monocytes, granulocytes, and also the newly discovered cytokine producing lineage negative cells known as innate lymphoid cells (ILC)^{11, 12, 13, 14, 15} (**Fig. 1.3**). Macrophages are activated by a variety of stimuli such as LPS, peptidoglycans and cytokines. Once they are activated, macrophages exhibit greater phagocytic activity and present antigen to T_H cells which makes macrophages an important connection between the innate immune system and the adaptive immune system. NK cells contain special proteins such as perforin and serine proteases known as granzymes that have the ability to destroy the pathogen. The NK cells play a significant role in defence against viruses and also produce two anti-viral cytokines IFN- γ and TNF- α . Dendritic cells are the major antigen presenting cells in the innate compartment. According to the immune compartment (skin, lung and digestive tract,) resident DC subsets can be vastly different, upon activation these DCs migrate to lymph nodes, and present antigens to T cells and initiate the adaptive immune cascade. The cytokines produced in the innate compartment by different immune cells play an important role at the first line of defense¹⁶ activating the DC and macrophages shaping the downstream adaptive immune outcomes (**Fig 1.4**).

1.1.2 Adaptive immune system.

The vast variability of antigenic structures and their ability to mutate to avoid host defence mechanisms have driven the evolution of the adaptive immune system¹⁷. Unlike the recognition receptors of the innate immune system, which are invariant, and germline encoded, the adaptive immune responses rely on receptors that are generated

Table 1.1. Elements of the innate immune system.

Cellular elements	Macrophages, mast cells, neutrophils, eosinophils, basophils, NK cells, dendritic cells, ILC
Humoral elements	Complement proteins, LPS binding protein, C-reactive protein, antimicrobial peptides, mannose-binding lectin
Receptors	Toll-like Receptors (TLR), NOD-like Receptors (NLR)

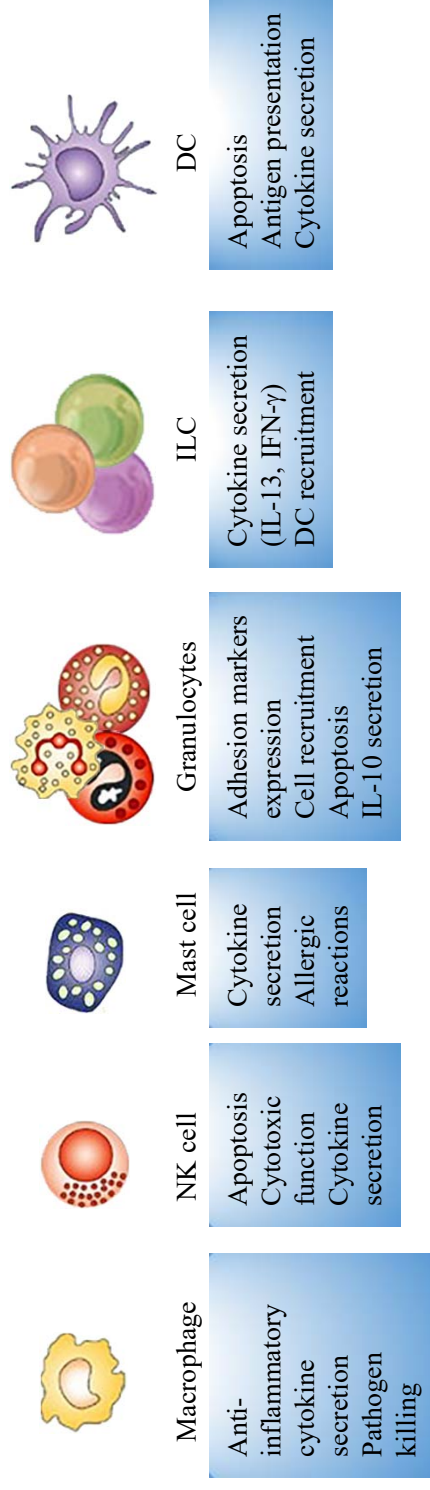


Fig. 1.3. The cells in innate immune system.

Macrophages, natural killer cells (NK cells), mast cells, granulocytes (neutrophils, basophils, and eosinophils), innate lymphoid cells (ILCs), dendritic cells (DC), are involved in generating innate immune responses.

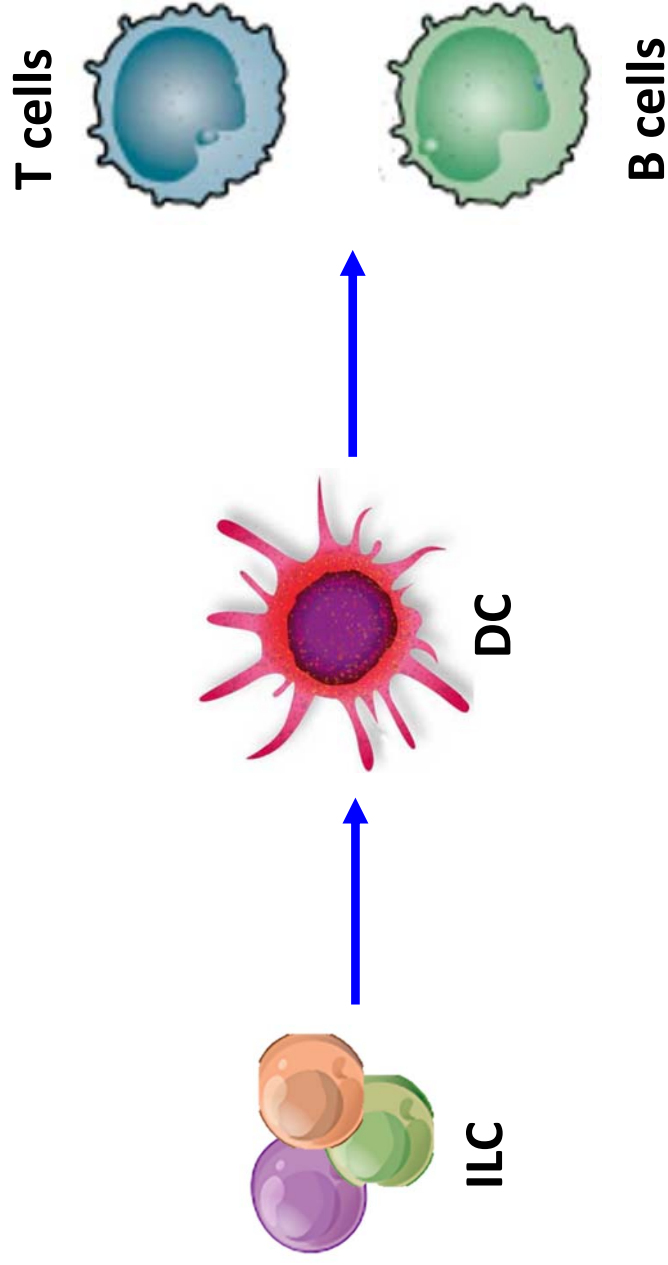


Fig 1.4. Innate lymphoid cells (ILCs) can manipulate downstream immunity.

ILC could be the the major cytokine producing cells in innate immune system. The cytokine milieu created by ILC most likely manipulate DC recruitment and the downstream adaptive immune outcomes.

by random somatic gene segment rearrangement^{18, 19, 20, 21, 22, 23}. After initial pathogen encounter, cells expressing these receptors can persist in the host for life, providing immunologic memory and capacity for rapid response in the event of re-exposure²⁴.

Cells of the adaptive immune system include the effectors of cellular immune responses, the T lymphocytes, which mature in the thymus, and antibody-producing cells, the B lymphocytes, which arise in the bone marrow^{25, 26}. These T and B lymphocytes use their antigen-specific receptors to drive targeted effector responses in two stages (**Fig. 1.5**). First, the antigen is presented to T or B cells by APC, and then T and B cells begin to prime, activate, and differentiate. This stage usually occurs in specialised environment of lymphoid tissues. Second, the effector response takes place, where activated T cells leave the lymphoid tissue and home to the site of infection, and similarly the activated B cells start to produce antibodies which can be found in blood and tissue fluids^{11, 24, 25, 26, 27, 28}.

1.2 The mucosal immune system.

The mucosal immune system is the first line of defence in humans and higher animals. It consists of a single-layer epithelium covered by mucus and antimicrobial secretes and fortified by both innate and adaptive components of host defence²⁹ (**Fig. 1.6**). Mucosal epithelium acts as a physical, chemical and a protective barrier, sensing and eliminating harmful pathogens (**Fig. 1.6**). The mucus secreted by goblet cells, forms a dense protective layer covering of the entire mucosal epithelium³⁰. The paneth cells are able to produce anti-microbial peptides or α -defensins, and epithelial cells produce β -defensins for host protection^{31, 32}. A network known as the mucosa-associated lymphoid tissue (MALT), plays an important role in initiating mucosal adaptive immune outcomes³³. According to the anatomical location, the MALT is divided into gut-

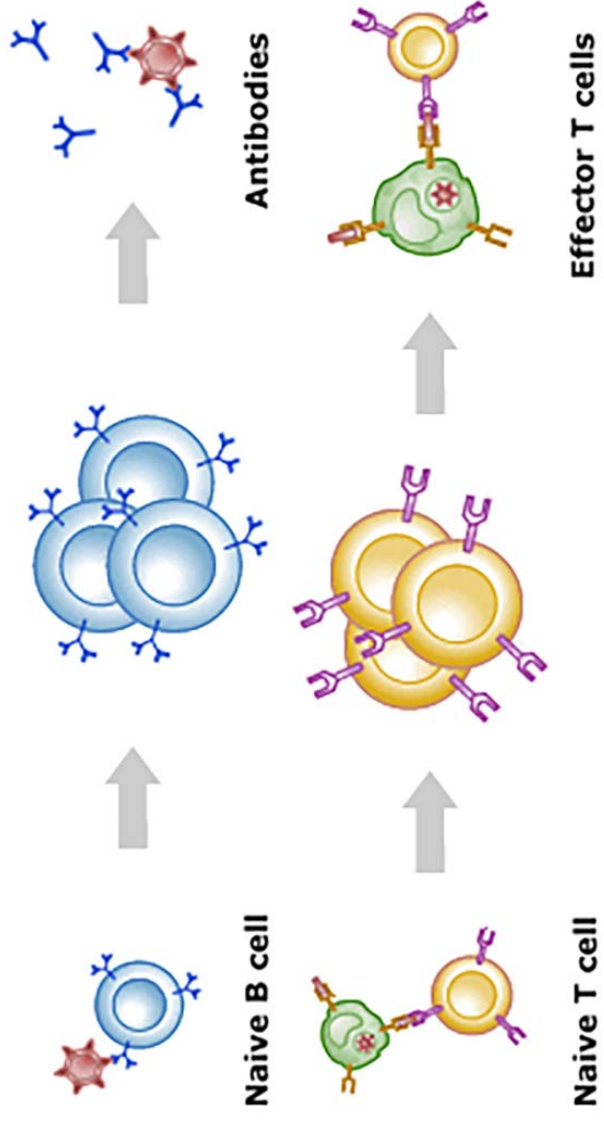


Fig. 1.5. Lymphocytes in the adaptive immune system.

T and B cells are the most important elements in the adaptive immune responses. T helper cells by producing different cytokines can help B cells to produce antibodies. CD4 and CD8 T cells, upon antigen encounter can differentiate into effector and memory T cells. Cytotoxic T cells which contain toxic granules (granzymes, perforins) has the ability to induce death of pathogen-infected cells.

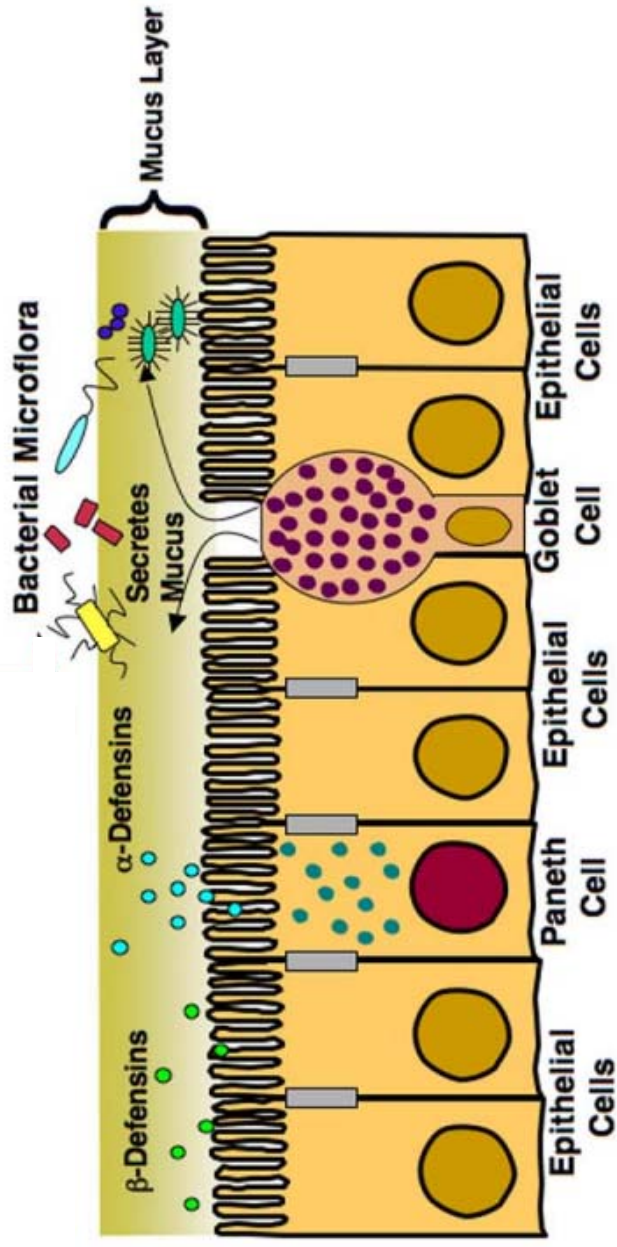


Fig. 1.6. The epithelial layer of the mucosal immune system.

In general mucosal tissues are comprised of a single-layer epithelium, covered in mucus and antimicrobial secretes. In this single-layer epithelium, the mucosal epithelial cells are the central position by providing both a physical barrier and innate immunity.

associated lymphoid tissue (GALT), nasopharynx-associated lymphoid tissue (NALT), bronchus-associated lymphoid tissue (BALT) and urogenital associated lymphoid tissue (**Fig. 1.7**).

GALT, is comprised of several lymphoid nodules; Peyer's patches, isolated lymphoid follicles, cryptopatches, and lymphoglandular complexes³⁴. Peyer's patches are extremely important for the initiation of immune responses in the gut, which contain large number of B cell zones and also small number of T cell zones³⁴. The subepithelial dome areas of Peyer's patches are rich in dendritic cells, T cells, and B cells. The isolated lymphoid follicles, located on the antimesenteric border of the small intestine are very similar to Peyer's patches and contain B cell follicles and an overlying follicle-associated epithelium containing microfold cells (M cells), and also scattered dendritic cells with few macrophages^{35, 36}. The M cells are unique to the mucosal compartment, which have a folded luminal surface and do not secrete digestive enzymes or mucus and lack microvilli unlike other mucosal epithelial cells (**Fig. 1.8**). M cells are directly exposed to micro-organisms and particles within the gut lumen and help antigen enter the Peyer's patches (**Fig. 1.8**)³⁷.

The NALT is composed of paired lymphoid aggregates in the caudoventral portion of the left and right nasal passages at the entrance to the nasopharyngeal duct³⁴. Compared to gut Peyer's patches, there are fewer intraepithelial lymphocytes in NALT, and the relative T and B cell zones areas are roughly equal in the NALT, unlike in the GALT where number of T cell zones are lower than B cell zones³⁴. Similar to GALT, the lymphoepithelium of NALT also contains M cells³⁸. BALT and urogenital associated lymphoid tissue also contain M cells. These M cells are known to uptake and present

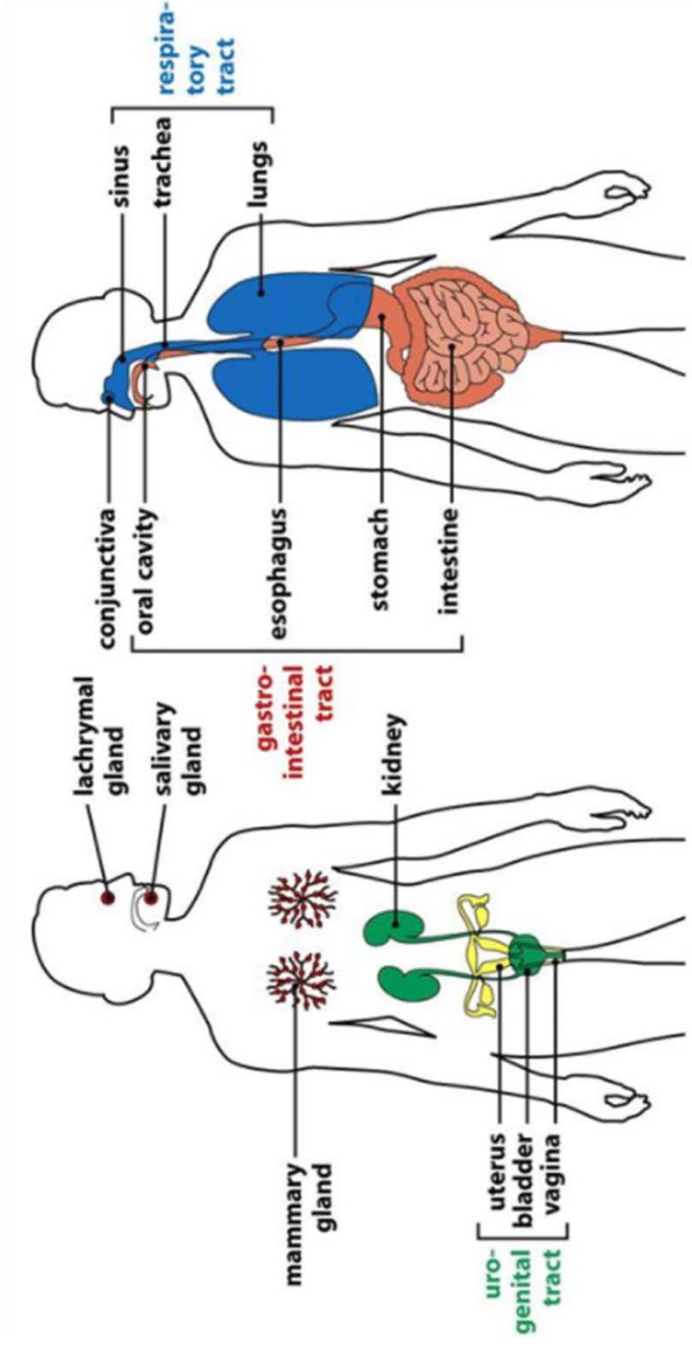


Fig. 1.7. The mucosal immune system.

Immune cells in mucosal surfaces form a specific network called the mucosal-associated lymphoid tissue (MALT).

MALT can be principally divided into gut-associated lymphoid tissue (GALT), nasopharynx-associated lymphoid tissue (NALT), bronchus-associated lymphoid tissue (BALT) and uro-genital-associated lymphoid tissue.

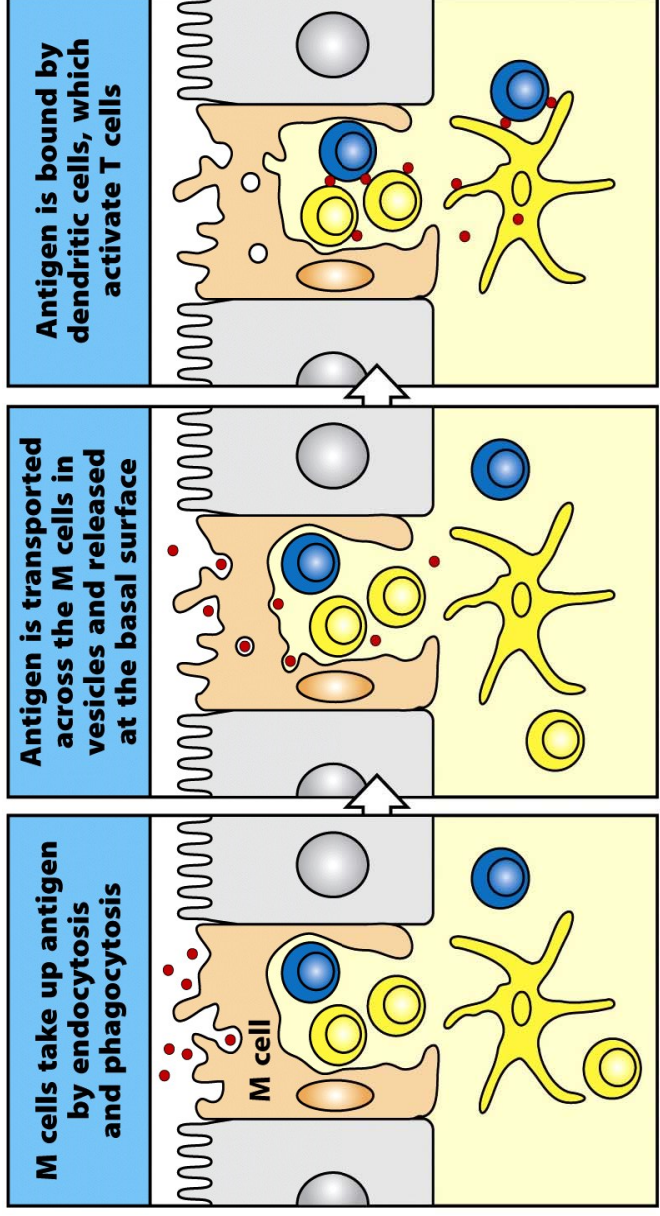


Figure 11-8 part 1 of 2 Immunobiology, 7ed. (© Garland Science 2008)

Adapted from Janeway's Immunology

Fig. 1.8. M cells in the mucosal compartment.

M cells are unique in the follicle-associated epithelium and they are important in taking up and transporting antigen to dendritic cells for antigen presentation.

antigens to mucosal dendritic cells, which in turn present antigens to T cells and initiate T cell homing³⁸.

1.3 Current state of HIV vaccines.

Since the first characterisation of Human Immunodeficiency Virus (HIV) and Acquired Immune Deficiency Syndrome (AIDS) in 1981³⁹, more than 25 million people have died of the disease⁴⁰. Currently according to WHO there are 36.7 million people living with HIV and 1.2 million have died in 2016 (UNAIDS global report 2017). Although effective anti-retroviral therapy is currently available, to effectively combat HIV, a vaccine with high efficacy is urgently needed, which is the only cost-effective solution, specifically in the developing countries. It is now well established that HIV is a mucosal infection as the transmission mainly occurs via the genito-rectal mucosae⁴¹. HIV infects CD4⁺ T cells, and the first CD4⁺ T cells depletion occurs in the gut⁴¹. Interestingly, despite HIV being a mucosal infection, not many mucosal vaccine strategies have been tested in the clinic. The main difficulties of HIV vaccine development have been associated to i) the diversity of HIV, the virus having different clades and makes it difficult to design a universal vaccine; ii) inability to induce effective neutralising antibodies; iii) viral latency, due to viral integration to the host genome; and iv) inability to design an effective vaccine that target both the mucosal and the systemic compartments^{42, 43, 44, 45}.

Over the past three decades, all human HIV clinical vaccine trials have used systemic route of delivery, and all these vaccines have yielded poor outcomes in humans (**Table 1.2**). Early clinical trials of HIV vaccines attempted to use recombinant subunits or synthetic peptide fragments to elicit neutralising antibodies against viral antigens, such as Env proteins gp120 and gp41. These vaccines although induced strong antibody

Table 1.2. Examples of selected phase II and III human HIV vaccine trials.

Type	Trial	Location	Phase	Results
Pox-protein	RV 144	Thailand	III	31% efficacy
DNA-Ad5	HVTN 505	US	IIb	No efficacy, stopped early
DNA-Ad5	HVTN 502	US	IIb	No efficacy, transient infection risk
DNA-Ad5	HVTN 503	RSA	IIb	No efficacy
Protein	VAX 003	Thailand	III	No efficacy
Protein	VAX 004	US	III	No efficacy

binding showed no neutralising ability, or CD8⁺ T cell immunity^{46, 47}. Following the VAX 004 trial using a recombinant HIV envelope glycoprotein subunit (rgp120) and a second envelope in alum adjuvant also showed no differences in protective efficacy among 3598 vaccines and 1805 placebo recipients^{48, 49, 50}. VAX 003 trial which used a similar approach also showed no protective efficacy^{51, 52}. DNA and adenovirus vector-based vaccines although successful in the animal models have yielded poor outcomes in humans^{53, 54}. The Thai phase RV144 trial which used recombinant canarypox prime followed by several gp120 Env boosters, has been the only trial that has shown any protective efficacy in humans (31%)⁵⁵. In this trial, the partial protection was mainly associated with Env-specific IgG antibodies not IgA, or CD8⁺ T cell responses^{56, 57}. Thus, it is now established that a vaccine strategy that can induce both high quality mucosal/systemic T cells and B cell immunity may be needed to induce full protection against HIV.

1.4 Mucosal HIV vaccines.

It is now well established that to induce effective, long-lasting mucosal immunity, a vaccine needs to be delivered to the mucosae, for example: intranasal, oral, rectal or intravaginal routes of delivery^{58, 59} (**Fig. 1.9a**), and systemic vaccination is unable to induce effective sustained immunity at the mucosae^{60, 61}. Studies have now clearly established that following vaccination the adaptive immune responses can be significantly manipulated by the route of delivery, vaccine adjuvants/vectors, and the cytokine milieu at the vaccination site^{61, 62, 63, 64}.

1.4.1 Vaccine vectors and routes of vaccine delivery.

Even though recombinant DNA vaccine strategies have shown to induce good immune responses against HIV in animal models^{65, 66, 67}, they have not been effective in clinical

trials, mainly due to their poor up-take. Specifically, mucosal delivery of DNA vaccines has not been effective in both animals and humans^{60, 65}. These complexities lead to the development of a range of live recombinant viral vector-based vaccines to deliver vaccine antigens against many chronic pathogens (for example malaria, HIV and TB)^{68, 69, 70, 71, 72}. For example, in the context of HIV, the Thailand RV 144 trial which showed partial protective efficacy (31.2%) used recombinant canarypox vector-based vaccine prime followed by several recombinant gp120 subunit vaccine booster vaccines⁵⁵. Also, in this trial, heterologous prime-boost vaccination was proven to be more effective than the use of recombinant HIV vaccine vector alone.

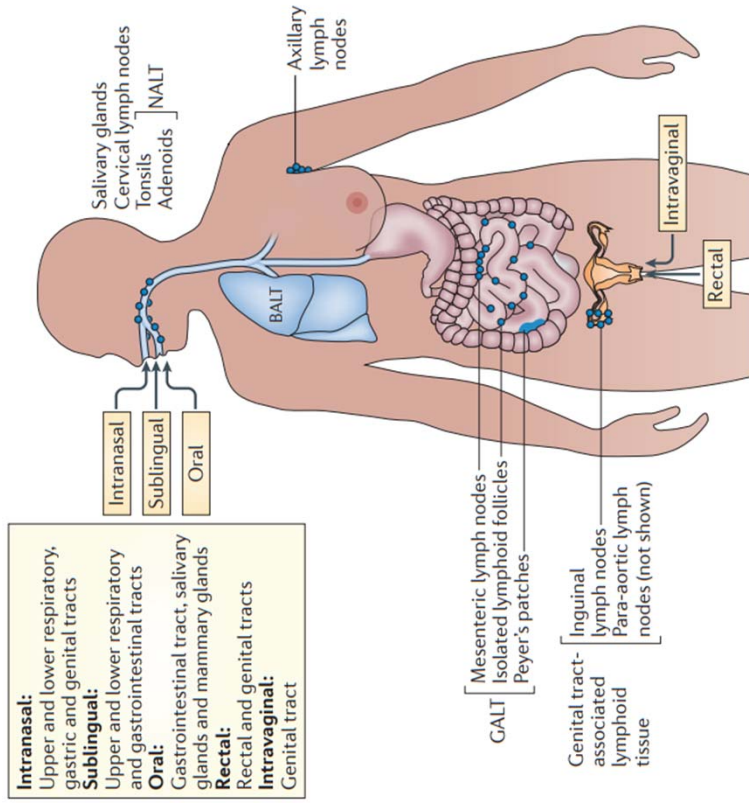
It is now well established that the route of delivery can significantly modulate the adaptive immune outcomes^{59, 61, 62}. Specifically, although nasal vaccination can induce immunity in the upper respiratory tract, gut and the genito-rectal mucosae; oral vaccination has shown to induce poor or no immunity in the genito-rectal mucosae. Similarly, rectal immunisation can induce immunity in the rectum and larger intestine, whilst vaginal vaccination only can induce immunity in the vagina⁴⁵ (**Fig. 1.9b**). Interestingly, systemic vaccination (for example intramuscular deliver), has shown to induce effective systemic immunity with transient immunity in the mucosae^{59, 73, 74}. Thus, given that most instances HIV initially encounters the host via the mucosae, when designing HIV vaccines, it is now established that a strategy that can induce strong sustained immunity in the mucosae, such as intranasal or intra rectal delivery would be of importance.

Our laboratory has performed extensive studies over a decade to understand different immune outcomes following different routes of prime-boost vaccination (systemic vs

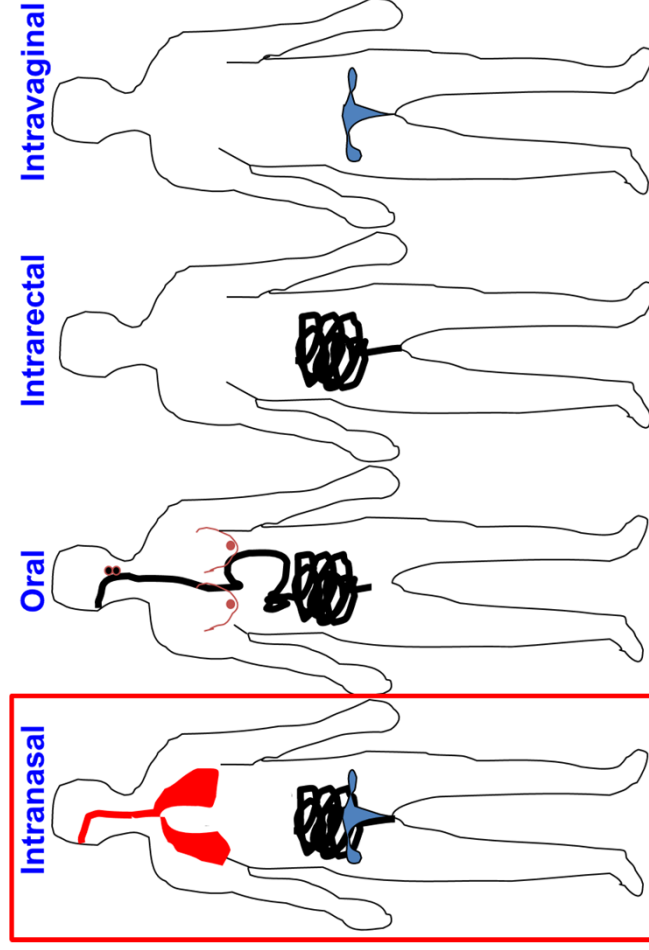
Fig. 1.9. Mucosal routes of vaccine delivery.

Traditional routes of mucosal immunization include oral and nasal routes. However, rectal, vaginal, sublingual, and transcutaneous routes can also induce mucosal immunity in different mucosal compartments **(a)**. Out of the mucosal vaccine routes tested, intra nasal deliver can induce immunity in the upper respiratory tract, gut and also the genito-rectal tract **(b)**.

a



b



mucosal) and the different vector combinations (for example recombinant DNA (rDNA), recombinant fowlpox (rFPV), Modified Vaccinia Ankara (MVA) and recombinant vaccinia virus (rVV) in mouse and non-human primate models^{60, 74, 75}. These studies have shown that i) rFPV is an excellent mucosal delivery vector compared to rDNA, rMVA or rVV^{60, 74}; ii) Intramuscular (i.m.) rDNA/intranasal (i.n.) rFPV prime-boost vaccine strategy can induce elevated HIV-specific systemic as well as mucosal T cell responses and IgG1, IgG2a and mucosal IgG, SIgA responses in mouse and macaque models^{60, 65}; iii) However, unlike rDNA prime-boost strategy, i.n. rFPV/i.m. rVV strategy can induce strong sustained HIV-specific CD8⁺ T cells with higher avidity and better protective efficacy^{60, 74}, iv) When designing viral vector-based vaccines vector combination plays an important role, where rFPV prime/rVV booster or influenza booster induce high avidity T cells whilst rVV or influenza prime induce low avidity T cell immunity⁷⁶ and v) The route of vaccine delivery plays a crucial role in modulating avidity and magnitude of T cell responses⁷⁵ where systemic delivery (intramuscular) induce low avidity HIV-specific CD8 T cells whereas, mucosal delivery (intranasal) can induce high avidity HIV-specific CD8⁺ T cells and this was associated with the level of IL-4 and IL-13 expressed by CD8 T cells^{75,77}.

1.4.2 Cytokine cell milieu.

Ranasinghe et al for the first time demonstrated that pure systemic route (intramuscular – i.m.) of vaccination can generate lower avidity of HIV-specific CD8⁺ T cells with higher levels of IL-4 and IL-13 production compared to pure mucosal (intranasal – i.n.) or mucosal/systemic routes (i.n./i.m.) of vaccination⁷⁷. Using IL-4 gene knock-out (IL-4^{-/-}) and IL-13 gene knock-out mice (IL-13^{-/-}), studies have shown that IL-4^{-/-} and IL-13^{-/-} mice are able to generate CD8⁺ T cells with higher avidity compared to WT mice given the same vaccination (i.n. FPV-HIV/i.m. VV-HIV)⁷⁷. Furthermore, these studies

showed that IL-4 and IL-13 can significantly dampen CD8 α expression on anti-viral CD8⁺ T cells, and reduce poly-functionality of these T cells (ability to produce a range of anti-viral cytokines- which is a hallmark of protective immunity)⁷⁸. Furthermore, these studies also established that following viral infection down regulation of IL-4 receptors α (IL-4R α) is associated with the induction of higher avidity CD8⁺ T cells⁷⁹. These studies clearly demonstrated that route of vaccination and IL-4/IL-13 levels play a detrimental role in modulating the quality of CD8⁺ T cells.

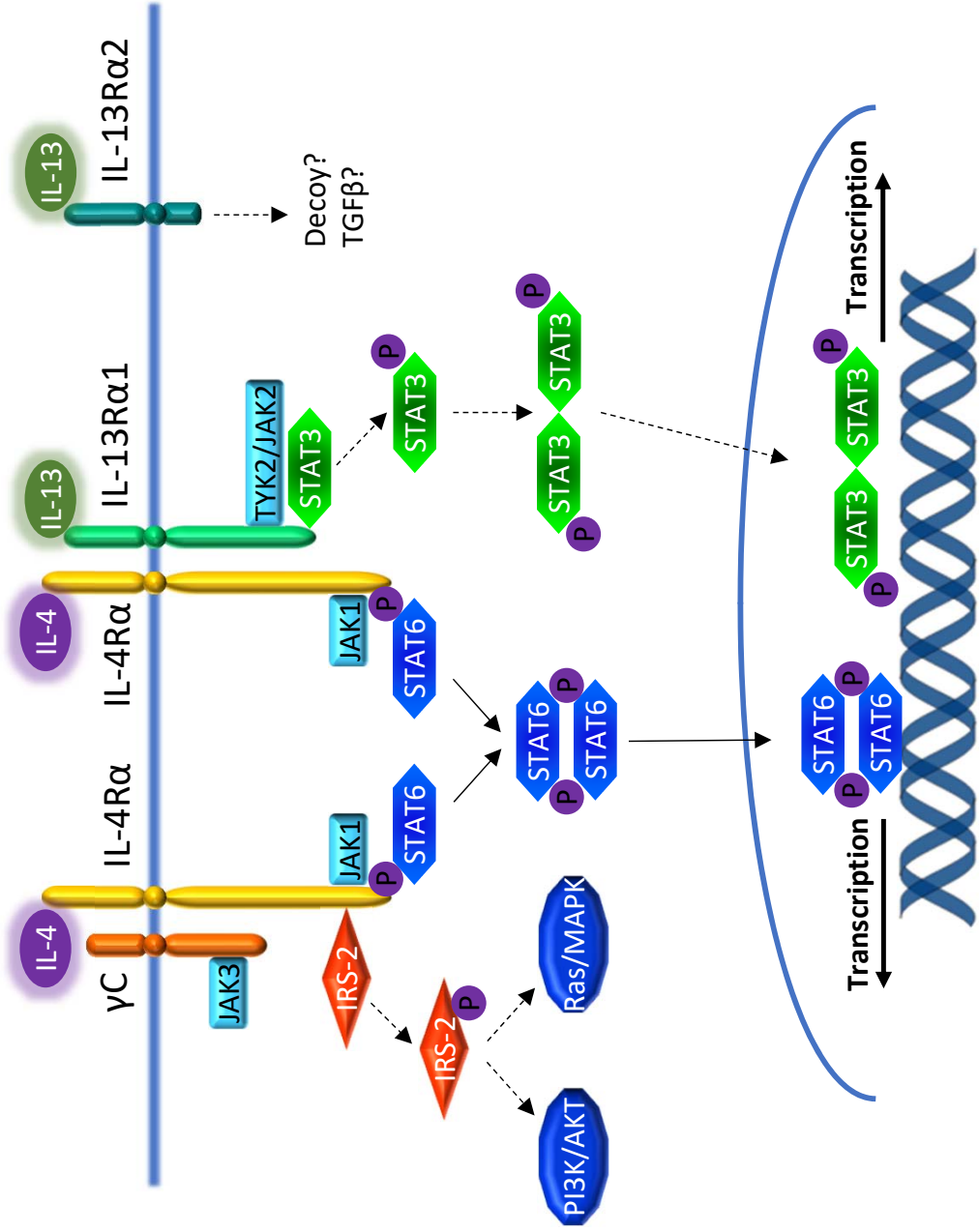
1.5 IL-4 and IL-13 signalling pathway.

IL-4 and IL-13 are two cytokines at the centre of type-2 inflammation, and since their discovery have been linked to allergy, asthma and atopic diseases^{80, 81}. IL-4 and IL-13 are secreted by CD4⁺ T cells^{82, 83}, CD8⁺ T cells^{84, 85, 86}, mast cells and basophils^{87, 88, 89}. In the last decade, the newly identified innate immune cell type 2 (ILC2) has also shown to express IL-13 and also IL-4 under certain conditions^{90, 91}.

IL-4 and IL-13 signal via a complex receptor system⁹² (**Fig. 1.10**). The type I IL-4 receptor complex consists of the IL-4 receptor α (IL-4R α) and common gamma chain (γ C). The type II IL-4 receptor complex contains IL-4R α and IL-13 receptor α 1 (IL-13R α 1)⁹³. IL-4 can signal via both type I and type II receptor complex by binding IL-4R α with very high affinity and then resulting in the recruitment of either γ C or IL-13R α 1^{94, 95}, followed by the initialization of Janus Kinase/Signal Transducer and Activator of Transcription 6 (JAK/STAT6) signalling^{96, 97, 98} (**Fig. 1.10**). It is also thought that under certain conditions IL-4 can also signal via the Insulin Receptor Substrate-1/2 (IRS-1/2) pathway^{97, 99, 100, 101, 102}, followed by the activation of Phosphoinositide 3-kinase (PI3-K)^{103, 104, 105},

Fig. 1.10. IL-4 and IL-13 signalling pathways.

A functional IL-4 receptor is composed of two transmembrane proteins. IL-4R α chain binds IL-4 with high affinity, leading to dimerization with either gamma common chain (γ C) or IL-13R α 1, forming the type I or type II receptor complexes, respectively. IL-13 binds to IL-13R α 1 with lower affinity, followed by heterodimerization with IL-4R α to form a high affinity complex. IL-13 also binds to IL-13R α 2 (the so-called “decoy receptor” in mice, but is active in humans) at the cell surface, or in soluble form, but this interaction fails to activate the JAK/STAT pathway and generally thought to be inhibitory to STAT6 signalling. It is postulated that IL-13R α 2 activates TGF- β via the activation of an not yet defined pathway.



Protein kinase B (also known as AKT)^{106, 107, 108, 109} and NF- κ B-driven gene transcription^{110, 111}. IL-13R α 1 is not only a subunit of the type II IL-4 receptor complex, but also the ligand binding subunit for IL-13. IL-13 binds IL-13R α 1 with low affinity leading to recruitment of the IL-4R α subunit and the activation of JAK/STAT6 signalling pathway⁹³.

IL-13 can also bind to IL-13 receptor α 2 (IL-13R α 2) with high affinity (pM conditions)¹¹². The IL-13R α 2 is considered as a decoy receptor for IL-13 in mice (not in humans) due to the lack of cytoplasmic tail signalling motifs¹¹². However, recent studies in our laboratory have shown that this may not be a decoy receptor even in mice¹¹³. In mice, IL-13R α 2 is found as a cell surface form and a soluble form^{114, 115} but only the cell surface form is found in human¹¹⁶. Studies have shown that IL-13R α 2 can bind to IL-4R α and inhibit IL-4/IL-13 signalling via the IL-13R α 1/IL-4R α type II complex and JAK/STAT6 pathway^{117, 118, 119, 120}. Also, in cancer studies IL-13R α 2 activation/signalling has been associated with TGF- β production in the absence of functional IL-4R α ¹²¹.

1.6 IL-4R antagonist and IL-13R α 2 adjuvanted mucosal HIV vaccines.

Knowing that low IL-4 and IL-13 can induce high avidity HIV-specific CD8⁺ T cells and this is vaccine route dependent^{75, 77}, in order to manipulate IL-4/IL-13 levels at the vaccination site, two pox viral vector-based vaccines were designed in our laboratory, i) IL-4R antagonist vaccine and ii) IL-13R α 2 adjuvanted vaccine. Both these vaccines were able to transiently inhibit IL-4 and/or IL-13 activity at the vaccination site^{113, 122} (**Fig. 1.11**). The IL-13R α 2 adjuvanted vaccine co-expressed HIV antigens together with soluble IL-13R α 2, which could sequester IL-13 at the vaccination site, when given to

wild type BALB/c mice were able to behave very similar to an IL-13 knockout animal¹²² (**Fig. 1.11a**). The IL-4R antagonist adjuvanted vaccine that co-expressed HIV antigens together with C-terminal deletion mutant of the mouse IL-4 (which is the essential tyrosine required for signalling), was able to bind to both type I and type II IL-4 receptor complex with high affinity, and transiently block both IL-4 and IL-13 signalling via the STAT6 pathway¹¹³ (**Fig. 1.11b**).

Using an intranasal/intramuscular prime-boost immunisation strategy, the IL-13R α 2 adjuvanted vaccine was shown to induce enhanced systemic HIV-specific CD8⁺ T cells with high avidity, broader cytokine and chemokine profiles and greater protective immunity¹²². This vaccine was also shown to induce excellent poly-functional mucosal CD8⁺ T cell responses in lung, genito-rectal nodes and Peyer's patch¹²². Interestingly, the IL-4R antagonist adjuvanted vaccine was not only able to induce enhanced mucosal/systemic HIV-specific poly-functional CD8⁺ T cells with high avidity, but also induce robust HIV gag-specific IgG1 and IgG2a antibody responses, unlike IL-13R α 2 adjuvanted vaccine where low antibody differentiation was detected¹¹³. Later studies in the laboratory showed that IL-4 and IL-13 levels at the vaccination site significantly modulate dendritic cell function. Specifically, using IL-13 and/or IL-4 inhibitor vaccines and IL-13^{-/-} mice, Trivedi *et al.* have demonstrated that low level of IL-13 and/or IL-4 induced elevated numbers of CD11b⁺ CD103⁻ conventional dendritic cells (cDC) at the lung mucosae¹²³ associated with the induction of high avidity, poly-functional HIV-specific CD8⁺ T cells¹²². While high level of IL-13 and/or IL-4 associated with rVV and rMVA vaccination induced reduced numbers of CD11b⁺ CD103⁻ dendritic cells, but elevated recruitment of cross presenting CD11b⁻ CD103⁺ dendritic cells which were directly linked to induction of poor quality HIV-specific CD8⁺ T cells¹²³.

Fig. 1.11a. Mechanisms of how IL-13R α 2 adjuvanted vaccine modulate IL-13 activity at the vaccination site.

The IL-13R α 2 adjuvanted vaccine co-expresses vaccine antigen together with soluble IL-13R α 2, which transiently inhibit IL-13 activity at the vaccination site, causing WT animals to behave (transiently) similar to an IL-13^{-/-} animal. In this situation, IL-4 will still bind to both type I and type II IL-4 receptor complexes and signal via the STAT6 pathway.

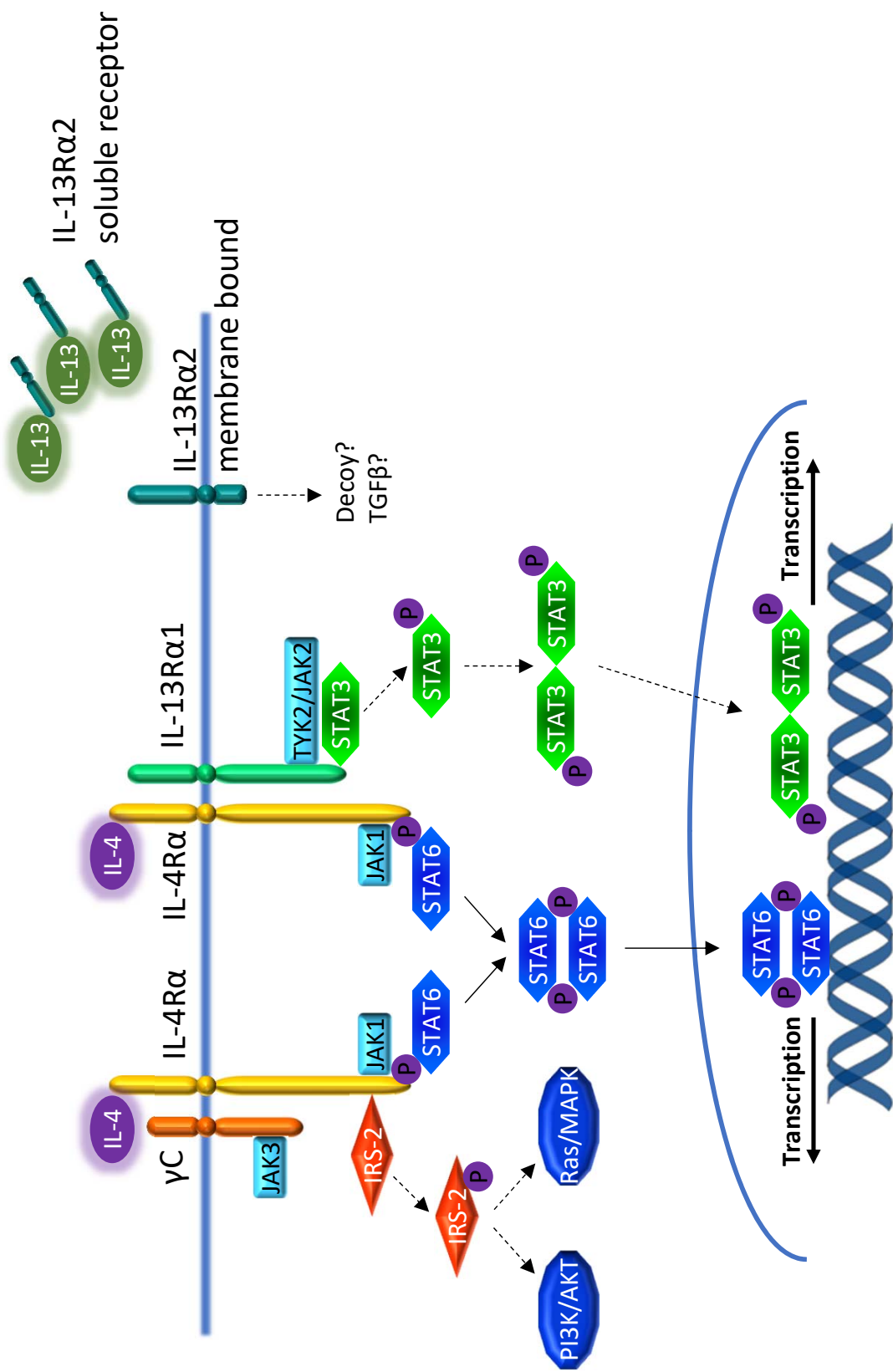
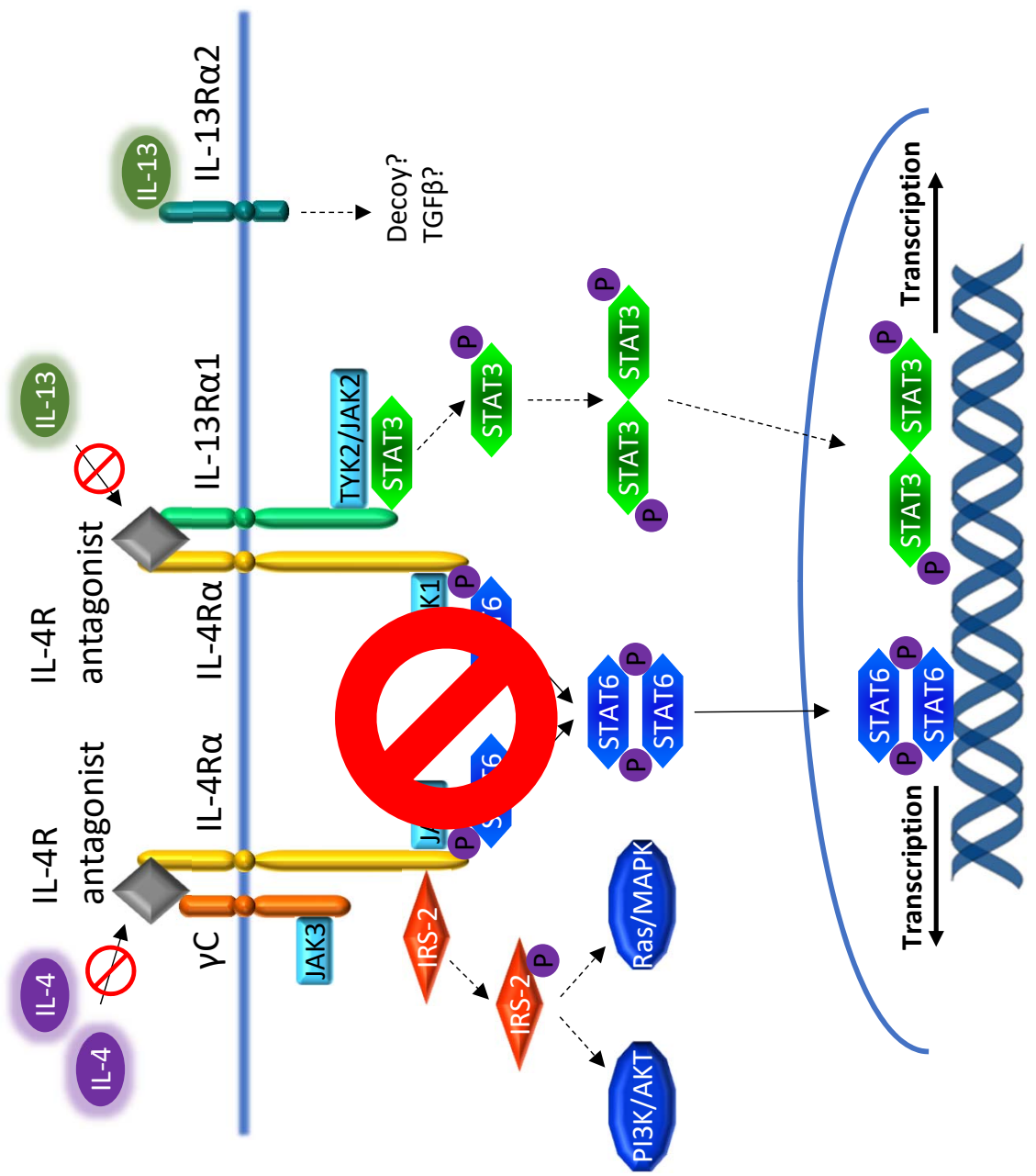


Fig. 1.11b. Mechanisms of how IL-4R antagonist adjuvanted vaccine modulate IL-13/IL-4 activity at the vaccination site.

The IL-4R antagonist adjuvanted vaccine co-express vaccine antigen together with a C-terminal deletion mutant of the mouse IL-4 without the essential tyrosine required for signalling. This mutant IL-4 will bind to both type I and type II IL-4 receptor complex with high affinity, and transiently block the signalling of both IL-4 and IL-13 via STAT6 pathway at the vaccination site. However, in this scenario, IL-13 still has the ability to signal via the not-well defined IL-13R α 2 pathway.



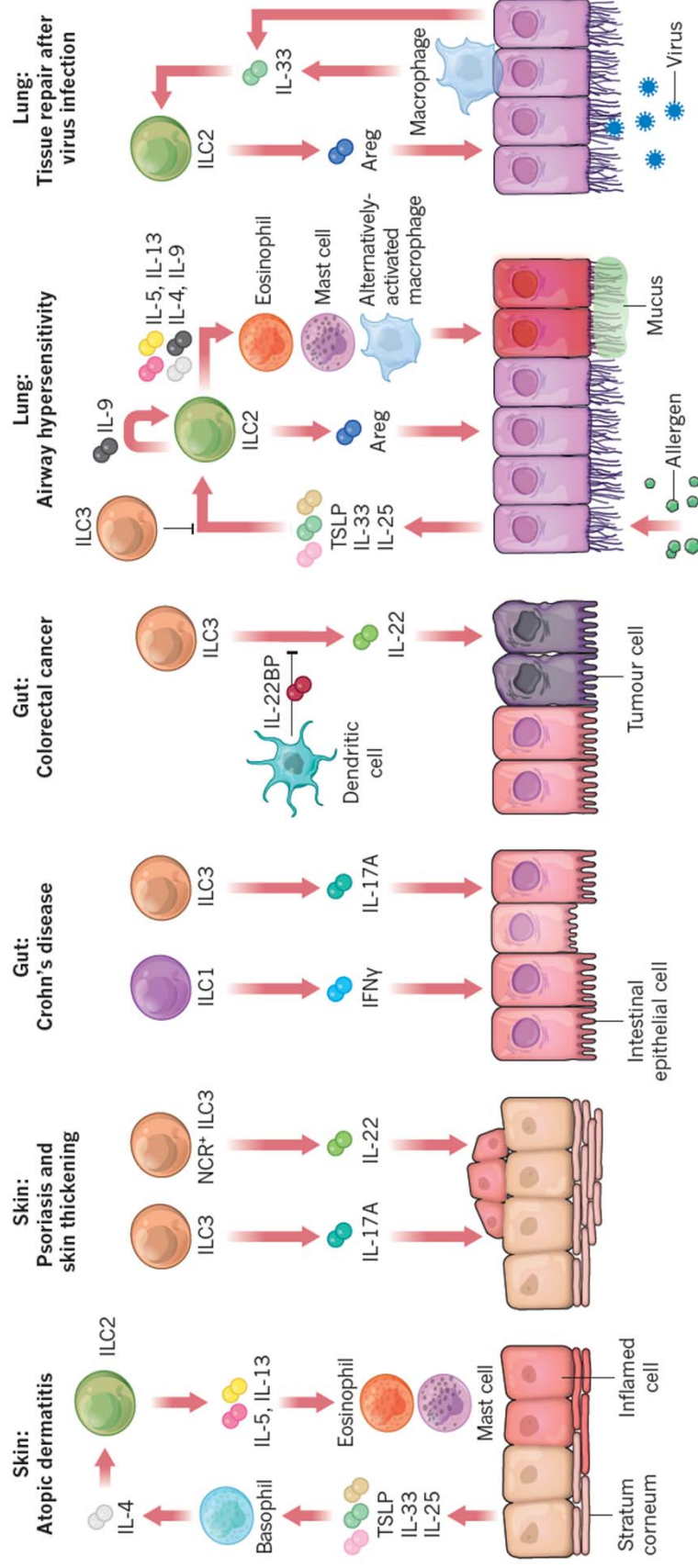
It is now established that HIV elite controllers, small number of individuals who naturally control HIV infection, possess high avidity HIV-specific CD8⁺ T cells as well as gag-specific antibodies with excellent ability to antibody differentiate^{124, 125, 126}. The immune outcomes of observed specifically with IL-4R antagonist adjuvanted vaccine, in murine and macaque models (Khanna, Ranasinghe et al in preparation) indicate that this vaccine strategy may have high potential to be a successful HIV vaccine in the future. This lead to the important question, “*what cells at the vaccination site produces IL-13 24 h post vaccination which are responsible for shaping the downstream immune outcomes?*” which forms the basis of this thesis.

1.7 Innate lymphoid cells (ILCs).

ILCs are a newly identified heterogeneous population of cells with diverse activity in the immune system^{127, 128, 129, 130} (**Fig. 1.12**). However, these cells neither express lymphoid differentiation lineage markers which means they are lineage- nor antigen receptors which make them different from T cells and B cells^{23, 131, 132, 133, 134, 135, 136, 137}. ILCs are classified as innate cells because they do not require the recombination activating genes RAG1 or RAG2 expression for their development, but since they are derived from the common lymphoid progenitor (CLP), they are considered as lymphoid cells¹³⁸, and were named as innate lymphoid cells. The ILC population is generally divided into three distinct groups ILC1, ILC2, and ILC3 on the basis of similarity in their cytokine production, development requirements and phenotypic markers^{132, 139, 140, 141}.

1.7.1 ILC2.

ILC2 are classified based on their ability to produce T helper 2 (Th2) cell associated cytokines including IL-5, IL-9, IL-13 and IL-4^{132, 142} and respond to IL-25, IL-33 and



Adapted from Artis 2015

Fig. 1.12. Innate lymphoid cells.

The ILC are newly discovered cytokine-producing cells, which neither express lymphoid differentiation lineage markers (lineage⁻) nor antigen receptors which making them different from other immune cells. ILCs are classified as innate cells because they do not require the RAG1 or RAG2 expression for development, but since they derive from the common lymphoid progenitor (CLP), they are considered as lymphoid cells. ILCs are mainly found on mucosal surfaces and also skin. According to the anatomical location, for example: gut, lung or skin, the ILC subtypes and their function (cytokine production) can be vastly different,

thymic stromal lymphopoietin (TSLP)^{127, 128, 129, 134, 135, 143, 144, 145}. Currently, ILC2 are divided into three subsets according to receptors they express, IL-33R/ST2⁺, IL-25R⁺, or TSLPR⁺. ILC2 are known to express of CD127, IL-33R (ST2), ICOS, Sca-1, and lack other lineage markers^{146, 147, 148}. The transcription factor GATA3 is often used as an intracellular marker to define ILC2¹⁴⁹. ILC2 are thought to be tissue resident, and large populations are found in the intestine and lung^{137, 142, 146, 150, 151}. Due to their Th2 cytokine production, specifically IL-5, IL-9, IL-13, and IL-4; ILC2 have been well studied in type 2 inflammation, helminth infections and allergic asthma /inflammation^{134, 135, 136, 146, 147, 152} (**Fig. 1.13**).

1.7.2 ILC1 and ILC3.

ILC1 are defined based on their capacity to produce type 1 cytokines especially IFN- γ ^{132, 142}. Some studies have also considered the conventional nature killer (NK) cells to be one subset of ILC1^{128, 153}. In fact, despite ILC1 and NK cells have the ability to produce IFN- γ and surface marker NKp46 (NKp44 in humans), they have several distinct features. Notably, NK cells are lineage⁺ cytotoxicity cells¹⁵⁴ while ILC1 are lineage-non-cytotoxicity IFN- γ producing cells^{140, 155, 156}. Secondly, NK cells are present in numerous sites as they recirculate between the blood and tissues, whereas ILC1 are thought to be tissue resident^{140, 150, 156, 157, 158, 159, 160, 161, 162}. ILC1 have been associated with the induction of immunity against intracellular bacteria and parasites^{140, 155, 156, 163} (**Fig. 1.14**).

ILC3 were initially described in human tissues as mucosal-associated lymphoid cells that express NKp44 and produce IL-22¹⁶⁴. Currently, three ILC3 subsets have been discovered based on the expression of various markers and cytokines, i) lymphoid tissue inducer (LTi) cells, ii) NKp46⁻ ILC3 and iii) NKp46⁺ ILC3^{128, 165, 166}. ILC3 can respond

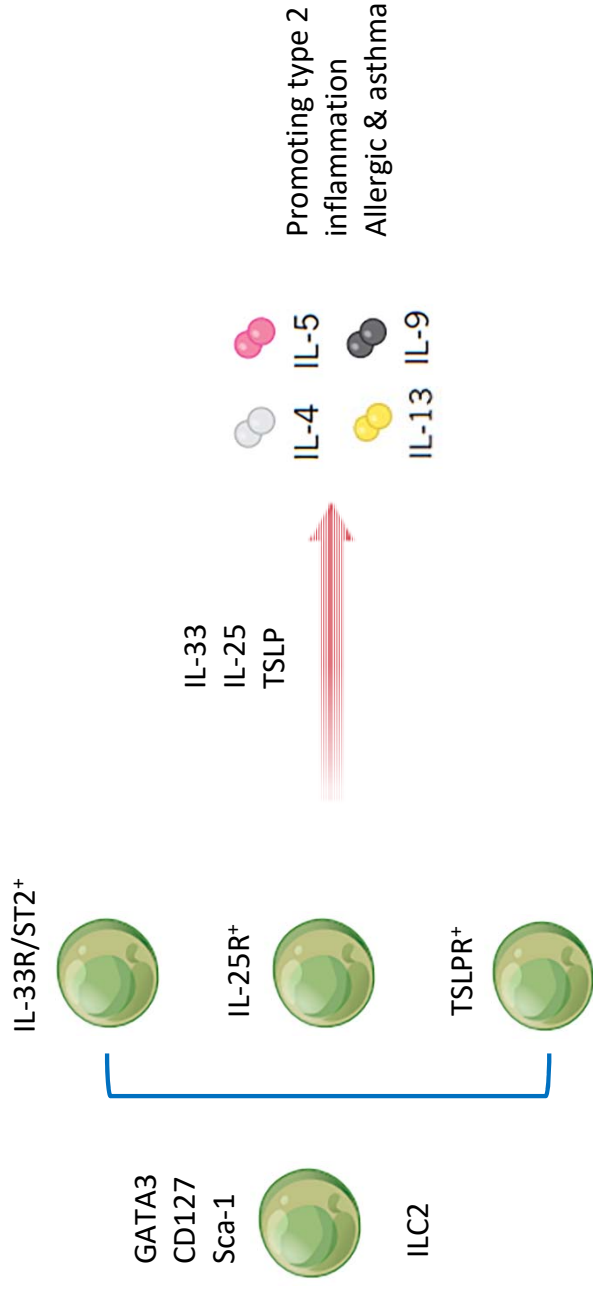


Fig. 1.13. Innate lymphoid cells type 2.

ILC2 are usually defined by expression of GATA3, CD127, Sca-1, and the lack of other lineage markers. Three types of ILC2 have been identified according to the surface receptors they express, IL-33R/ST2⁺, IL-25R⁺, or TSLPR⁺. ILC2 can respond to IL-25, IL-33, and TSLP, and produce T helper 2 (Th2) cell associated cytokines including IL5, IL-9, IL-13 and IL-4. Due to their ability to produce Th2 cytokines, ILC2 have been well studied in the context of allergy, asthma and inflammatory conditions.

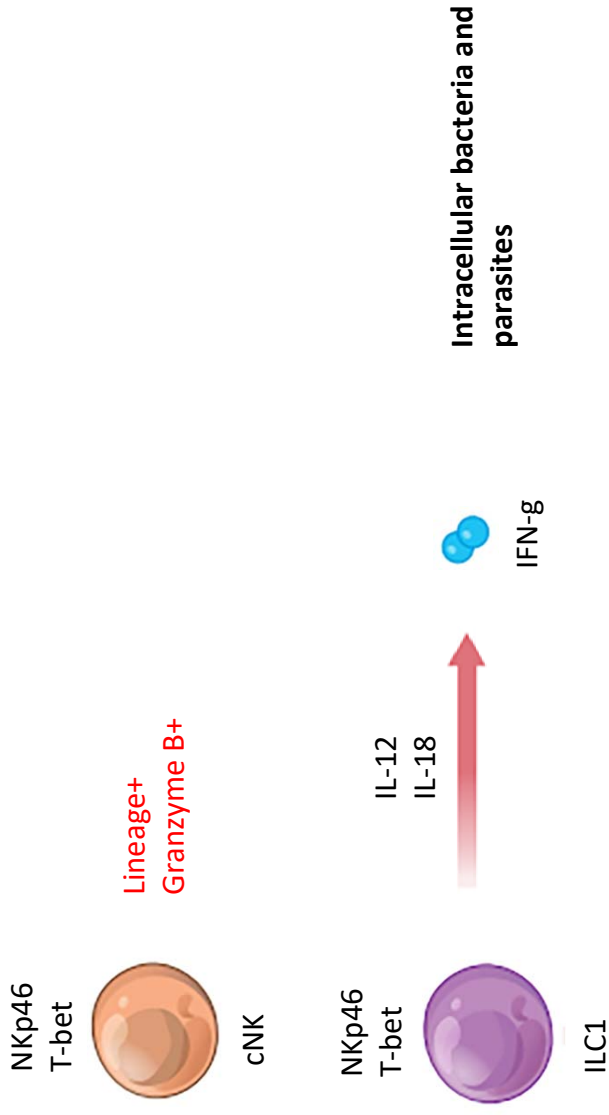


Fig. 1.14. Innate lymphoid cells type 1 and NK cells.

Some studies have considered the conventional NK cells as one subset of ILC1 population. However, NK cells and ILC1 have several distinct features. Firstly, NK cells are lineage⁺ cytotoxicity cells (produce granzymes), while ILC1 are lineage- and are non-cytotoxic IFN- γ producing cells. Secondly, NK cells are present in numerous sites as they recirculate between the blood and tissues, whereas ILC1 are thought to be tissue resident. ILC1 can respond to IL-12 and IL-18 and produce IFN- γ . ILC1 have been shown to be involved in immunity to intracellular bacteria and parasites.

to IL-1 β and IL-23 and produce IL-17A, IL-22 and also IFN- γ , and these cells have been shown to play important roles in antibacterial immunity, chronic inflammation and tissue repair^{164, 167, 168, 169, 170} (**Fig 1.15**). Interestingly, according to the stimuli they encounter ILC3 have shown to be highly plastic^{163, 165, 166}.

1.7.3 ILC development.

ILCs derive from bone marrow lymphoid progenitors (CLP)^{140, 171, 172, 173, 174, 175, 176, 177}. Downstream of the CLP is the common innate lymphoid progenitor (CILP) which gives rise to all the different ILC subtypes and conventional NK cells but not T or B cells^{140, 173, 178, 179}. The transcriptional regulator inhibitor of DNA binding 2 (Id2) is essential for the CILPs to develop into common helper innate lymphoid cell progenitors (CHILP) (**Fig. 1.16**)^{134, 178, 180}, and Id2 is expressed in high amounts in all ILC lineages^{149, 181}. The CHILP consists of both promyeloid leukaemia zinc finger (PLZF)⁺ and PLZF⁻ progenitors^{141, 182}, and they give rise to all ILC subsets including the LTi cells¹⁴⁰ but not conventional NK cells¹⁴⁰. Further development and differentiation of ILC is driven by the activation of different transcription factors including GATA3, retinoic acid receptor-related receptor- α (ROR α), T-bet, and ROR γ ^t^{140, 141, 149, 183, 184, 185, 186, 187} (**Fig. 1.16**).

1.7.4 ILC in inflammation and asthma.

Since the discovery of ILC, these cells have been intensively studied in inflammation and asthma. Specifically, due to the expression of Th2 cytokines, ILC2 have been widely studied in inflammation^{23, 132}. ILC2 have been shown to respond to cytokines IL-25, IL-33, and TSLP and play an important role in type 2 inflammation by producing IL-5, IL-9, IL-13 and IL-4^{188, 189, 190, 191, 192, 193}. In the lesions of atopic dermatitis patients, TSLP has been shown to expand ILC2s^{194, 195}. Interestingly, studies have shown that ILC2 can also cooperate with dendritic cells and CD4⁺ T cells at mucosal

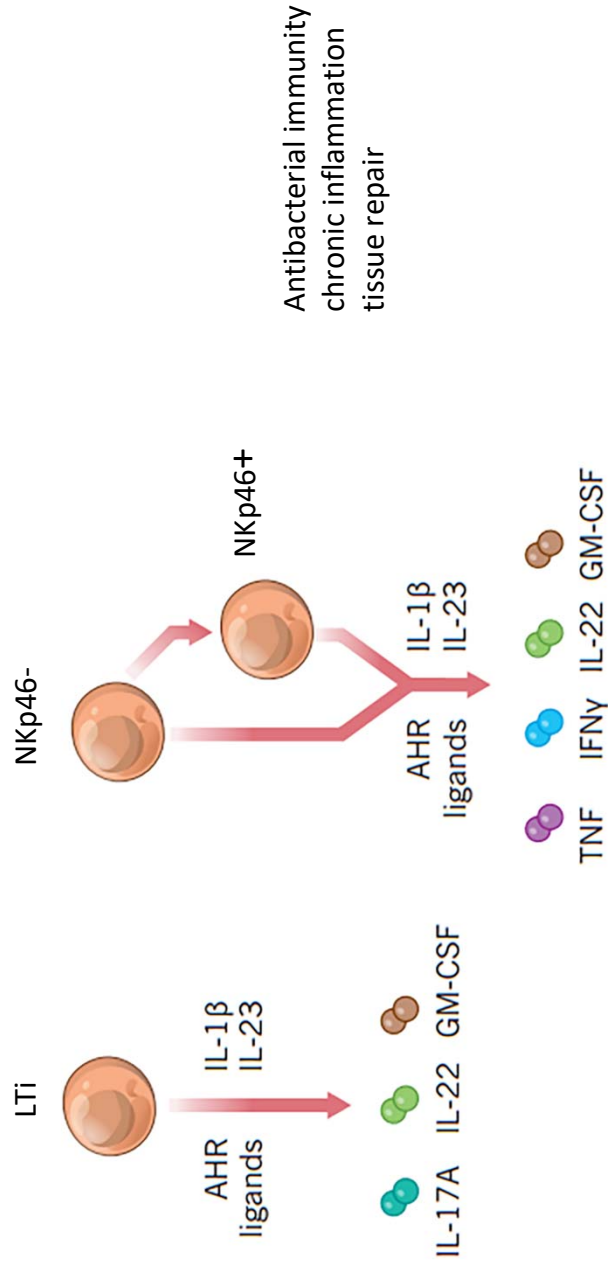


Fig. 1.15. Innate lymphoid cells type 3.

ILC3 were initially described in human tissues as mucosal-associated lymphoid cells that express NKp44 and produce IL22.

Currently, three ILC3 subsets have been identified based on the expression of various cell surface markers and cytokines: lymphoid tissue inducer (LTI) cells, NKp46⁻ ILC3 and NKp46⁺ ILC3. ILC3 can respond to IL-1 β and IL-23 and produce IL-17A, IL-22 and also IFN- γ , and these cells have been shown to play important roles in antibacterial immunity, chronic inflammation and tissue repair. However high plasticity of these cells have been reported according to the stimuli they encounter.

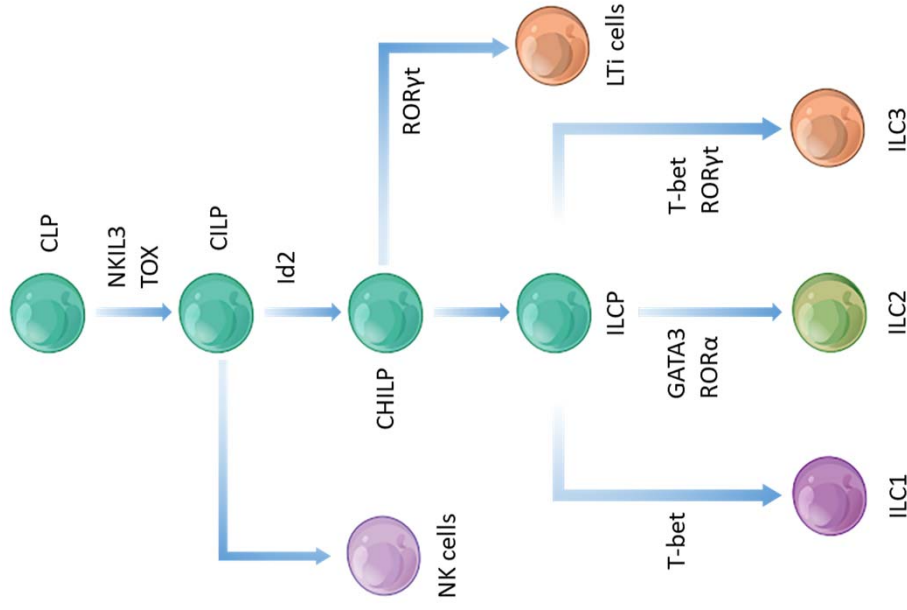


Fig. 1.16 Innate lymphoid cells development.

ILCs derive from a common lymphoid progenitor cell (CLP). After the common innate lymphoid progenitor (CILP), lineage divergence of ILC populations occurs through the common helper-like innate lymphoid progenitor (CHILP) The CHILP can give rise to all different ILC subsets including the LTI cells.

sites to regulate T cell responses in allergic airway inflammation condition^{196, 197}. ILC1 and IFN- γ producing ILC3 have also been reported to have the ability to induce inflammation in mice^{156, 170}. Also, IFN- γ producing ILCs and IL-17A producing ILC3 have been shown play a significant role in inflammatory bowel disease for example; Crohn's disease^{155, 156, 170, 198}. Specifically, IL-22 producing ILC3 have been shown to promote tissue repair and regeneration of inflamed intestine¹⁹⁹.

1.7.5 ILC in parasitic and helminth infections.

ILC have also been shown to play an important role in immune responses against parasite and helminth infections. Specifically, IL-13 produced by ILC2 have been associated with inflammatory responses against extracellular helminth and parasitic infections^{23, 132, 200}. For example, following infection with *Nippostrongylus brasiliensis* parasite in mice ILC2 have shown to be the dominant source of IL-13 apart from T cells¹³⁶. In the context of cerebral malaria infection, exogenous IL-33 was shown to promote expansion of ILC2 that produced type-2 cytokines (IL-4, IL-5 and IL-13) and prevented the development of experimental cerebral malaria in mice with down regulation of inflammatory mediators such as IFN- γ , IL-12 and TNF- α ²⁰¹. Moreover, ILC2 have also been shown to play an important role in controlling filarial infection and related humoral responses^{202, 203}. In the context of parasite and helminth infections, ILC1 are thought to be the main producers of protective IFN- γ and TNF- α at the early stage of infection (eg; *Toxoplasma gondii* infection)²⁰⁴.

1.7.6 ILC in viral infection.

Although ILC have been studied intensively in inflammation and asthma conditions, not much attention has been given to ILC activation/function following viral infection.

Studies of influenza virus^{146, 191} and rhinovirus infection²⁰⁵ have shown that ILC2 play an important role in exacerbating asthma responses and tissue repair following viral infection^{146, 205}. Interestingly, ILC also have been shown to play a role in HIV-1 infection. For example, a recent study has shown that all ILC subsets were depleted during both acute and chronic HIV-1 infection and it was associated with epithelial gut breakdown²⁰⁶. Moreover, depletion of ILC3 in the GALT was also detected during acute SIV infection in macaques²⁰⁷. These findings suggest that ILC most likely play an important role in HIV-1 infection/pathology. Interestingly, how the different ILC derived cytokines profiles are modulated during viral infection/vaccination is poorly understood.

1.7.7 Plasticity of ILCs.

Recent studies into ILC, indicate that there is high plasticity between the different ILC subsets (**Fig. 1.17**), making it difficult to classify the different ILC subsets under different conditions. The first observations of high plasticity of ILC were observed between ILC1/ILC3, and ILC1/ILC3 can differentiate to each other under certain conditions^{163, 208, 209}. Studies have shown that under IL-12 and IL-23 stimulation conditions subset of ROR γ t⁺ ILC3 can down regulate ROR γ t and increase T-bet and IFN- γ expression^{163, 166, 208, 209, 210}. Moreover, Bernink *et al* have shown that CD127⁺ ILC1 can differentiate to ILC3 in the presence of IL-2, IL-23, and IL-1 β ²⁰⁹. Similarly, high plasticity of ILC2 has also been reported and ILC2 can differentiate to both ILC1 and ILC3. For example, ILC2s isolated from human blood, when cultured in the presence of IL-1 β were shown to express IL-12 receptor. Interestingly, when IL-12 was then added into the culture condition, these ILC2 were shown to express IFN- γ , and down regulate IL-5 and IL-13 expression²¹¹. In another study following influenza virus

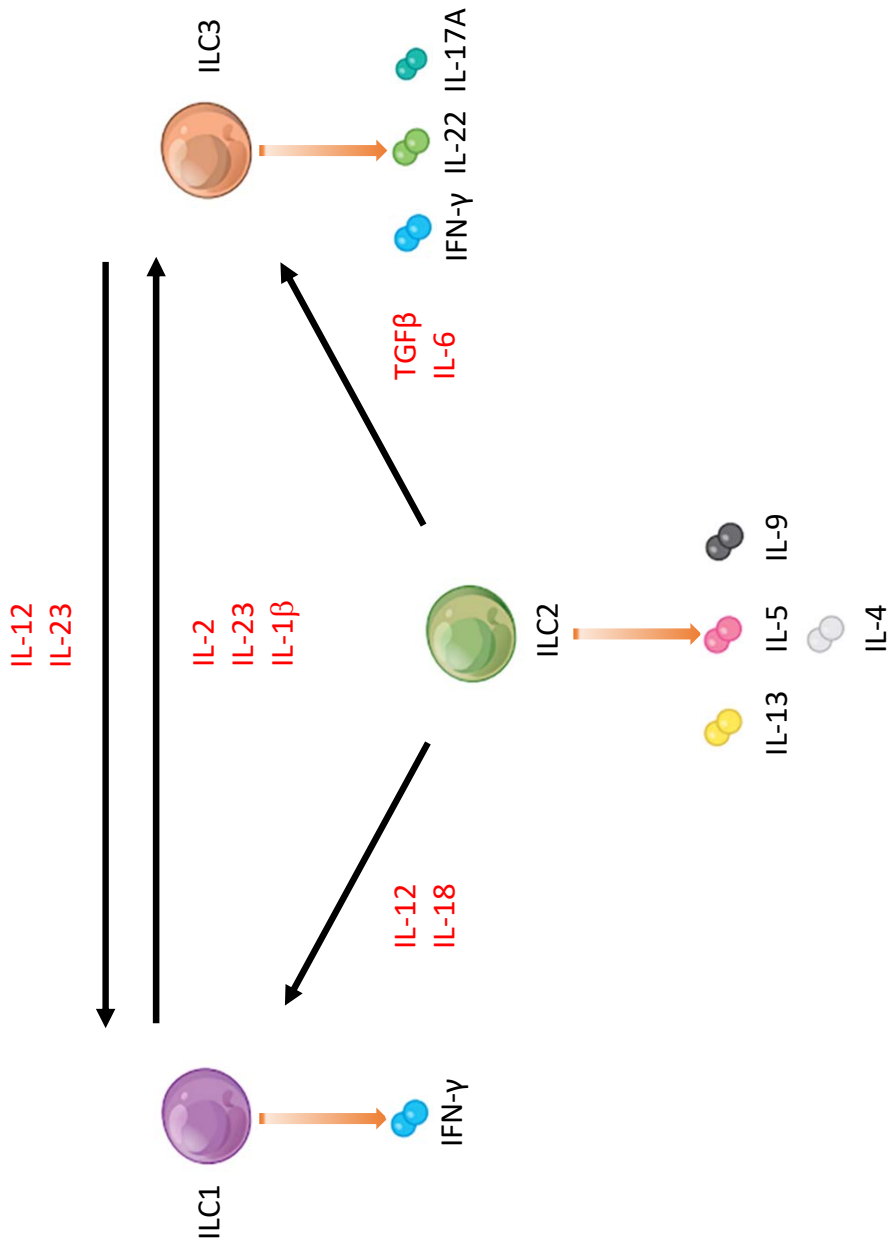


Fig. 1.17. Plasticity of innate lymphoid cells.

There is a high plasticity between different ILC subsets. One subset of ILC can change phenotype and become another subset under certain conditions. It has been shown that ILC2 have the ability to become either ILC1 or ILC3. ILC1 and ILC3 can differentiate to each other under different scenarios. However, ILC1 or ILC3 have not shown to differentiate into ILC2.

infection, upon stimulation with IL-12 and IL-18, ILC2 were shown to down regulate GATA3 expression and convert to ILC1 and express IFN- γ ²¹². Moreover, another study has shown that under IL-6 and transforming growth factor- β (TGF- β) culture condition, ILC2 can become ILC3-like cells and produce IL-17A²¹³ (**Fig. 1.17**).

These recent studies clearly indicate that the current understanding of ILC is limited, and the ILC regulation following inflammation and vaccination/infection could be vastly different. Specifically, ILC plasticity/regulation most likely is dependent on different stimulation conditions, which forms the basis of this thesis.

1.8 Scope of this PhD thesis.

Viral vector-based vaccine studies in our laboratory for the last decade have shown that IL-13 plays a crucial role in modulating the efficacy of a vaccine in a route dependent manner, where mucosal vaccination was shown to induce high avidity CD8 T cells with better protective efficacy by inducing lower IL-13, compare to systemic vaccination. Recent studies in the laboratory have shown that IL-13R α 2 and IL-4R antagonist adjuvanted viral vector-based vaccines that transiently inhibited IL-4/IL-13 activity at the vaccination site, induced excellent high avidity T cells with better protective efficacy, including excellent differentiated Gag-specific antibodies in mice and also in non-human primates. Thus, the main purpose of this study was to dissect the mechanisms of how IL-13 modulated T and B cell activity at the innate immune cell level, specifically at the ILC following pox viral vector-based vaccination.

Hypotheses:

1. ILC2s are the main source of IL-13 at the vaccination site 24h post vaccination, and route of vaccination and different adjuvants can significantly modulate ILC function at the vaccination site.
2. IL-25 plays a more predominant role in modulating ILC2 function following viral vector vaccination compared to IL-33.

3. ILC2-derived IL-13 and ILC1/ILC3-driven IFN- γ regulate the ILC balance at the vaccination site.

Aims:

1. Identify which cells are the predominant source of IL-13 at the vaccination site and how FPV-HIV unadjuvanted vaccine, FPV-HIV-IL-4R antagonist and FPV-HIV-IL-13R α 2 adjuvanted vaccines that transiently inhibit IL-4 and/or IL-13, manipulate the different ILC subsets at the vaccination site. (Hypothesis 1)
2. Evaluate the different ILC subsets recruited to lung and muscle following intranasal (mucosal) versus intramuscular (systemic) viral vector vaccination. (Hypothesis 1)
3. Evaluate how FPV-IL-33BP and FPV-IL-25BP adjuvanted vaccines, that transiently block IL-25 and IL-33 respectively, modulate ILC activity at the vaccination site. (Hypothesis 2)
4. Evaluate ILCs at the vaccination site in IL-13, IL-4 and STAT6 knockout mice following intranasal rFPV vaccination. (Hypothesis 3)
5. Evaluate the expression of IL-4/IL-13 receptors (γ C, IL-4R α , IL-13R α 1, and IL-13R α 2) on ILC subsets and assess how they regulate IL-13 and IFN- γ at the vaccination site. (Hypothesis 3)

Chapter 3 studies: Studies in our laboratory have found that IL-13 plays an important role in modulating anti-viral CD8⁺ T cells avidity, but it is still unclear which cells are the predominant source of IL-13 at the vaccination site. Also, since few studies have been focused on ILC in viral infection conditions, how different ILC subsets are modulated during this process is still poorly understood. Thus, in Chapter 3, these questions were answered by evaluating ILC subsets following i.n./i.m. rFPV, IL-4R

antagonist and IL-13R α 2 adjuvanted vaccination (which block IL-4/IL-13 at the vaccination site) of BALB/c mice and evaluating the different ILC subsets at 0-7 days post vaccination.

Chapter 4 studies: According to the current knowledge, ILC2 can be stimulated by IL-33, IL-25 and TSLP. The surface receptors found on ILC2 can be different according to the tissue/mucosal compartment. For example: ST2/IL-33R⁺ ILC has been associated with lung, whereas TSLPR⁺ ILC2 in skin. However, the development of ILC2 and also ILC1/ILC3 following viral vaccination is poorly understood. Notably, whether there is a hierarchy in the expression of these different cytokines (specifically IL-25 vs IL-33) is not yet characterised. Thus, in this chapter rFPV co-expressing HIV antigen together with IL-25R binding protein (FPV-HIV-IL-25BP), or IL-33 binding protein (FPV-HIV-IL-33BP), which can transiently sequester IL-25 or IL-33 at the vaccination site respectively were constructed. BALB/c mice were vaccinated intranasally with the adjuvanted vaccines or the unadjuvanted control vaccine (FPV-HIV), and the lung ILC profiles were evaluated 24 h post vaccination.

Chapter 5 Studies: In this chapter, ILC function was further evaluated in IL-13^{-/-}, IL-4^{-/-}, and STAT6^{-/-} mice (permanent blockage of these cytokines) following i.n. rFPV vaccination and 24h post vaccination the lung ILC subsets and their cytokine expression were evaluated. In this chapter, transient versus permanent blockage of IL-4, IL-13 and STAT6 signalling and the potential role of IL-13 and IFN- γ in the context of antibody differentiation was assessed.

Chapter 6 studies: IL-4 and IL-13 signalling via a common receptor system, however, the role of IL-13R α 2 is still well characterised. In this chapter the expression receptors

associated with IL-4 and IL-13 (γ C, IL-4R α , IL-13R α 1, and IL-13R α 2) on different ILC subsets were assessed in i) WT BALB/c mice following FPV-HIV unadjuvanted or IL-4R antagonist and IL-13R α 2 adjuvanted vaccines, and ii) IL-13^{-/-}, IL-4^{-/-}, and STAT6^{-/-} mice, following FPV-HIV unadjuvanted vaccination using multicolour flow cytometry to understand how ILC2-derived IL-13 and ILC1/ILC3-derived IFN- γ are regulated, and test whether IL-13R α 2 is involved in this process. This was performed specifically, given that i) level of IL-13 expressed by ILC2 are known to be much lower than T cells and ii) in chapter 3 & 4 studies it was established that ILC2-driven IL-13 modulated ILC1/ILC3 function. Thus, taken together IL-13R α 2 being the high affinity receptor for IL-13 (pM affinity) compared to IL-13R α 1 (nM affinity), it was hypothesised that IL-13R α 2 may be involved in ILC2-driven IL-13 regulation.

Chapter 2.

General Materials and Methods.

2.1 Materials.

Table 2.1 Medium.

Name	Component	Source	Catalogue number
Complete RPMI medium	RPMI-1640 medium (500 ml)	Sigma	R8758
	HI-FCS (35 ml)	GIBCO	10099-133
	1 M HEPES (10 ml)	GIBCO	15630-080
	100 mM sodium pyruvate (10 ml)	GIBCO	11360-070
	Pen-Strep (0.5 ml)	JCSMR	N/A
	β -mercaptoethanol (4 μ l)	Sigma	M6250
RPMI medium	RPMI-1640 medium (500 ml)	Sigma	R8758
	1 M HEPES (10 ml)	GIBCO	15630-080
Minimum Essential Medium Eagle (MEM)	MEM	Sigma	M4655
	5% (v/v) HI-FCS	GIBCO	10099-133

Table 2.2 Buffers and solutions.

Name	Component	Source	Catalogue number
Lung tissue digestion buffer	1 mg/ml Collagenase	Sigma	C2139
	1.2 mg/ml Dispase	GIBCO	17105-041
	5 Units/ml DNase	Calbiochem	26095
	Complete RPMI medium	Sigma	R8758
Quadriceps muscle digestion buffer	0.5 mg/ml Collagenase	Sigma	C2139
	2.4 mg/ml Dispase	GIBCO	17105-041
	5 Units/ml DNase	Calbiochem	26095
	Complete RPMI medium	Sigma	R8758
Red blood cell	0.16 mM NH ₄ Cl	Sigma	A-0171

lysis buffer	0.17 M Tris HCl (pH 7.65)	MERCK	108382
Brefeldin A (BFA)	1:1000 working dilution in complete RPMI medium	eBioscience	00-4506-51
FACS buffer	1X PBS 2% FCS	JCSMR GIBCO	N/A 10099-133
IC-FIX buffer	1X IC-FIX	BioLegend	420801
IC-PERM buffer	10% 10X IC-PERM 90% dH ₂ O	eBioscience JCSMR	00-8333-56 N/A
PFA	2% (w/v) PFA in PBS	Sigma	P-6148
PBS	1X PBS	Sigma	D8537
TrypLE	TrypLE EXPRESS	GIBCO	1813304

Table 2.3 Antibodies.

Antibody	Fluorochrome	Clone	Source	Working dilution	
Lineage cocktail	CD3	FITC	17A2	BioLegend	1:200
	CD19	FITC	6D5	BioLegend	1:100
	CD11b	FITC	M1/70	PharMingen	1:200
	CD11c	FITC	N418	BioLegend	1:100
	CD49b	FITC	HM α 2	BioLegend	1:200
	Fc ϵ RI	FITC	MAR1	BioLegend	1:100
CD45	APC/Cy7	30-F11	BioLegend	1:200	
ST2	PE	DIH9	BioLegend	1:100	
ST2	PerCP/Cy5.5	DIH9	BioLegend	1:100	
Sca-1	APC	D7	BioLegend	1:100	

IL-25R	APC	9B10	BioLegend	1:100
CD127	Brilliant Violet 605	A7R34	BioLegend	1:100
NKp46	Brilliant Violet 421	29A1.4	BioLegend	1:100
TSLPR	APC	FAB5461A	R&D	1:100
GATA3	PerCP/Cy5.5	16E10A23	BioLegend	1:200
IL-13	PE-eFlour 610	EBio13A	eBioscience	1:100
IL-4	Brilliant Violet 421	11B11	BioLegend	1:100
IL-17A	Alexa Flour 700	TC11-18H10.2	BioLegend	1:100
IFN- γ	Brilliant Violet 510	XMG1.2	BioLegend	1:100
IL-22	APC	Poly5164	BioLegend	1:100
Granzyme B	PE	16G6	eBioscience	1:200
IL-4R α	PE	I015F8	BioLegend	1:200
IL-13R α 1	PE	13MOKA	eBioscience	1:200
γ -c chain	PE	554457	PharMingen	1:200
IL-13R α 2	Biotin	BAF539	R&D	1:50
Streptavidin	PE	N/A	BioLegend	1:200
Isotype control	PE	EBio299Arm	eBioscience	1:200
FC block	N/A	2.4G2	PharMingen	1:200

Table 2.4 Mice and vaccine strategies.

Chapter	Mice	Vaccination strategies	
3	BALB/c	i.n.	FPV-HIV
	BALB/c	i.n.	FPV-HIV-IL-4R antagonist
	BALB/c	i.n.	FPV-HIV-IL-13R α 2
	BALB/c	i.m.	FPV-HIV
	BALB/c	i.m.	FPV-HIV-IL-4R antagonist
	BALB/c	i.m.	FPV-HIV-IL-13R α 2
4	BALB/c	i.n.	FPV-HIV
	BALB/c	i.n.	FPV-HIV-IL-25BP
5 (Part I)	BALB/c	i.n.	FPV-HIV
	IL-13 ^{-/-}	i.n.	FPV-HIV
	IL-4 ^{-/-}	i.n.	FPV-HIV
	STAT6 ^{-/-}	i.n.	FPV-HIV
5 (Part II)	BALB/c	i.n.	FPV-HIV
	BALB/c	i.n.	FPV-HIV-IL-4R antagonist
	BALB/c	i.n.	FPV-HIV-IL-13R α 2
	IL-13 ^{-/-}	i.n.	FPV-HIV
	IL-4 ^{-/-}	i.n.	FPV-HIV
	STAT6 ^{-/-}	i.n.	FPV-HIV

i.n. = intranasal, i.m. = intramuscular, IL-13^{-/-} = IL-13 knockout mice, IL-4^{-/-} = IL-4 knockout mice, STAT6^{-/-} = STAT6 knockout mice, FPV = Fowlpox virus

2.2 Methods.

2.2.1 Mice.

5-6 weeks old specific-pathogen free female WT BALB/c, IL-13^{-/-}, IL-4^{-/-} and STAT6^{-/-} mice were obtained from the Australian Phenomics Facility, the Australian National University. Gene knockout mice (GKO) were from BALB/c background. All animals were maintained, and experiments were performed in accordance with the Australian NHMRC guidelines within the Australian Code of Practice for the Care and Use of Animals for Scientific Purposes and in accordance with guidelines approved by the Australian National University Animal Experimentation and Ethics Committee (AEEC). Work in this thesis was conducted under the AEEC approved protocol numbers A2011/018, A2014/14, and A2017/15.

2.2.2 Primary chicken embryo skin culture.

All recombinant viruses used in this thesis were grown in primary chicken embryo skin cells (CES) which were stored in liquid nitrogen. Frozen CES were thawed rapidly and transferred to a 50 ml Falcon tube containing 30 ml MEM (as per described in **Table 2.1**) at room temperature. Cells were centrifuged for 5 min at 1200 RPM (335×g) using a Beckman ALLEGRA X-12R centrifuge. The supernatant was discarded, 8 ml MEM was added, cells were transferred to T25 flask (Thermo Nunc EasYFlask) and cultured for 5 days at 37°C with 5% CO₂ in a Forma Scientific water-jacketed incubator. Next CES cells were split into four T175 flasks. Specifically, medium was firstly removed, cells were washed once with 1×PBS. Then 1.5 ml TrypLE (as per described in **Table 2.2**) was added and incubated for 5 min. Next 4.5 ml fresh MEM was added mixed thoroughly, and 1.5 ml cells were transferred to each T175 flask, followed by 30 ml fresh MEM. Cells were cultured for 5 days at 37°C with 5% CO₂ in a Forma Scientific

water-jacketed incubator. CES cells were split every 5 days and maintained for no more than 8-9 splits.

2.2.3 Recombinant virus stock preparation.

To grow the recombinant fowl pox vector-based vaccine virus stocks used in this study (**Table 2.4**), CES cells were firstly cultured for 5 days as per described in **2.2.2**, infected with rFPV at a rate of 0.5 multiplicity of infection for 1.5 h, and 20 ml fresh MEM was added and cultured for 4-5 days at 37°C with 5% CO₂. To harvest virus, the infected cells were scraped from flasks and centrifuged for 10 min at 2300 rpm (1200×g) at 4°C using a Beckman ALLEGRA X-12R centrifuge. Then the cells were resuspended in 1 ml sterile PBS and sonicated 3 times 15s on ice at 50 outputs using a Branson Sonifier 450 until cell clumps were no longer visible. Then the virus stock was aliquoted and stored at -80°C.

2.2.4 Recombinant virus titration.

CES cells were subculture at 1×10⁶ cells per well in a 6-well tissue culture plates (Costar Corning CellBIND Surface), incubated overnight at 37°C with 5% CO₂. The rFPV stock was serially diluted (10 fold, from 10⁻¹ to 10⁻⁶). 100 µl of each dilution was added to CES cells in 6-well plates respectively. Plates were incubated for 1.5 h at 37°C with 5% CO₂ and gently shaken to make sure virus was evenly distributed in each well. Then 2 ml of fresh MEM was added to each well and cells were cultured for a further 4-5 days. Next, media was removed, and cells were stained with 0.5 ml crystal violet (0.1% (w/v) in 20% ethanol) for 5 min to visualize plaques. Plaques were then counted, and the following equation was used to calculate the plaque forming unit (PFU)/ml:

$$PFU/ml = \frac{\text{Average \# plaques}}{\text{dilution factor} \times \text{volume of diluted virus added}}$$

2.2.5 Immunization.

For both intranasal and intramuscular vaccination, 1×10^7 PFU of each vaccine was given to mice under mild isoflurane anaesthesia. The i.n. vaccines were given in 10-15 μ l per nostril (total 25-30 μ l volume) and i.m. vaccines 50 μ l per quadriceps muscle. All vaccines were diluted in sterile PBS and sonicated 3 times 15s on ice at 50 outputs using a Branson Sonifier 450 prior to use.

2.2.6 Preparation of lung lymphocytes.

The mice were euthanised using cervical dislocation according to the approved AEEC guidelines. Lung tissues were removed and kept in complete RPMI medium on ice until processing. Single cell suspensions of lung tissues were prepared as described previously^{8, 122, 123}. Specifically, the lung tissues were first cut into small pieces, and then enzymatically digested in 1 ml of lung digestion buffer containing 1 mg/ml collagenase (Sigma-Aldrich, St Louis, MO), 1.2 mg/ml Dispase (Gibco, Auckland, NZ), 5 Units/ml DNase (Calbiochem, La Jolla, CA) in complete RPMI as indicated in **Table 2.2**. During digestion, samples were vortexed every 10 min and incubated in a 37°C water bath for 45 min. The digested lung tissues were mashed and passed through a 100 μ m Falcon cell strainer. The strainer was then washed with complete RPMI medium and the resulting lung cell suspensions were centrifuged for 15 min at 1500 RPM (524 \times g) at 4°C using a Beckman ALLEGRA X-12R centrifuge. Next, the supernatants were removed, and cells were resuspended in 5 ml red blood cell lysis buffer containing 0.16 mM NH₄Cl and 0.17 M Tris HCl (pH 7.65) at room temperature for 3 min, then 30 ml with RPMI medium was added to each sample and centrifuged at 1500 RPM (524 \times g) for 5 min at 4°C. It is noteworthy that to ensure maximum RBC lysis efficiency, the RBC lysis buffer was aliquoted and equilibrated to room temperature before use. The resulting supernatant was removed, washed once more and cells were resuspended in

RPMI medium and passed through sterile gauze to remove any remaining debris. Then the cells were washed twice using RPMI medium, and cell pellets were resuspended in 0.5 ml complete RPMI medium. Lung cells from each sample were counted using a hemocytometer (Tiefe Depth Profondeur 0.100 mm). Next 2×10^6 cells per sample were plated in U-bottomed 96-well plates (Falcon) and were rested overnight (16 h) at 37°C with 5% CO₂ in a Forma Scientific water-jacketed incubator to allow the recovery of cell surface markers before performing the surface and intracellular staining¹²².

2.2.7 Preparation of muscle lymphocytes.

The mice were euthanised using cervical dislocation according to the approved AEEC guidelines. Quadriceps muscle was removed from both rear legs and kept in complete RPMI medium on ice until processing. To prepare quadriceps muscle single cell suspensions, muscle tissues were cut into small pieces and digested in buffer containing 0.5 mg/ml Collagenase (Sigma-Aldrich, St Louis, MO), 2.4 mg/ml Dispase (Gibco, Auckland, NZ), and 5 Units/ml DNase (Calbiochem, La Jolla, CA) in complete RPMI as indicated in **Table 2.2**. 0.5 – 1 ml of digestion buffer was used to digest each muscle. During digestion, samples were gently vortexed every 10 min and incubated in a 37°C water bath for 45 min. The digested muscle tissues were gently passed through a 100 µm Falcon cell strainer without mashing too much to avoid creating smaller debris. The strainer was then washed with RPMI medium and the resulting muscle cell suspensions were centrifuged for 15 min at 1500 RPM (524×g) at 4°C using a Beckman ALLEGRA X-12R centrifuge. The muscle cells were resuspended in RPMI medium and passed through sterile gauze similar to lung to further remove debris and then was washed twice with RPMI medium (Note that muscle tissues were not treated with RBC lysis buffer). Cell pellets were resuspended in 0.5 ml complete RPMI medium. Muscle cells for each sample were counted using a hemocytometer (Tiefe Depth Profondeur 0.100

mm). 3.5×10^5 cells per sample were plated into U-bottomed 96-well plates (Falcon) and were rested overnight (16 h) at 37°C with 5% CO₂ in a Forma Scientific water-jacketed Incubator as per the lung samples.

2.2.8 Surface and intracellular staining of ILC.

Prior to staining, 1 × Brefeldin A (BFA) was added to each sample and incubated at 37°C with 5% CO₂ for 5 h to prevent cytokine release. Surface and intracellular staining were performed according to protocols established in our laboratory¹²². Specifically, cells were first centrifuged at 1300 RPM (524×g) for 2 min at 4°C using a Sigma 3K1S centrifuge and the supernatant was discarded, cells were washed twice with FACS buffer (**Table 2.2**). Next, Fc block antibodies were added, and cells were incubated on ice in the dark for 20 min. The cells were washed with FACS buffer and supernatant was discarded. Next, surface staining antibodies (dilution in **Table 2.3**) were added to each sample in a total volume of 40 µl and cells were incubated on ice in the dark for 40 min. After surface staining, all cells were washed three times with FACS buffer and then resuspended in 100 µl IC-FIX buffer and incubated on ice in the dark for 10 min. After fixation, cells were washed with FACS buffer and permeabilised using IC-PERM buffer at room temperature in the dark for 10 min. Then the cells were centrifuged under the same condition and supernatant was discarded. The intracellular antibodies (dilution in **Table 2.3**) were diluted in IC-PERM buffer and were added to each sample in a total volume of 25 µl, cells were incubated on ice in the dark for 40 min and then washed twice with FACS buffer. The resulting cell pellets were resuspended in 100 µl 0.5% PFA and then transferred to cluster tubes and run on a BD LSR Fortessa on the same day of staining. From each lung sample 1400000 events were acquired, and 200000 events were acquired for each quadriceps muscle sample. Data were analysed using Tree Star FlowJo software version 10.0.7 for Windows.

2.2.9 General ILC gating strategy.

2.2.9.1 Fluorescence minus one (FMO) and single colour controls.

In this thesis to assess the different ILC populations and cytokine expression (**Fig. 2.1 and 2.2**) single colour controls and fluorescent minus one (FMO) controls were used to setup the gates. The red boxes indicate the positive populations.

2.2.9.2 Lung ILC gating strategy.

Lung samples from each experiment were stained as described in **2.2.6**. The ILC were gated as indicated in **Fig. 2.3**. Firstly, CD45⁺ cells were gated from total lung cells, and then from CD45⁺ cells lymphocytes were gated as FSC^{low} SSC^{low} cells. Next within the lymphocyte gate, lineage⁺ cells were gated out using the FITC-conjugated lineage cocktail (as indicated in **Table 2.3** and **Table 2.5**). In the lineage⁻ population, ILC2 were identified as lineage⁻ ST2/IL-33R⁺ cells. In this study Sca-1 and CD127 (IL-7R) expression profiles were also evaluated on lineage⁻ cells.

2.2.9.3 Quadriceps muscle ILC gating strategy.

After muscle tissues were digested and stained as per described in **2.2.7** and **2.2.8**, CD45⁺ cells and lymphocytes were gated from total muscle cells. Next, within the lymphocyte gate, ILC2 were identified as Lineage⁻ IL-25R⁺ cells (as no ST2/IL-33R⁺ or TSLPR⁺ cells were detected in muscle). Then the lineage⁻ ST2/IL-33R⁻ cells (ILC1& ILC3) were stained with NKp46 (**Fig. 2.4**).

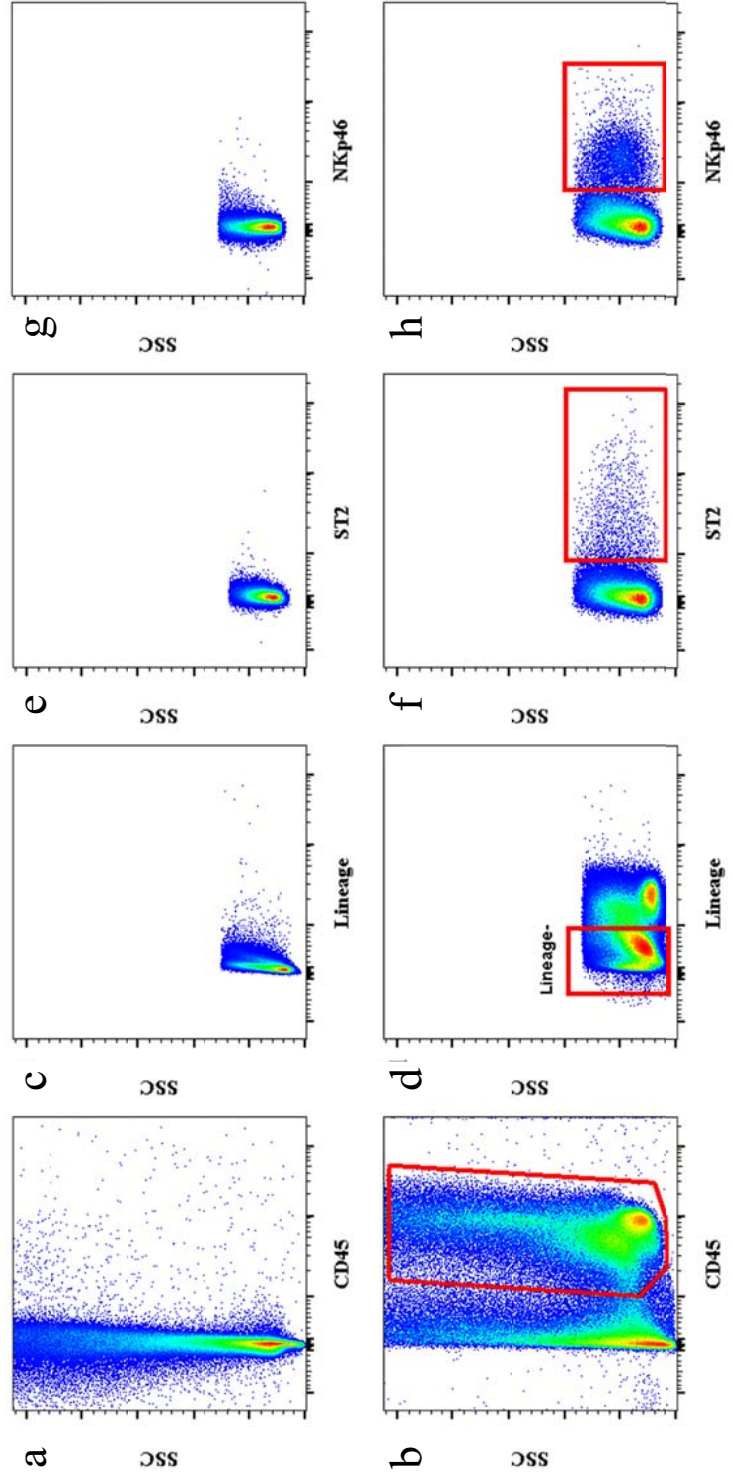


Fig. 2.1. Surface staining fluorochrome minus one (FMOs) and single colour controls.

General ILC population gates were based on single colour controls and FMOs. CD45 FMO **(a)**, CD45 single colour control **(b)**; lineage FMO **(c)**, lineage single colour control **(d)**; ST2/IL-33R FMO **(e)**, ST2/IL-33R single colour control **(f)**; NKp46 FMO **(g)**, NKp46 single colour control **(h)**.

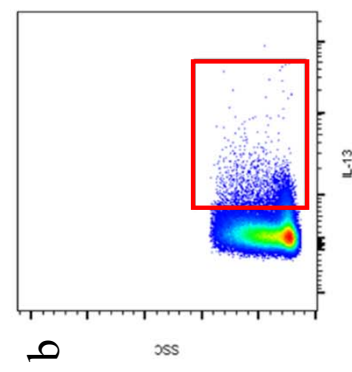
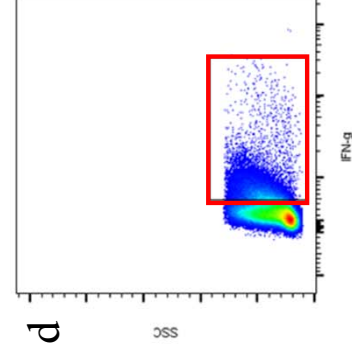
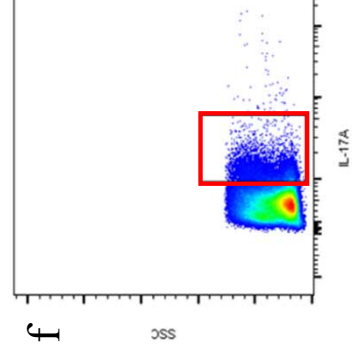
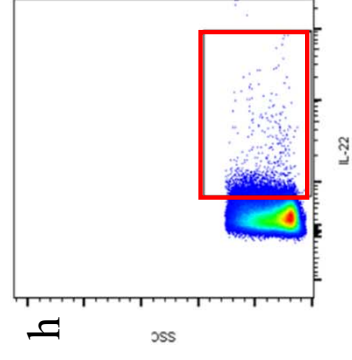
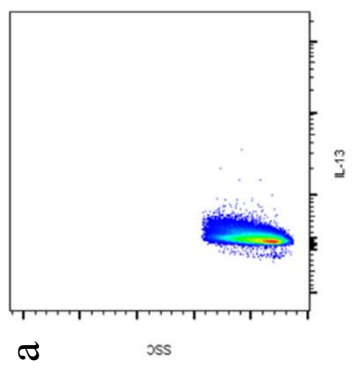
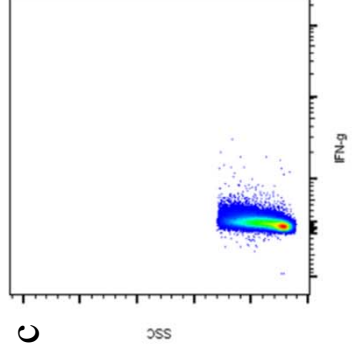
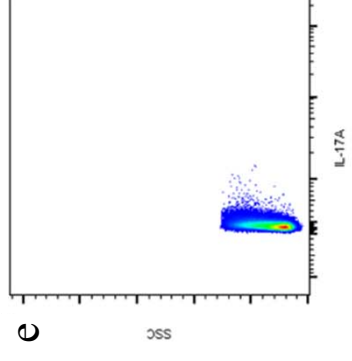
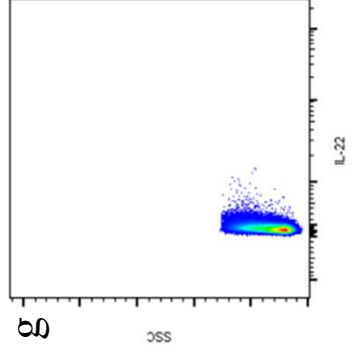


Fig. 2.2. Intracellular staining fluorochrome minus one (FMOs) and single colour controls.

Cytokine gates were based on single colour controls and FMOs. IL-13 FMO **(a)**, IL-13 single colour control **(b)**; IFN- γ FMO **(c)**, IFN- γ single colour control **(d)**; IL-17A FMO **(e)**, IL-17A single colour control **(f)**; IL-22 FMO **(g)**, IL-22 single colour control **(h)**.

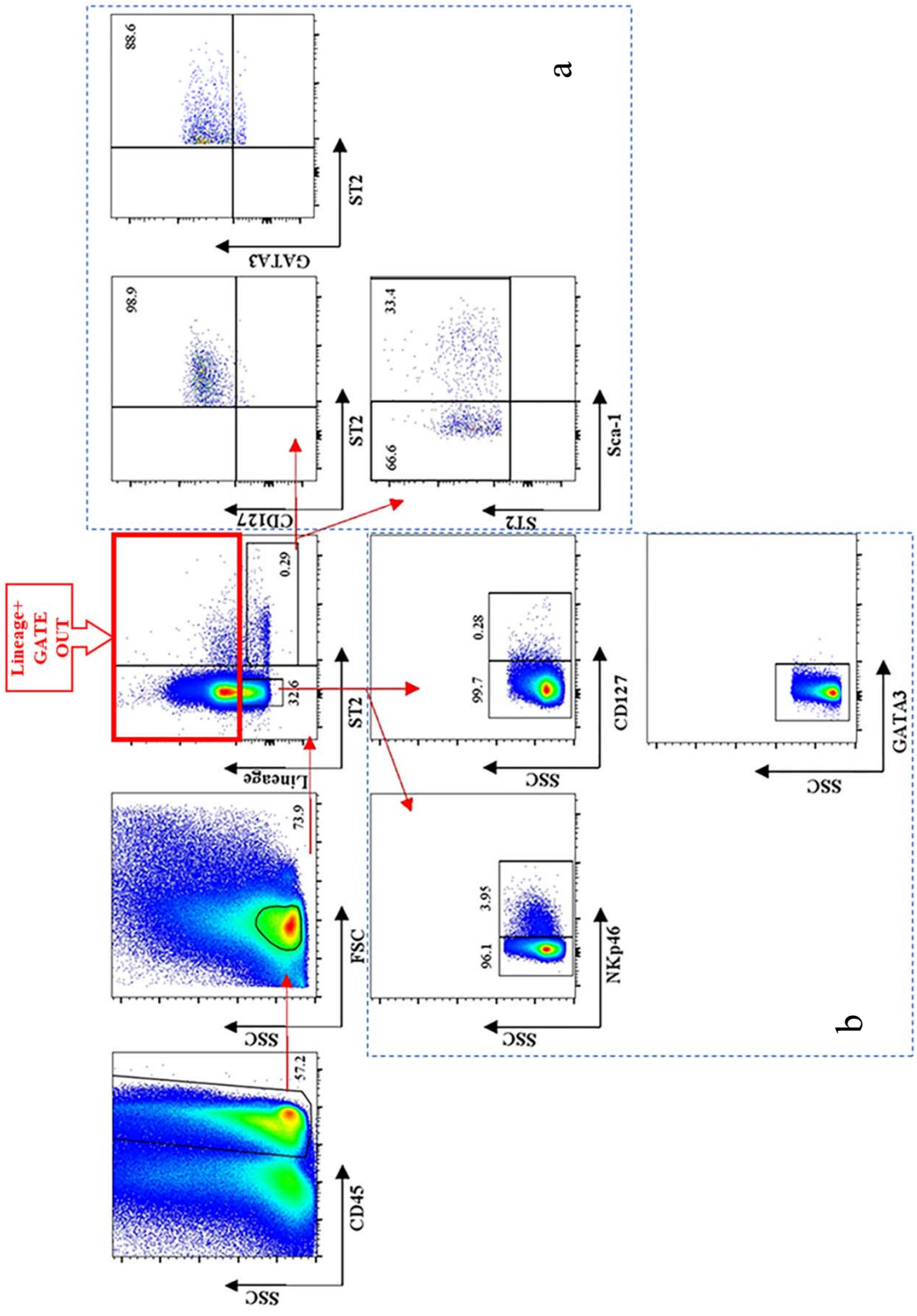


Fig. 2.3. Lung ILC general gating strategy.

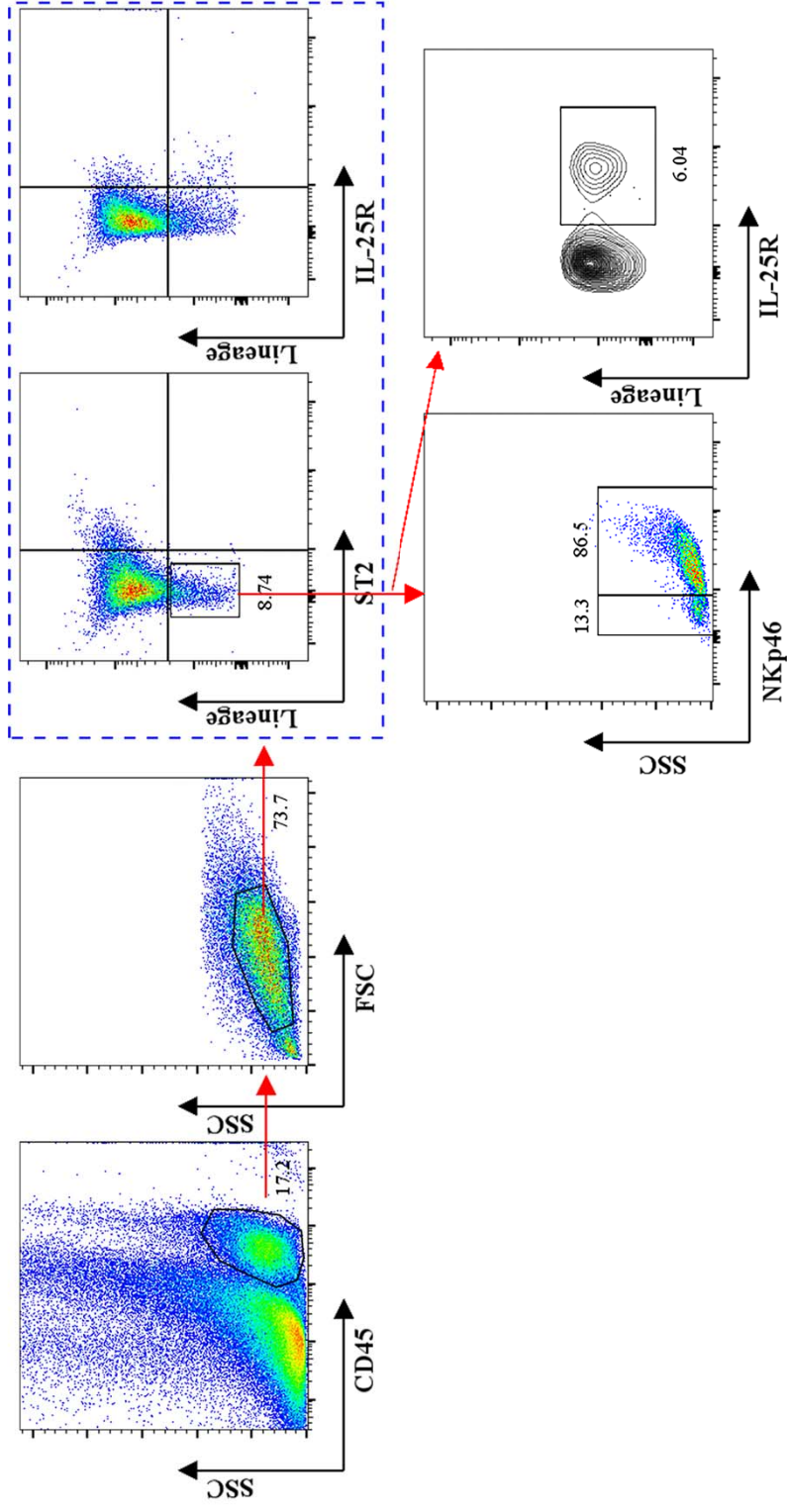
Lung ILCs from BALB/c mice were evaluated 24h post FPV-HIV immunization as per described in Materials and Methods. Firstly, from total lung cells, CD45⁺ cells and lymphocytes were gated. Next within the lymphocyte gate, lineage⁺ cells were gated out as indicated in red box. ILC2 were identified as lineage⁻ ST2/IL-33R⁺ cells and their IL-13 and IL-4 expression were further evaluated. ILC1/3 cells were gated as lineage⁻ ST2/IL-33R⁻ cells and divided into NKp46^{+/+} cells. Sca-1, CD127 (IL-7R) and GATA3 expression profiles were also evaluated on lineage⁻ cells.

Table 2.5. Lineage cocktail. All lineage cocktail antibodies were FITC conjugated and lineage⁺ cells were gated out based on single color controls and FMO controls.

Antibodies	To gate out	
FITC conjugated	CD3	T cells
	CD19	B cells
	CD11b	Macrophages
	CD11c	Dendritic cells
	CD49b	Nature killer cells, platelets, fibroblasts
	FcεRI	Mast cells, basophils

Fig. 2.4. Quadriceps muscle ILC general gating strategy.

Muscle ILCs from BALB/c mice were evaluated 24h post FPV-HIV immunization. From total muscle cells, CD45⁺ cells and lymphocytes were gated as per lung, and assessed for lineage⁻ ST2/IL-33R⁺ and lineage⁻ IL-25R⁺ cells. ILC2 were identified as lineage⁻ ST2/IL-25R⁺ cells and ILC1/3 were identified as lineage⁻ ST2/IL-33R⁻ NKp46^{+/-} cells.



2.2.10 Calculation of cell numbers.

The ILC subsets were characterized using the gating strategies described in section 2.2.8. In this study, the cell numbers were back calculated to CD45⁺ gate as there was no significant differences in the total CD45⁺ cells among different mice groups or vaccines groups tested. This was performed by back-calculating cell numbers of each ILC subsets to CD45⁺ population and then normalizing to 1×10⁶ cells. The following equation was used to calculate the cell numbers:

$$Cell\ number = \frac{X}{CD45^+ cell\ number} \times 1 \times 10^6$$

X = the absolute cell numbers in the specific gate.

2.2.11 Statistical analysis.

Data in this thesis, n = 3 to 6 mice per group were used and all experiments were repeated at least three times, and 24h experiments were repeated six times. Data are represented as the mean and standard deviation (s.d.). Statistical analysis was performed using GraphPad Prism software (version 6.05 for Windows). One-way ANOVA using Tukey's multiple comparisons test and unpaired T-test were used. The P-values are denoted as: ns - p≥0.05, * - p<0.05, ** - p<0.01. *** - p<0.001, **** - p<0.0001.

Chapter 3.

Vaccination route can significantly alter the innate lymphoid cell subsets: A feedback between IL-13 and IFN- γ .

3.1 Abstract.

This study demonstrates that the efficacy of a vaccine is influenced by the cytokines produced by the innate lymphoid cells (ILC) recruited to the vaccination site and is vaccine route and adjuvant dependent. Intranasal virus vaccination induced ST2/IL-33R⁺ ILC2 in lung, while intramuscular vaccination induced exclusively IL-25R⁺ ILC2 in muscle. Interestingly, a larger proportion of IL-13⁺ ILC2s were detected in muscle following i.m. viral vector vaccination compared to lung post i.n. delivery. These observations revealed that, ILC2 were the main source of IL-13 at the vaccination site (24h post vaccination) responsible for inducing T cells of varying avidities. Moreover, recombinant fowlpox viral vector-based vaccines expressing adjuvants that transiently block IL-13 signalling at the vaccination site using different mechanisms (IL-4R antagonist or IL-13R α 2 adjuvants), revealed that the level of IL-13 present in the milieu also significantly influenced IFN- γ , IL-22 or IL-17A expression by ILC1/ILC3. Specifically, an early IL-13 and IFN- γ co-dependency at the ILC level may also be associated with shaping the downstream antibody responses, supporting the notion that differentially regulating IL-13 signalling via STAT6 or IL-13R α 2 pathways can modify ILC function and the resulting adaptive T and B cell immune outcomes reported previously. Moreover, unlike chronic inflammatory or experimentally induced conditions, viral vector vaccination induced uniquely different ILC profiles (i.e. expression of CD127 only on ILC2 not ILC1/ILC3; expression of IFN- γ in both NKP46⁺ and NKP46⁻ ILCs). Collectively, data highlight that, tailoring a vaccine vector/adjuvant to modulate the ILC cytokine profile according to the target pathogen, may help design more efficacious vaccines in the future.

3.2 Introduction.

Innate lymphoid cells (ILCs) are a recently identified class of immune cells which do not express antigen receptors nor surface markers characteristic of other immune cells, i.e. lineage negative²¹⁴. ILCs are known to play a multi-factorial role at the mucosae¹⁶, for example, in tissue remodelling²³, allergy and inflammation^{146, 215}, Crohn's disease²¹⁴, and immunity towards helminth and intracellular parasitic infections^{146, 215, 216}. ILCs are thought to develop from a common lymphoid progenitor^{214, 217}, and according to the transcription factors and cytokines they express, ILC have been broadly classified into three main categories. ILC1 respond to IL-12, IL-18 and IL-15 and express transcription factor T-bet, interferon (IFN)- γ and tumour necrosis factor (TNF)- α . ILC2 subsets are characterised by surface receptors IL-33R⁺ (ST2⁺), IL-25R⁺ (IL-17RB⁺) or TSLPR⁺ and can be stimulated by IL-33, IL-25 (IL-17E) or thymic stromal lymphopoietin (TSLP), respectively. Activated ILC2 express GATA3, IL-13, IL-5, IL-9 or IL-4. In contrast, ILC3 respond to IL-1 β and IL-23 and express ROR γ t, IL-22 and IL-17A^{90, 214, 217}. However, recent studies indicate strong plasticity between ILC2, ILC1 and ILC3 subsets according to the tissue environment and the external stimuli they encounter^{209, 218, 219}.

Studies have shown that influenza virus^{146, 191} and rhinovirus infection stimulate ILC2 IL-13 expression and exacerbate asthma responses²⁰⁵, and HIV infection causes an irreversible loss of ILC function during acute infection²²⁰. However, how different ILC subsets are modulated during viral infection or vaccination and influence vaccine-specific immunity is poorly understood. A range of recombinant viruses, including Avipoxviruses (canarypox and fowlpox viruses) used in the HIV RV144 Thai trial²²¹, Modified Vaccinia Ankara (MVA) and Adenovirus-5 are being developed as vectors to deliver vaccines for human diseases, However, the mechanisms by which these different

vaccine vectors modulate innate immunity is not fully understood. MVA is known to stimulate TLR2, TLR6 and NALP3 inflammasome pathways, with vigorous IFN- β and IL-1 β expression by macrophages²²². While ILC2 IL-13 expression licences CD11b⁺ CD103⁻ conventional dendritic cells to stimulate CD4⁺ T helper 2 (Th2) responses²²³. However, the influence of ILC interacting with professional antigen presenting cells in stimulating of antiviral Th1 immunity is not known. Thus, understanding how these vaccine vectors interact with the innate immune response and influence resulting adaptive immunity is paramount for developing efficacious vaccine technologies in the future.

Our previous studies, have revealed that i) recombinant poxvirus HIV-1 antigen vaccines delivered via the mucosa induce high avidity, poly-functional HIV-specific CD8⁺ T cells with reduced IL-4 and IL-13 expression⁷⁷, ii) IL-13R α 2 and IL-4R antagonist adjuvanted vaccines transiently blocking IL-13 and/or IL-4 signalling at the vaccination site induce higher avidity/multi-functional HIV specific effector/memory CD8⁺ T cells with improved CD8⁺ T cell mediated protective efficacy^{113, 122} and iii) IL-4R antagonist adjuvant vaccine also induces HIV gag-specific IgG1 and IgG2a antibodies¹¹³. (The IL-13R α 2 adjuvanted vaccine co-expresses HIV antigens together with soluble IL-13R α 2 and can block IL-13 activity at the vaccination site. Whereas the IL-4R antagonist adjuvanted vaccine co-expresses HIV antigens and C-terminal deletion mutant of the mouse IL-4 without the essential tyrosine required for signalling, which can bind to both type I and type II IL-4 receptor complexes with high affinity, and transiently block both IL-4 and IL-13 signalling at the vaccination site)¹²³. Interestingly, the responses observed with the adjuvanted vaccines in mice were similar to what has been reported for elite controllers who naturally control HIV infection and do not progress to clinical AIDS^{126, 224, 225}. While we have gained some understanding of

how IL-4/IL-13 regulates CD8⁺ T cell avidity at the adaptive immune level^{78, 79, 226}, it is still unclear which cells in the innate immune compartment are involved in IL-4, IL-13 and IFN- γ expression and/or regulation at the vaccination site, responsible for the downstream T and B cell outcomes.

3.3 Materials and Methods.

3.3.1 Mice and immunisation.

5-6 weeks old pathogen free female WT BALB/c mice were obtained from the Australian Phenomics Facility, the Australian National University, and were maintained and handled under protocols indicated in **2.2.1**. 1×10^7 PFU unadjuvanted FPV-HIV, FPV-HIV-IL-4R antagonist adjuvanted, and FPV-HIV-IL-13R α 2 adjuvanted vaccines were administered to WT BALB/c mice (n = 3 to 6 per group) intranasally or intramuscularly, under mild isoflurane anaesthesia as per described in **2.2.5**. Lungs were harvested in 2 ml of complete RPMI at 24 h, 3 days, and 7 days post immunisation, and single cell suspension was prepared as per described in **2.2.6**. Quadriceps muscles were harvested in 2 ml of complete RPMI at 24 h post immunisation, and single cell suspension was prepared as per described in **2.2.7**.

3.3.2 Surface and intracellular staining.

Surface and intracellular staining were performed as per described in **2.2.8** using antibodies listed in **Table 2.3**. Specifically,

ILC2 staining: APC/Cy7-conjugated anti-mouse CD45, and FITC-conjugated lineage cocktail were used to identify lineage⁻ cells. PE-conjugated anti-mouse ST2/IL-33R, APC-conjugated anti-mouse IL-25R, APC-conjugated anti-mouse TSLPR were used to identify the different ILC2 subsets. APC-conjugated anti-mouse Sca-1, Brilliant Violet

605-conjugated anti-mouse CD127, and PerCP/Cy5.5-conjugated anti-mouse GATA3 (stained intracellularly) were used to further confirm that the CD45⁺ lineage⁻ ST2/IL-33R⁺ cells were true ILC2s. Brilliant Violet 421-conjugated anti-mouse IL-4 and PE-eFlour 610-conjugated anti-mouse IL-13 were used to evaluate intracellular expression of these cytokines in ILC2s.

ILC1/3 staining: APC/Cy7-conjugated anti-mouse CD45, and FITC-conjugated lineage cocktail were used to identify lineage⁻ cells. PE-conjugated anti-mouse ST2/IL-33R, Brilliant Violet 421-conjugated anti-mouse CD335 (NKp46), and Brilliant Violet 605-conjugated anti-mouse CD127 were used to identify ILC1/3 populations. Brilliant Violet 510-conjugated anti-mouse IFN- γ , APC-conjugated anti-mouse L-22, and Alexa Fluor 700-conjugated anti-mouse IL-17A were used to evaluate intracellular expression of these cytokines in ILC1 and ILC3. PerCP/Cy5.5-conjugated anti-mouse GATA3 was also used to make sure ILC1/3 subsets did not contain any ILC2.

Granzyme B staining: In this thesis, ILC1 and ILC3 were divided into lineage⁻ ST2/IL-33R⁻ NKp46⁺ or lineage⁻ ST2/IL-33R⁻ NKp46⁻ cells, since NKp46 is also a common marker of conventional NK cells. Thus, to confirm that lineage⁻ ST2/IL-33R⁻ NKp46⁺ population did not contain any conventional NK cell contamination, a Granzyme B staining was performed (Note that Granzyme B is expressed in conventional NK cells, but are not expressed in ILC). In NK cell staining, APC/Cy7-conjugated anti-mouse CD45, and FITC-conjugated lineage cocktail were used to identify lineage^{+/-} cells. Brilliant Violet 421-conjugated anti-mouse CD335 (NKp46) and PE-conjugated anti-mouse Granzyme B were used to identify conventional NK cells.

All ILC subsets were gated as per described in **2.2.9**. Granzyme B expression in conventional NK cells and lineage⁻ NKp46^{+/+} cells was assessed using gating strategies described in the results section.

3.4 Results.

3.4.1 Intranasal vaccination induces lineage⁻ ST2/IL-33R⁺ ILC2s expressing IL-13 at the lung mucosae and IL-4R antagonist/IL-13R α 2 adjuvanted vaccines inhibit this activity.

Previous studies in our laboratory have shown that 24 h post intranasal IL-4R antagonist and IL-13R α 2 adjuvanted vaccination can alter IL-4/IL-13 signalling at the vaccination site¹²² and this directly influences the activity of antigen presenting cells (APC) at the lung mucosae resulting in high avidity CD8⁺ T cell mediated immunity¹²³. In this study, we have embarked upon understanding how the expression of IL-4 and/or IL-13 by ILC at the lung mucosae can modulate adaptive immune outcomes following intranasal vaccination using i) FPV-HIV unadjuvanted, ii) FPV-HIV-IL-4R antagonist and iii) FPV-HIV-IL-13R α 2 adjuvanted vaccines. Firstly, 12h to 7 days post i.n. vaccination the lung ILC2 were evaluated as described in **2.2.6.1 (Fig. 3.1a)**. ILC2 were gated as CD45⁺ FSC^{low}, SSC^{low}, lineage⁻ and ST2/IL-33R⁺ cells (**Fig. 2.1**).

At 12 h although no differences in the ST2/IL-33R⁺ ILC2 percentages were detected, significant differences were detected 24 h post vaccination (**Fig. 3.1b**). Interestingly, compared to the control unadjuvanted vaccine, the IL-13R α 2 adjuvanted vaccine sequestering IL-13 in the cell milieu, showed significant suppression of ILC2 at the lung mucosae 24 h to 7 days post vaccination, suggesting a requirement for free IL-13 in maintaining ILC2 cells. In contrast, IL-4R antagonist vaccine which blocked both IL-

4 and IL-13 cell-signalling via IL-4R/STAT6 pathway showed significantly elevated percentages of ST2/IL-33R⁺ ILC2, 24 h post vaccination compared to the other two vaccines tested (**Fig. 3.1b**). It is noteworthy that very low ILC2 were detected in naïve mice lung, average 0.074% (**Fig. 3.2**) vs unadjuvanted vaccinated 0.29%.

When IL-13 expression was evaluated in the lung lineage⁻ ST2/IL-33R⁺ ILC2, higher IL-13 expression was detected in mice that received the unadjuvanted vaccine compared to the IL-4R antagonist or IL-13R α 2 vaccines ($p < 0.0001$) (**Fig. 3.1c**). Interestingly, although IL-4R antagonist and IL-13R α 2 vaccines activated different overall percentages of ST2/IL-33R⁺ ILC2 at the lung mucosae, both vaccines significantly inhibited IL-13 expression by ST2/IL-33R⁺ ILC2, at 24 h to 7 days post vaccination compared to the control unadjuvanted FPV-HIV vaccine (**Fig. 3.1d**). It is noteworthy that the trend of ST2/IL-33R⁺ IL-13⁺ cells observed overtime presented as percentage or total cell number were similar (**Fig. 3.1d**). In all three vaccinated groups, lineage⁻ ST2/IL-33R⁺ ILC2 did not express IL-4 at any of the time points tested. Furthermore, lineage⁻ ST2/IL-33R⁺ ILC2 obtained from unimmunised controls (**Fig. 3.2**) and importantly the lineage⁺ ST2/IL-33R⁺ cells obtained from vaccinated and non-vaccinated groups (**Fig. 3.3**) also did not show any expression of IL-4 or IL-13. This was further confirmed by staining each lineage marker separately for IL-4 and IL-13 (**Fig. 3.4**), and data clearly indicated that the lineage⁻ ST2/IL-33R⁺ cells did not contain any contaminating mast cells or basophils.

Stem cell marker Sca-1 expression²²⁷ was found to be inversely related to the percentage of CD45⁺ lineage⁻ ST2/IL-33R⁺ ILC2 over time regardless of adjuvant treatment (**Fig. 3.1e & 3.1f**). Few Sca-1⁺ ILC2 were detected at 12 h in all three vaccine

Fig. 3.1. Evaluation of lung ILC2 and IL-13 expression following intranasal vaccination.

In this study ILC2 cells were identified as CD45⁺ FSC^{low} SSC^{low} lineage⁻ ST2/IL-33R⁺ cells using flow cytometry **(a)**. BALB/c mice were immunized intranasally with FPV-HIV (normal IL-13 condition), FPV-HIV-IL-4 antagonist, and FPV-HIV-IL-13R α 2 (IL-13 activity transiently inhibited or sequestered) vaccines and the percentage and number of lung lineage⁻ ST2/IL-33R⁺ ILC2 **(b)** and their IL-13 expression **(c,d)** were assessed at 12 h, 24 h, 3 days, and 7 days post vaccination. The FACS plots **(c)** are representative of the 24h data points for each vaccination. The left graph represents percentage of ST2/IL-33R⁺ IL-13⁺ cells and right graph the total cell number **(d)**. The lineage⁻ ST2/IL-33R⁺ cells were further analysed for Sca-1 and IL-13 expression **(e-h)**. Data indicate that IL-13 was only detected in lineage⁻ ST2/IL-33R⁺ Sca-1⁺ ILC2 whilst no IL-13 was detected in lineage⁻ ST2/IL-33R⁺ Sca-1⁻ ILC2 **(g-h)**. The graphs represent the mean and standard deviation (s.d.). The p-values were calculated using GraphPad Prism software (version 6.05 for Windows). *p<0.05, **p<0.01, ***p<0.001, ****p<0.0001. For each time point experiments were repeated minimum of three times.

Note that during early time points no significant inflammatory infiltrates were detected and the absolute cell numbers obtained were very similar.

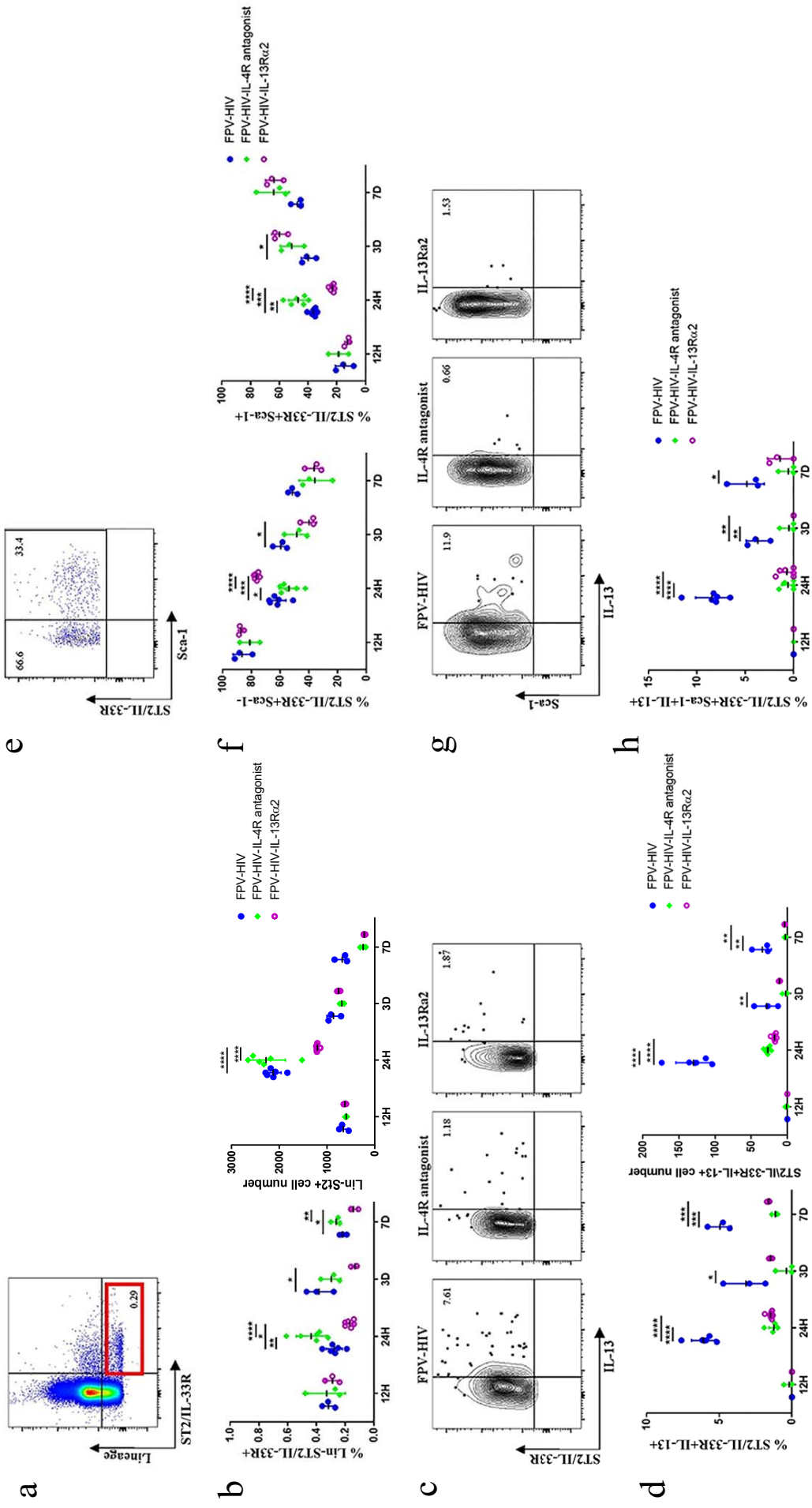


Fig. 3.2. Evaluation of IL-13, IFN- γ , and IL-22 expression by different ILC subsets in naïve

BALB/c mice.

Lung ILC from naïve BALB/c mice were prepared and stained as described in Materials and Methods. In naïve mice no IL-13 expression by ILC2 cells were detected **(a)**. Although no IFN- γ expression was detected in NKp46⁺ and NKp46⁻ ILC1 and ILC3 **(b)** some IL-22 expression was detected in NKp46⁻ ILC1 and ILC3 **(c)**.

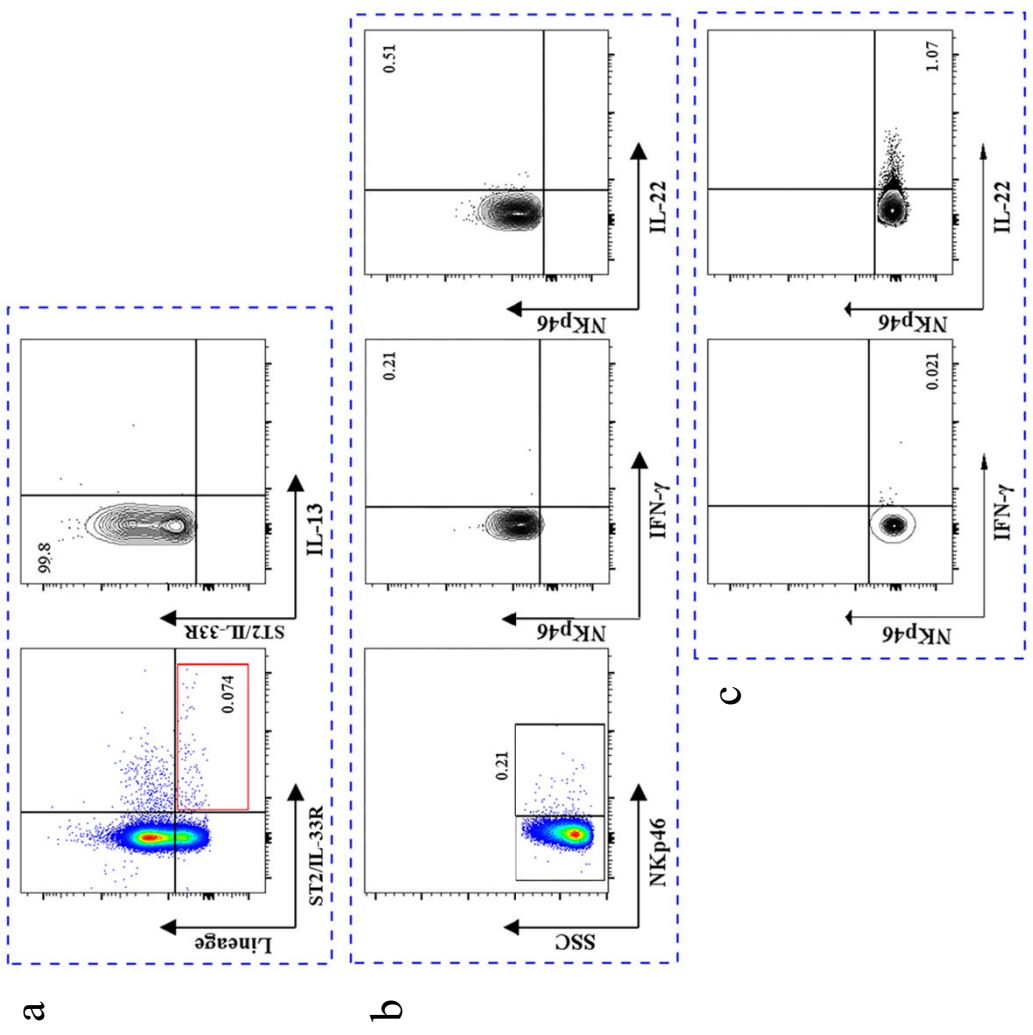


Fig. 3.3. Evaluation of IL-13 expression by lung lineage⁺ ST2/IL-33R⁺ cells following i.n. rFPV immunisation.

BALB/c mice were immunized intranasally with FPV-HIV, FPV-HIV-IL-4R antagonist adjuvanted, and FPV-HIV-IL-13R α 2 adjuvanted vaccines and IL-13 expression by lineage⁺ ST2/IL-33R⁺ cells was evaluated at 24 h post vaccination and compared with unimmunized naïve mice. Data indicated that no IL-13 expression (0%) was detected in lineage⁺ ST2/IL-33R⁺ cells under all three vaccine conditions.

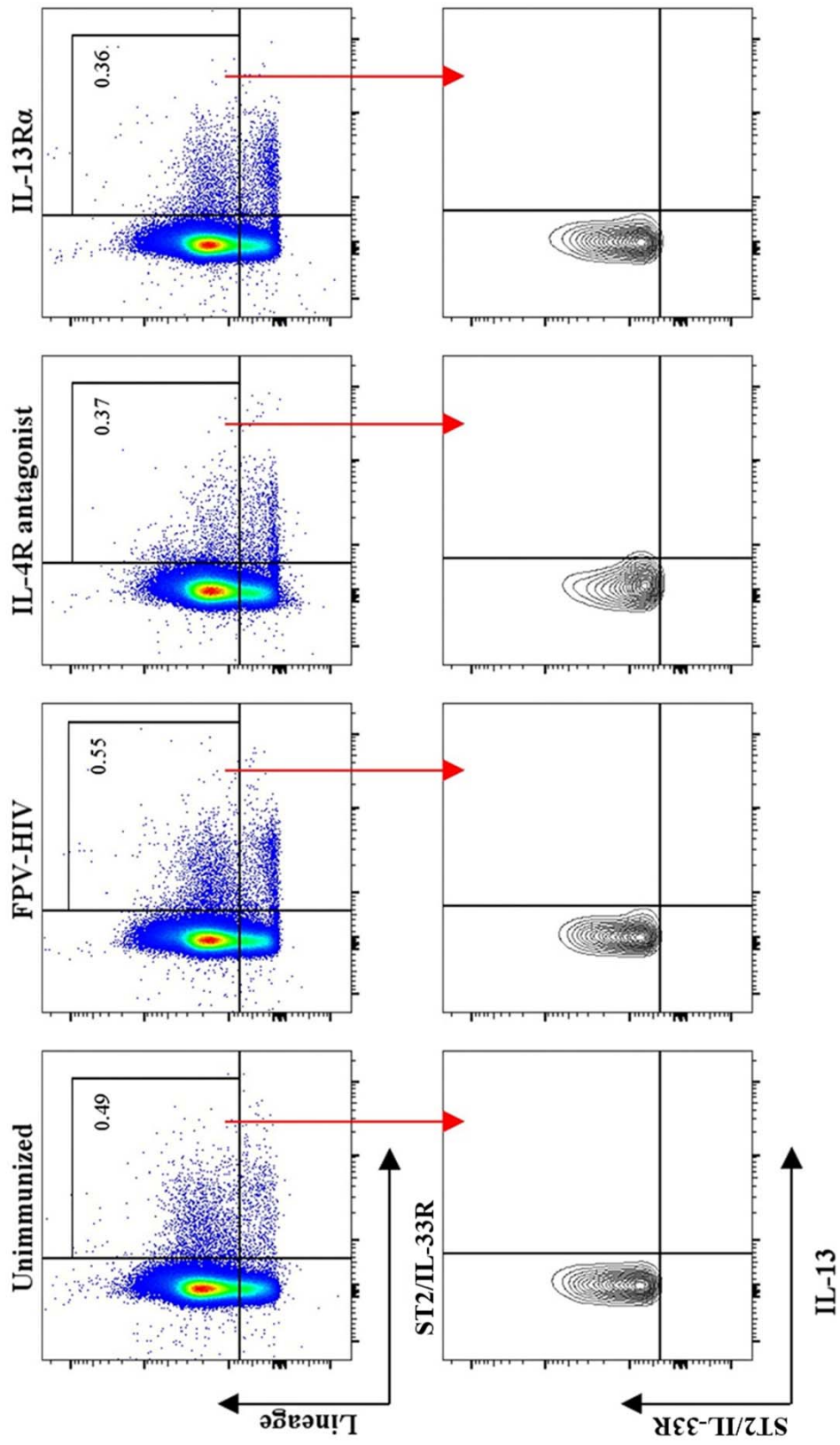
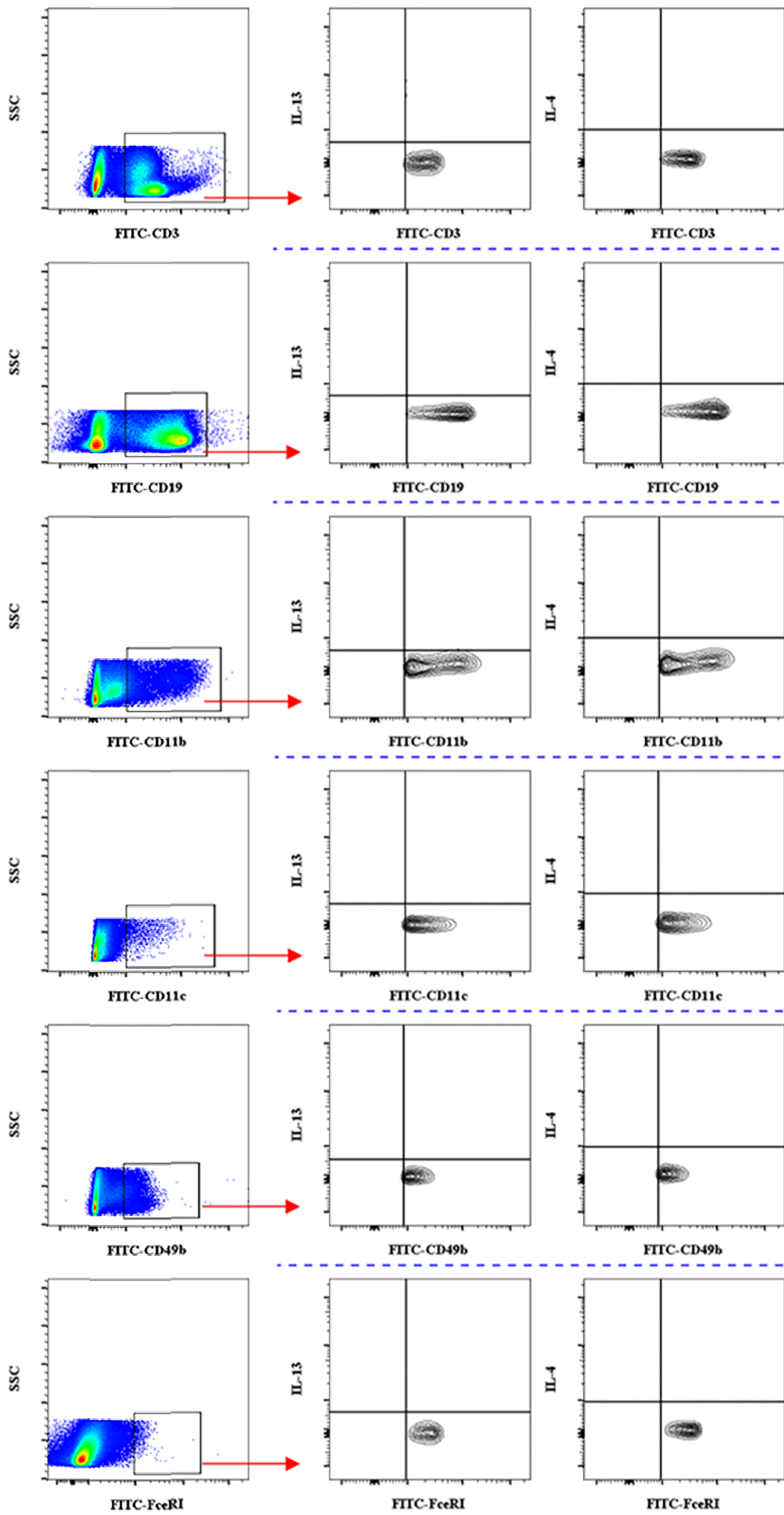


Fig. 3.4. Evaluation of IL-13 and IL-4 expression by each lineage⁺ cell subset following i.n. rFPV immunisation.

BALB/c mice were immunized intranasally with FPV-HIV vaccine, lung cells were stained with each lineage marker separately. IL-13, and IL-4 expression were evaluated at 24 h post vaccination. Data revealed that none of the lineage⁺ cell subsets expressed IL-13 or IL-4, further confirming that the ILC2 cells were not contaminated with any lineage⁺ cells.



groups tested, however by 24 h post vaccination CD45⁺ lineage⁻ ST2/IL-33R⁺ ILC2s following IL-4R antagonist adjuvanted vaccine showed significantly elevated Sca-1 expression compared to the other two vaccines. Although Sca-1⁻ subset did not express IL-13, the Sca-1⁺ ST2/IL-33R⁺ ILC2 subset was positive for IL-13 in the unadjuvanted vaccine, while the IL-4R antagonist and IL-13R α 2 adjuvanted vaccines showed complete inhibition of IL-13 expression (**Fig. 3.1h & 3.1g**). These results indicated that Sca-1 is a general activation marker for ST2/IL-33R⁺ ILC2, and not necessary dependent on IL-13 expression.

3.4.2 Expression of IFN- γ and IL-22 by NKp46⁺ ILC subset is differentially regulated following FPV-HIV-IL-13R α 2 and FPV-HIV-IL-4R antagonist vaccination at the lung mucosae.

According to the micro environment/cell milieu, high plasticity of ILC1 and ILC3 has been observed and classifying ILC1 and ILC3 according to their cell surface marker expression has been a difficult task^{142, 228, 229, 230}. Thus, in this viral vector-based vaccination study, for better clarity the ILC subsets (ILC1 and ILC3) were identified as lineage⁻ NKp46⁺ ILC and lineage⁻ NKp46⁻ ILC and assessed according to their cytokines production. Unlike the lineage⁻ ST2/IL-33R⁺ cells that were CD127⁺ and GATA3⁺, 99.7% of the lineage⁻ ST2/IL-33R⁻ cells were found to be CD127⁻ and GATA3⁻ (**Fig. 2.1**). Furthermore, to confirm that the ILCs were not conventional NK cells, granzyme B expression was evaluated on the lineage⁺ NKp46⁺ and lineage⁻ NKp46⁺ subsets (**Fig. 3.5b & d**), as expected in the lineage⁻ population, no granzyme B was detected (**Fig. 3.5b**), whereas in the lineage⁺ NKp46⁺ population, both IFN- γ and granzyme B were detected (**Fig. 3.5e**). These data clearly confirmed that no

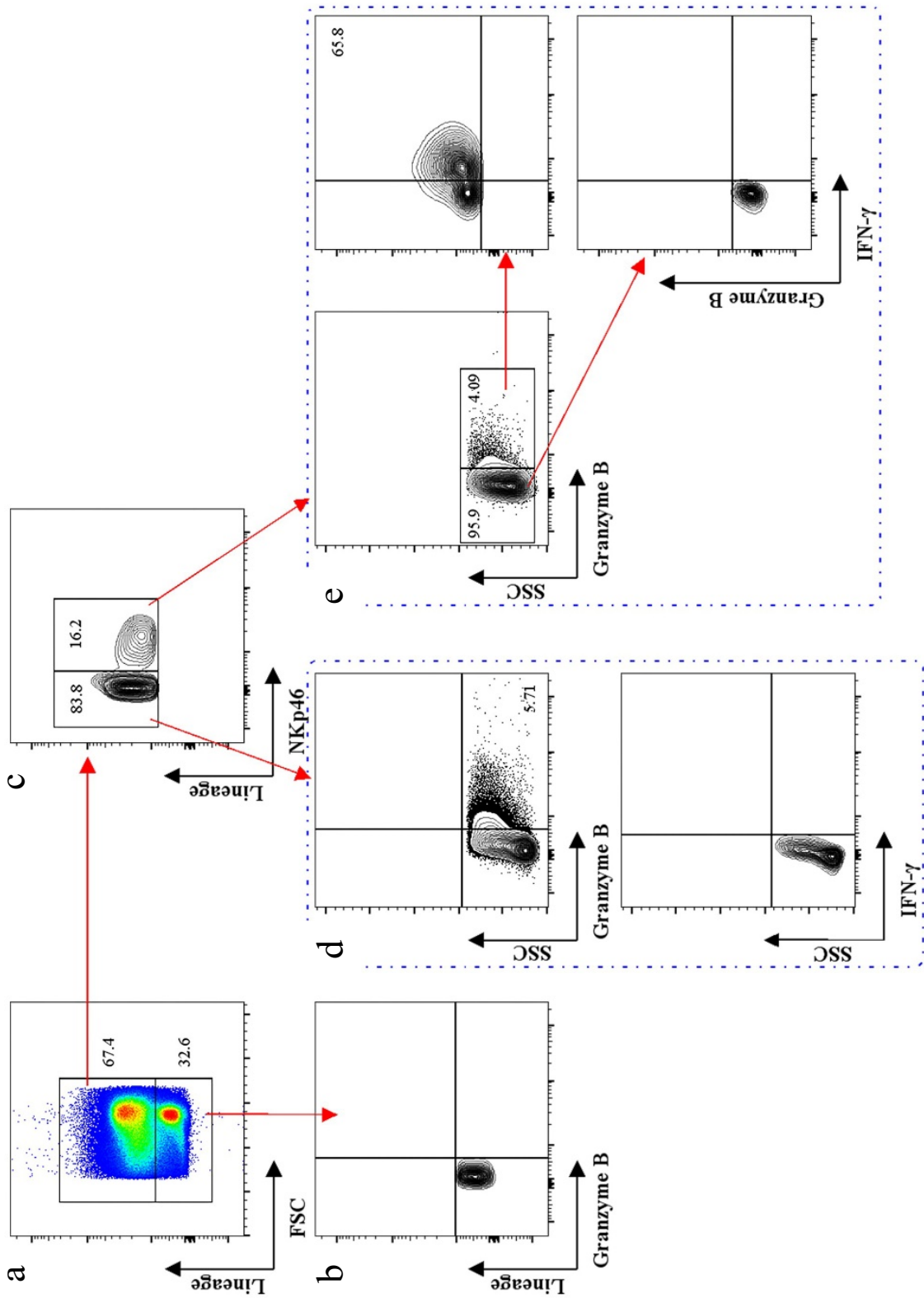


Fig. 3.5. Determination of the absence of conventional NK cells in CD45⁺, lineage- population.

Lung cells from BALB/c mice immunized with FPV-HIV control vaccine were firstly gated on CD45⁺, FSC^{low} and SSC^{low} followed by lineage⁻ and lineage⁺ populations (**a**), and granzyme B expression was evaluated on these subsets respectively (**b & c**). The lineage⁺ cells were further divided into NKp46⁺ and NKp46⁻ populations (**c**), and their granzyme B and IFN- γ production were evaluated (**d & e**). Data indicated that granzyme B was only expressed by lineage⁺ cells (NKp46⁺ and NKp46⁻) not lineage⁻ cells (**b**), and IFN- γ expression was also detected in conventional NK cells, which were determined as lineage⁺ NKp46⁺ Granzyme B⁺. Numbers on FACS plots represent cell percentage.

conventional NK cells were present in the lineage⁻ population. Interestingly, 24 h post vaccination, the IL-4R antagonist vaccinated group showed elevated IFN- γ expression by the lineage⁺ NKp46⁺ (conventional NK cells) subset (~22%) compared to the control unadjuvanted (~15%) or IL-13R α 2 adjuvanted vaccine groups tested (~7%) (**Fig. 3.6**). Interestingly, very low NKp46⁺ ILC were detected in naïve mice lung, average 0.21% (**Fig. 3.2**) vs unadjuvanted vaccinated 3.95%.

Lineage⁻ ST2/IL-33R⁻ NKp46⁺ ILC were detected in all three vaccine groups tested 24 h post vaccination (**Fig. 3.7b**) but the highest percentage was detected in the IL-4R antagonist vaccinated group ($p < 0.0001$) (**Fig. 3.7b**). In the context of IFN- γ expression by NKp46⁺ ILC, control unadjuvanted and IL-4R antagonist vaccinated groups showed similar IFN- γ expression profile compared to the lower IL-13R α 2 adjuvanted vaccine group, although only control unadjuvanted showed statistical significance to IL-13R α 2 adjuvanted vaccine ($p < 0.01$) (**Fig. 3.7c-d**). Unlike IFN- γ , the IL-22 production by NKp46⁺ ILCs was significantly reduced in both IL-4R antagonist and IL-13R α 2 vaccine groups compared to the control at 24 h ($p < 0.0001$) (**Fig. 3.7e**). However, at all time points tested the level of IL-22 was much lower in animals that received FPV-HIV-IL-13R α 2 vaccine (**Fig. 3.7f**).

3.4.3 FPV-HIV-IL-4R antagonist vaccine significantly increases IFN- γ production by NKp46⁻ ILC at the lung mucosae.

When the lineage⁻ ILCs were assessed post i.n. delivery, most of the cells were found to be ST2/IL-33R⁻ NKp46⁻ ILCs (**Fig. 3.8a**). There was no significant difference in the percentages of NKp46⁻ ILC numbers between the vaccine groups tested, except for 24 h time point (**Fig. 3.8b**). Next when cytokine expression was evaluated in ST2/IL-33R⁻

Fig. 3.6. Evaluation of IFN- γ expression by lung conventional NK cells following adjuvanted and unadjuvanted i.n. rFPV immunisation.

BALB/c mice were immunized intranasally with FPV-HIV, FPV-HIV-IL-4R antagonist adjuvanted, and FPV-HIV-IL-13R α 2 adjuvanted vaccines and IFN- γ expression by conventional NK cells were evaluated at 24 h post vaccination in lung. Conventional NK cells were gated as CD45⁺, lineage⁺, and NKp46⁺, and their IFN- γ expression was evaluated using intracellular cytokine staining (**a & b**). The graphs represent the mean and standard deviation (s.d.). The p-values were calculated using GraphPad Prism software (version 6.05 for Windows). *P<0.05, **p<0.01, ***P<0.0001 (one-way ANOVA). For each time point experiments were repeated minimum of three times. Data indicate that 24 h post vaccination, the IL-4R antagonist adjuvanted vaccinated group showed elevated IFN- γ expression by the lung lineage⁺ NKp46⁺ (conventional NK cells) subset (~22%) compared to the control unadjuvanted (~15%) or IL-13R α 2 adjuvanted vaccine groups tested (~7%).

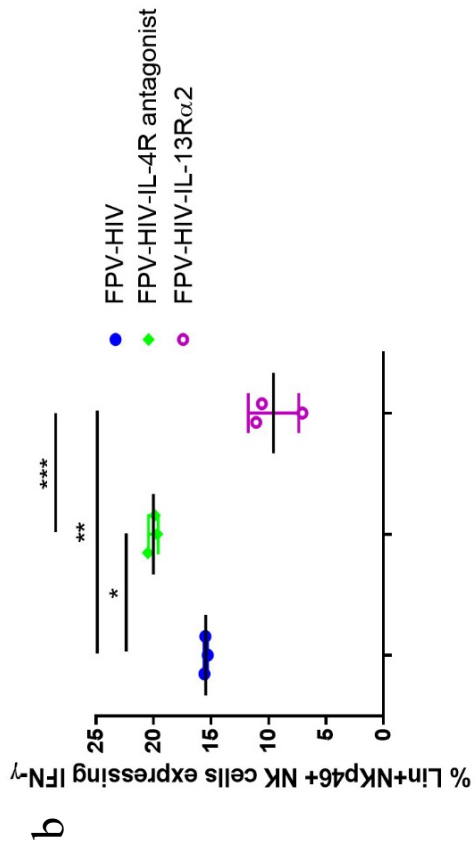
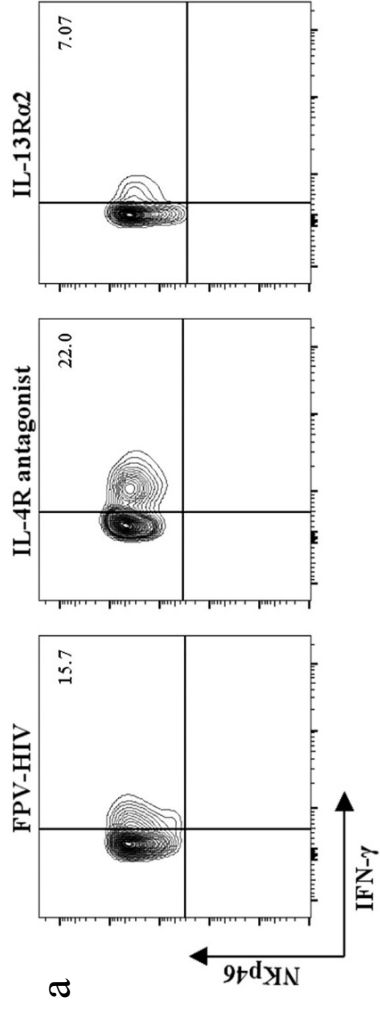


Fig. 3.7. Expression of IFN- γ and IL-22 by NKp46⁺ ILC following i.n. rFPV immunisation.

BALB/c mice were immunized intranasally with FPV-HIV, FPV-HIV-IL-4 antagonist, and FPV-HIV-IL-13R α 2 vaccines and the percentage of lung NKp46⁺ ILC cells were evaluated at 12 h, 24 h, 3 days, and 7 days post vaccination. Cells were gated as CD45⁺, FSC^{low}, SSC^{low}, lineage⁻, ST2/IL-33R⁻ NKp46⁺, (**a & b**) and IFN- γ (**c & d**) and IL-22 (**e & f**) expression was evaluated using intracellular cytokine staining. The graphs represent the mean and standard deviation (s.d.). The p-values were calculated using GraphPad Prism software (version 6.05 for Windows). *P<0.05, **p<0.01, ***P<0.0001 (one-way ANOVA). For each time point experiments were repeated minimum of three times.

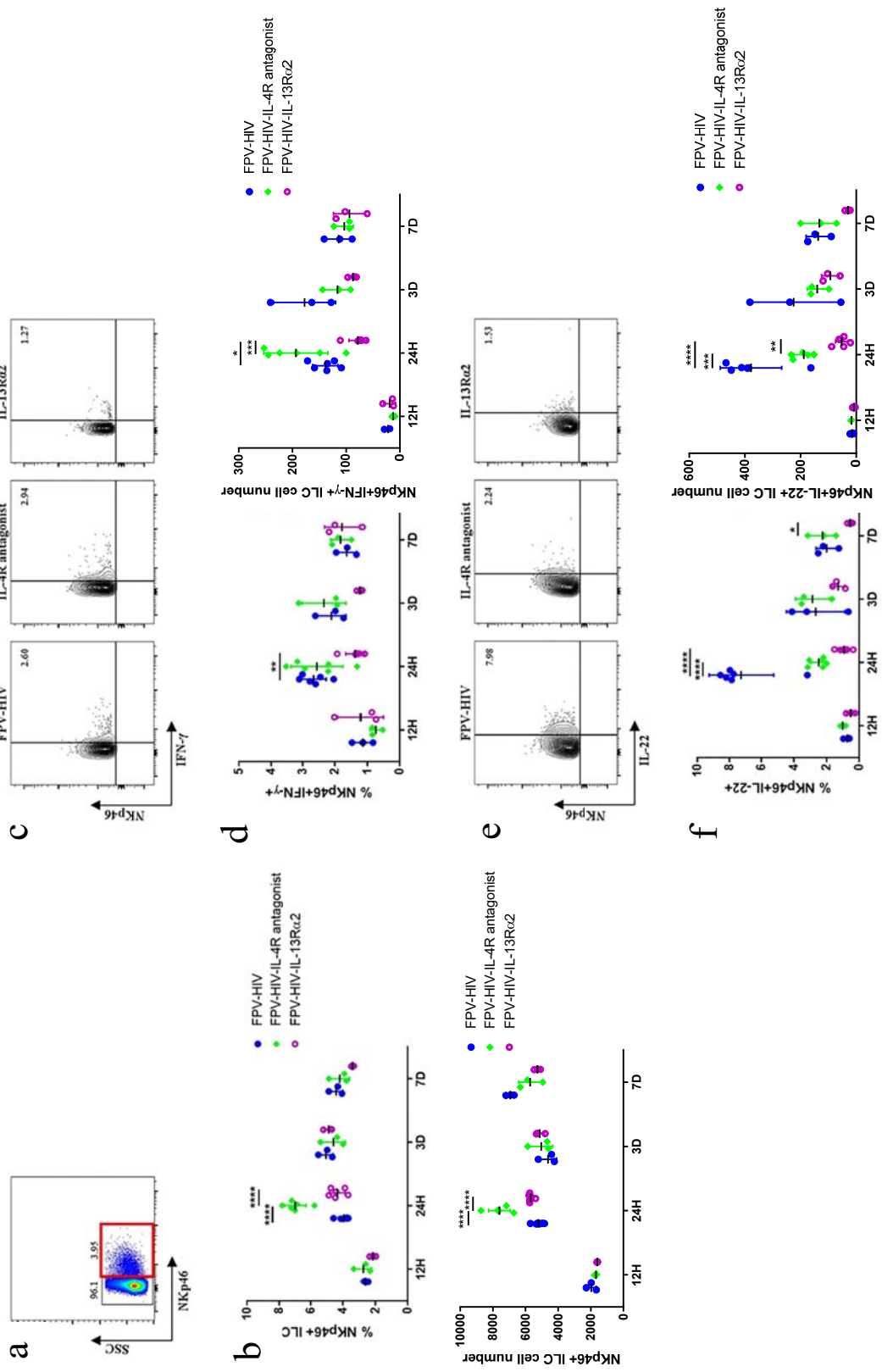
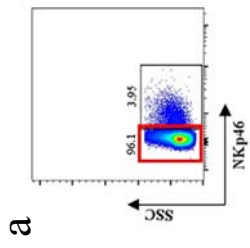
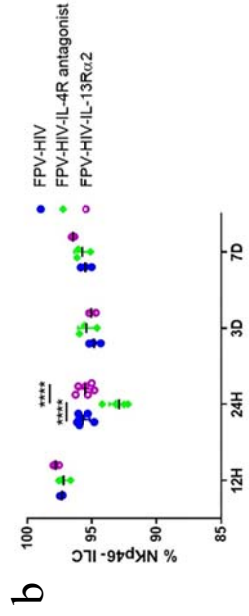
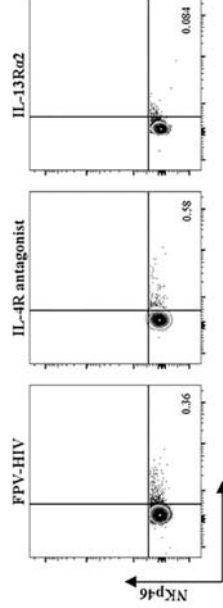


Fig. 3.8. Expression of IFN- γ and IL-22 by NKp46⁻ ILC cells post rFPV immunisation.

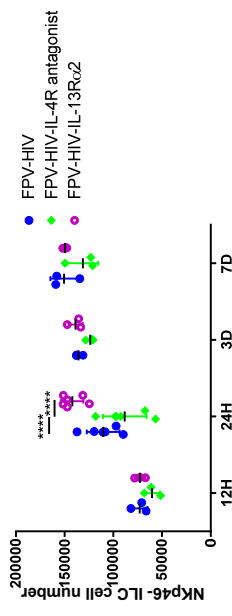
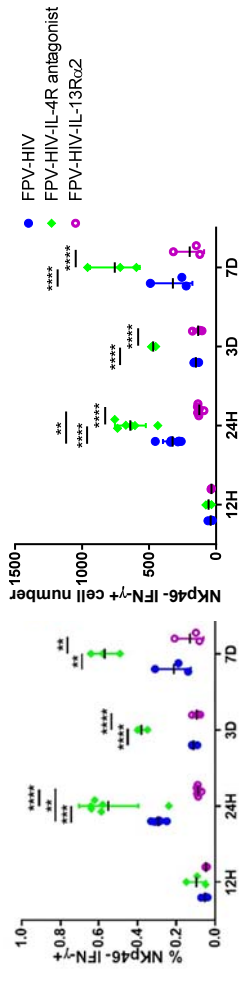
BALB/c mice were immunized intranasally with FPV-HIV, FPV-HIV-IL-4 antagonist, and FPV-HIV-IL-13R α 2 vaccines and the percentage of lung NKp46⁻ ILC cells were evaluated at 12 h, 24 h, 3 days, and 7 days post vaccination. Cells were gated as CD45⁺, FSC^{low}, SSC^{low}, lineage⁻, ST2/IL-33R⁻ NKp46⁻, (**a & b**) and IFN- γ (**c & d**) and IL-22 (**e & f**) expression was evaluated using intracellular cytokine staining. The graphs represent the mean and standard deviation (s.d.). The p-values were calculated using GraphPad Prism software (version 6.05 for Windows). *P<0.05, **p<0.01, ***P<0.0001 (one-way ANOVA). For each time point experiments were repeated minimum of three times.



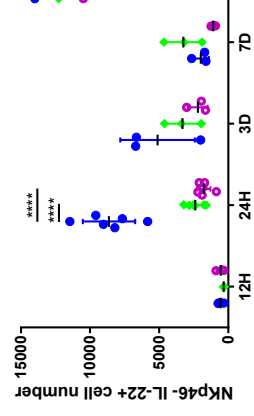
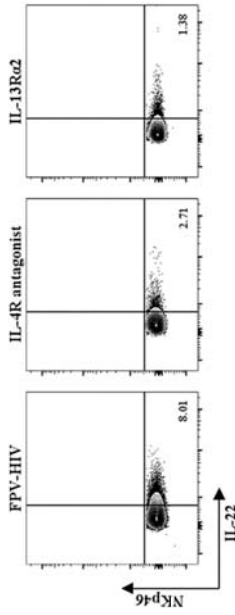
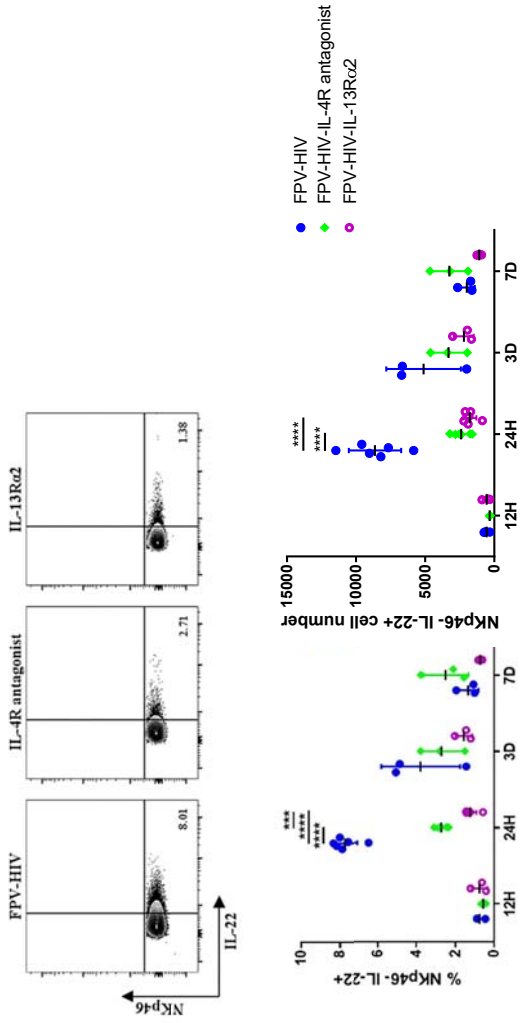
c



d



f



NKp46⁻ ILCs, significantly elevated IFN- γ expression was detected in FPV-HIV-IL-4R antagonist group compared to the control unadjuvanted group and FPV-HIV-IL-13R α 2 group from 24 h to 7 days post vaccination ($p < 0.0001 - 0.01$) (**Fig. 3.8c, d**). At 24 h post vaccination, similar to the ST2/IL-33R⁻ NKp46⁺ ILC, IL-22 production by ST2/IL-33R⁻ NKp46⁻ ILC was significantly lower in both FPV-HIV-IL-4R antagonist and FPV-HIV-IL-13R α 2 adjuvanted vaccine groups compared to the control unadjuvanted group (**Fig. 3.8e, f**).

3.4.4 Intramuscular vaccination induces exclusive lineage⁻ IL-25R⁺ ILC2 subset at the vaccination site.

Next when BALB/c mice were immunised intramuscularly (i.m.) and ILC2s were evaluated, no IL-33R⁺ ILC2s were detected in muscle and only IL-25R⁺ ILC2 were observed (**Fig. 3.9a&b**). ST2/IL-33R⁺ ILC2s were only found in the lung following intranasal vaccination (**Fig. 3.10**). However, no IL-25R⁺ or IL-33R⁺ ILC2s were detected in naïve quadriceps muscle of BALB/c mice (**Fig. 3.11**). More interestingly, compared to the other two vaccines FPV-HIV-IL-4R antagonist vaccine significantly suppressed the IL-25R⁺ ILC2s while FPV-HIV-IL-13R α 2 adjuvanted vaccine significantly increased the IL-25R⁺ ILC2 number (**Fig. 3.9c**). When IL-13 expression by lineage⁻ ST2/IL-33R⁻ IL-25R⁺ ILC2 subset was assessed, significantly higher IL-13 expression was detected in control unadjuvanted vaccines compared to the FPV-HIV-IL-4R antagonist and FPV-HIV-IL-13R α 2 adjuvanted vaccines ($p < 0.0001$) (**Fig. 3.9d**). Interestingly, although FPV-HIV-IL-4R antagonist and FPV-HIV-IL-13R α 2 adjuvanted vaccines activated different overall percentages of IL-25R⁺ ILC2 numbers, both vaccines were able to significantly down-regulate the IL-13 production by IL-25R⁺ ILC2 compared to control unadjuvanted FPV-HIV vaccine (**Fig. 3.9e**). In all vaccine groups tested, no IL-4 production was detected in IL-25R⁺ ILC2.

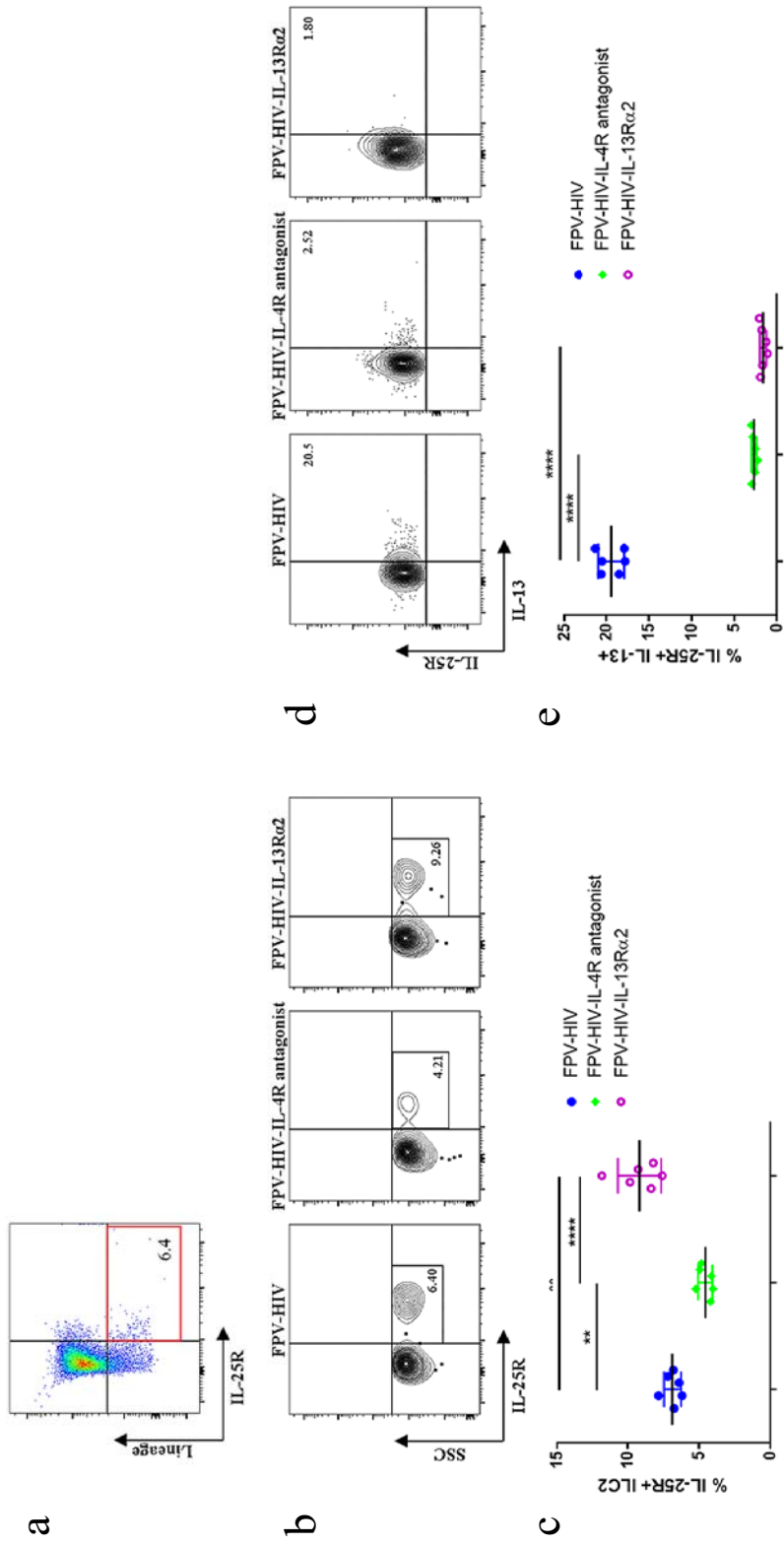


Fig. 3.9. Evaluation of ILC2 subtypes and cytokines they express in the quadriceps muscle 24 h post intramuscular vaccination.

BALB/c mice were immunized intramuscularly with FPV-HIV, FPV-HIV-IL-4 antagonist, and FPV-HIV-IL-13R α 2 vaccines and the percentage of ILC2 in muscle cells was evaluated 24 h post vaccination (note that no ST2/IL-33R⁺ ILC2 were detected in muscle). In this study ILC2 cells were identified as CD45⁺ FSC^{low} SSC^{low} lineage⁻ ST2/IL-33R⁻ IL-25R⁺ cells using flow cytometry (**a & b**). The FACS plots are representative of each vaccination (**b**) and the collected data are presented in graph (**c**). The expression of IL-13 by IL-25R⁺ ILC2s were also assessed (**d & e**). The graphs represent mean and standard deviation (s.d.). The p-values were calculated using GraphPad Prism software (version 6.05 for Windows). *P<0.05, **p<0.01, ***P<0.0001 (one-way ANOVA). For each time point experiments were repeated three times.

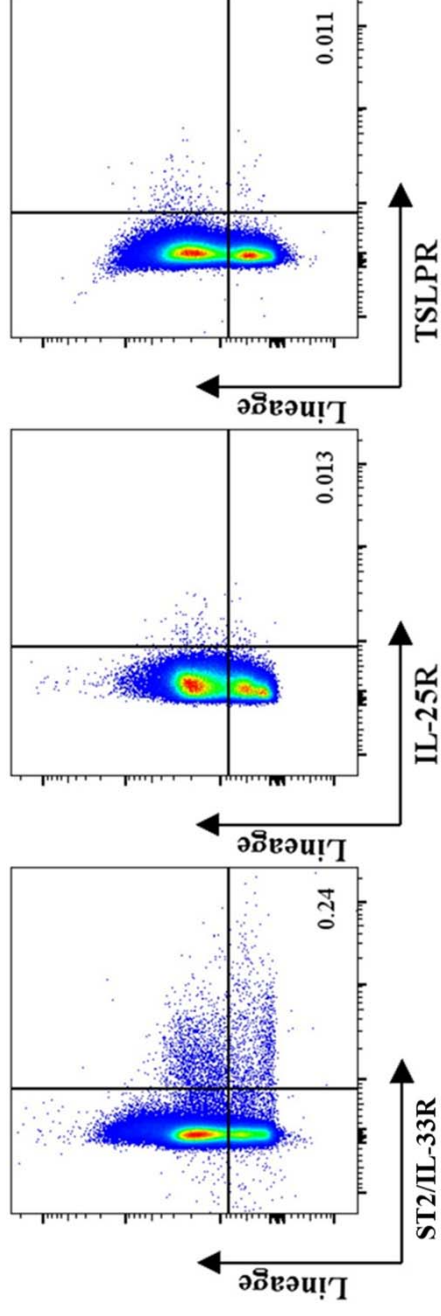


Fig. 3.10. Staining of lung tissue for different ILC2 subsets.

Cells were gated from $CD45^+$ and lymphocytes as shown in supplementary Figure 1 and lineage $^-$ ST2/IL-33R $^+$, lineage $^-$ IL-25R $^+$, and lineage $^-$ TSLPR $^+$ lung ILC2 subsets were evaluated 24 h post FPV-HIV immunization. Following rFPV immunization, all lung ILC2s were found to be ST2/IL-33R $^+$. Numbers on FACS plots represent cell percentage.

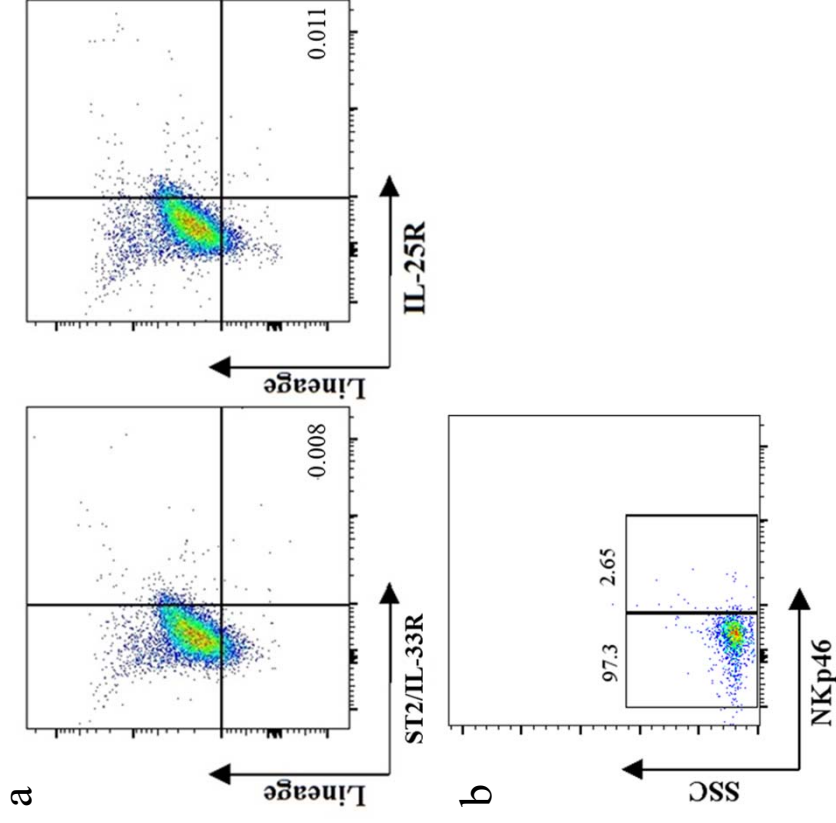


Fig. 3.11. Evaluation of different ILC2 subsets in naïve mice quadriceps muscle.

Cells were gated from CD45⁺ and lymphocytes as per described in materials and methods. No or extremely low ST2/IL-33R⁺ (0.008%) and IL-25R⁺ (0.011%) ILC2 cells were detected in quadriceps muscle in naïve BALB/c mice **(a)**. Very low NKp46⁺ ILC (18.3%) were detected in quadriceps muscle in naïve BALB/c mice **(b)**.

3.4.5 Intramuscular vaccination induces uniquely different lineage⁻ NKp46⁻ and NKp46⁺ ILC subsets at the vaccination site.

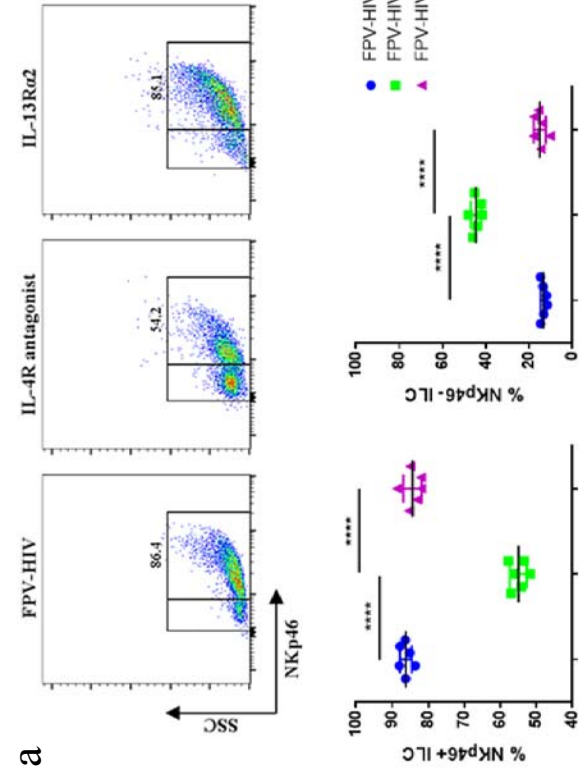
When lineage⁻ IL-25R⁻ (also ST2/IL-33R⁻) NKp46⁺ and NKp46⁻ ILC subsets were evaluated 24 h post vaccination, the FPV-HIV-IL-4R antagonist vaccinated group showed very low NKp46⁺ ILC and elevated percentage of NKp46⁻ ILC compared to the control unadjuvanted and FPV-HIV-IL-13R α 2 vaccines (**Fig. 3.12a**). Interestingly, in naïve mice very low NKp46⁺ ILC were detected compared to unadjuvanted vaccinated, average 2.65% (**Fig. 3.11**) vs 86.4%. When cytokine profiles were evaluated in these two subsets, significantly elevated IFN- γ and IL-22 expression was detected in NKp46⁺ ILC obtained from FPV-HIV-IL-13R α 2 adjuvanted vaccinated group compared to the IL-4R antagonist vaccine group ($p < 0.05$ - 0.0001) (**Fig. 3.12b & Fig. 3.13**). Also, the percentage of IL-25R⁻ NKp46⁺ ILC that expressed IFN- γ ($p < 0.001$) and IL-17A ($p < 0.01$) was significantly higher in FPV-HIV-IL-13R α 2 adjuvanted group compared to the control (**Fig. 3.12b & Fig. 3.13a**). Overall, the HIV-IL-13R α 2 vaccinated group showed elevated percentage of lineage⁻ IL-25R⁻ NKp46⁺ ILC expressing IFN- γ , IL-22 and IL-17A compared to the other two groups tested.

Unlike IL-22 and IL-17A that was detected in both lineage⁻ IL-25R⁻ NKp46⁺ and NKp46⁻ ILC subsets, no IFN- γ expression was detected IL-25R⁻ NKp46⁻ ILC. Although there was no significant difference in IL-22 and IL-17A production by NKp46⁻ ILC subsets between control unadjuvanted and FPV-HIV-IL-4R antagonist vaccinated groups, FPV-HIV-IL-13R α 2 adjuvanted vaccinated group showed significantly reduced percentage of NKp46⁻ ILC expressing IL-17A compared to the other two vaccine groups tested ($p < 0.001 - 0.0001$) (**Fig. 3.14**). No NKp46⁺ or NKp46⁻ ILC subsets were positive for both IL-22 and IL-17A.

Fig. 3.12. Evaluation of NKp46⁺/- ILC and their IFN- γ expression in the quadriceps muscle 24 h post intramuscular vaccination.

BALB/c mice were immunized intramuscularly with FPV-HIV, FPV-HIV-IL-4 antagonist, and FPV-HIV-IL-13R α 2 vaccines and the percentage of NKp46⁺ and NKp46⁻ ILC in muscle cells was evaluated 24 h post vaccination. The NKp46⁺ and NKp46⁻ ILCs were evaluated exactly as per lung tissue **(a)**. Data represent percentage NKp46⁺ cells expressing IFN- γ , no IFN- γ expression was detected in NKp46⁻ population **(b)**. The graphs represent the mean and standard deviation (s.d.). The p-values were calculated using GraphPad Prism software (version 6.05 for Windows). *P<0.05, **p<0.01, ***P<0.0001 (one-way ANOVA). For each time point experiments were repeated three times.

a



b

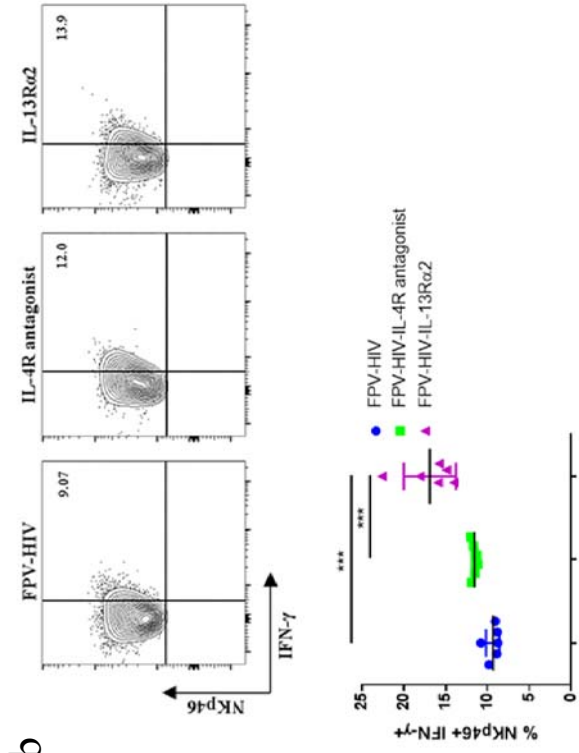


Fig. 3.13. Evaluation of NKp46^{+/−} ILC IL-22 expression in the quadriceps muscle 24 h post intramuscular vaccination.

BALB/c mice were immunized intramuscularly with FPV-HIV, FPV-HIV-IL-4 antagonist, and FPV-HIV-IL-13R α 2 vaccines and the percentage of NKp46⁺ and NKp46[−] ILC in muscle cells was evaluated 24 h post vaccination. Data represent percentage NKp46⁺ and NKp46[−] cells expressing IL-22 (**a & b**). The graphs represent the mean and standard deviation (s.d.). The p-values were calculated using GraphPad Prism software (version 6.05 for Windows). *P<0.05, **p<0.01, ***P<0.0001 (one-way ANOVA). For each time point experiments were repeated three times.

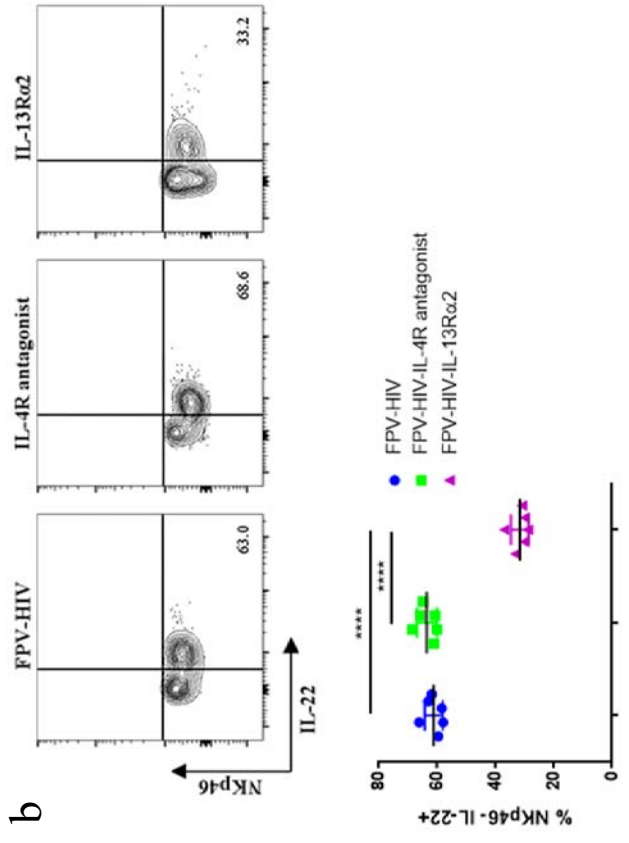
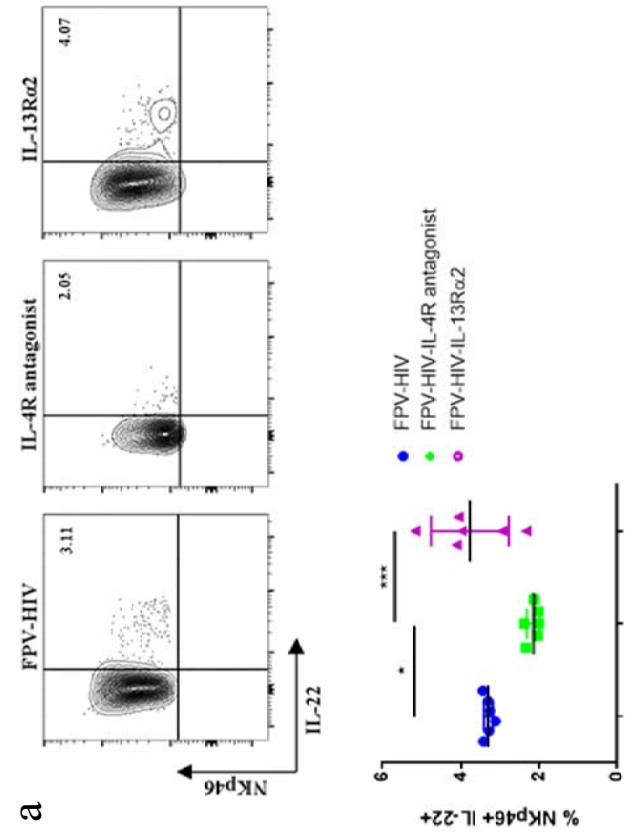
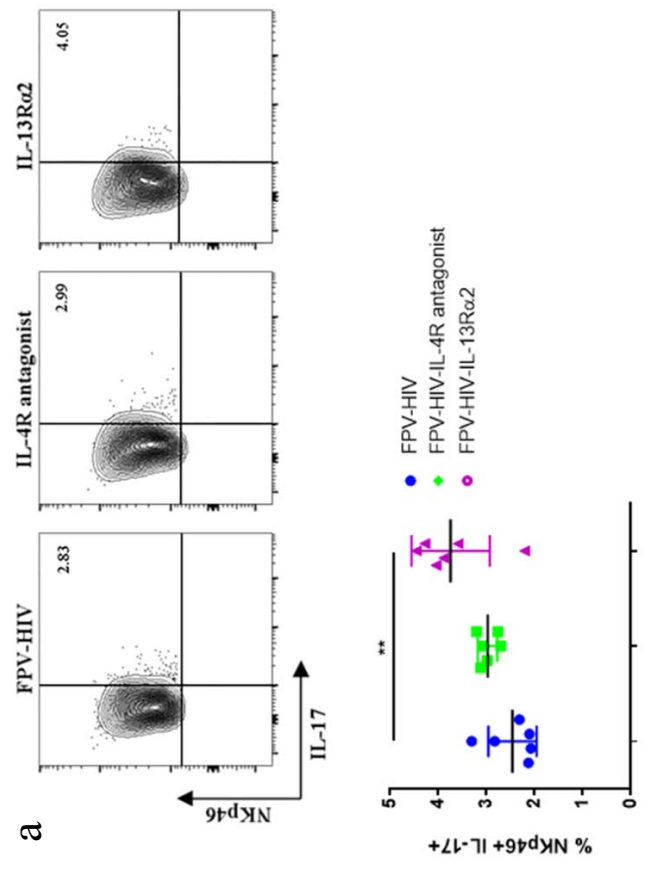
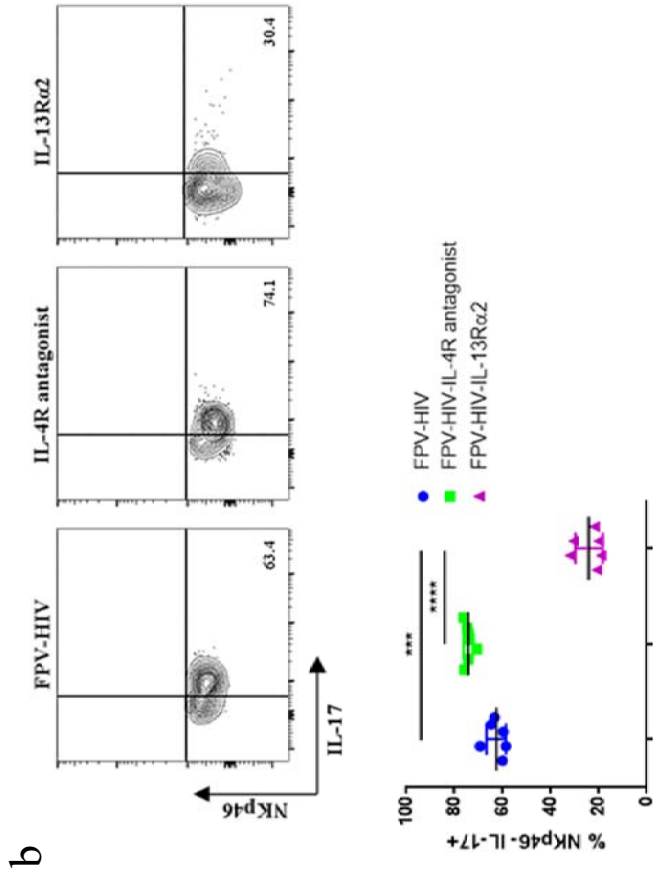


Fig. 3.14. Evaluation of NKp46^{+/-} ILC IL-17A expression in the quadriceps muscle 24 h post intramuscular vaccination.

BALB/c mice were immunized intramuscularly with FPV-HIV, FPV-HIV-IL-4 antagonist, and FPV-HIV-IL-13R α 2 vaccines and the percentage of NKp46⁺ and NKp46⁻ ILC in muscle cells was evaluated 24 h post vaccination. Data represent percentage NKp46⁺ and NKp46⁻ cells expressing IL-17A (**a & b**). The graphs represent the mean and standard deviation (s.d.). The p-values were calculated using GraphPad Prism software (version 6.05 for Windows). *P<0.05, **p<0.01, ***P<0.0001 (one-way ANOVA). For each time point experiments were repeated three times.



3.5 Discussion.

In this study, our approach of characterising lineage⁻ ILC subsets based principally upon cytokine expression without preconceived expectations of cell surface markers have shown that ILC induced following viral vector vaccination are uniquely different to what has been reported under experimentally induced or chronic inflammation conditions. Following rFPV vaccination although ILC2 were found to express CD127, NKp46⁺ and NKp46⁻ ILC1 and ILC3 populations did not express CD127. This was not entirely surprising as a recent study had shown that CD127 was not strictly required for the development of any ILC subsets²³¹. These observations highlight the caveats of using conventional flow cytometry analysis that relies only on surface marker expression (i.e. Sca-1, CD127 or NKp46) to study ILCs under different conditions (i.e. vaccination or acute infection), especially given the high plasticity of ILC subsets^{142, 209, 218, 219, 228, 229, 230}.

Different ILC2 subsets arise from a common progenitor cell and under different cytokine conditions/ anatomical location differentiate into ILC2 that are IL-33R⁺, IL-25R⁺ or TSLPR⁺²³². Here we have for the first time demonstrated that route of vaccination can alter the ILC recruitment profile at the vaccination site. Following i.n. rFPV vaccination only ST2/IL-33R⁺ ILC2 (lung resident “natural” ILC) were detected in lung, while exclusively IL-25R⁺ ILC2s were detected in muscle following i.m. rFPV vaccination. IL-25R⁺ ILC2 in muscle were most likely circulatory “inflammatory” ILC2²¹³ as naive muscle did not show any significant ILC2 subsets (**Fig. 3.11**). Both lung IL-33R⁺ ILC2s and muscle IL-25R⁺ ILC2s although expressed IL-13, did not express IL-4. As lineage⁺ cells did not express any IL-13 at 12 h or 24 h post vaccination, ILC2 were the only or major source of IL-13 at the vaccination site at these specific timepoints. Interestingly, a larger proportion of IL-13⁺ ILC2s were detected in

muscle following i.m. FPV-HIV vaccination compared to lung post i.n. delivery. These observations revealed that, what is observed at the ILC level could be directly translated into T cells level, where intramuscular poxviral vaccination has shown to induce elevated IL-13 expression by CTL responsible for low avidity T cells compared to mucosal delivery⁷⁵.

Moreover, IL-13R α 2 and IL-4R antagonist adjuvanted vaccines that induced high avidity CTL^{113, 122} showed significant inhibition of IL-13 expression by lung IL-33R⁺ ILC2 compared to control non-adjuvant vaccination. Taken together the ability of IL-13 to modulate dendritic cell recruitment to the vaccination site 24 h post vaccination⁷⁷, current findings clearly propose that level of IL-13 expressed by ILC2, could directly modulate dendritic cell recruitment to the vaccination site, responsible for the generation of uniquely different T cell immune outcomes (i.e. under low IL-13 condition recruitment of CD11b⁺ CD103⁻ conventional DC responsible for induction high avidity CTLs⁷⁷). Interestingly, under allergic lung inflammation conditions IL-13 but not IL-4 expressed by ILC2s have shown to promote migration of activated lung dendritic cells into the draining lymph nodes responsible for CD4⁺ T helper 2 cell activation¹⁹⁷. Halim *et al.* have further demonstrated that IL-13⁺ ILC2 licence CD11b⁺ CD103⁻ conventional DC to express CCL17 and promotes Th2 responses²²³, and our studies showed that blocking IL-13 activity likely inhibit this process and forces stronger Th1 mediated immunity¹²³. In summary, these findings indicate that the ILC2 bias (IL-25R⁺ or IL-33R⁺) observed at the different vaccination sites and the amount of IL-13 produced by these ILC2, play a critical role in defining the efficacy of a vaccine. This may also explain how and why mucosal vaccination (which induce low IL-13 expression by ILC2) induce high avidity CTL with better protective efficacy against mucosal pathogens compared to systemic vaccination^{65, 73, 75}.

IL-13 and IL-4 share a common receptor system comprised of IL-4R α /IL-13R α 1, Type II IL-4 receptor complex^{233, 234}, while IL-4 can also signal via Type I IL-4 receptor complex comprised of the common- γ chain and IL-4R α ²³⁵. Both these receptor complexes activate STAT6 signalling. IL-13R α 2 and IL-4R antagonist adjuvanted vaccines inhibited IL-13 expression by ILC2s compared to the control non-adjuvanted vaccine. Sequestering IL-13 (IL-13R α 2 adjuvanted vaccination) also reduced the overall percentage of ST2/IL-33R⁺ ILC2 suggesting an IL-13 autocrine role in maintaining ILC2 function. Surprisingly, sequestering IL-13 from the milieu versus blocking conventional IL-4R α /IL-13R α 1/STAT6 signalling using IL-4R antagonist vaccines resulted in differing ILC1/ILC2 responses. These observations indicate that IL-13 signalling via an alternative pathway, most likely IL-13R α 2 may possibly be responsible for the responses observed with the latter vaccination strategy. This can be further corroborated by the findings that under certain conditions, a physical interaction between cytoplasmic domains of IL-13R α 2 and IL-4R α regulating IL-4R α /IL-13R α 1 receptor function²³⁶, and also IL-13 signalling via the not well defined high-affinity IL-13R α 2 pathway has been reported²³⁷.

Furthermore, IL-13R α 2 adjuvanted vaccination was associated with lower IFN- γ expression by both NKp46^{+/+} ILC and conventional NK cell (**Fig. 3.6**) compared to the other two vaccines tested. Interestingly, a recent study has demonstrated that IL-1 β , IL-12 and IL-18 drive the plasticity between ILC2 and IFN- γ ⁺ ILC1 populations²³⁸. Thus, the very low starting population of ILC2 induced under IL-13R α 2 adjuvanted vaccine may account for the reduced IFN- γ ⁺ NKp46^{+/+} ILC populations. However, whether this would directly affect the IFN- γ expression by conventional NK cell is not yet known (**Fig. 3.6**). In contrast, our study demonstrated that IFN- γ expression by lung NKp46⁻

ILC was elevated up to the day 7 experimental period, while IFN- γ expression by “ex-ILC3” NKp46⁺ cells was largely unaffected following IL-4R antagonist adjuvant vaccination. It is accepted that IL-4/IL-13/STAT6 signalling is antagonistic to IFN- γ expression²³⁹. Thus, it is not entirely surprising that blocking the conventional IL-4R α /IL-13R α 1 pathway resulted in elevated IFN- γ expression by both NKp46⁺ ILC and conventional NK cells. We have previously shown that vaccination using the IL-4R antagonist vaccine resulted in robust IgG1 and IgG2a antibody responses, whereas the IL-13R α 2 adjuvanted vaccine resulted in reduced IgG2a antibodies¹¹³. Interestingly, one major difference between the two adjuvanted vaccines were the level of IFN- γ expression by NKp46⁺ ILC and NK cells suggesting this may ultimately influence APC activation and CD4⁺ T helper cells required for antibody isotype class switching. Blocking autocrine signalling via the IL-4R/IL-13R α 1 (blocking STAT6 signalling) may account for reduced ILC2 IL-13⁺ cell number, it has also been shown that ILC1 IFN- γ expression can suppress IL-13 expression by tissue-resident natural ILC2 cells²⁴⁰. IFN- γ has shown to significantly inhibit IL-13 production by ILC2^{240, 241, 242}, while also up-regulating extracellular expression of IL-13R α 2²³⁹. The above and our current findings indicate a complex interaction between IFN- γ and IL-13 signalling at the vaccination site, and the early IL-13 and IFN- γ co-dependency at the ILC level most likely playing an important role in shaping the downstream antibody immunity.

Previous inflammation and asthma mouse models indicate NKp46⁺ ILC1 express IFN- γ , NKp46⁺ ILC3 express IL-17A and NKp46⁻ ILC3 express IL-22^{167, 168, 243}. Interestingly, in this study, following intranasal viral vaccination both NKp46⁺ and NKp46⁻ ILC1 and ILC3 were found to express IFN- γ and IL-22, but not IL-17A. In contrast, following intramuscular vaccination NKp46⁺ ILC1 and ILC3 were found to express IFN- γ , IL-22

and IL-17A, while NKp46⁻ ILCs only expressed IL-22 and IL-17A, not IFN- γ . These findings clearly indicate the ILC1/ILC3 and ILC2 populations induced are uniquely different depending upon the route of vaccination. Furthermore, the adjuvanted vaccine studies demonstrated that unlike i.n. delivery, the NKp46⁺ and NKp46⁻ ILC1/ILC3 subsets induced following i.m. vaccination have significantly different responsiveness to IL-13. For example: unadjuvanted and the IL-4R adjuvant vaccines showed significantly elevated IL-22 and IL-17A expression by NKp46⁻ ILC1/ILC3 compared to IL-13R α 2 adjuvanted vaccine. Also, a larger proportion of IL-13⁺ ILC2s were detected following i.m. FPV-HIV vaccination compared to i.n. delivery. Taken together our previous studies on CD8⁺ T cells, where IL-13 has shown to modulate IL-17A activity²²⁶, we postulate that IL-17A expression in ILC1 and ILC3 is tightly regulated by IL-13-driven ILC2. In summary, these observations evoke the possibility that the NKp46⁺ or NKp46⁻ ILC1 and ILC3 plasticity at vaccination site is co-dependent on the amount of IL-13 produced by different ILC2 subsets (IL-25R⁺ vs IL-33R⁺).

Collectively, results indicate that within the first 24 h post-vaccination, according to the route of delivery and adjuvants used, different types of IL-13-driven ILC2 and IFN- γ /IL-17A/IL-22 expressing NKp46⁺ or NKp46⁻ (ILC1 and ILC3) are recruited to the vaccination site. The IL-13 and IFN- γ /IL-17A balance induced by these ILCs, play a crucial role in shaping the resulting APC recruitment/activation and B and T cell immunity. Our data suggest that altering the functions of these different ILC subsets at the vaccination site, by regulating IL-13 signalling to induce the desired protective immune outcome needed according to the target pathogen (bacteria, viruses or parasites), may give rise to more efficacious vaccines in the future.

Chapter 4.

Transient inhibition of IL-25 at the lung mucosae can significantly modulate ILC2 development and function.

4.1 Abstract.

Intranasal immunisation with recombinant fowlpox viral vector-based vaccine co-expressing an adjuvant that transiently sequesters IL-25 (FPV-HIV-IL-25BP) at the vaccination site was shown to induce ST2/IL-33R⁺, IL-25R⁺, and TSLPR⁺ ILC2 subsets in lung unlike unadjuvanted vaccine which only induced ST2/IL-33R⁺ ILC2. At 24 h post vaccination, all these lung ILC2 subsets expressed significantly different levels of IL-13, and the TSLPR⁺ ILC2 subset also expressed IL-4. Surprisingly, sequestration of IL-33 did not have any impact on lung ILC function, although the major ILC2 subset in lung following i.n. vaccination was ST2/IL-33R⁺ (Chapter 3), thus the current data suggest that during early lung ILC2 development cytokine IL-33 may not play an important role as IL-25. Interestingly, FPV-HIV-IL-25BP adjuvanted vaccination also induced elevated IL-17A and IFN- γ expression by ILC1/ILC3 in lung, suggesting that the level of ILC2-derived IL-13 in the milieu, can regulate ILC1/ILC3. Moreover, sequestration of IL-25 induced a uniquely different lineage⁻ ST2/IL-33R⁻ IL-25R⁻ TSLPR⁻ ILC2 population that expressed elevated IL-13 and IL-4. Taken together with previous findings, where elevated IL-4/IL-13 has been associated with induction of low avidity T cells following viral vector vaccination, current observations suggest that intranasal IL-25BP adjuvant delivery may promote the development of low avidity T cells. Collectively, these inhibitor studies indicate that IL-25 plays a more predominant role in early ILC development than IL-33, suggesting that IL-25 may be the master regulator of ILC at the lung mucosae.

4.2 Introduction.

The discovery of ILC2s began with the identification of a new subset of cells in RAG-deficient mice (lacking B cells and T cells) that produced IL-5 and IL-13 in response to IL-25²⁴⁴. After a decade of research, in 2010, a group of type 2 cytokine-producing cells

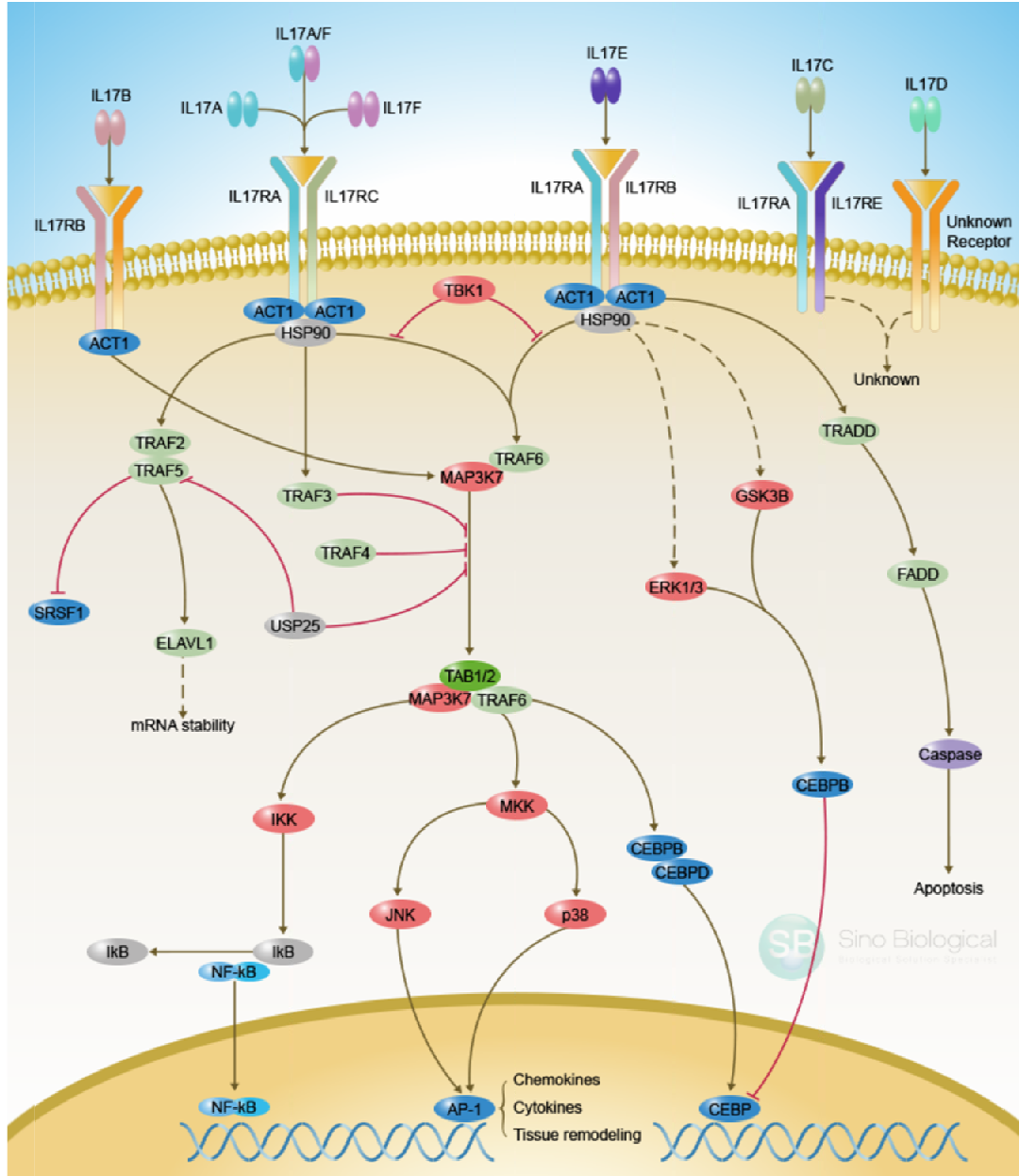
which have the ability to produce IL-5 and IL-13 in response to IL-25 and IL-33 were identified and named as ILC2^{134, 135, 136}. Later studies characterised these ILC2s into three different subsets (IL-33R/ST2⁺, IL-25R⁺, and TSLPR⁺) depending on their receptor expression in response to cytokines IL-33, IL-25, and TSLP^{135, 195, 245, 246, 247}. Interestingly, large number of studies have now shown that IL-33, IL-25, and TSLP differentially modulate ILC2 activity. Specifically, in the context of tissue remodelling, allergy, and inflammation.^{134, 135, 144, 145, 149, 194, 248}

Chapter 3, studies established that intranasal vaccination with rFPV induced IL-33R/ST2⁺ ILC2 in the lung, whereas intramuscular rFPV vaccination induced IL-25R⁺ ILC2 in muscle. In naïve BALB/c lung only IL-33R/ST2⁺ ILC2 were detected, however neither IL-33R/ST2⁺ nor IL-25R⁺ ILC2 subsets were detected in naïve BALB/c muscle. These results indicated that IL-33R/ST2⁺ ILC2 are resident ILC in the lung mucosae, while IL-25R⁺ ILC2 are more likely ‘inflammatory’ ILC2 that migrate to muscle from blood²¹³. The inflammatory ILC2 are characterized by their high expression of the maturation marker KLRG1 and the IL-25R but not IL-33R/ST2²¹³. In addition, these inflammatory ILC2 have not only shown to play an important role in mediating anti-helminth immunity, they also have shown to express RORγt and produce IL-17 in *Candida albicans* infection²¹³ which has indicated that there is high plasticity between ILC2 and ILC3. Interestingly, the IL-33R/ST2⁻ IL-25R⁺ inflammatory ILC2s have also shown to develop into IL-33R/ST2⁺ ILC2s both in vivo and in vitro under certain conditions²¹³. Taken together these observations, we postulate that IL-25R⁺ ILC may be the precursor ILC that differentiate into ILC1, ILC2, and ILC3 under different stimulatory conditions.

Therefore, to further understand the role of IL-33 and IL-25 in ILC development specifically in the context of intranasal vaccination, in this study two novel rFPV vaccines were constructed to transiently inhibit IL-33 and IL-25 activity at the vaccination site, the lung mucosae. i) FPV-HIV-IL-33BP vaccine that co-expressed HIV antigen together with an IL-33 binding protein, that can sequester IL-33 temporarily at the vaccination site, and ii) FPV-HIV-IL-25BP vaccine that co-expressed HIV antigen together with an IL-25 binding protein, that can sequester IL-25 temporarily at the vaccination site (**Fig 4.1**). Knowing that IL-33R/ST2⁺ ILC2s were only detected in lung and IL-25R⁺ ILC2s were only observed in muscle following vaccination (Chapter 3), when WT BALB/c mice were intranasally vaccinated with FPV-HIV-IL-33BP, no differences in ILC recruitment or cytokine expression were observed in lung. However, when mice were vaccinated intramuscularly with FPV-HIV-IL-25BP adjuvanted vaccine, significantly different ILC and cytokine profiles were detected (Jackson and Ranasinghe unpublished observations). These findings indicated that IL-25 most likely play a more important role in modulating ILC development and function than IL-33. Therefore, to understand this process further, specifically to establish how IL-25 cytokine impact development of lung and muscle ILC development, in this study, rFPV vaccine co-expressing the IL-25R (FPV-HIV-IL-25RBP), was delivered intranasally and ILC and their cytokine expression profiles were evaluated 24 h post vaccination (This time point was chosen as in Chapter 3, data clearly established that ILC were significantly modulated at 24 h post viral vector vaccination).

Fig. 4.1 IL-17 signaling pathway.

The IL-17 family consists of six members IL-17A-F, while the IL-17 receptor family consists of five members IL-17RA to IL-17RE. IL-17RA is a common receptor that forms heterodimeric complexes with IL-17RB, IL-17RC, and IL-17RE. IL-17A and IL-17F signals through the IL-17RA-RC complex, triggering TRAF6-dependent target gene transcription. IL-17E (IL-25) signaling through the IL-17RA-RB receptor complex induces Th2 responses by activating MAPK and NF- κ B pathways.



Adapted from Sino Biological

4.3 Materials and Methods.

4.3.1 Mice and immunisation.

5-6 weeks old pathogen free female WT BALB/c mice were obtained from the Australian Phenomics Facility, the Australian National University, and were maintained and handled under protocols indicated in **2.2.1**. 1×10^7 PFU unadjuvanted FPV-HIV, and FPV-HIV-IL-25BP adjuvanted vaccines prepared as per described in **2.2.3** and **2.2.4** were administered to WT BALB/c mice (n = 6 per group) intranasally, under mild isoflurane anaesthesia as per described in **2.2.5**. Lungs were harvested in 2 ml of complete RPMI 24 h post immunisation, and single cell suspension was prepared as per described in **2.2.6**.

4.3.2 Surface and intracellular staining.

Surface and intracellular staining were performed as per described in **2.2.8**, using antibodies details in **Table 2.3**. Specifically,

ST2/IL-33R⁺ and IL-25R⁺ ILC2 staining: APC/Cy7-conjugated anti-mouse CD45, and FITC-conjugated lineage cocktail were used to identify the lineage⁻ cells. PE-conjugated anti-mouse ST2/IL-33R, and APC-conjugated anti-mouse IL-25R were used to identify the different ILC2 subsets. Brilliant Violet 421-conjugated anti-mouse IL-4 and PE-eFlour 610-conjugated anti-mouse IL-13 were used to evaluate intracellular expression of these cytokines in ILC2. The gating strategy indicated in **Fig. 2.3** was used to identify the different ILC2 subsets and their cytokine expression.

ST2/IL-33R⁺ & TSLPR⁺ ILC2 staining: APC/Cy7-conjugated anti-mouse CD45, and FITC-conjugated lineage cocktail were used to identify the lineage⁻ cells as per before. PerCP/Cy5.5-conjugated anti-mouse ST2/IL-33R, and APC-conjugated anti-mouse TSLPR were used to identify different ILC2 subsets. (In this staining cocktail, since the

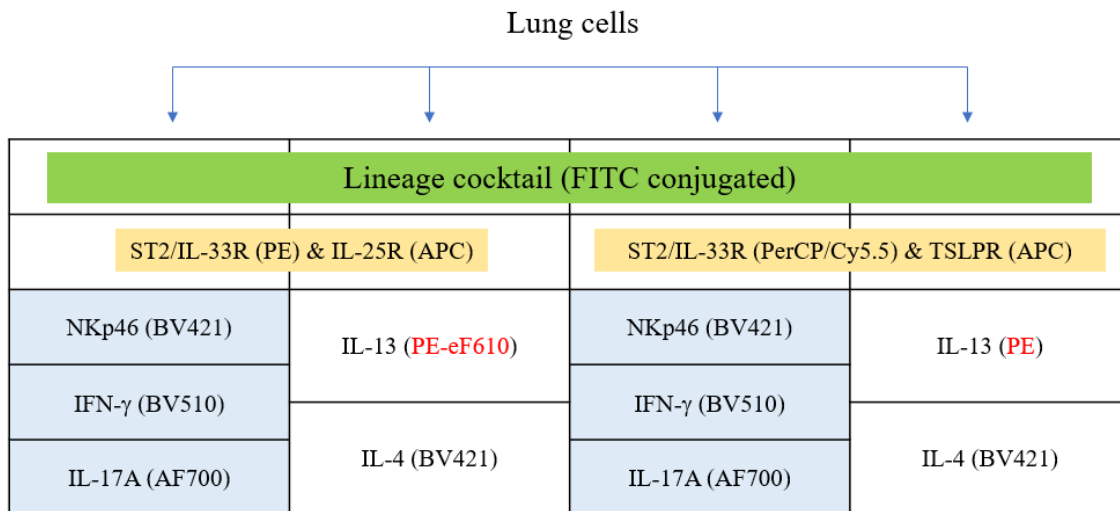
TSLPR antibody was found to interact with PE-conjugated anti-mouse ST2/IL-33R antibody, PerCP/Cy5.5-conjugated anti-mouse ST2/IL-33R was used). To avoid spectral overlap, Brilliant Violet 421-conjugated anti-mouse IL-4 and PE-conjugated anti-mouse IL-13 were used to evaluate the intracellular cytokine expression in ILC2.

ILC1 and ILC3 staining: APC/Cy7-conjugated anti-mouse CD45, and FITC-conjugated lineage cocktail were used to identify lineage⁻ cells. PE-conjugated anti-mouse ST2/IL-33R, and Brilliant Violet 421-conjugated anti-mouse CD335 (NKp46) were used to identify the ILC1 and ILC3 populations. Brilliant Violet 510-conjugated anti-mouse IFN- γ , APC-conjugated anti-mouse IL-22, and Alexa Fluor 700-conjugated anti-mouse IL-17A were used to evaluate the intracellular cytokine expression in ILC1 and ILC3 subsets.

Staining strategy of the novel ST2/IL-33R⁻ IL-25R⁻ TSLPR⁻ ILC2 subset:

1x10⁶ lung cells were stained in four different wells using range of fluorochromes as per indicated in the **flow chat 4.1**. Specifically, IL-25R and TSLPR were stained separately to avoid spectral overlap using PE-conjugated ST2/IL-33R and PerCP/Cy5.5-conjugated ST2/IL-33R respectively. (In this staining cocktail, as the TSLPR antibody was found to interact with PE-conjugated anti-mouse ST2/IL-33R antibody, PerCP/Cy5.5-conjugated anti-mouse ST2/IL-33R was used). IL-13 and IL-4 expression in all known ILC2 subsets (ST2/IL-33R⁺, IL-25R⁺, and TSLPR⁺), including the lineage⁻ ST2/IL-33R⁻ IL-25R⁻ TSLPR⁻ population were evaluated. NKp46, IFN- γ , and IL-17A were also stained to established that ILC1 and ILC3 cells did not express IL-4 or IL-13

Flowchart 4.1: ST2/IL-33R⁻ IL-25R⁻ TSLPR⁻ ILC2 staining strategy.



4.4 Results.

4.4.1 Following i.n. FPV-IL-25BP vaccination lineage⁻ IL-33R/ST2⁻ IL-25R⁺ and lineage⁻ IL-33R/ST2⁻ TSLPR⁺ ILC2 subsets were recruited to the lung mucosae.

WT BALB/c mice were vaccinated intranasally with the unadjuvanted FPV-HIV vaccine or the FPV-HIV IL-25BP adjuvanted vaccine (which sequestered IL-25 at the vaccination site). As ILC subsets were shown to be manipulated mainly at 24 h post vaccination (Chapter 3), in this study, different ILC subsets and their cytokines expression were evaluated only at 24 h post vaccination. Data indicated that while the unadjuvanted vaccine only induced lineage⁻ IL-33R/ST2⁺ ILC2 in lung (**Fig. 4.2a**), the FPV IL-25BP adjuvanted vaccine not only induced lineage⁻ IL-33R/ST2⁺ ILC2s but also induced lineage⁻ IL-33R/ST2⁻ IL-25R⁺ and lineage⁻ IL-33R/ST2⁻ TSLPR⁺ ILC2 subsets in the lung mucosae (**Fig. 4.2a**). Although no significant differences in the lineage⁻ IL-33R/ST2⁺ ILC2 cell numbers were observed between unadjuvanted control and IL-25BP adjuvanted vaccination (**Fig. 4.2b**), significantly elevated numbers of lineage⁻ IL-33R/ST2⁻ IL-25R⁺ ILC2 (p=0.0004) (**Fig. 4.2c**) and

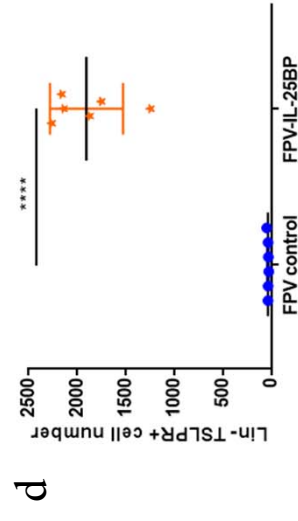
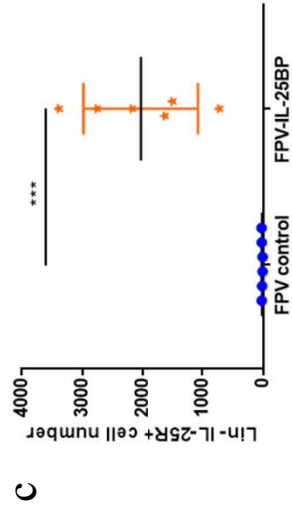
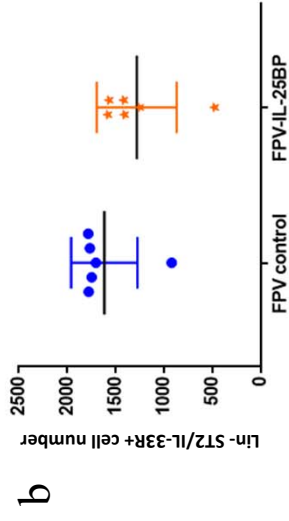
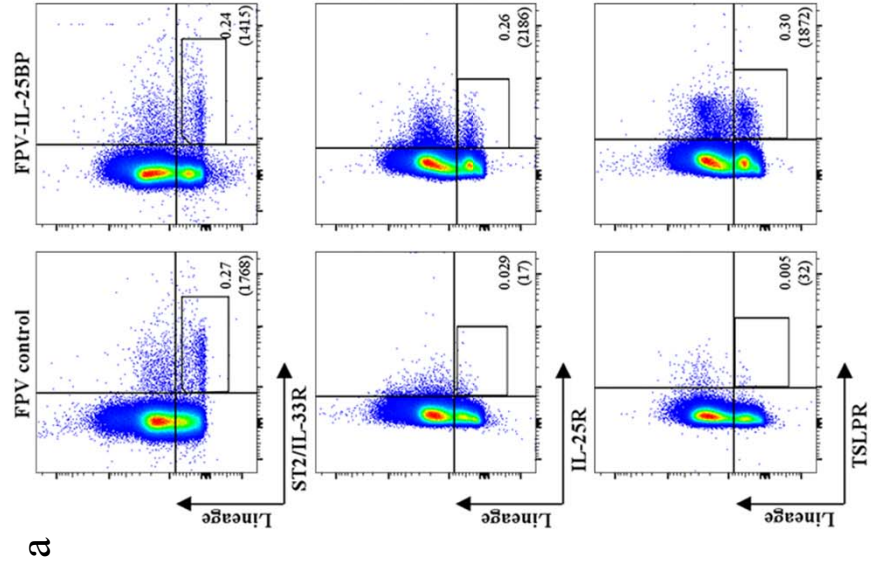


Fig. 4.2. Evaluation of lung lineage⁻ ILC2 subsets in WT BALB/c mice following intranasal IL-25BP adjuvanted vaccination.

WT BALB/c (each group n = 6) were immunized intranasally with unadjuvanted FPV-H1V vaccine or IL-25BP adjuvanted vaccine. Using the flow cytometry gating strategy indicated in materials and methods, ILC2s were defined as CD45⁺ FSC^{low} SSC^{low} Lin⁻ IL-33R/ST2⁺, CD45⁺ FSC^{low} SSC^{low} Lin⁻ IL-25R⁺, or CD45⁺ FSC^{low} SSC^{low} Lin⁻ TSLPR⁺ cells. The FACS plots indicate the percentage of different lung ILC2 subsets (lineage⁻ IL-33R/ST2⁺, lineage⁻ IL-25R⁺, and lineage⁻ TSLPR⁺) at 24 h post vaccination, the number of cells in each quadrant is indicated within brackets below the cell percentage **(a)**. Graph represents number of lineage⁻ IL-33R/ST2⁺ ILC2s back calculated to CD45⁺ population as described in materials and methods at 24 h post vaccination **(b)**. Graph represents number of lineage⁻ IL-33R/ST2⁻ IL-25R⁺ ILC2s back calculated to CD45⁺ population as described in materials and methods at 24 h post vaccination **(c)**. Graph represents number of lineage⁻ IL-33R/ST2⁻ TSLPR⁺ ILC2s back calculated to CD45⁺ population as described in materials and methods at 24 h post vaccination **(d)**. The error bars represent the mean and standard deviation (s.d.). The p-values were calculated using GraphPad Prism software (version 6.05 for Windows). * = p<0.05, ** = p<0.01, *** = p<0.001, **** = p<0.0001. For each group experiments were repeated minimum three times.

lineage⁻ IL-33R/ST2⁻ TSLPR⁺ ILC2 ($p < 0.0001$) (**Fig. 4.2d**) were observed in FPV-IL-25BP vaccinated group compared to the unadjuvanted control.

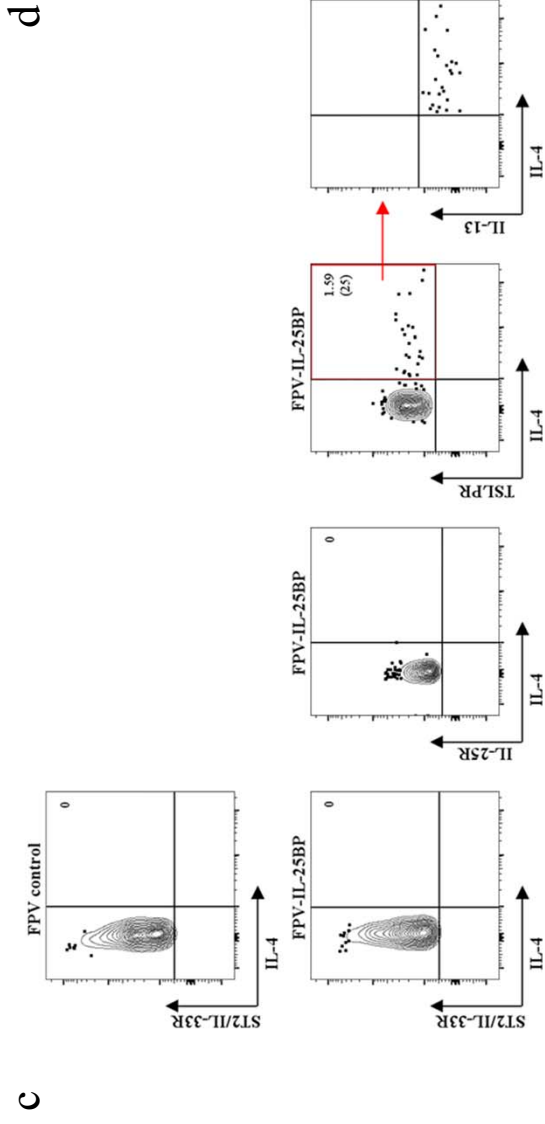
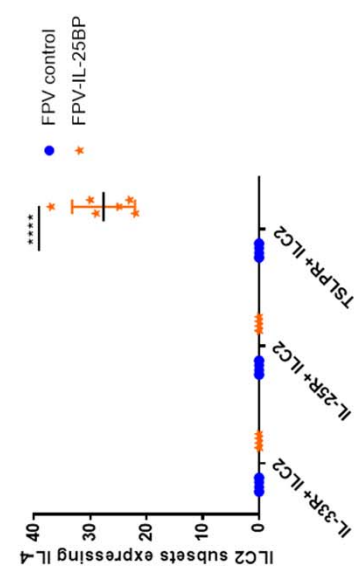
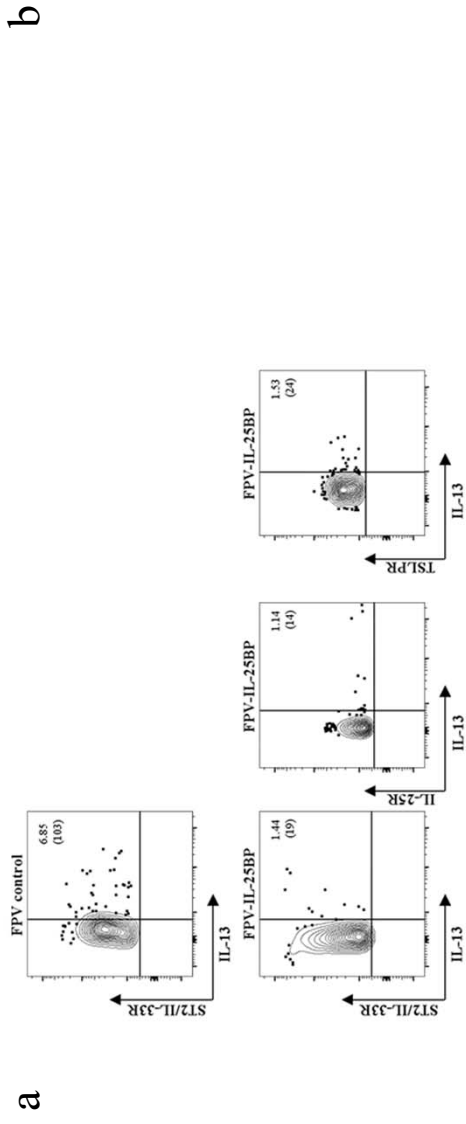
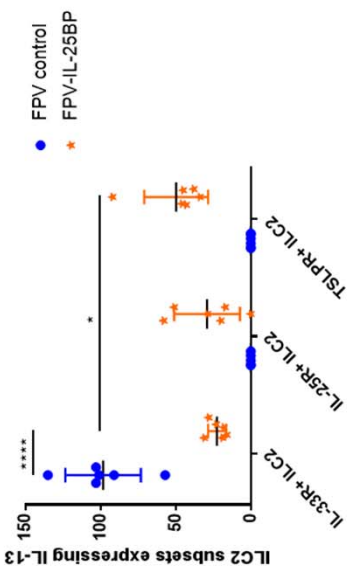
4.4.2 Following FPV-IL-25BP vaccination distinctive IL-13 and IL-4 expression profiles were detected in the different lung ILC2 subsets.

Next when IL-13 expression in ILC2 subsets was evaluated, post intranasal FPV-HIV-IL-25BP vaccination, all three ILC2 subsets (IL-33R/ST2⁺ ILC2, IL-25R⁺ ILC2 and TSLPR⁺ ILC2) were shown to express IL-13 (**Fig. 4.3a**). Specifically, compared to the unadjuvanted vaccine group, FPV-HIV-IL-25BP adjuvanted group showed significantly reduced IL-13 expression by IL-33R/ST2⁺ ILC2s ($p < 0.0001$) (**Fig. 4.3b**). In contrast, IL-13 expression in IL-33R/ST2⁻ IL-25R⁺ and IL-33R/ST2⁻ TSLPR⁺ ILC2 subsets (which were not observed following unadjuvanted vaccination) were significantly elevated (**Fig. 4.3b**). Interestingly, in mice given FPV-HIV-IL-25BP vaccination, IL-33R/ST2⁻ TSLPR⁺ ILC2s showed significantly elevated IL-13 expression compare to IL-33R/ST2⁺ ILC2 subset ($p = 0.0126$) (**Fig. 4.3b**).

All vaccines tested in Chapter 3 (specifically vaccine that transient inhibited IL-4/IL-13) did not show any IL-4 expression by IL-33R/ST2⁺ ILC2s. However interestingly, following intranasal FPV-HIV-IL-25BP adjuvanted vaccination, elevated IL-4 expression was detected in lineage⁻ IL-33R/ST2⁻ TSLPR⁺ ILC2, but not the other two ILC2 subsets (**Fig. 4.3c & d**). The IL-33R/ST2⁻ TSLPR⁺ ILC2 subset that expressed IL-13 were not positive for IL-4 (**Fig. 4.3c**).

Fig. 4.3. Evaluation of IL-13 and IL-4 expression by different ILC2 subsets in WT BALB/c mice following intranasal IL-25BP adjuvanted vaccination.

The three different ILC2 subsets were further analysed for IL-13 and IL-4 expression. The FACS plots indicate the representative plots from WT BALB/c mice vaccinated with unadjuvanted control FPV-HIV vaccine and IL-25BP adjuvanted vaccine at 24 h post vaccination **(a)**. The graph represents IL-13 expression by different ILC2 subsets, cell numbers were back calculated to CD45⁺ population as described in materials and methods **(b)**. The FACS plots indicate the representative plots from WT BALB/c mice vaccinated with unadjuvanted control FPV-HIV vaccine and IL-25BP adjuvanted vaccine at 24 h post vaccination **(c)**. The graph represents IL-4 expression by different ILC2 subsets, cell numbers were back calculated to CD45⁺ population as described in materials and methods **(d)**. The error bars represent the mean and standard deviation (s.d.). The p-values were calculated using GraphPad Prism software (version 6.05 for Windows). * = p<0.05, ** = p<0.01, *** = p<0.001, **** = p<0.0001. For each group experiments were repeated minimum three times.



4.4.3 Following FPV-HIV-IL-25BP vaccination lineage⁻ IL-33R/ST2⁻ NKp46^{+/-} ILCs were found to express IFN- γ and IL-17A.

When lineage⁻ IL-33R/ST2⁻ NKp46⁺ ILCs in lung were assessed 24 h post intranasal FPV-HIV-IL-25BP adjuvanted vaccination, significantly elevated numbers of lineage⁻ IL-33R/ST2⁻ NKp46⁺ ILCs were observed compared to the unadjuvanted vaccine (**Fig. 4.4a**). The lineage⁻ IL-33R/ST2⁻ NKp46⁺ ILCs obtained from the IL-25BP adjuvanted vaccinated group expressed elevated IFN- γ compared to unadjuvanted vaccine group, $p < 0.0001$) (**Fig. 4.4b**), and more interestingly, were also found to express elevated IL-17A (**Fig. 4.4c**). Unlike IFN- γ and IL-17A, in the context of IL-22 expression, FPV-HIV-IL-25BP adjuvanted vaccine showed significantly reduced IL-22 expression by lineage⁻ IL-33R/ST2⁻ NKp46⁺ ILC compared to the unadjuvanted vaccine ($p < 0.001$) (**Fig. 4.4d**).

Next when the lineage⁻ IL-33R/ST2⁻ NKp46⁻ ILCs were assessed following intranasal FPV-HIV-IL-25BP vaccination, most of the lineage⁻ IL-33R/ST2⁻ cells were found to be NKp46⁻ (**Fig. 4.5a**). However, unlike the lineage⁻ IL-33R/ST2⁻ NKp46⁺ cells, there were no significant differences in the lineage⁻ IL-33R/ST2⁻ NKp46⁻ ILCs cell numbers (**Fig. 4.5a**) and their IFN- γ expression between the adjuvanted and unadjuvanted groups (**Fig. 4.5b**). Interestingly, similar to the lineage⁻ IL-33R/ST2⁻ NKp46⁺ cells, elevated IL-17A expression was detected in the lineage⁻ IL-33R/ST2⁻ NKp46⁻ ILCs following FPV-HIV-IL-25BP vaccination (**Fig. 4.5c**). In contrast, significantly reduced IL-22 expression ($p < 0.0001$) was detected in lineage⁻ IL-33R/ST2⁻ NKp46⁻ ILCs (**Fig. 4.5d**).

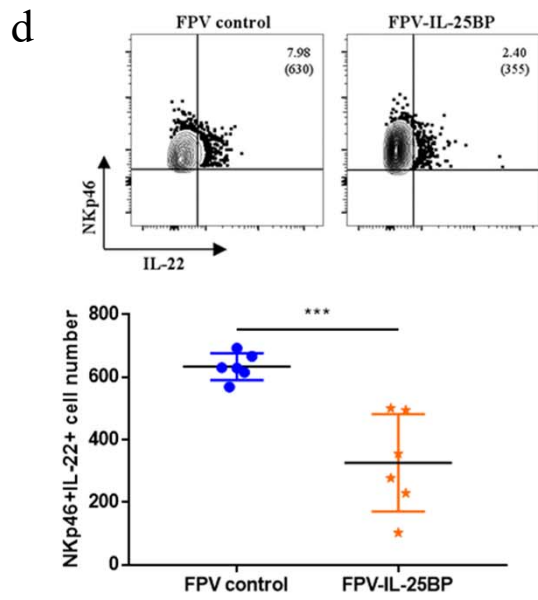
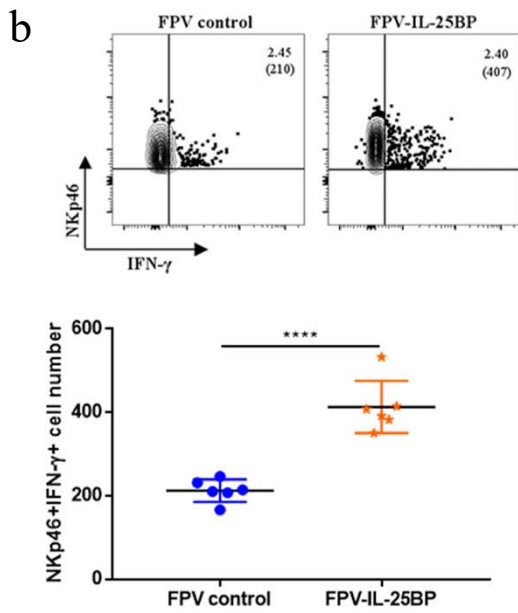
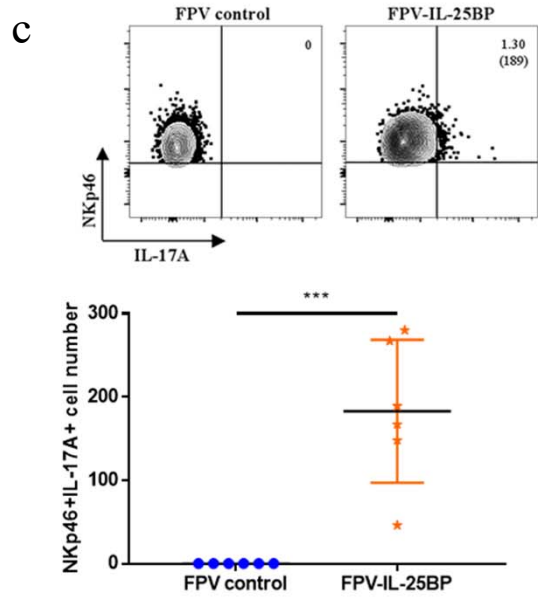
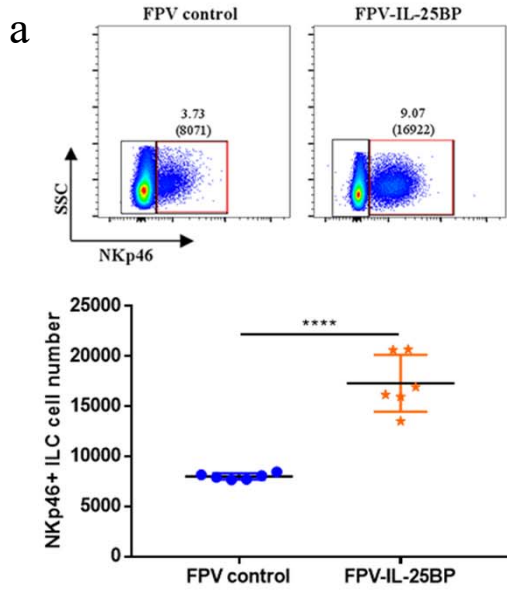


Fig. 4.4. Evaluation expression of IFN- γ , IL-22 and IL-17A by lineage⁻ IL-33R/ST2⁻ NKp46⁺ ILC in WT BALB/c mice following intranasally IL-25BP adjuvanted FPV vaccination.

WT BALB/c mice (each group n = 6) were immunized intranasally with unadjuvanted FPV-HIV vaccine or IL-25BP adjuvanted FPV vaccine. As described in materials and methods, NKp46⁺ ILCs were gated as CD45⁺ FSC^{low} Lin⁻ ST2⁻ NKp46⁺. The representative FACS plots of lineage⁻ IL-33R/ST2⁻ NKp46⁺ ILC for each vaccine group at 24 h post vaccination **(a)**. The graph represents number of lineage⁻ IL-33R/ST2⁻ NKp46⁺ ILC back calculated to CD45⁺ cells as per indicated in materials and methods. After lineage⁻ IL-33R/ST2⁻ NKp46⁺ ILC were gated, their IFN- γ , IL-22 and IL-17A expression were evaluated using intracellular cytokine staining. The FACS plots are representative plots for lineage⁻ IL-33R/ST2⁻ NKp46⁺ ILC IFN- γ **(b)**, IL-22 **(c)** and IL-17A **(d)** expression in each group. The graphs indicate the number of IFN- γ **(b)**, IL-22 **(c)** and IL-17A **(d)** expressing lineage⁻ IL-33R/ST2⁻ NKp46⁺ ILC in WT BALB/c mice immunized with different vaccines. The error bars represent the mean and standard deviation (s.d.). The p-values were calculated using GraphPad Prism software (version 6.05 for Windows). * = p<0.05, ** = p<0.01, *** = p<0.001, **** = p<0.0001. For each group experiments were repeated minimum three times.

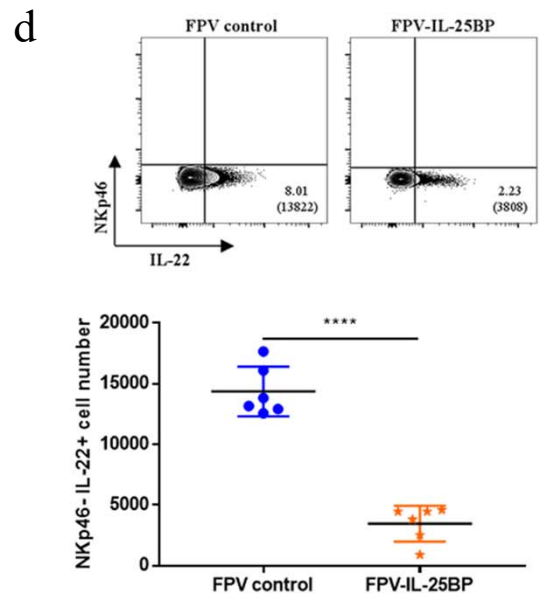
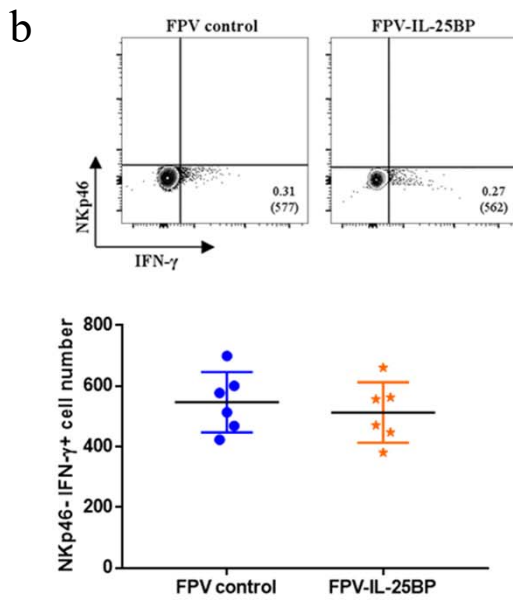
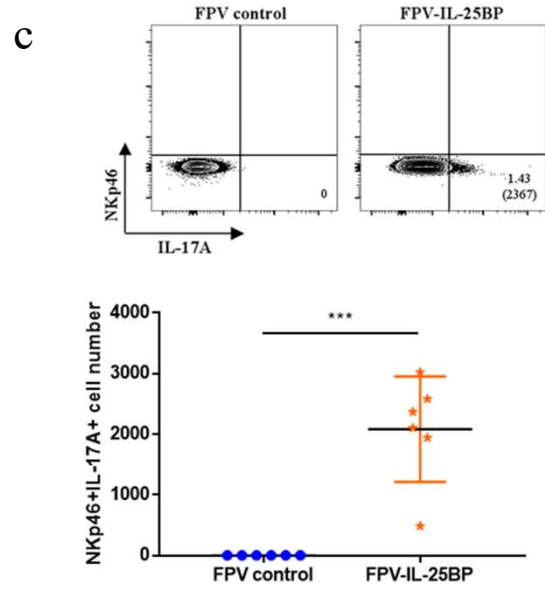
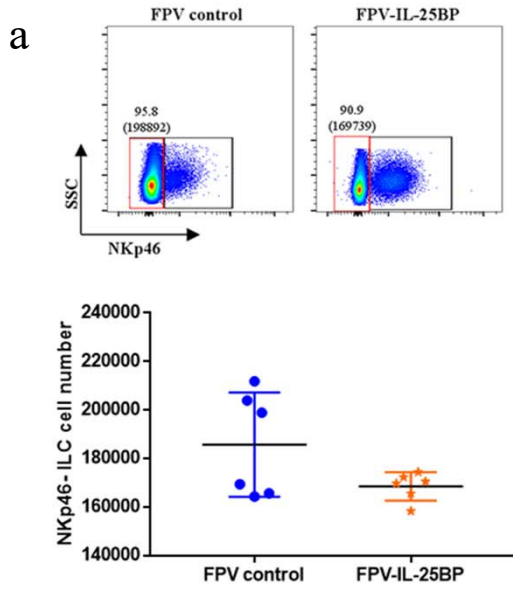


Fig. 4.5. Evaluation expression of IFN- γ , IL-22 and IL-17A by lineage⁻ IL-33R/ST2⁻ NKp46⁻ ILC in WT BALB/c mice following intranasally IL-25BP adjuvanted FPV vaccination.

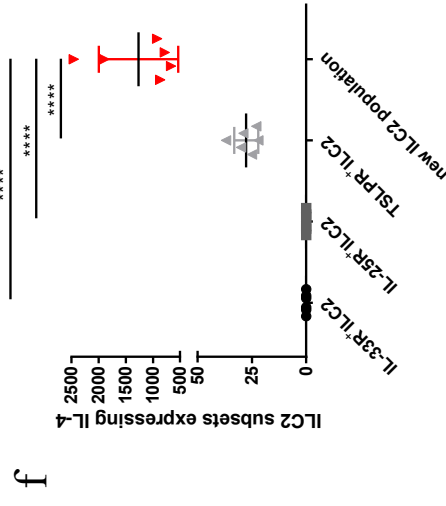
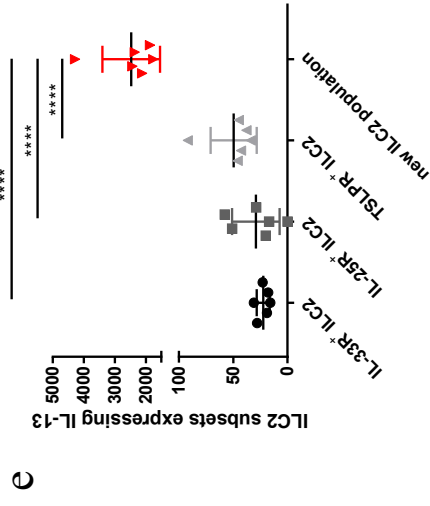
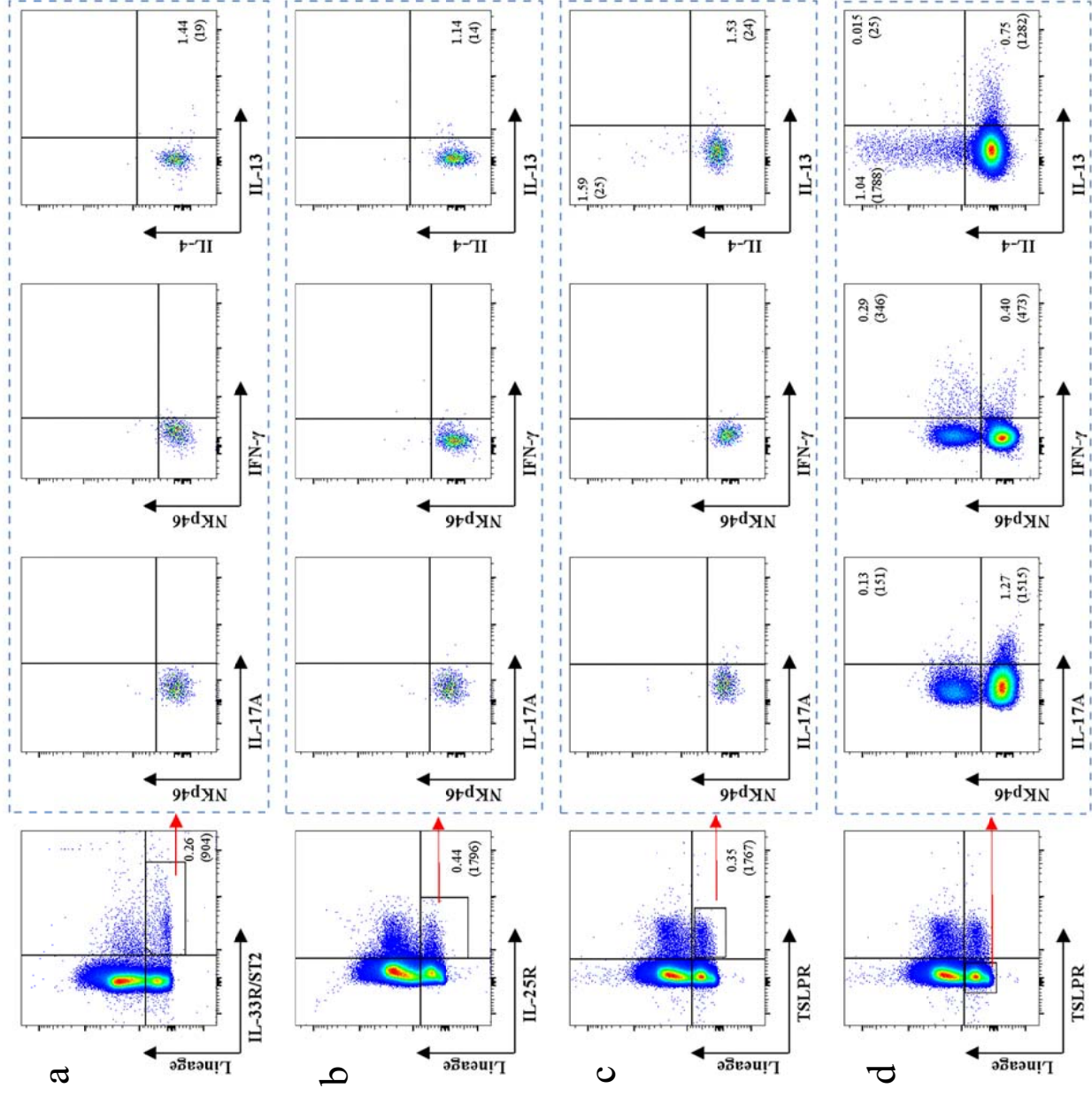
WT BALB/c mice (each group n = 6) were immunized intranasally with unadjuvanted FPV-HIV vaccine or IL-25BP adjuvanted FPV vaccine. As described in materials and methods, NKp46⁻ ILCs were gated as CD45⁺ FSC^{low} SSC^{low} Lin⁻ ST2⁻ NKp46⁻. The representative FACS plots of lineage⁻ IL-33R/ST2⁻ NKp46⁻ ILC for each vaccine group at 24 h post vaccination **(a)**. The graph represents number of lineage⁻ IL-33R/ST2⁻ NKp46⁻ ILC back calculated to CD45⁺ cells as per indicated in materials and methods. After lineage⁻ IL-33R/ST2⁻ NKp46⁻ ILC were gated, their IFN- γ , IL-22 and IL-17A expression were evaluated using intracellular cytokine staining. The FACS plots are representative plots for lineage⁻ IL-33R/ST2⁻ NKp46⁻ ILC IFN- γ **(b)**, IL-22 **(c)** and IL-17A **(d)** expression in each group. The graphs indicate the number of IFN- γ **(b)**, IL-22 **(c)** and IL-17A **(d)** expressing lineage⁻ IL-33R/ST2⁻ NKp46⁻ ILC in WT BALB/c mice immunized with different vaccines. The error bars represent the mean and standard deviation (s.d.). The p-values were calculated using GraphPad Prism software (version 6.05 for Windows). * = p<0.05, ** = p<0.01, *** = p<0.001, **** = p<0.0001. For each group experiments were repeated minimum three times.

4.4.5 Following intranasal FPV-HIV-IL-25BP vaccination a novel lineage⁻ IL-33R/ST2⁻ IL-25R⁻ TSLPR⁻ ILC2 cell subset expressing IL-13 and IL-4 was discovered.

FPV-HIV-IL-25BP adjuvanted vaccination induced all three known ILC2 subsets (lineage⁻ IL-33R/ST2⁺, lineage⁻ IL-33R/ST2⁻ IL-25R⁺ and lineage⁻ IL-33R/ST2⁻ TSLPR⁺), and they were found to express IL-13 and the TSLPR⁺ subset also expressed IL-4. As expected, these ILC2 subsets did not express IL-17A or IFN- γ (**Fig. 4.6a-c**). Surprisingly, in the lineage⁻ IL-25R⁻ IL-33R/ST2⁻ TSLPR⁻ cell population, group of cells were found not only to express IL-13 but also IL-4. In this subset, the IL-4/IL-13 expression was much greater than the other three ILC2 subsets ($p < 0.0001$) (**Fig. 4.6d-f**). A small subset was also found to be double positive for both IL-13 and IL-4 (**Fig. 4.6d**). These observations suggested that lineage⁻ IL-25R⁻ IL-33R/ST2⁻ TSLPR⁻ population could contain a not yet defined ILC2 subset. In this analysis the lineage⁻ IL-33R/ST2⁻ TSLPR⁻ NKp46⁺ and NKp46⁻ cells that produced IL-17A and IFN- γ were most likely classic ILC1 and ILC3, not ILC2 as none of the known ILC2s express these two cytokines (**Fig. 4.6d**).

Fig. 4.6 Evaluation IL-17A, IFN- γ , IL-13 and IL-4 cytokines expression in lineage IL-33R/ST2⁺, lineage IL-33R/ST2-IL-25R⁺, lineage IL-33R/ST2-TSLPR⁺ and lineage IL-33R/ST2-TSLPR⁻ population following intranasally IL-25BP adjuvanted FPV vaccination.

WT BALB/c mice (each group n = 6) were immunized intranasally with IL-25BP adjuvanted FPV vaccine. Lineage IL-33R/ST2⁺, lineage IL-33R/ST2-IL-25R⁺, lineage IL-33R/ST2-TSLPR⁺ and lineage IL-33R/ST2-TSLPR⁻ cells were gated as described in materials and methods. Their IL-17A, IFN- γ , IL-13 and IL-4 expression were evaluated using intracellular cytokine staining. The FACS plots are representative plots for IL-17A, IFN- γ , IL-13 and IL-4 expression by lineage IL-33R/ST2⁺ (**a**), lineage IL-33R/ST2-IL-25R⁺ (**b**), lineage IL-33R/ST2-TSLPR⁺ (**c**), and lineage IL-33R/ST2-TSLPR⁻ cells (**d**). The graph represents IL-13 (**e**) and IL-4 (**f**) expression by different ILC2 subsets, cell numbers were back calculated to CD45⁺ population as described in materials and methods. The error bars represent the mean and standard deviation (s.d.). The p-values were calculated using GraphPad Prism software (version 6.05 for Windows). * = p<0.05, ** = p<0.01, *** = p<0.001, **** = p<0.0001. For each group experiments were repeated minimum three times.



e

f

4.5 Discussion.

Following intranasal FPV-HIV-IL-25BP vaccination, where IL-25 was temporarily sequestered from the vaccination site, significant impact on ILC development/function in lung mucosae were observed, similar to that of muscle following intramuscular vaccination. Specifically, in relation to lung ILC2, not only ST2/IL-33⁺ ILC2, but also IL-25R⁺, TSLPR⁺ ILC2 and also a unique lineage⁻ IL-33R/ST2⁻ IL-25R⁻ TSLPR⁻ ILC2 subsets that expressed IL-13 or IL-4 were detected 24 h post vaccination, unlike mice given the unadjuvanted FPV-HIV vaccination. Interestingly, knowing that sequestration of IL-33 (FPV-HIV-IL-33BP adjuvanted vaccine) had no impact on ILC2 development/function in lung, although the major ILC2 subset in lung following i.n. vaccination was ST2/IL-33R⁺ (Chapter 3), these unexpected finding suggested a hierarchical role of IL-25 in ILC2 development compared to IL-33.

Different ILC2 subsets arise from a common progenitor cell and under different cytokine conditions/anatomical location differentiate into ILC2 that are IL-33R⁺, IL-25R⁺ or TSLPR⁺^{232, 249}. Chapter 3 studies have shown that in naïve mice, IL-33R/ST2⁺ ILC2 are the resident ILC population in lung, while IL-25R⁺ ILC2 (which are known as the “inflammatory” ILC²¹³) were recruited to the muscle only following i.m. vaccination. Current study demonstrated that transient inhibition of IL-25 at the vaccination site can promote some ILC2s at the lung mucosae to express both IL-13 as well as IL-4. Interestingly, the IL-4 expressing ILC2s induced by FPV-HIV-IL-25BP adjuvanted vaccination did not express IL-13, suggesting that these were two distinct ILC2 populations. Recent studies have also shown that addition of IL-25 and IL-33 can promote differential cytokine expression by lung IL-33R/ST2⁺ ILC2. For example, when lung IL-33R/ST2⁺ ILC2 were cultured in the presence of IL-25 in vitro, these cells were shown to produce elevated IL-13 but reduced IL-5 whereas the inverse was

reported when cells were cultured in the presence of IL-33^{250, 251}. Furthermore, *Chen et al* using IL-13-GFP reporter mice have also shown that compared to IL-33, intranasal administration of recombinant IL-25 can induce elevated IL-13 expression by lung ILC2²⁵⁰. Interestingly, the current study demonstrated that removal of IL-25 from the cell milieu can have a much profound impact on ILC2 differentiation (induction of range of ILC2 subsets) including IL-13/IL-4 expression by these ILC2s, unlike overexpression of IL-25. These observations further support the notion that IL-25 may play a more important role in ILC2 development in lung than IL-33.

Our previous studies have shown that mucosal vaccination induced high avidity CD8⁺ T cells and this was associated with low level of IL-13 expressed by T cells⁷⁷. In contrast, systemic vaccination induced low avidity CD8⁺ T cells associated with elevated level of IL-13⁷⁷. Transient inhibition of IL-4 and IL-13 at the vaccination site has shown to induce i) T cells of high avidity and ii) unlike IL-13R α 2 adjuvanted vaccination IL-4R antagonist vaccination has also shown to induce excellent antibody differentiation^{113, 122}, suggesting IL-13 plays an important role in modulating both T and B cell immunity^{78, 79}. These studies also showed that level of IL-4/IL-13 at the vaccination site can significantly alter the activity of antigen presenting cells¹²³. When trying to dissect which cells at the vaccination site produced IL-13, Chapter 3 studies have clearly established that ILC2 are the major source of IL-13 at the vaccination site 24 h post viral vector vaccination. Interestingly, low IL-4/IL-13 levels were associated with recruitment of CD11b⁺ CD103⁻ conventional DCs, and induction of high avidity HIV-specific CD8⁺ T cells¹²³. Intranasal FPV-HIV-IL-25BP adjuvanted vaccination was shown to induce significantly elevated level of both IL-4 and IL-13 by ILC2 at the lung mucosae 24 h post vaccination. Taken together our previous findings and the elevated IL-13 observed following intranasal FPV-HIV-IL-25BP adjuvanted vaccination, data

suggest that sequestration of IL-25 at the lung mucosae may be detrimental for the induction of high avidity T cells. However, intramuscular FPV-HIV-IL-25BP vaccination significantly inhibited both IL-4 and IL-13 expression by ILC2 in muscle (Jackson and Ranasinghe unpublished data), suggesting that IL-25BP could be a highly efficacious intramuscular but not an intranasal adjuvant.

Interestingly, FPV-HIV-IL-25BP adjuvanted vaccination not only manipulated the ILC2 differentiation/function but also ILC1 and ILC3 at the vaccination site. This was highly unexpected as cytokine IL-25 was thought to be an activator of ILC2 but not ILC1/ILC3²⁴⁹. Surprisingly, compared to the unadjuvanted rFPV vaccination, transient removal of IL-25 at the lung mucosae was induced elevated expression of IL-17A by lineage⁻ IL-33R/ST2⁻NKp46^{+/-} ILC1 and ILC3. Ravichandran *et al.* have previously demonstrated that IL-4 and IL-13 can differentially regulate IL-17A in antigen-specific CD8⁺ T cells²²⁶. As FPV-HIV-IL-25BP vaccination also significantly manipulated IL-4 and IL-13 expression by the different ILC2 subsets (IL-33R/ST2⁺, IL-25R⁺, TSLPR⁺, and the unique lineage⁻ IL-33R/ST2⁻ IL-25R⁻ TSLPR⁻ ILC2 subsets), we postulate that the significant changes in IL-17A production in ILC1/ILC3 could be associated with the high level of IL-4/IL-13 expressed by the different ILC2 subsets, including the novel lineage⁻ IL-33R/ST2⁻ IL-25R⁻ TSLPR⁻ ILC2 subset. Moreover, IL-25 (IL-17E), signals via the IL-25 receptor complex IL-17RA/IL-17RB, and IL-17RA/ IL-17RC is the major receptor complex for IL-17A signaling^{252, 253}(**Fig. 4.1**). Therefore, following IL-25BP vaccination the elevated IL-17A expressed by ILC1/ILC3 could also be associated with the balance of IL-17A and IL-25 signalling. For example; sequestration of IL-25 initiating the IL-17A signalling via NF-κB, Activator Protein 1 (AP-1) and CCAAT-enhancer-binding-protein (C/EBP) pathways (**Fig 4.1**). This could be similar to what has been observed during transient inhibition of IL-13, in which IL-4 signalling via the

STAT6 pathway was initiated^{113, 122}(Chapter 3). The level of IL-13 expressed by ILC2 was also shown to alter the expression of IFN- γ by ILC1 and ILC3 (Chapter 3). Specifically, transient blockage of IL-4/IL-13 signalling via STAT6 pathway, compared to transient inhibition of IL-13 at the vaccination site differentially regulated IL-13 expression by ILC2 and IFN- γ expression by ILC1/ILC3. These findings support the notion that in the context of viral vector vaccination, IL-13 produced by ILC2 could be the master regulator of ILC1 and ILC3 activity, specifically the IFN- γ , IL-17 and also IL-22 expression by these cells 24 h post vaccination.

This study clearly established that manipulating IL-25 at the lung mucosae can have not only dramatic impact on ILC2 and their IL-13/IL-4 expression, but also have significant effects on ILC1/ILC3 cells and their IFN- γ /IL-22/IL-17A production. Several studies, including ours have shown that IL-25 and IL-33 may have different impacts on ILC development and function^{147, 194, 254}. Stier *et al.* have shown that IL-33 plays a crucial role in promoting ILC2 egress from the bone marrow²⁵⁵. Hence, we propose that IL-33 may be critical for ILC homing and trafficking to tissue²⁵⁵, whereas IL-25 may be important for initial ILC development and function. Following IL-25 sequestration, the lineage⁻ IL-33R/ST2⁻ IL-25R⁻ TSLPR⁻ ILC2 population observed, could be an undifferentiated ILC2 subset (i.e. similar to CD4⁻ CD8⁻ T cell development) or a not yet defined ILC2 subset. However, in context given the expression of IL-4 and IL-13 by these cells, the latter explanation appears to be may be more valid. In conclusion, current findings further substantiate that the adjuvants used and the route of delivery play an important role in modulating ILC-driven cytokine expression at the vaccinations site, and these early events need to be seriously taken into consideration when designing effective vaccines against chronic pathogens. Following IL-25 sequestration, as TSLPR⁺ ILC2 were found to express IL-4 and IL-13, it would also be of interest to

study the impact of inhibition or sequestration TSLP at the vaccination site, and this warrants further investigation.

Chapter 5.

Evaluation of ILC subsets in IL-4, IL-13 and STAT6 knockout mice following intranasal rFPV vaccination.

5.1 Abstract.

This study demonstrated that ILC and their cytokine expression profiles (IL-13, IFN- γ and IL-22) were vastly different during permanent (gene knockout) versus transient blockage of IL-13, IL-4, and STAT6 at the vaccination site. STAT6^{-/-} mice given the FPV-HIV vaccine showed elevated ST2/IL-33R⁺ ILC2-driven IL-13 expression whilst reduced IFN- γ expression by both NKp46^{+/+} ILC1/ILC3 24 h post intranasal vaccination. In contrast, when STAT6 signalling was transiently blocked in BALB/c mice using FPV-HIV-IL-4R antagonist vaccination, the opposing effect was observed, eliciting high IFN- γ expression. When IL-13^{-/-} mice were vaccinated with FPV-HIV significantly elevated lung lineage⁻ ST2/IL-33R⁺ ILC2s were detected compared to BALB/c mice given the FPV-HIV-IL-13R α 2 adjuvanted vaccine (transient inhibition of IL-13), and their NKp46^{+/+} ILC1/ILC3-driven IFN- γ expression was significantly lower compared to transient inhibition of STAT6. In previous studies when IL-13 was inhibited, no or low HIV gag specific IgG1 and IgG2a antibody differentiation has been reported, unlike STAT6 inhibition. Thus, current data further corroborate that ST2/IL-33R⁺ ILC2-derived IL-13 plays a crucial role in modulating downstream B cell immune outcomes. Specifically, co-regulation of ST2/IL-33R⁺ ILC2-derived IL-13 and NKp46^{+/+} ILC1/ILC3-derived IFN- γ may play an important role in modulating IgG1 to IgG2a antibody differentiation process in a STAT6 independent manner via the IL-13R α 2 pathway.

5.2 Introduction.

Cytokines IL-13 and IL-4 have been well studied in models which are related to Th2 immunity such as allergy, asthma, parasitic and helminth infections^{80, 81, 82, 256, 257}. The

roles of these two cytokines have been characterised as the regulators of Th1 and Th2 immune responses^{80, 81, 258}.

The two poxviral vector based HIV vaccines, IL-13R α 2 adjuvanted and IL-4R antagonist adjuvanted vaccines described in Chapter 3, that can temporarily manipulate IL-13 and IL-4 activity at the vaccination site, have shown to induce higher avidity/multi-functional HIV specific effector/memory CD8 T cells with improved CD8 T cell mediated protective efficacy¹²². Moreover, in the context of antibody immunity, the FPV-HIV-IL-4R antagonist adjuvant vaccine has also shown to induce HIV gag-specific IgG1 and IgG2a antibody differentiation, but not the FPV-HIV-IL-13R α 2 adjuvanted vaccine¹¹³. To further understand the role of IL-13 in IgG1/IgG2a antibody differentiation, IL-13^{-/-}, IL-4^{-/-}, and STAT6^{-/-} mice were vaccinated with FPV-HIV/VV-HIV (unadjuvanted) prime-boost strategy. Although IL-4^{-/-} and STAT6^{-/-} animals showed enhanced IgG2a antibody responses, IL-13^{-/-} showed very low IgG2a antibodies (Hamid *et al* EJI accepted). More interestingly, when STAT6^{-/-} mice were given the FPV-HIV-IL-13R α 2 adjuvanted vaccine, which sequestered IL-13 at the vaccination site, elevated IgG1 but low IgG2a antibody responses were detected similar to the IL-13^{-/-} mice (Hamid *et al* EJI accepted). These observations clearly indicated that i) unlike T cell immunity, presence of IL-13 was critical for B cell differentiation, and ii) taken together the STAT6^{-/-} and IL-4R antagonist data indicated that signalling via IL-13R α 2 pathway may be involved in this process (Hamid *et al* EJI accepted). Knowing that IFN- γ plays an important role in antibody differentiation^{259, 260, 261, 262, 263}, and chapter 3 showing that ILC2 are the major source of IL-13 at the vaccination site and IL-13R α 2 adjuvanted vaccine and IL-4R antagonist vaccines, differentially regulated IFN- γ at the vaccination site, we postulate that balance between ILC2-driven IL-13 and ILC1/ILC3-driven IFN- γ at the vaccination site most likely play a critical role in shaping the downstream B cell immune responses.

IL-13 and IFN- γ have shown to regulate each other under different conditions^{264, 265, 266, 267, 268}. Under inflammation condition, IFN- γ has shown to inhibit ILC2 activation and IL-5 production²⁶⁹, however, the relationship between IL-13 and IFN- γ at the ILC level under viral vector vaccination is still poorly understood. Thus, in this study we have used IL-13, IL-4, and STAT6 gene knockout mice (permanent versus transient blockage -Chapter 3) to further understand the roles of these different ILC subsets following rFPV viral vector vaccination and to gain better understanding of how the balance of ILC2-driven IL-13 and ILC1/3-driven IFN- γ at the vaccination site modulate B cell activation.

5.3 Materials and Methods.

5.3.1 Mice and immunisation.

5-6 weeks old pathogen free female WT BALB/c, IL-13^{-/-}, IL-4^{-/-}, STAT6^{-/-} mice were obtained from the Australian Phenomics Facility, the Australian National University, and were maintained and handled under protocols indicated in **2.2.1**. 1 \times 10⁷ PFU unadjuvanted FPV-HIV vaccine was administered to each mice group (n = 3 - 6 per group) intranasally under mild isoflurane anaesthesia as per described in **2.2.5**. Lungs were harvested in 2 ml of complete RPMI at 24 h, 3 and 7 days post immunisation, single cell lung suspensions were prepared, stained and analysed as per described in **2.2.6 and 2.2.8**.

5.3.2 Surface and intracellular staining.

Surface and intracellular staining were performed as per described in **2.2.8** using antibodies listed in **Table 2.3**. Specifically,

ILC2 staining: APC/Cy7-conjugated anti-mouse CD45, and FITC-conjugated lineage cocktail were used to identify lineage⁻ cells. PE-conjugated anti-mouse ST2/IL-33R, APC-conjugated anti-mouse Sca-1 were used to identify the ILC2. Brilliant Violet 421-conjugated anti-mouse IL-4 and PE-eFlour 610-conjugated anti-mouse IL-13 were used to evaluate intracellular expression of these cytokines in ILC2s.

ILC1/3 staining: APC/Cy7-conjugated anti-mouse CD45, and FITC-conjugated lineage cocktail were used to identify lineage⁻ cells. PE-conjugated anti-mouse ST2/IL-33R, and Brilliant Violet 421-conjugated anti-mouse CD335 (NKp46) were used to identify ILC1/3 populations. Brilliant Violet 510-conjugated anti-mouse IFN- γ , APC-conjugated anti-mouse IL-22, and Alexa Fluor 700-conjugated anti-mouse IL-17A were used to evaluate intracellular expression of these ILC1/3 cytokines in ILC1 and ILC3.

All ILC subsets were gated and analysed as per described in **2.2.9**.

5.4 Results.

5.4.1 Following i.n. rFPV vaccination lung lineage⁻ IL-33R/ST2⁺ ILC2 in IL-4^{-/-}, IL-13^{-/-} and STAT6^{-/-} mice were significantly different compared to WT BALB/c mice.

In this study, WT BALB/c, IL-13^{-/-}, IL-4^{-/-}, and STAT6^{-/-} mice (each group n = 3 - 6) were vaccinated intranasally with the unadjuvanted FPV-HIV vaccine and lung lineage⁻ IL-33R/ST2⁺ ILC2 were evaluated 24 h, 3 and 7 days post vaccination, using multicolour flow cytometry as described in Materials and Methods. Data revealed that compared to WT BALB/c mice, all knockout animals showed significantly elevated lung lineage⁻ IL-33R/ST2⁺ ILC2 24 h post vaccination (WT BALB/c vs IL-13^{-/-},

$p < 0.0001$; WT BALB/c vs IL-4^{-/-}, $p = 0.0013$; WT BALB/c vs STAT6^{-/-} $p < 0.0001$). However, interestingly, at day 3 post vaccination, lineage⁻ IL-33R/ST2⁺ ILC2 numbers in lung decreased significantly in knockout mice compared to the control WT BALB/c (**Fig. 5.1a & 1b**). Consistent with what was observed in the previous chapter, at 7 days post vaccination very low numbers of lung lineage⁻ IL-33R/ST2⁺ ILC2 were detected in all groups tested.

Unlike transient inhibition of IL-13 at the vaccination site with IL-13R α 2 adjuvanted vaccine described in Chapter 3, IL-13^{-/-} mice showed significantly elevated numbers of lung lineage⁻ IL-33R/ST2⁺ ILC2 24 h post vaccination ($p < 0.0001$) (**Fig 5.1c**). Similarly, STAT6^{-/-} mice (where no IL-13 and IL-4 signalling occur via STAT6 pathway), showed significantly higher lung lineage⁻ IL-33R/ST2⁺ ILC2 24 h post vaccination compared to IL-4^{-/-}, IL-13^{-/-} and WT BALB/c mice (**Fig. 5.1b**). Interestingly, out of the three knockout mice groups tested the lowest number of lung lineage⁻ IL-33R/ST2⁺ ILC2s were detected in IL-4^{-/-} 24 h post vaccination.

5.4.2 In KO mice the Sca-1 regulation on lung lineage⁻ IL-33R/ST2⁺ ILC2 was mainly observed at 24 h post vaccination.

Next when stem cell marker Sca-1 expression was evaluated on lineage⁻ IL-33R/ST2⁺ ILC2, unlike WT BALB/c mice where an increase in Sca-1⁺ ILC were detected over time, in gene knock-out mice differences in Sca-1⁺ ILC were only observed at 24 h post vaccination (**Fig. 5.2a**). Furthermore, compared to the other two knockout mice groups, relatively low Sca-1 expression was detected in IL-4^{-/-} lineage⁻ IL-33R/ST2⁺ ILC2 (**Fig. 5.2b**). In contrast, elevated numbers of Sca-1⁺ lineage⁻ IL-33R/ST2⁺ ILC2 were detected in both IL-13^{-/-} mice and STAT6^{-/-} mice at 24 h post vaccination (**Fig. 5.2b & c**). In general, the trend of Sca-1 expression 24 h to 7 days post immunisation was

Fig. 5.1. Evaluation of lung lineage⁻ IL-33R/ST2⁺ ILC2 in knockout mice following intranasal vaccination.

WT BALB/c, IL-13^{-/-}, IL-4^{-/-} and STAT6^{-/-} mice (BALB/c background) (each group n = 3-6) were immunized intranasally with unadjuvanted FPV-HIV vaccine. Using the flow cytometry gating strategy indicated in materials and methods, ILC2s were defined as CD45⁺ FSC^{low} SSC^{low} Lin⁻ IL-33R/ST2⁺ cells. The FACS plots indicate the percentage of lung lineage⁻ ST2⁺ ILC2 cells at 24 h and 3 days post vaccination, the number of cells in each quadrant is indicated within brackets below the cell percentage **(a)**. Graphs represent number of lineage⁻ IL-33R/ST2⁺ ILC2s in each population back calculated to CD45⁺ population as described in Materials and Methods at 24 h to 7 days post vaccination**(b)**. Lineage⁻ IL-33R/ST2⁺ ILC2 cell numbers were also compared to WT BALB/c and IL-13^{-/-} mice immunized with unadjuvanted FPV-HIV vaccine and WT BALB/c immunized with IL-13R α 2 adjuvanted vaccine indicated in Chapter 3 **(c)**. The error bars represent the mean and standard deviation (s.d.). The p-values were calculated using GraphPad Prism software (version 6.05 for Windows). * = p<0.05, ** = p<0.01, ***= p<0.001, ****= p<0.0001. For each time point experiments were repeated minimum three times.

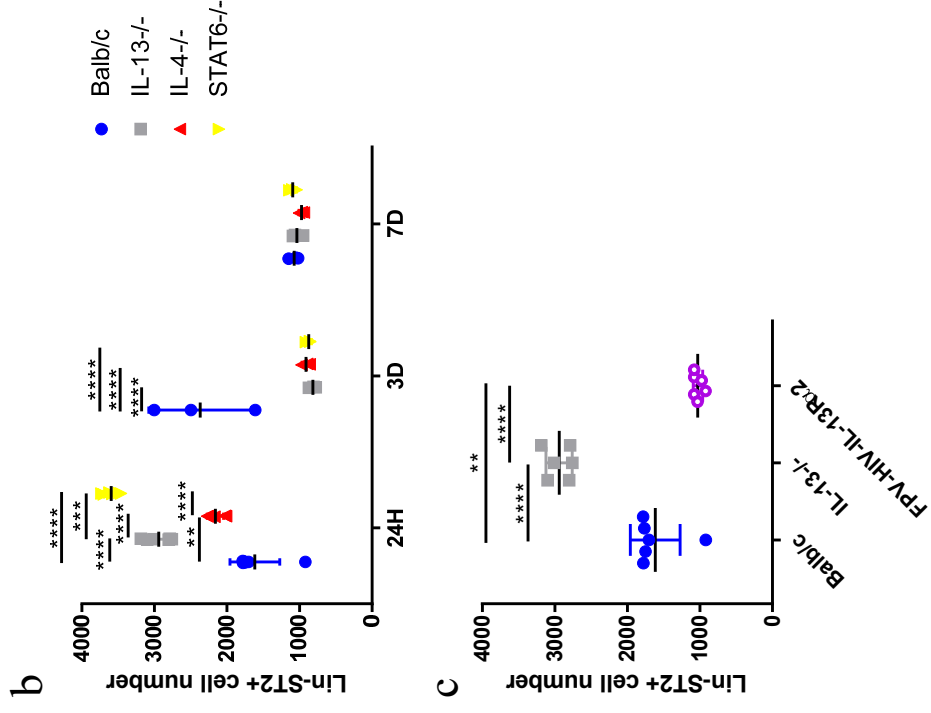
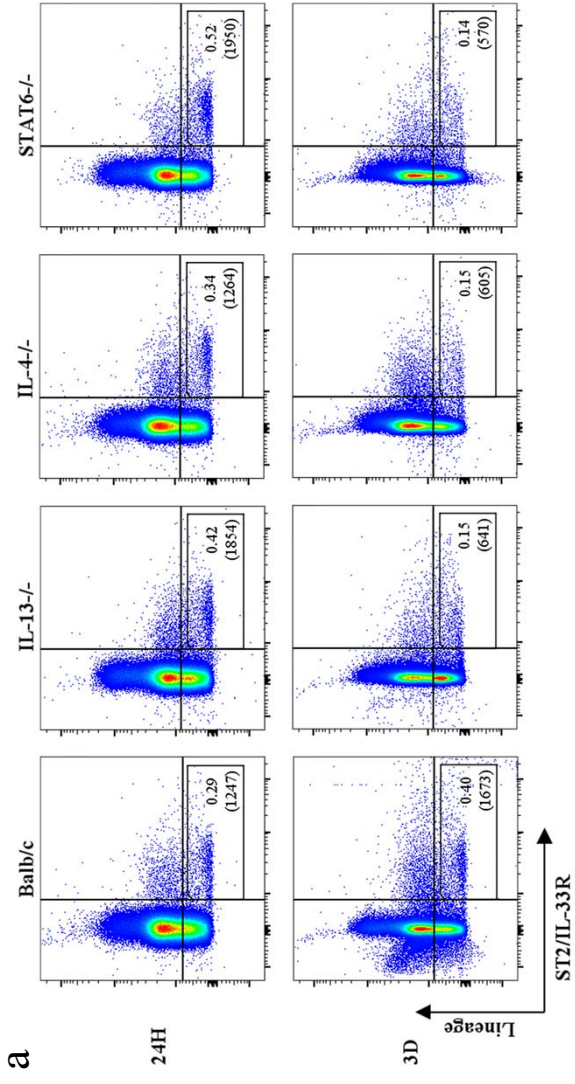
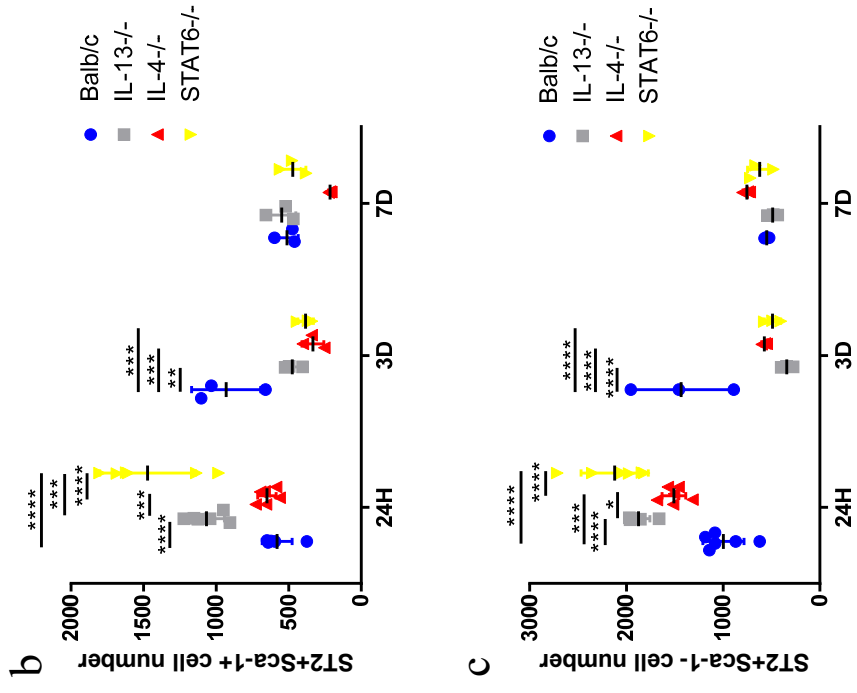
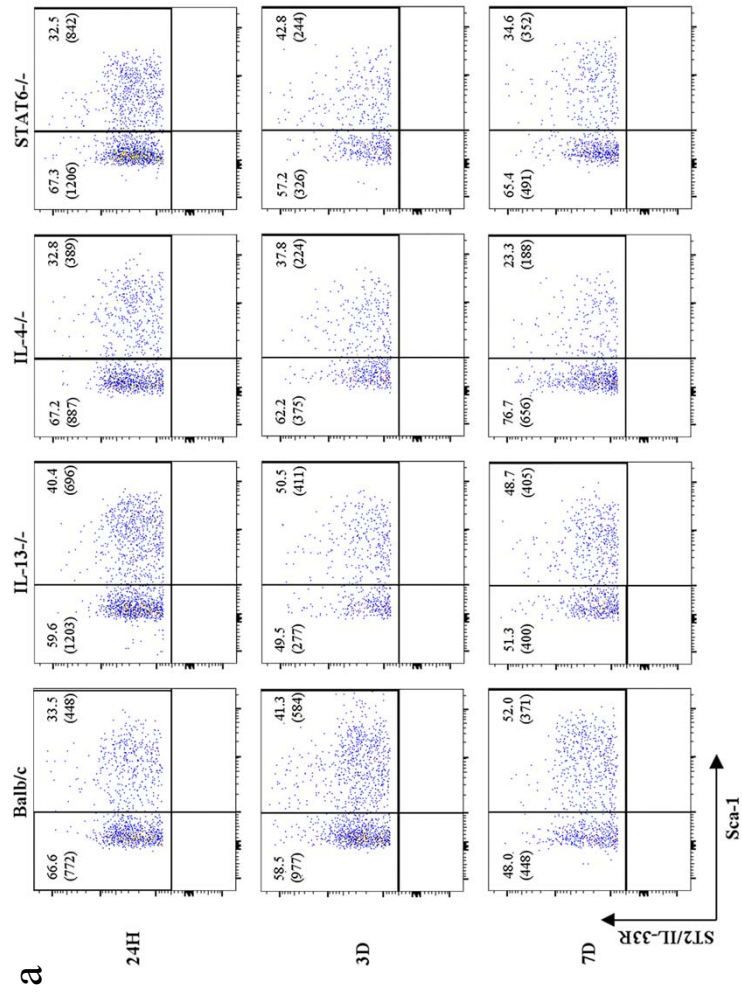


Fig. 5.2. Evaluation of lung lineage IL-33R/ST2⁺ ILC2 Sca-1 expression in knockout mice following intranasal vaccination.

After lineage IL-33R/ST2⁺ ILC2 were gated as described in materials and methods, stem cell marker Sca-1 expression was assessed at 24 h, 3 days, and 7 days post vaccination. Representative FACS plots of IL-13^{-/-}, IL-4^{-/-} and STAT6^{-/-} and WT BALB/c lung showing ILC2 Sca-1 expression at 24 h, 3 and 7 days post vaccination (a). Graphs represent Sca-1⁺ and Sca-1⁻ ILC2 numbers back calculated to CD45⁺ population as described in Materials and Methods and compared with WT BALB/c mice (b & c). The error bars represent the mean and standard deviation (s.d.). The p-values were calculated using GraphPad Prism software (version 6.05 for Windows). * = p<0.05, ** = p<0.01, *** = p<0.001, **** = p<0.0001. For each time point experiments were repeated minimum three times.



significantly different in IL-13, IL-4 and STAT6 gene knock-out mice compared to the WT control BALB/c mice.

5.4.3 WT BALB/c and STAT6^{-/-} mice showed elevated numbers of lung lineage⁻ IL-33R/ST2⁺ ILC2 expressing IL-13 compared to IL-4^{-/-} mice.

Next when IL-13 expression was evaluated in lung lineage⁻ IL-33R/ST2⁺ ILC2, all time points tested significantly lower IL-13 levels were detected in IL-4^{-/-} mice compared to WT BALB/c and STAT6^{-/-} mice (**Fig. 5.3a & b**). Although the IL-13 expression in STAT6^{-/-} lineage⁻ IL-33R/ST2⁺ lung ILC2 was significantly higher than WT BALB/c at 24 h post vaccination (**Fig. 5.3a & b**), no IL-13 expression was detected 3 days post vaccination (**Fig. 5.3b**). Moreover, no IL-4 expression was detected in any of the lung lineage⁻ IL-33R/ST2⁺ ILC2 obtained from knockout mice or WT control BALB/c, including IL-13^{-/-} mice.

5.4.4 Lung lineage⁻ IL-33R/ST2⁻ NKp46^{+/+} ILC1/ILC3 numbers were regulated differently in IL-13^{-/-}, IL-4^{-/-}, and STAT6^{-/-} mice.

When lineage⁻ IL-33R/ST2⁻ NKp46^{+/+} lung ILC (ILC1 /ILC3) were assessed following i.n. rFPV vaccination in gene knockout mice, significantly reduced numbers were observed compared to WT BALB/c mice (**Fig. 5.4a**). This reduction was more pronounced 3 to 7 days post vaccination (**Fig. 5.4b**). Although there was no significant difference in the lung lineage⁻ IL-33R/ST2⁻ NKp46^{+/+} ILC numbers in all three KO mice groups at day 3 post vaccination, at 24 h, these ILC numbers were significantly elevated in the IL-4^{-/-} group, compared to IL-13^{-/-} group these (**Fig. 5.4b**). Moreover, 7 days post vaccination, lung lineage⁻ IL-33R/ST2⁻ NKp46^{+/+} ILC numbers in STAT6^{-/-} mice were slightly elevated compared to IL-4^{-/-} mice (**Fig. 5.4b**).

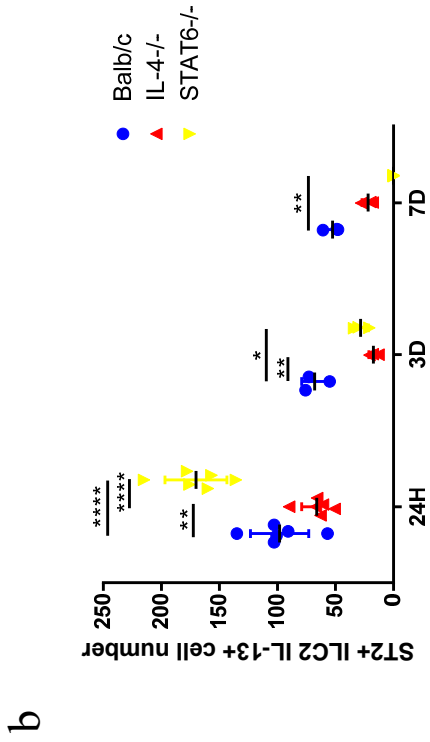
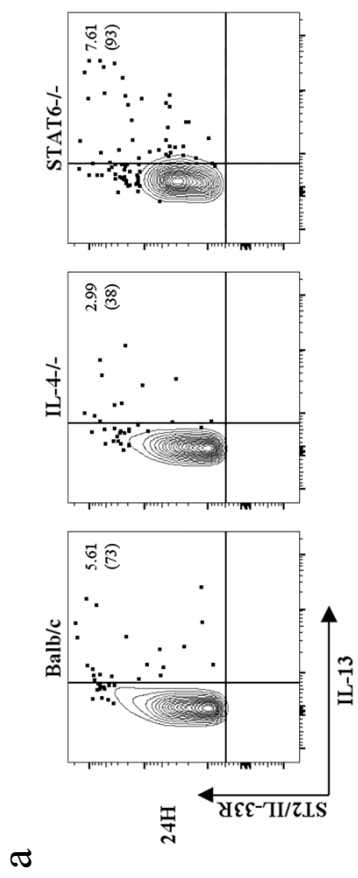


Fig. 5.3. Evaluation of lung lineage⁻ IL-33R/ST2⁺ ILC2 IL-13 expression in knockout mice following intranasal vaccination.

The lineage⁻ IL-33R/ST2⁺ ILC2 cells were further analysed for IL-13 expression. The FACS plots indicate the representative plots from IL-4^{-/-} STAT6^{-/-} and WT BALB/c mice **(a)**. The graphs represent IL-13 expression by ILC2, cell numbers back calculated to CD45⁺ population as described in Materials and Methods **(b)**. The error bars represent the mean and standard deviation (s.d.). The p-values were calculated using GraphPad Prism software (version 6.05 for Windows). * = $p < 0.05$, ** = $p < 0.01$, *** = $p < 0.001$, **** = $p < 0.0001$. For each time point experiments were repeated minimum three times.

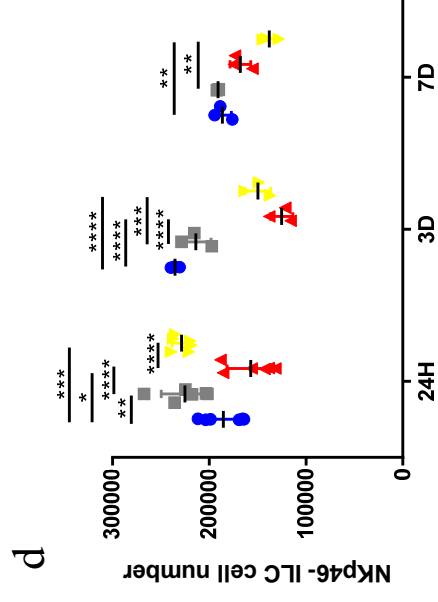
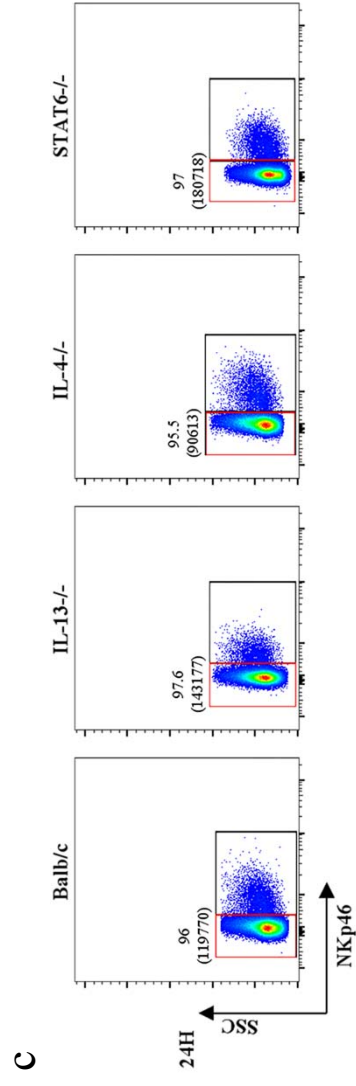
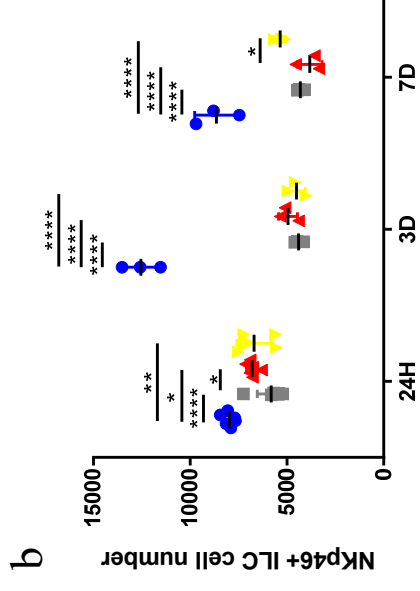
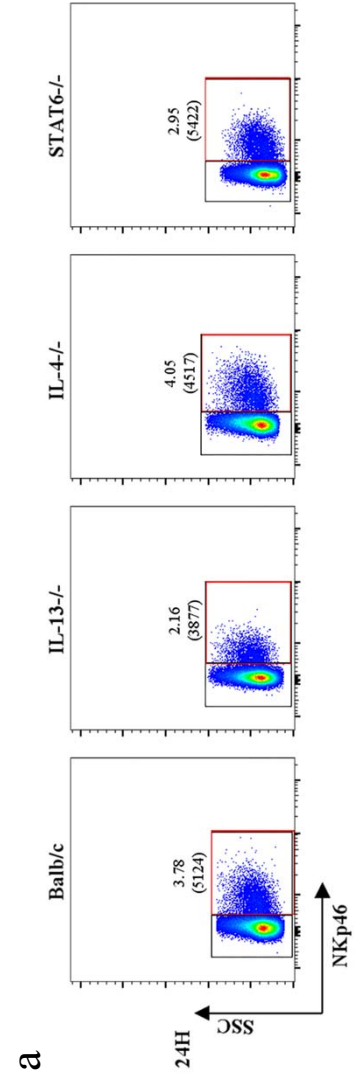


Fig. 5.4. Identification of lung lineage IL-33R/ST2⁻ NKp46^{+/-} ILC in knockout mice following intranasal vaccination.

WT BALB/c, IL-13^{-/-}, IL-4^{-/-} and STAT6^{-/-} mice (each group n = 3-6) were immunized intranasally with unadjuvanted FPV-HIV vaccine. As described in materials and methods, NKp46^{+/-} ILC were gated as CD45⁺ FSC^{low} SSC^{low} lineage⁻ ST2⁻ NKp46^{+/-}. The representative FACS plots for each mouse group 24 h post vaccination (**a & c**). The graphs represent number of lineage⁻ IL-33R/ST2⁻ NKp46^{+/-} ILC (ILC1/ILC3) back calculated to CD45⁺ cells as per indicated in Materials and Methods (**b & d**). The error bars represent the mean and standard deviation (s.d.). The p-values were calculated using GraphPad Prism software (version 6.05 for Windows). *p<0.05, **p<0.01, ***p<0.001, ****p<0.0001. For each time point experiments were repeated minimum three times.

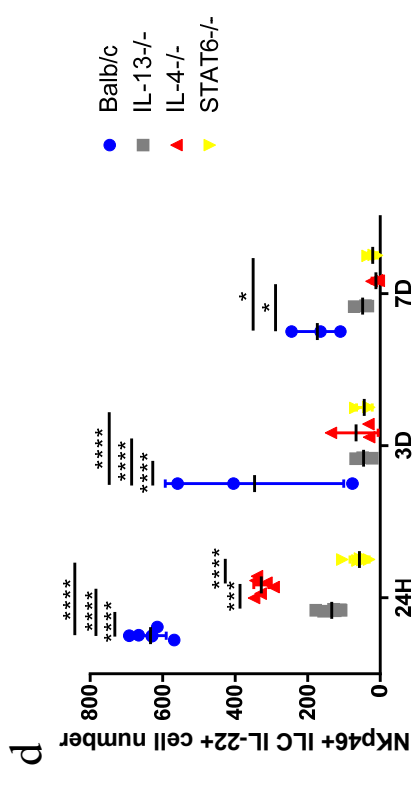
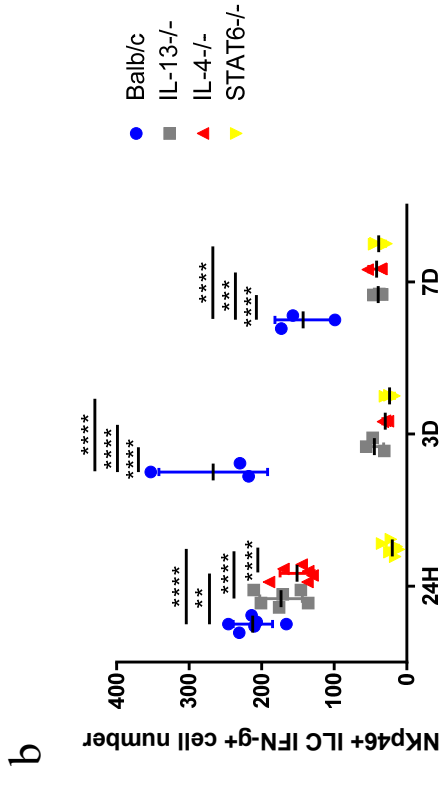
Unlike lung lineage⁻ IL-33R/ST2⁻ NKp46⁺ ILCs, when lung lineage⁻ IL-33R/ST2⁻ NKp46⁻ ILC in KO mice were assessed, significant differences were observed between the four mice groups at all time points tested (**Fig. 5.4c**). Specifically, whilst lineage⁻ IL-33R/ST2⁻ NKp46⁻ ILC numbers in WT BALB/c mice and IL-13^{-/-} mice showed similar trends overtime, IL-4^{-/-} mice showed no significant changes at 24 h, 3 and 7 days post intranasal vaccination (**Fig. 5.4d**). Compared to all KO mice tested, IL-4^{-/-} mice showed the lowest number of NKp46⁻ ILC at 24 h post vaccination. Interestingly, elevated numbers of lineage⁻ IL-33R/ST2⁻ NKp46⁻ ILC were detected in IL-13^{-/-} mice and STAT6^{-/-} compared to both control WT BALB/c and IL-4^{-/-} mice at 24h post vaccination (**Fig. 5.4d**). However, the STAT6^{-/-} mice showed significantly reduced NKp46⁻ ILC at 3 and 7 days post vaccination compared to both WT BALB/c and IL-13^{-/-} mice. The profiles at 3 and 7 days post vaccination in IL-4^{-/-} mice were similar to STAT6^{-/-} mice (**Fig. 5.4d**).

5.4.5 Following intranasal vaccination, STAT6^{-/-} mice showed extremely low lung lineage⁻ IL-33R/ST2⁻ NKp46^{+/-} ILC1/ILC3 expressing IFN- γ and IL-22.

Although IFN- γ and IL-22 expression in lung lineage⁻ IL-33R/ST2⁻ NKp46⁺ ILC were significantly lower in KO mice compared to WT BALB/c mice, STAT6^{-/-} mice showed the lowest expression of both cytokines at all time points tested (**Fig. 5.5a - d**). The low IFN- γ and IL-22 expression by lineage⁻ IL-33R/ST2⁻ NKp46⁺ ILC at 3 to 7 days post vaccination (**Fig. 5.5b & d**), was reflective of the overall low numbers of lineage⁻ IL-33R/ST2⁻ NKp46⁺ ILC in KO mice at these time points (**Fig. 5.4**). Unlike IFN- γ , in the context of IL-22 expression, IL-4^{-/-} mice shows much elevated levels compared to IL-13^{-/-} (**Fig. 5.5d**). In all groups tested, none of the NKp46⁺ ILC were found to express IL-17A.

Fig. 5.5. Evaluation expression of IFN- γ and IL-22 by lineage⁻ IL-33R/ST2⁻ NKp46⁺ ILC in knockout mice following intranasal vaccination.

After lineage⁻ IL-33R/ST2⁻ NKp46⁺ ILC (ILC1/ILC3) were gated, their IFN- γ (**a & b**) and IL-22 (**c & d**) expression were evaluated using intracellular cytokine staining. The FACS plots are representative of the 24 h data points for each group (**a & c**). The graphs indicate the number of IFN- γ and IL-22 expressing lineage⁻ IL-33R/ST2⁻ NKp46⁺ ILC, KO mice compared to WT BALB/c mice (**b & d**). The error bars represent the mean and standard deviation (s.d.). The p-values were calculated using GraphPad Prism software (version 6.05 for Windows). * = p<0.05, ** = p<0.01, *** = p<0.001, **** = p<0.0001. For each time point experiments were repeated minimum three times.



When IFN- γ , IL-22 and IL-17A cytokines expression was evaluated in lineage⁻ IL-33R/ST2⁻ NKp46⁻ ILC, extremely low IFN- γ expression was detected in STAT6^{-/-} mice at all time points tested (**Fig. 5.6a & b**). In IL-13^{-/-} mice, although significantly reduced IFN- γ expression was detected at 24 h post vaccination (**Fig. 5.6a & b**), elevated levels were detected after 3 days post vaccination (**Fig. 5.6b**). No significant difference in IFN- γ expression by lineage⁻ IL-33R/ST2⁻ NKp46⁻ ILC were detected in IL-4^{-/-} mice and WT BALB/c mice at 24 h post vaccination (**Fig. 5.6a & b**), and rapid reduction in IFN- γ expression was observed 3 days post vaccination, unlike IL-13^{-/-} mice (**Fig. 5.6b**). In the context of IL-22 expression by lineage⁻ IL-33R/ST2⁻ NKp46⁻ ILC, IL-13^{-/-} mice and STAT6^{-/-} mice showed significantly reduced IL-22 expression at all time points tested (**Fig. 5.6c & d**). IL-4^{-/-} mice showed significantly elevated level of IL-22 expression by NKp46⁻ ILC compared to IL-13^{-/-} and STAT6^{-/-} mice at 24 h post vaccination (**Fig. 5.6d**). Similar to lineage⁻ IL-33R/ST2⁻ NKp46⁺ ILC, none of the lineage⁻ IL-33R/ST2⁻ NKp46⁻ ILC were found to express IL-17A.

5.4.6 Following viral vector vaccination, ILC2-driven IL-13 and ILC1/ILC3-driven IFN- γ expression were inversely correlated.

Next, the IL-13 expression profile of lung IL-33R/ST2⁺ ILC2, and IFN- γ expression by both NKp46^{+/+} ILC1/ILC3 obtained from BALB/c mice given the FPV-HIV-IL-4R antagonist and IL-13^{-/-}, FPV-HIV-IL-13R α 2 adjuvanted vaccines were compared with IL-13^{-/-}, STAT6^{-/-}, and IL-4^{-/-} mice given the control unadjuvanted vaccine (**Fig. 5.7a**). STAT6^{-/-} and IL-4^{-/-} mice showed elevated IL-13 expression by ILC2 compared to the BALB/c mice given the adjuvanted vaccines (**Fig. 5.7a**). However, ILC2-driven IL-13 expression was significantly higher in STAT6^{-/-} mice compared to IL-4^{-/-} mice (**Fig. 5.7a**). When IFN- γ expression by both NKp46^{+/+} ILC1/ILC3 were evaluated, the FPV-

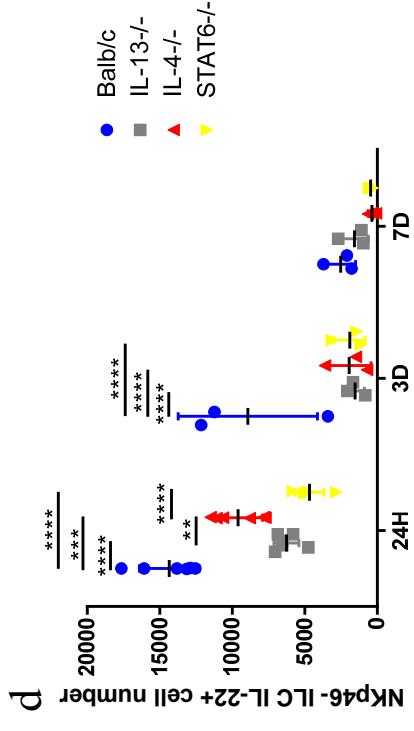
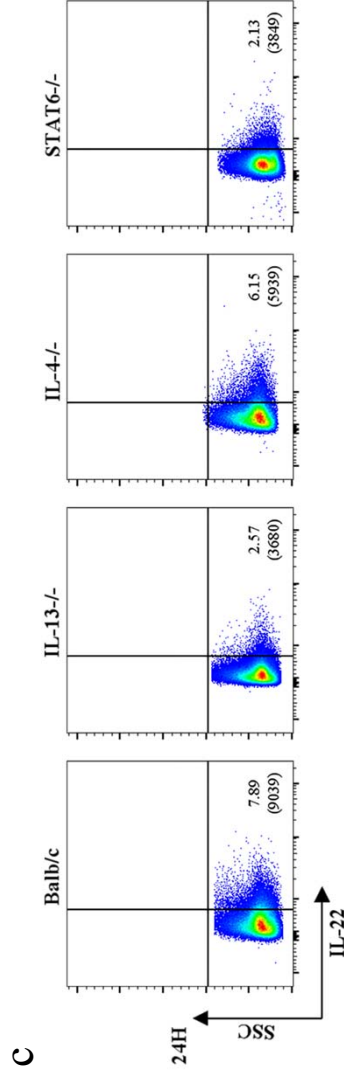
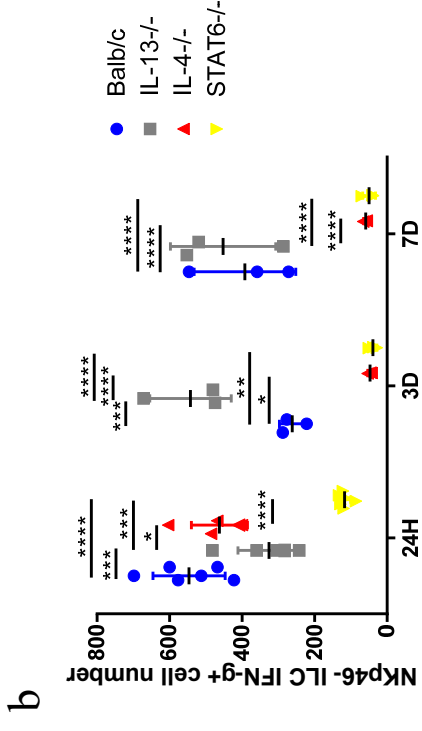
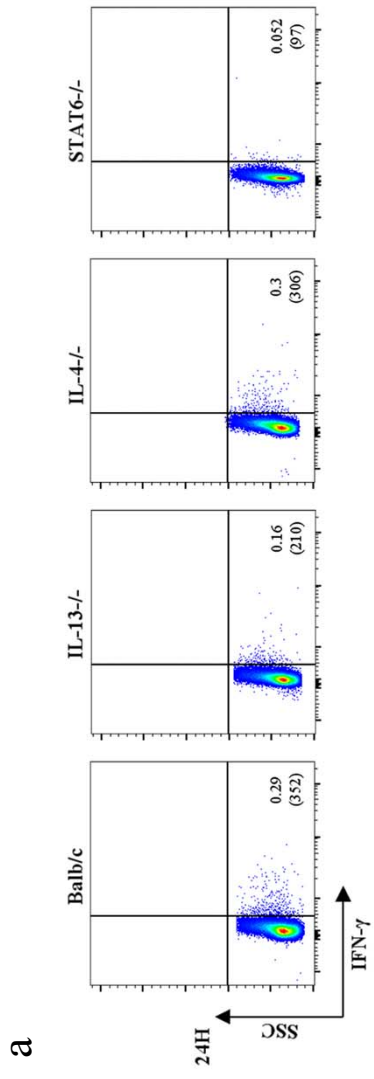


Fig. 5.6. Expression of IFN- γ and IL-22 by lineage⁻ IL-33R/ST2⁻ NKp46⁻ ILC in knockout mice following intranasal vaccination.

After lineage⁻ IL-33R/ST2⁻ NKp46⁻ ILC were gated, their IFN- γ (**a & b**) and IL-22 (**c & d**) expression were evaluated using intracellular cytokine staining. The FACS plots are representative of the 24 h data points for each group of mice (**a & c**). The graphs indicate the number of IFN- γ and IL-22 expressing lineage⁻ IL-33R/ST2⁻ NKp46⁻ ILC, in KO mice compared to WT BALB/c mice (**b & d**). The error bars represent the mean and standard deviation (s.d.). The p-values were calculated using GraphPad Prism software (version 6.05 for Windows). * = $p < 0.05$, ** = $p < 0.01$, *** = $p < 0.001$, **** = $p < 0.0001$. For each time point experiments were repeated minimum three times.

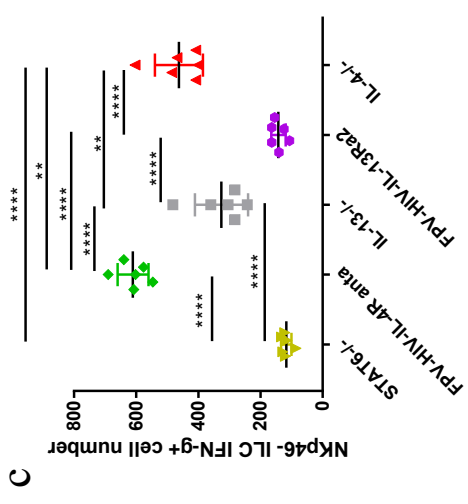
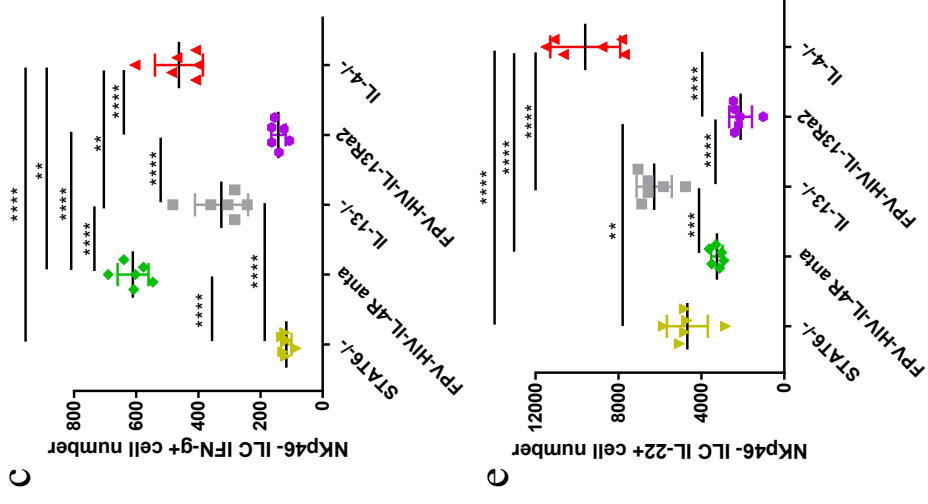
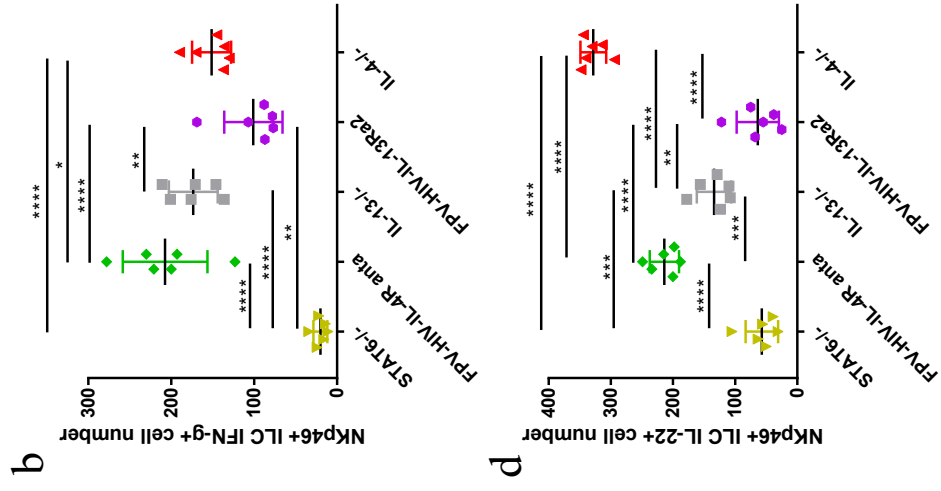
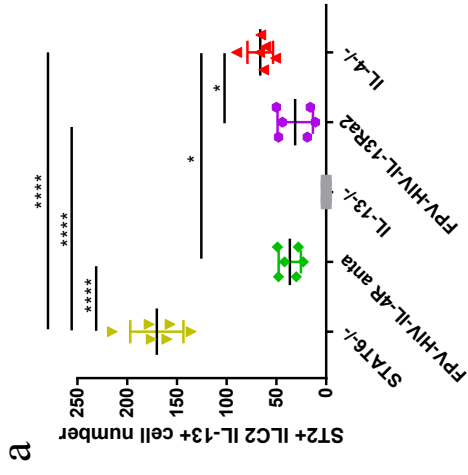
HIV-IL-4R antagonist vaccine group showed elevated IFN- γ expression by both NKp46^{+/−} ILCs, whilst STAT6^{−/−} mice vaccinated with unadjuvanted vaccine showed very low expression of IFN- γ (**Fig. 5.7b & c**). In contrast, compared to the FPV-HIV-IL-13R α 2 adjuvanted vaccine group, the IL-13^{−/−} mice given the unadjuvanted vaccine showed higher level of IFN- γ expression by both NKp46^{+/−} ILC1/ILC3 (**Fig. 5.7b & c**). Moreover, expression of IL-22 by both NKp46^{+/−} ILC1/ILC3s was significantly lower in FPV-HIV-IL-13R α 2 group compared to IL-13^{−/−} mice given FPV-HIV vaccine (**Fig. 5.7d & e**). Although there was no significant difference in NKp46[−] ILC1/ILC3-driven IL-22, significantly elevated IL-22 expression by NKp46⁺ ILC1/ILC3 were observed in FPV-HIV-IL-4R antagonist vaccinated group compared to STAT6^{−/−} mice given FPV-HIV (**Fig. 5.7d & e**). Interestingly, in each vaccine group tested the expression profile of NKp46⁺ ILC1/ILC3-driven IL-22 and IFN- γ were very similar, unlike NKp46[−] ILC1/ILC3, suggesting that NKp46⁺ and NKp46[−] subsets most likely are differentially regulated (**Fig 5.7b & d**).

5.5 Discussion.

This study revealed that ILC and their cytokine expression profile (IL-13, IFN- γ , and IL-22) at the vaccination site is vastly different in the scenario of transient sequestration verses permanent blockage of in IL-13, IL-4, and STAT6. Moreover, IL-17A was not detected in lung NKp46^{+/−} ILC at any time points tested, unlike when IL-25 was transiently sequestered at vaccination site (Chapter 4). Data further supported the notion that the balance of ILC-2 driven IL-13 and ILC1/ILC3-driven IFN- γ play an important role in shaping downstream immune outcomes. Specifically, at 24 h post vaccination when IL-13 was permanently blocked (IL-13^{−/−}), significantly elevated number of lung lineage[−] ST2/IL-33R⁺ ILC2s were detected at the vaccination, compared to transiently

Fig. 5.7. Comparison of ILC2-driven IL-13 and ILC1/ILC3-driven IFN- γ and IL-22 expression following permanent vs transient blockage of IL-13, IL4 and STAT6.

Graphs represent IL-13 expression by ILC2 (a), IFN- γ (b & c) and IL-22 (d & e) by ILC1/ILC3 following IL-13^{-/-}, STAT6^{-/-} and IL-4^{-/-} mice given the control unadjuvanted vaccine (FPV-HIV) compared to BALB/c mice given FPV-HIV-IL-4R antagonist and FPV-HIV-IL-13R α 2 adjuvanted vaccines. Note that in the figure FPV-HIV-IL-4R anta = FPV-HIV-IL-4R antagonist.



inhibition of IL-13 in BALB/c mice (FPV-HIV-IL-13R α 2 adjuvanted vaccine) which showed the opposing effect. Interestingly, when STAT6^{-/-} mice were given FPV-HIV, where IL-13 was unable to signal via the JAK/STAT6 pathway, and transient inhibition of STAT6 signalling in BALB/c mice (FPV-HIV-IL-4R antagonist adjuvanted vaccine) both showed elevated ST2/IL-33R⁺ ILC2s compared to WT control. These data clearly indicated that in the knockout scenario, different compensatory mechanism may be involved in modulating the ST2/IL-33R⁺ ILC2 at the vaccination site. For example, under STAT6 inhibitory condition, IL-13 may signal via the not well-defined IL-13R α 2 pathway described by Hamid *et al* 2018 (Hamid *et al* EJI accepted). In this scenario, it is plausible that IL-13R α 2 may have the potential to complex with IL-13R α 1 to promote STAT3 signalling²⁷⁰.

STAT6^{-/-} mice given the FPV-HIV vaccine showed elevated ST2/IL-33R⁺ ILC2-driven IL-13 expression whilst reduced IFN- γ expression by both NKp46^{+/-} ILC1/ILC3. However, when STAT6 signalling was transiently blocked in BALB/c mice using FPV-HIV-IL-4R antagonist vaccination, the opposing effect was observed. Interestingly, IL-13^{-/-} mice given the FPV-HIV showed elevated expression of IFN- γ by NKp46^{+/-} ILC1/ILC3, whereas BALB/c mice given the FPV-HIV-IL-13R α 2 adjuvanted vaccine showed low ST2/IL-33R⁺ ILC2-driven IL-13 expression and low NKp46^{+/-} ILC1/ILC3-driven IFN- γ . It is now established that IL-13 can modulate IFN- γ expression^{265, 266}. These findings indicate that the balance between ST2/IL-33R⁺ ILC2-driven IL-13 and NKp46^{+/-} ILC1/ILC3-driven IFN- γ at vaccination site is differentially modulated under IL-13 and STAT6 permanent verses transient inhibitory conditions.

Our previous studies have demonstrated that the FPV-HIV-IL-4R/VV-HIV-IL-4R antagonist adjuvanted prime-boost vaccination can induce the HIV gag-specific IgG1 to

IgG2a antibody differentiation. unlike FPV-HIV-IL-13R α /VV-HIV-13R α adjuvanted vaccine strategy¹¹³. Similarly, IL-4^{-/-}, STAT6^{-/-} given FPV-HIV/VV-HIV was shown to induce elevated gag-specific IgG2a unlike IL-13^{-/-} mice (Hamid *et al* EJI accepted), indicating that IL-13 signalling was detrimental for IgG1/IgG2a antibody differentiation (**Fig.5.8a & b**). When STAT6 signalling pathway was interrupted by FPV-HIV-IL-4R antagonist vaccine, elevated IFN- γ expression by both NKp46^{+/-} ILC1/ILC3 were observed (**Fig. 5.9a**). It is now established that i) IFN- γ is required for antibody differentiation^{259, 260, 261, 262, 263}, and IL-13 plays an important role in this process (Hamid *et al* EJI accepted), ii) IL-13R α 2 can act as an inhibitor of IL-4R α chain and STAT6 signalling¹¹⁹, and iii) also IL-4R α and STAT6 signalling can inhibit IFN- γ expression by CD4⁺ T cells²⁷¹. Moreover, IL-13 signalling via IL-13R α 2 pathway is involved in induction of TGF- β production^{272, 273}, and TGF- β is known to be a key regulator for IgG2a antibody induction^{274, 275, 276}. Thus, we postulate that in IL-4R antagonist inhibitor scenario, IL-13 may act on NKp46^{+/-} ILC1/ILC3 to regulate IFN- γ expression. Specifically, via the IL-13R α 2 pathway and modulate IgG1/IgG2a antibody differentiation process. In STAT6^{-/-} mice given the unadjuvanted vaccine scenario (**Fig. 5.9b**), where low NKp46^{+/-} ILC1/ILC3-driven IFN- γ expression and high ST2/IL-33R⁺ ILC2-driven IL-13 expression was observed, the IgG1/IgG2a antibody differentiation process is likely regulated by the balance of IL-13 and IFN- γ at the vaccination site, still via the IL-13R α 2 pathway.

Interestingly, in IL-4^{-/-} mice given the unadjuvanted vaccine (**Fig. 5.10**), lower ST2/IL-33R⁺ ILC2-derived IL-13 expression was observed compared to STAT6^{-/-} mice or WT BALB/c. This is not surprising as studies have shown that IL-4^{-/-} lymphocytes express

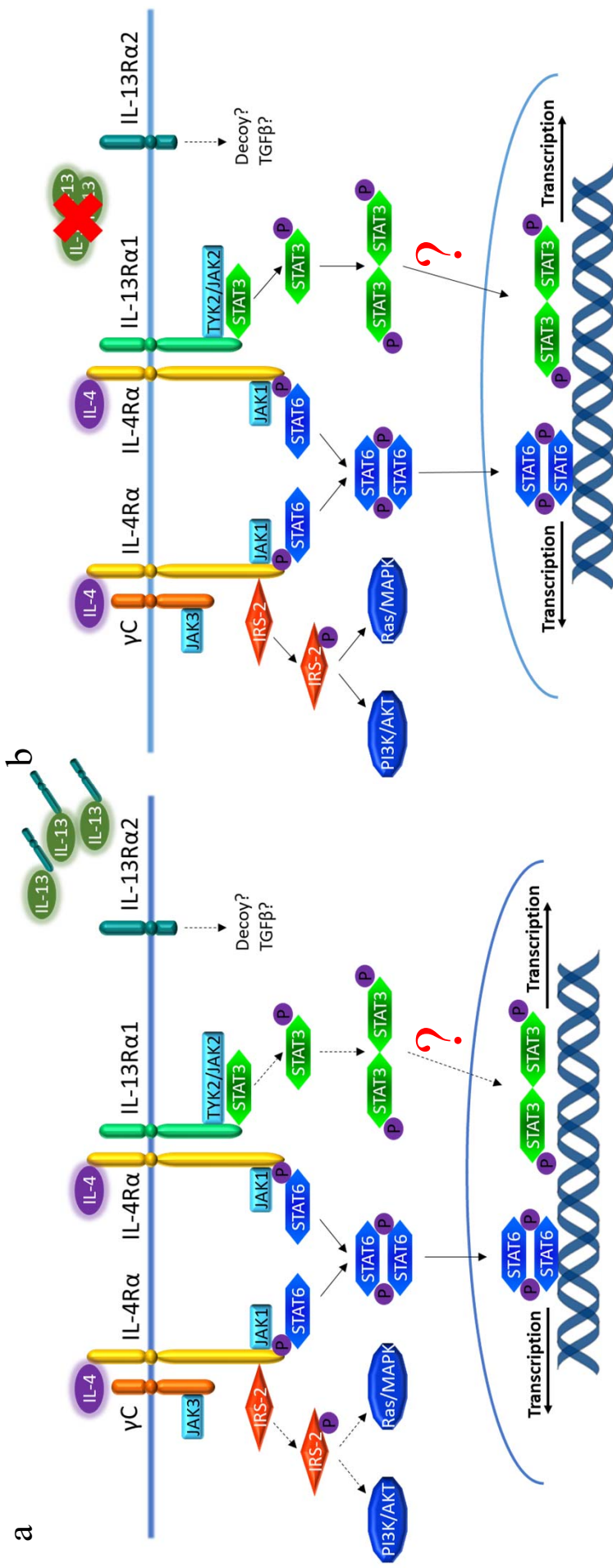


Fig. 5.8. IL-4/IL-13 signaling following BALB/c mice given the FPV-HIV-IL-13Rα2 adjuvanted vaccine (a) and IL-13^{-/-} mice given the control unadjuvanted vaccine (FPV-HIV) (b).

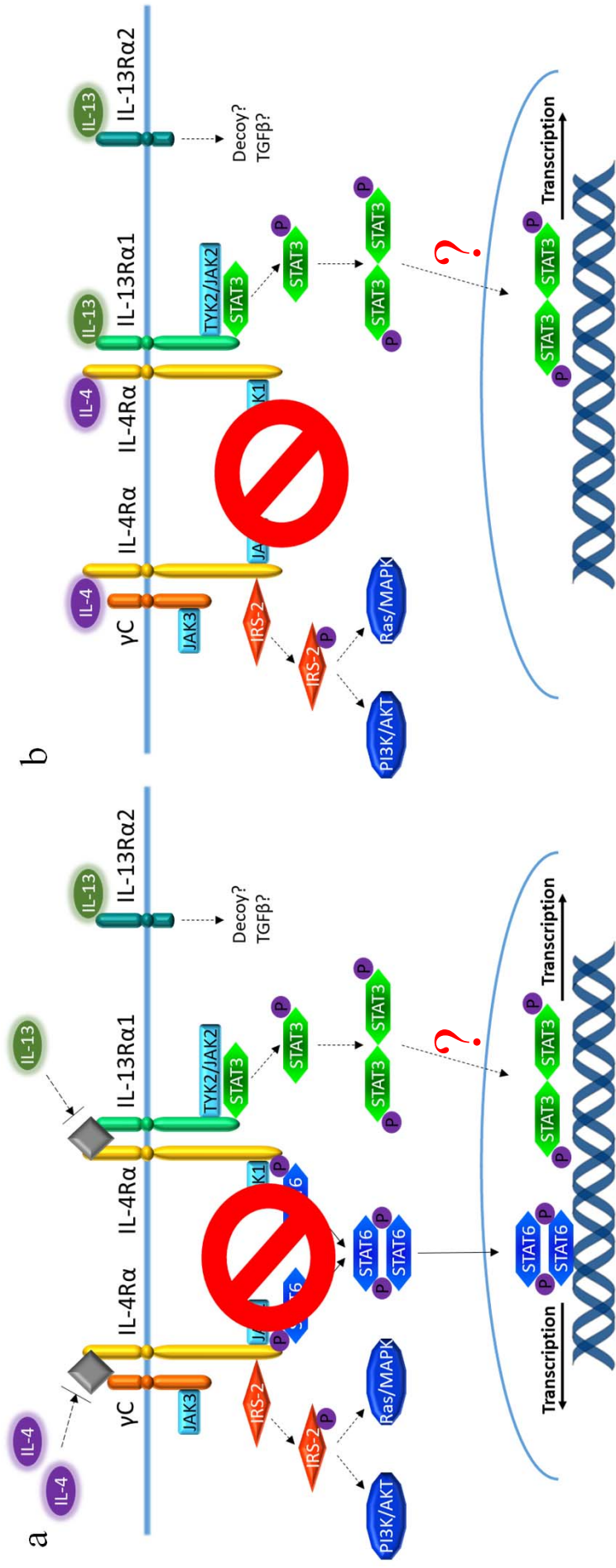


Fig. 5.9. IL-4/IL-13 signaling following BALB/c mice given the FPV-HIV-IL-4R antagonist vaccine (a) and STAT6^{-/-} mice given the control unadjuvanted vaccine (FPV-HIV) (b).

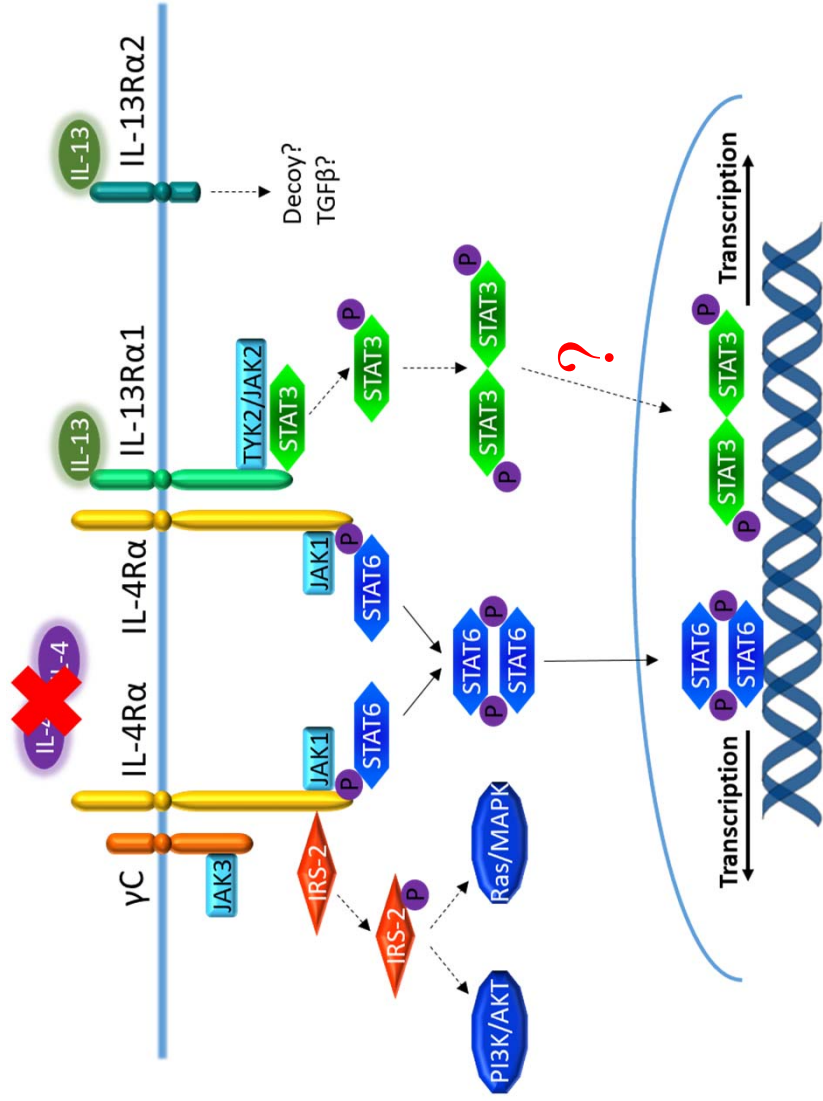


Fig. 5.10. IL-4/IL-13 signaling in IL-4^{-/-} mice following control unadjuvanted vaccination (FPV-HIV).

low IL-13^{77, 277, 278}. Thus, knowing that IL-13R α 2 is the high affinity receptor for IL-13, we postulate that in IL-4^{-/-} condition, IL-13 may act on NKp46^{+/-} ILC1/ILC3 via the IL-13R α 2 to regulate IFN- γ expression and promote IgG1/IgG2a antibody differentiation. The lower IgG2a observed in IL-13^{-/-} could be associated with redundancies in the knockout system, where compensatory mechanisms induce IgG1/IgG2a antibody differentiation, which is completely different to a transient inhibition of IL-13 (**Fig 5.8a & b**). In contrast, in WT BALB/c mice this could be associated with IL-4R α /STAT6 signalling pathway competing with IL-13R α 2, knowing that IL-4R α prevents IL-13R α 2 interaction with type II complex²⁷⁹.

Taking together the previous findings in our laboratory, current data indicated that if no ST2/IL-33R⁺ ILC2-derived IL-13 was detected at the vaccination site, no IgG2a antibody differentiation was observed regardless of the presence or absence of NKp46^{+/-} ILC1/ILC3-derived IFN- γ (**Table 5.1**). These findings support the notion that i) ILC2-derived IL-13 is a master regulator of the initial IgG1/IgG2a antibody differentiation process, likely associated with IL-13 signalling via STAT6 independent IL-13R α 2 pathway and ii) co-regulation of ST2/IL-33R⁺ ILC2-derived IL-13 and NKp46^{+/-} ILC1/ILC3-derived IFN- γ (specifically NKp46⁻ ILC) play an important role in this process (**Table 5.1**). The mechanisms at the ILC level, involved in these processes warrant further investigation.

Table 5.1 Comparison of antibody differentiation data (from previous studies in the laboratory) and ILC activation under different IL-4/IL-13 signaling conditions.

Condition	Antibody differentiation	IL-13 level (by ILC2)	IL-13 signal (via IL-13R α 2)	STAT6 signalling	IFN- γ level (by Nkp46 ⁺ ILC)	IFN- γ level (by Nkp46 ⁺ ILC)
Control	+	+++	?	√	+++	+++
IL-4R antagonist	++++	±	√	×	+++++	+++
STAT6 ^{-/-}	++++	+++++	√	×	+	+
IL-13R α 2 vaccine	±	±	×	√	+	+
IL-13 ^{-/-}	+	-	×	√	++	+++
IL-4 ^{-/-}	++++	++	√	√	+++	++

- absent, ± weak, + low, +++ medium, +++++ high, ++++++ very high, +++++++ extremely high

Chapter 6.

Evaluation of IL-13R α 2, type I and II IL-4 receptor complexes on different ILC subsets following rFPV vaccination.

6.1 Abstract.

This study demonstrated that the expression of IL-13R α 2, type I and II IL-4 receptor complexes on ST2/IL-33R⁺ ILC2 and NKp46⁻ ILC1/ILC3 were co-regulated, 24 h post intranasal rFPV vaccination. Inhibition of STAT6 signalling significantly impacted the IL-13R α 2 expressions on both ST2/IL-33R⁺ ILC2 and NKp46⁻ ILC1/ILC3, unlike IL-13 inhibition, suggesting that under STAT6 inhibition conditions, IL-13 could signal via IL-13R α 2 pathway. As elevated number of ST2/IL-33R⁺ ILC2 expressing IL-13R α 2 were detected in BALB/c mice given the FPV-HIV-IL-4R antagonist vaccine also indicated an autocrine regulation of IL-13 at the ILC2 via IL-13R α 2. The IL-4/IL-13 receptor expression profile on NKp46⁺ ILC1/ILC3 and NKp46⁻ ILC1/ILC3 were vastly different, suggesting that these cells may play different roles in downstream immune outcomes.

6.2 Introduction.

Data in previous chapters have demonstrated that ILC2-driven IL-13 can significantly modulate ILC1/ILC3 function (specifically, IFN- γ expression) and is a master regulator of the initial T and B cell activation in a STAT6 independent manner. However, the molecular mechanism by which ILC2-derived IL-13 regulating ILC1/ILC3 activity is not well understood.

IL-4 and IL-13 signal via a complex receptor system⁹². The type I and type II IL-4 receptor complexes consist of the γ C/IL-4R α and IL-4R α /IL-13R α 1 respectively⁹³ (**Fig. 1.10**). IL-4 can signal via both type I and type II receptor complex by binding IL-4R α ⁹⁴,⁹⁵, signalling via the JAK/STAT6 pathway^{96, 97, 98}. IL-13 can also bind to IL-13R α 1 (type II IL-4 receptor complex) with low affinity (nM concentrations) and signal via the

JAK/STAT6 pathway⁹³. Furthermore, under low IL-13 conditions (pM concentrations), it is also thought that IL-13 can signal via IL-13R α 2 pathway¹¹² using a not yet characterised mechanism. Studies have shown that IL-13R α 2 can bind to IL-4R α and inhibit IL-4/IL-13 signalling via the IL-13R α 1/IL-4R α type II complex and JAK/STAT6 pathway^{117, 118, 119, 120}. Also, in cancer studies IL-13R α 2 activation/signalling has been associated with TGF- β production in the absence of functional IL-4R α ¹²¹. The dis-regulation of IL-13R α 2 in cancers^{280, 281, 282, 283} suggest that maintaining the optimal balance of IL-13 may be crucial for cell homeostasis and immune regulation.

Given that i) IL-13R α 2 being the high affinity receptor for IL-13 compared to IL-13R α 1, and ii) recent studies in the laboratory including Chapter 5 studies indicating that IL-13R α 2 could be involved in ILC2-driven IL-13 and ILC1/ILC3-driven IFN- γ regulation (specifically in the context of antibody differentiation), in this chapter, the possible mechanisms involved in this processes were assessed 24 h post vaccination. Specifically, by evaluating the IL-4/IL-13 receptors (IL-13R α 2, IL-13R α 1, IL-4R α , and γ C) on ILC subsets in i) WT BALB/c mice following FPV-HIV unadjuvanted or IL-4R antagonist and IL-13R α 2 adjuvanted vaccines, and ii) IL-13^{-/-} and STAT6^{-/-} mice following FPV-HIV unadjuvanted vaccination. (Note that in this study 24 h time point was chosen as Chapters 3-5 studies clearly demonstrated that ILC were mainly regulated at this timepoint).

6.3 Materials and Methods.

6.3.1 Mice and immunisation.

5-6 weeks old pathogen free female WT BALB/c, IL-13^{-/-}, and STAT6^{-/-} mice were obtained from the Australian Phenomics Facility, the Australian National University, and were maintained and handled under protocols indicated in **2.2.1**. 1×10^7 PFU unadjuvanted FPV-HIV, FPV-HIV-IL-4R antagonist, or FPV-HIV-IL-13R α 2 adjuvanted vaccines were administered to BALB/c mice (n = 4 per group) intranasally under mild isoflurane anaesthesia as per described in **2.2.5**. IL-13^{-/-} and STAT6^{-/-} mice (n = 4 per group) were intranasally vaccinated with 1×10^7 PFU unadjuvanted FPV-HIV vaccine. Lungs were harvested in 2 ml of complete RPMI 24 h post vaccination, single cell lung suspensions were prepared, stained and analysed as per described in **2.2.6 and 2.2.8**.

6.3.2 Surface staining.

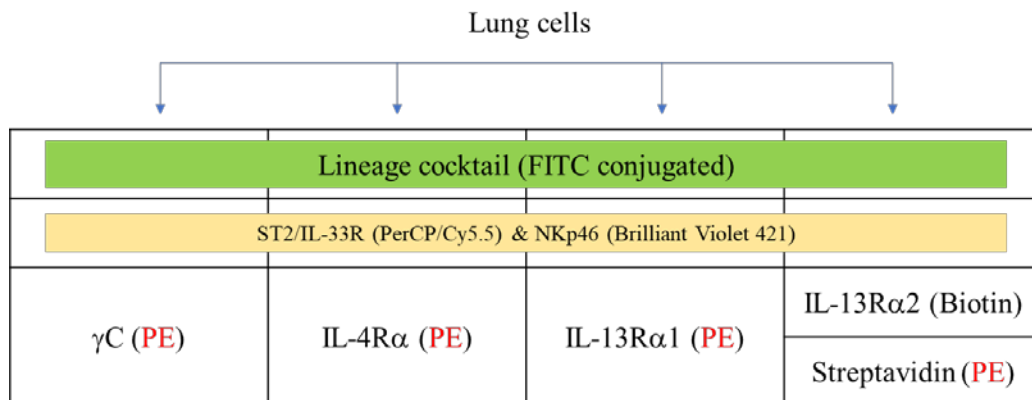
Surface staining was performed as per described in **2.2.8** using antibodies listed in **Table 2.3**. Specifically,

ILC staining: APC/Cy7-conjugated anti-mouse CD45, and FITC-conjugated lineage cocktail were used to identify lineage⁺ cells. PerCP/Cy5.5-conjugated anti-mouse ST2/IL-33R was used to identify the ILC2. Brilliant Violet 421-conjugated anti-mouse CD335 (NKp46) were used to identify ILC1/3 populations.

IL-13R α 2, IL-13R α 1, IL-4R α , and γ C staining: PE-conjugated anti-mouse γ C (CD132), PE-conjugated anti-mouse IL-4R α (CD124), PE-conjugated anti-mouse IL-13R α 1, and Biotin-conjugated anti-mouse IL-13R α 2 were used to evaluate type I (γ C and IL-4R α) and type II (IL-4R α and IL-13R α 1) IL-4 receptor complex and IL-13R α 2

expression on different ILC subsets. PE-conjugated streptavidin was used as secondary antibody to detect the Biotin-conjugated IL-13R α 2 antibody. All receptors antibodies were stained separately to avoid spectral overlap as indicated in the **Flowchart 6.1**. Specifically, γ C (PE), IL-4R α (PE), IL-13R α 1 (PE) and IL-13R α 2 (Biotin) were stained with ILC master mix antibodies. Then γ C, IL-4R α , and IL-13R α 1 stained samples were directly fixed with 0.5% PFA as per described in **2.2.8**. The IL-13R α 2 stained samples were washed once with FACS buffer and then stained with PE-conjugated Streptavidin for 15 min on ice in the dark, followed by washing and fixing with 0.5% PFA. All samples were analysed using a BD LSR Fortessa as per described in **2.2.8**. All ILC subsets and their γ C, IL-4R α , IL-13R α 1, and IL-13R α 2 expression were analysed based on the FMO controls as per described in **Fig. 6.1**.

Flowchart 6.1. ILC γ C, IL-4R α , IL-13R α 1, and IL-13R α 2 staining strategy.



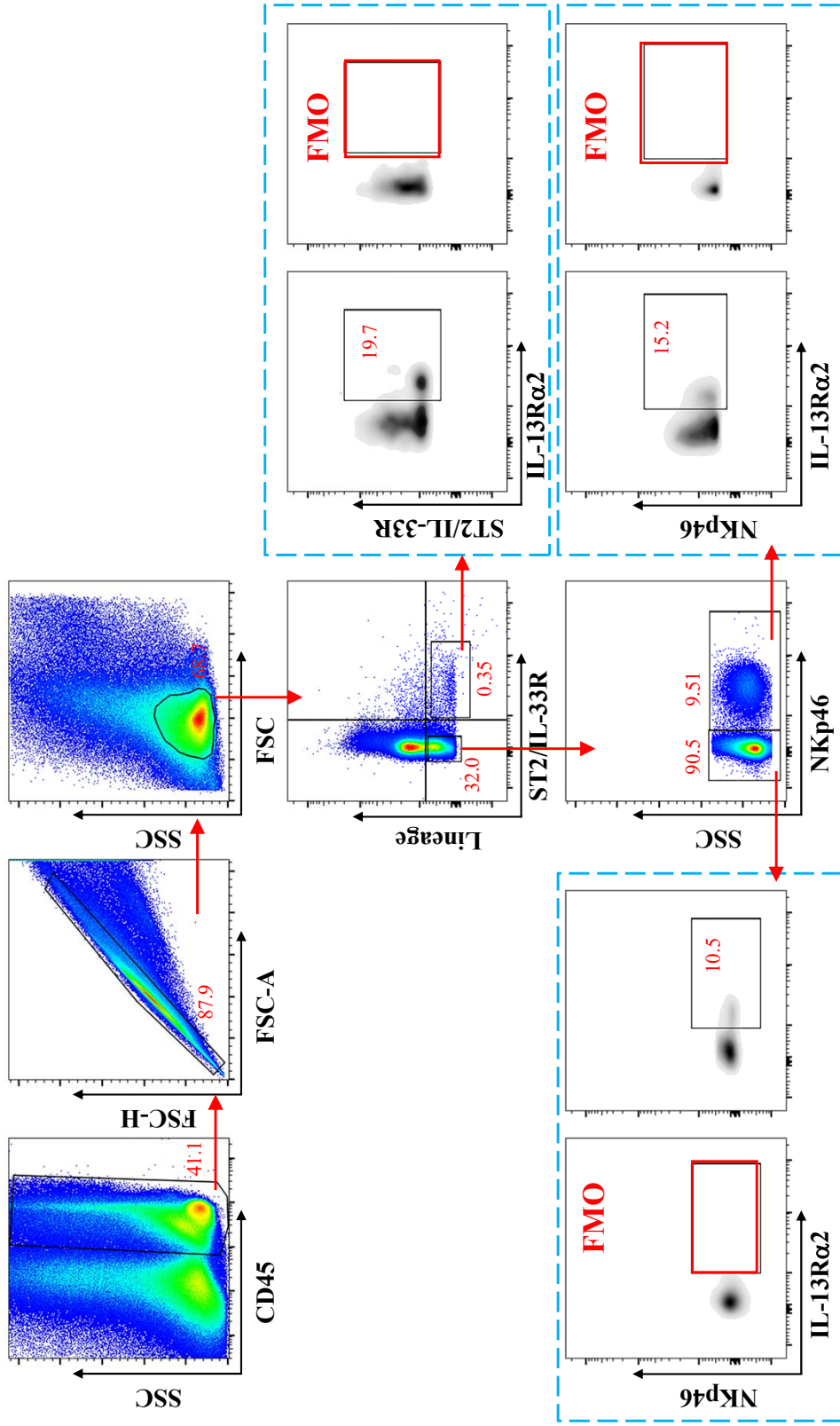


Fig. 6.1. Lung ILC IL-13R α 2 expression gating strategy.

Lung ILCs from BALB/c mice were evaluated 24 h post FPV-HIV immunization as per described in Materials and Methods. ILC2 were gated as CD45⁺ FSC^{low} SSC^{low} lineage⁻ IL-33R/ST2⁺ cells. ILC1/ILC3 were identified as CD45⁺ FSC^{low} SSC^{low} lineage⁻ IL-33R/ST2⁻ NKp46^{+/-} ILCs. γ C, IL-4R α , IL-13R α 1, and IL-13R α 2 expression on different ILC subsets were assessed based on FMO controls. The FACS plots are representative gating strategy for IL-13R α 2 expression on ILC2 and NKp46^{+/-} ILC1/ILC3.

6.4 Results.

6.4.1 Elevated number of ST2/IL-33R⁺ ILC2 and NKp46⁻ ILC1/ILC3 were found to express IL-13R α 2 following FPV-HIV-IL-4R antagonist vaccination.

To examine type I and type II IL-4 receptor complexes and IL-13R α 2 expression profiles on different ILC subsets, WT BALB/c mice were vaccinated intranasally with the unadjuvanted and adjuvanted vaccines and ILC subsets were evaluated using multicolour flow cytometry as per described in Materials and Methods. Data revealed that at 24 h post rFPV vaccination, IL-13R α 2, IL-13R α 1, IL-4R α , and γ C were expressed on both ST2/IL-33R⁺ ILC2 and NKp46^{+/+} ILC1/ILC3 (**Fig. 6.2a-d**).

When transient versus permanent inhibition of STAT6 (FPV-HIV-IL-4R antagonist vs STAT6^{-/-}), elevated number of ST2/IL-33R⁺ ILC2 were found to express IL-13R α 2 following IL-4R antagonist adjuvanted vaccination compared to BALB/c mice given the unadjuvanted FPV-HIV vaccination ($p < 0.05$) (**Fig. 6.3a**). In contrast, no ST2/IL-33R⁺ ILC2 obtained from STAT6^{-/-} mice given the unadjuvanted vaccine were found to express IL-13R α 2 (**Fig. 6.3a**). However, no significant difference in ST2/IL-33R⁺ ILC2 IL-13R α 1 expression was observed in any of the groups tested (**Fig. 6.3b**). Although no differences in γ C and IL-4R α expression were detected in BALB/c mice vaccinated with IL-4R antagonist adjuvanted and unadjuvanted vaccines, significantly lower number of ST2/IL-33R⁺ ILC2 from STAT6^{-/-} mice given unadjuvanted FPV-HIV vaccine expressed these two receptors (**Fig. 6.3c & d**).

When the densities of the different receptors on ILC subsets were assessed, no significant differences in IL-13R α 2 and IL-13R α 1 were detected on ST2/IL-33R⁺

Fig. 6.2. Evaluation of type I (γ C chain and IL-4R α) and type II (IL-4R α and IL-13R α 1) IL-4 receptor complexes and IL-13R α 2 expression on ILC following intranasal rFPV vaccination.

WT BALB/c mice (each group n = 4) were immunized intranasally with unadjuvanted FPV-HIV vaccine. Using the flow cytometry gating strategy indicated in materials and methods, ILC2s were defined as CD45⁺ FSC^{low} SSC^{low} lineage⁻ IL-33R/ST2⁺ cells, ILC1/ILC3 were identified as CD45⁺ FSC^{low} SSC^{low} lineage⁻ IL-33R/ST2⁻ NKp46^{+/-} ILCs. The histogram FACS plots indicate the expression of IL-13R α 2 (a), IL-13R α 1 (b), IL-4R α (c), and γ C chain (d) on different ILC subsets in unimmunized WT BALB/c mice (black line) and 24 h post intranasal unadjuvanted rFPV vaccinated WT BALB/c mice (blue line) compared to isotype control.

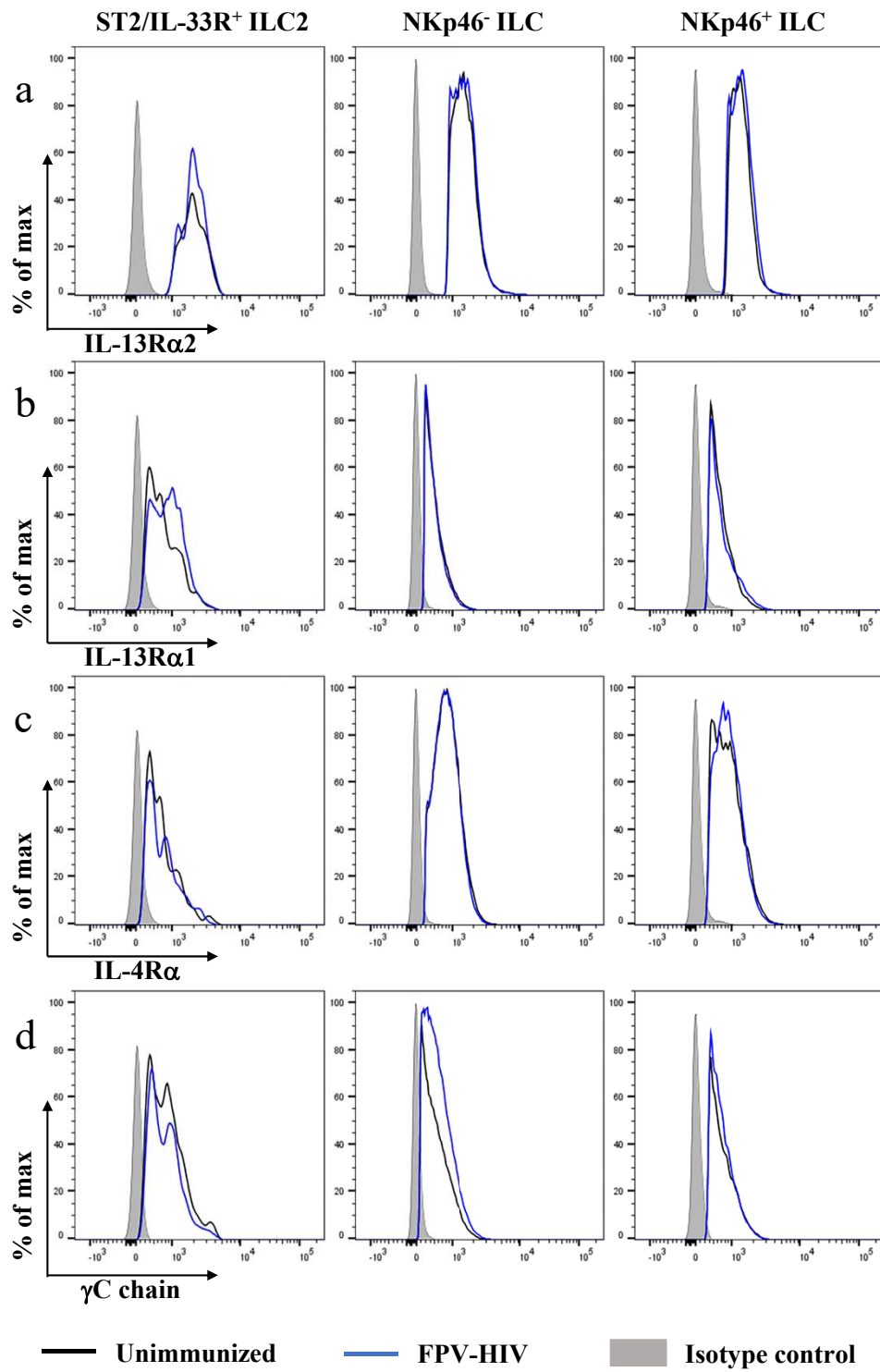
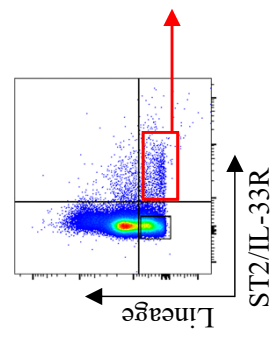
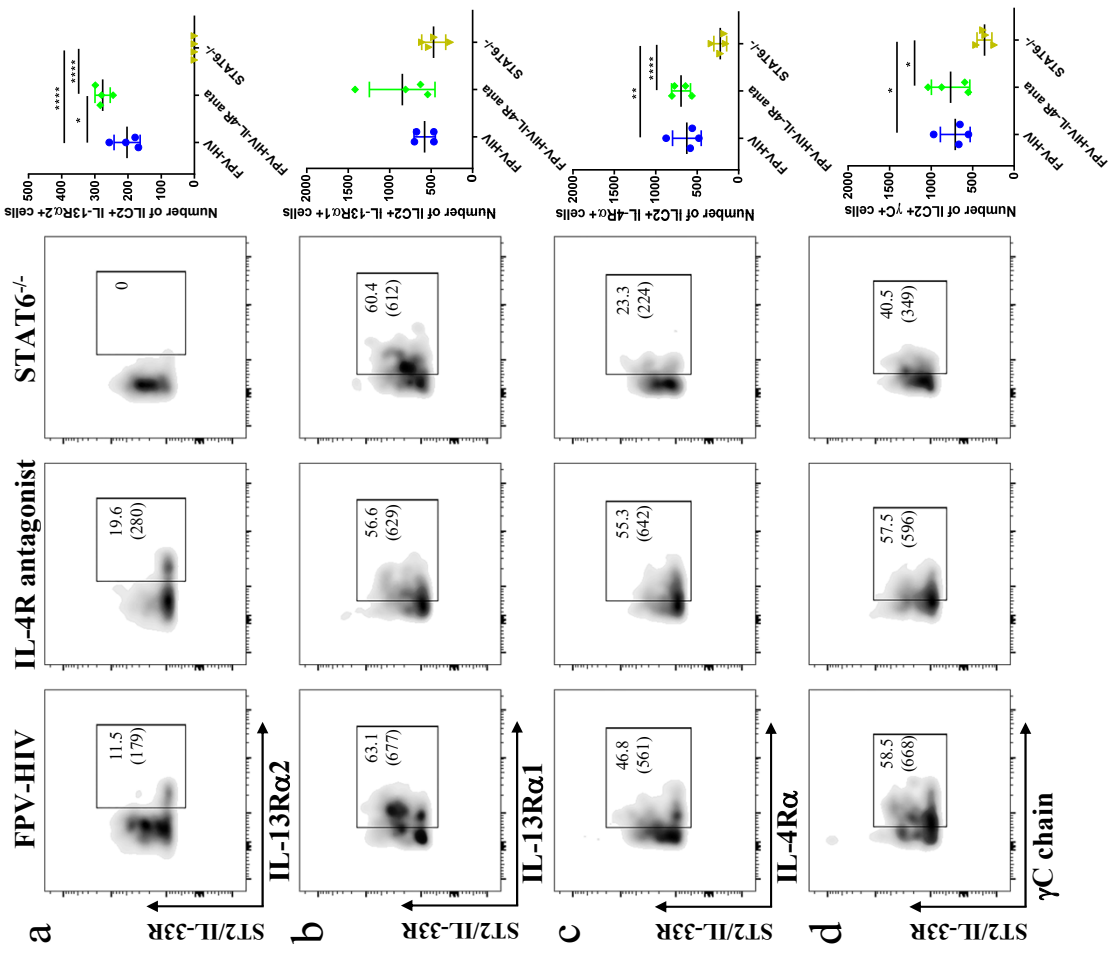


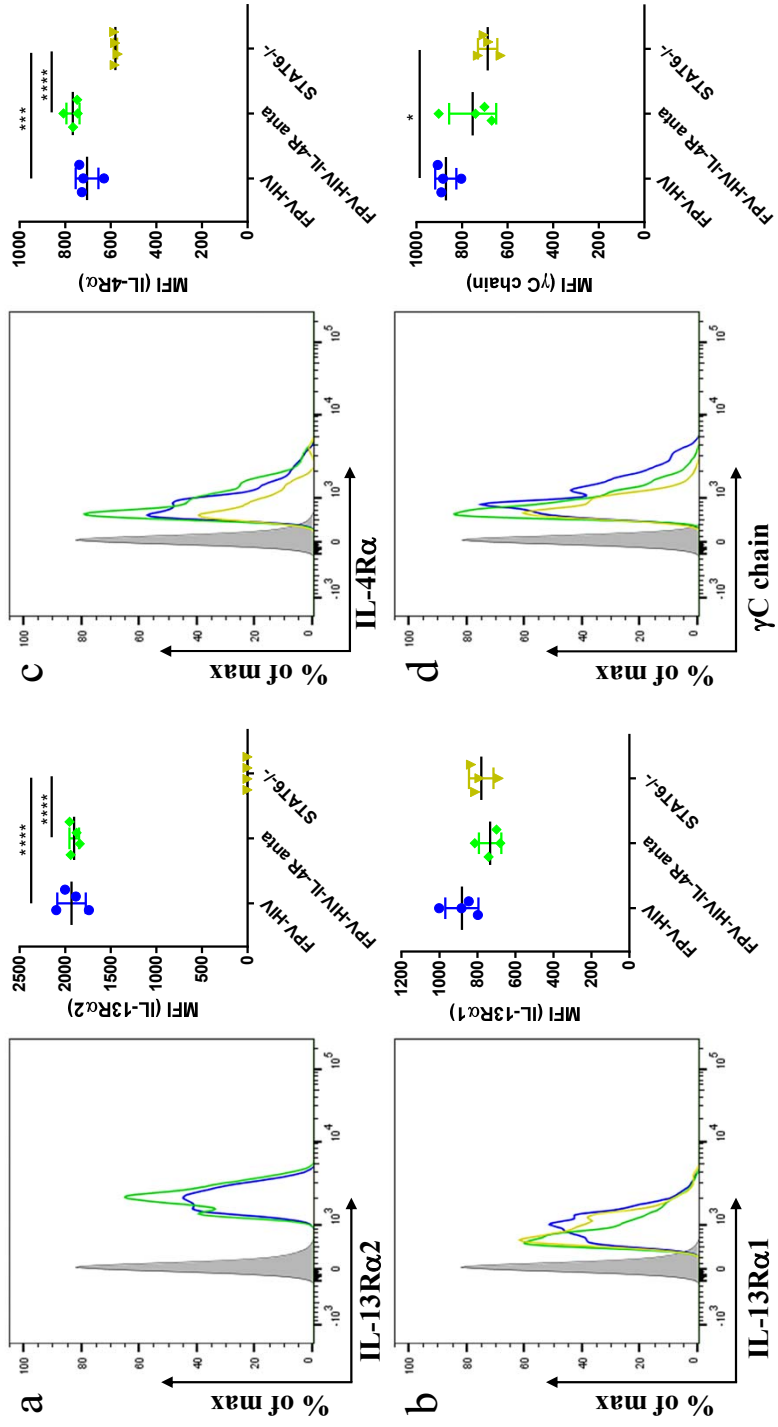
Fig. 6.3. Evaluation of number of lung lineage⁻ IL-33R/ST2⁺ ILC2 expressing type I (γ C chain and IL-4R α) and type II (IL-4R α and IL-13R α 1) IL-4 receptor complex and IL-13R α 2 – (permanent vs transient inhibition of STAT6 signalling).

WT BALB/c and STAT6^{-/-} mice (each group n = 4) were immunized intranasally with unadjuvanted FPV-HIV or FPV-HIV-IL-4R antagonist vaccines. Lung ILC2 were evaluated as CD45⁺ FSC^{low} SSC^{low} lineage⁻ IL-33R/ST2⁺ cells. The FACS plots in each panel indicate the percentage of ILC2 expressing IL-13R α 2 **(a)**, IL-13R α 1 **(b)**, IL-4R α **(c)**, and γ C chain **(d)** in each group. The bracket below the cell percentage indicates the number of cells in each gate. Graph in each panel represents number of ILC2s expressing the different receptors back calculated to CD45⁺ population as described in materials and methods (24 h post vaccination). The error bars represent the mean and standard deviation (s.d.). The p-values were calculated using GraphPad Prism software (version 6.05 for Windows). * = p<0.05, ** = p<0.01, *** = p<0.001, **** = p<0.0001. For each group experiments were repeated minimum three times.



ILC2s (**Fig. 6.4a & b**). However, IL-4R α densities on ST2/IL-33R⁺ ILC2 obtained from STAT6^{-/-} mice given the unadjuvanted vaccine were significantly down-regulated compared to BALB/c mice given the adjuvanted or the unadjuvanted vaccines (p<0.0001 and p<0.001 respectively) (**Fig. 6.4c**). Similarly, down regulation of γ C on ST2/IL-33R⁺ ILC2 was also observed in STAT6^{-/-} mice compared to BALB/c given the unadjuvanted vaccine (**Fig. 6.4d**).

Following rFPV vaccination, similar to ST2/IL-33R⁺ ILC2, elevated number of NKp46⁻ ILC1/ILC3 were found to express IL-13R α 2 in FPV-HIV-IL-4R antagonist adjuvanted vaccine group compared to both BALB/c and STAT6^{-/-} mice given unadjuvanted FPV-HIV vaccination (p<0.01) (**Fig. 6.5a**). Interestingly, STAT6^{-/-} mice given unadjuvanted FPV-HIV vaccine showed down-regulation of the IL-13R α 1 on NKp46⁻ ILC1/ILC3 compared to both BALB/c mice given unadjuvanted FPV-HIV or FPV-HIV-IL-4R antagonist adjuvanted vaccines (**Fig. 6.5b**). Moreover, transient inhibition of STAT6 signalling (FPV-HIV-IL-4R antagonist) down-regulated the expression of IL-4R α on NKp46⁻ ILC1/ILC3s (**Fig. 6.5c**). Similarly, γ C was also down-regulated on FPV-HIV-IL-4R antagonist vaccinated NKp46⁻ ILC1/ILC3s compared to unadjuvanted vaccination (p<0.05) (**Fig. 6.5d**). In the context of IL-4/IL-13 receptor densities, STAT6^{-/-} mice given the unadjuvanted vaccine showed significant down-regulation of IL-13R α 2 on NKp46⁻ ILC1/ILC3 compared to the other vaccine groups tested (**Fig. 6.6a**). Interestingly, IL-13R α 1 or IL-4R α was not modulated on NKp46⁻ ILC1/ILC3 (**Fig. 6.6b & c**), although STAT6 inhibition resulted in down-regulation of γ C expression on these cells (**Fig. 6.6d**).



— FPV-HIV — FPV-HIV-IL-4R antagonist — STAT6^{-/-} — Isotype control

Fig. 6.4. IL-13R α 2, IL-13R α 1, IL-4R α , and γ C receptor densities on ILC2 following rFPV vaccination – (permanent vs transient inhibition of STAT6 signalling).

WT BALB/c mice and STAT6^{-/-} mice (each group n = 4) were immunized intranasally with unadjuvanted FPV-HIV or FPV-HIV-IL-4R antagonist vaccines. Lung ILC2 were gated as CD45⁺ FSC^{low} SSC^{low} lineage⁻ IL-33R/ST2⁺ cells. The histogram plots show cell surface expression of IL-13R α 2 **(a)**, IL-13R α 1 **(b)**, IL-4R α **(c)**, and γ C chain **(d)** on ILC2s as MFI, [WT BALB/c mice given unadjuvanted FPV-HIV (blue lines) or FPV-HIV-IL-4R antagonist (green lines), and STAT6^{-/-} mice given unadjuvanted FPV-HIV (yellow lines)]. Graphs represent the mean fluorescence intensity of each receptor. The error bars represent the mean and standard deviation (s.d.). The p-values were calculated using GraphPad Prism software (version 6.05 for Windows). * = p<0.05, ** = p<0.01, *** = p<0.001, **** = p<0.0001. For each group experiments were repeated minimum three times.

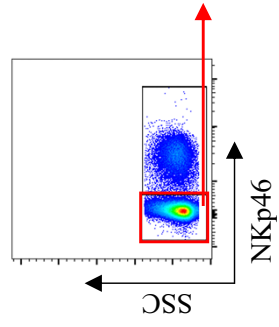
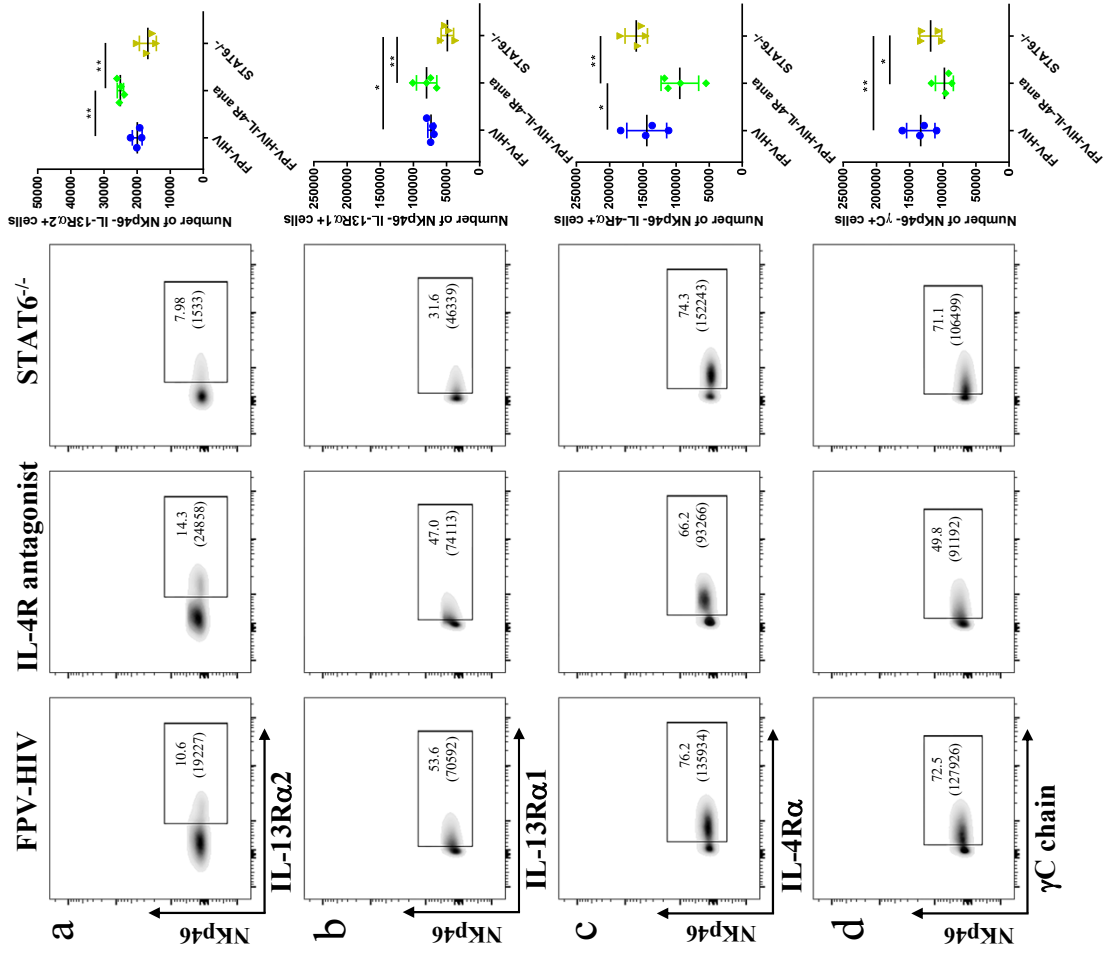
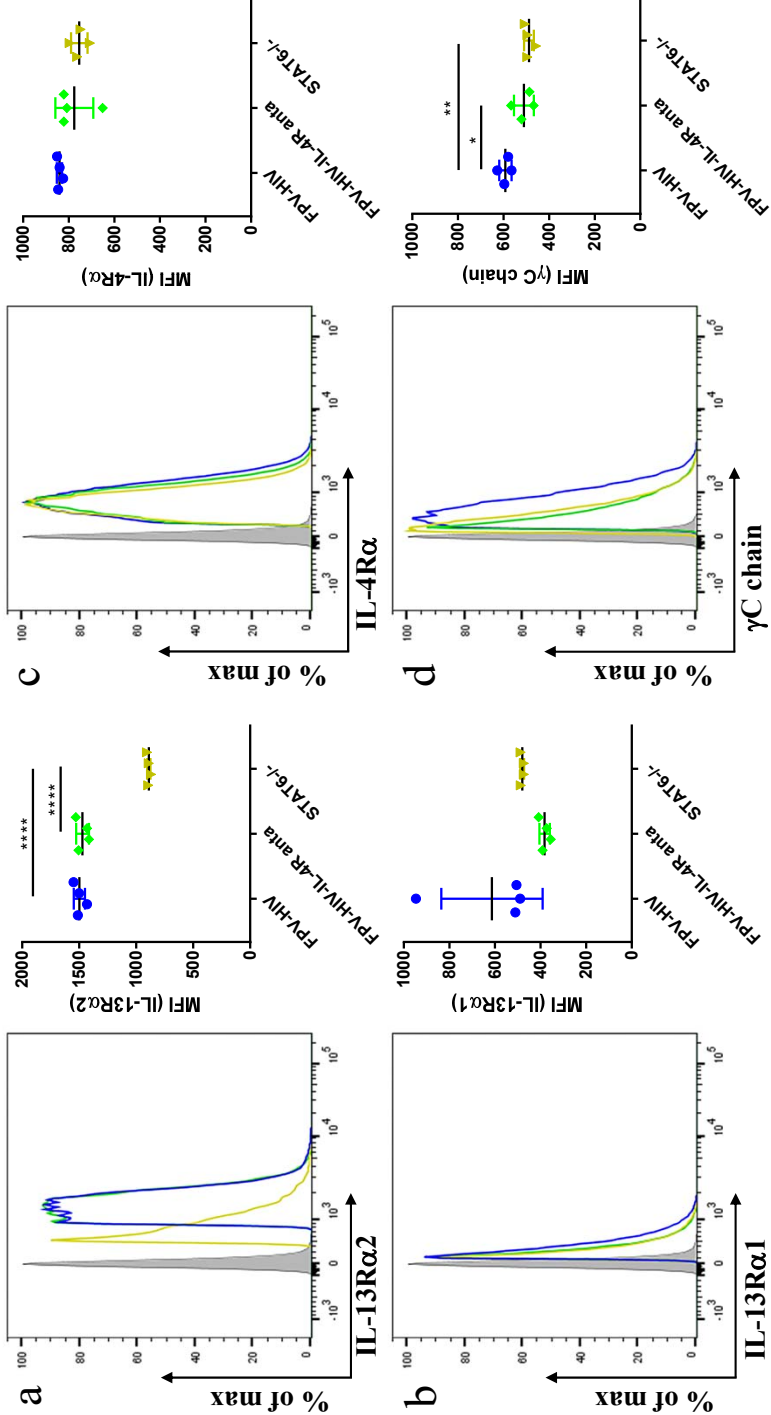


Fig. 6.5. Evaluation of number of lung lineage⁻ IL-33R/ST2⁻ NKp46⁻ ILC1/ILC3 expressing IL-13R α 2, IL-13R α 1, IL-4R α , and γ C chain - (permanent vs transient inhibition of STAT6 signalling).

WT BALB/c and STAT6^{-/-} mice (each group n = 4) were immunized intranasally with unadjuvanted FPV-HIV or FPV-HIV-IL-4R antagonist vaccines. Lung NKp46⁻ ILC1/ILC3 were gated as CD45⁺ FSC^{low} lineage⁻ IL-33R/ST2⁻ NKp46⁻ cells. The FACS plots in each panel indicate the percentage of NKp46⁻ ILC1/ILC3 expressing IL-13R α 2 **(a)**, IL-13R α 1 **(b)**, IL-4R α **(c)**, and γ C chain **(d)**. The bracket below the cell percentage indicates the number of cells in each gate. Graph in each panel represents number of NKp46⁻ ILC1/ILC3s expressing the different receptors back calculated to CD45⁺ population as described in materials and methods at (24 h post vaccination). The error bars represent the mean and standard deviation (s.d.). The p-values were calculated using GraphPad Prism software (version 6.05 for Windows). * = p<0.05, ** = p<0.01, *** = p<0.001, **** = p<0.0001. For each group experiments were repeated minimum three times.



— FPV-HIV
 — FPV-HIV-IL-4R antagonist
 — STAT6^{-/-}
 Isotype control

Fig. 6.6. IL-13R α 2, IL-13R α 1, IL-4R α , and γ C receptor densities on lineage⁻ IL-33R/ST2⁻ NKp46⁻ ILC1/ILC3 following rFPV vaccination - (permanent vs transient inhibition of STAT6 signalling).

WT BALB/c mice and STAT6^{-/-} mice (each group n = 4) were immunized intranasally with unadjuvanted FPV-HIV or FPV-HIV-IL-4R antagonist vaccines. Lung NKp46⁻ ILC1/ILC3 were gated as CD45⁺ FSC^{low} SSC^{low} lineage⁻ IL-33R/ST2⁻ NKp46⁻ cells. The histogram plots in each panel show cell surface expression of IL-13R α 2 (**a**), IL-13R α 1 (**b**), IL-4R α (**c**), and γ C chain (**d**) on lung NKp46⁻ ILC1/ILC3, [WT BALB/c mice given unadjuvanted FPV-HIV (blue lines) or FPV-HIV-IL-4R antagonist (green lines), and STAT6^{-/-} mice given unadjuvanted FPV-HIV (yellow lines)]. Graphs represent the mean fluorescence intensity of each receptor. The error bars represent the mean and standard deviation (s.d.). The p-values were calculated using GraphPad Prism software (version 6.05 for Windows). * = p<0.05, ** = p<0.01, *** = p<0.001, **** = p<0.0001. For each group experiments were repeated minimum three times.

6.4.2 Following FPV-HIV-IL-13R α 2 adjuvanted vaccination, IL-13R α 2 was not regulated on ST2/IL-33R $^+$ ILC2 or NKp46 $^-$ ILC1/ILC3.

Next when IL-4/IL-13 receptor expression on ST2/IL-33R $^+$ ILC2 were examined under transient versus permanent inhibition of IL-13 (FPV-HIV-IL-13R α 2 vs IL-13 $^{-/-}$), although expression of IL-13R α 2 on ST2/IL-33R $^+$ ILC2 was not modulated, IL-13R α 1 expression was significantly down regulated on IL-13 $^{-/-}$ mice given the unadjuvanted vaccine ($p < 0.05$) (**Fig. 6.7a & b**). Interestingly, in this scenario, elevated number of ST2/IL-33R $^+$ ILC2 were found to express both γ C and IL-4R α following FPV-HIV-IL-13R α 2 adjuvanted vaccination, unlike IL-13 $^{-/-}$ mice given unadjuvanted FPV-HIV vaccine ($p < 0.001$ and $p < 0.0001$ respectively) (**Fig. 6.7c & d**). Furthermore, compare to the BALB/c mice given the unadjuvanted vaccine, mice that received FPV-HIV-IL-13R α 2 adjuvanted vaccine showed significant regulation of type I IL-4 receptor complex on ST2/IL-33R $^+$ ILC2 (**Fig. 6.7c & d**). In the context of IL-4/IL-13 receptor densities on ST2/IL-33R $^+$ ILC2, the IL-13 $^{-/-}$ mice given the unadjuvanted vaccine showed significantly lower IL-4R α / γ C expression (**Fig. 6.8c & d**). Interestingly, IL-13R α 1 and IL-13R α 2 were not regulated in any of the groups tested (**Fig. 6.8a & b**).

Under different IL-13 inhibition conditions, the IL-4/IL-13 receptor expression profiles were vastly different between ST2/IL-33R $^+$ ILC2 and NKp46 $^-$ ILC1/ILC3. Significantly elevated number of NKp46 $^-$ ILC1/ILC3 were found to express IL-13R α 2 in the IL-13 $^{-/-}$ mice given the unadjuvanted vaccine (**Fig. 6.9a**). However surprisingly, transient inhibition of IL-13 showed elevated number of NKp46 $^-$ ILC1/ILC3 expressing IL-13R α 1 compared to both BALB/c and IL-13 $^{-/-}$ mice given the unadjuvanted vaccine (**Fig. 6.9b**). Elevated number of NKp46 $^-$ ILC1/ILC3 were found to express IL-4R α (**Fig. 6.9c**), but not γ C (**Fig. 6.9d**) obtained from IL-13 $^{-/-}$ mice given unadjuvanted FPV-HIV

Fig. 6.7. Evaluation of number of lung lineage⁻ IL-33R/ST2⁺ ILC2 expressing IL-13R α 2, IL-13R α 1, IL-4R α , and γ C - (permanent vs transient inhibition of IL-13).

WT BALB/c and IL-13^{-/-} mice (each group n = 4) were immunized intranasally with unadjuvanted FPV-HIV or FPV-HIV-IL-13R α 2 adjuvanted vaccines. Lung ILC2 were gated as CD45⁺ FSC^{low} SSC^{low} lineage⁻ IL-33R/ST2⁺ cells. The FACS plots in each panel indicate the percentage of ILC2s expressing IL-13R α 2 (a), IL-13R α 1 (b), IL-4R α (c), and γ C chain (d). The bracket below the cell percentage indicates the number of cells is each gate. Graph in each panel represents number of ILC2s expressing the different receptors back calculated to CD45⁺ population as described in materials and methods (24 h post vaccination). The error bars represent the mean and standard deviation (s.d.). The p-values were calculated using GraphPad Prism software (version 6.05 for Windows). * = p<0.05, ** = p<0.01, *** = p<0.001, **** = p<0.0001. For each group experiments were repeated minimum three times.

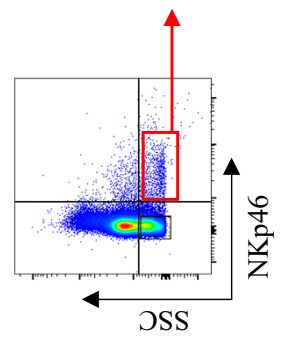
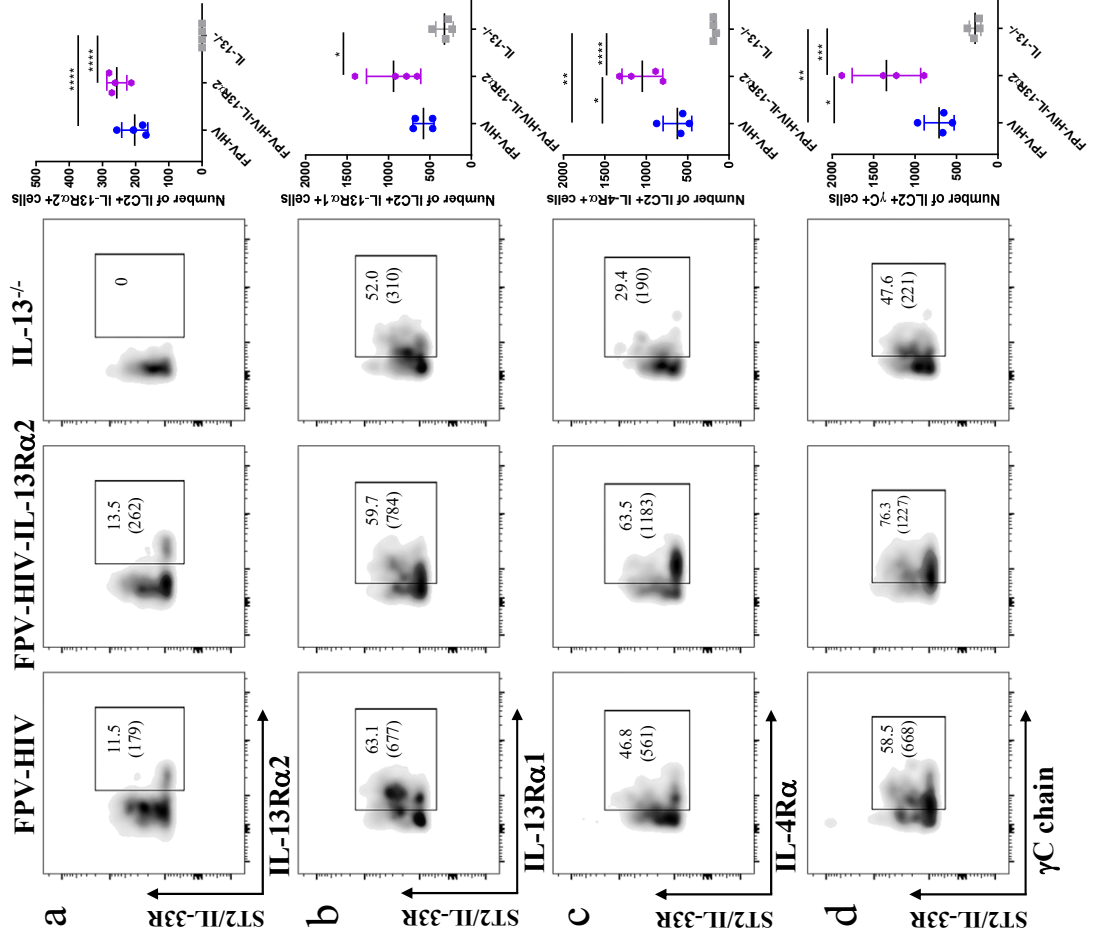


Fig. 6.8. IL-13R α 2, IL-13R α 1, IL-4R α , and γ C receptor densities on ILC2 following unadjuvanted and IL-13R α 2 adjuvanted vaccination.

WT BALB/c mice and IL-13^{-/-} mice (each group n = 4) were immunized intranasally with unadjuvanted FPV-HIV or FPV-HIV-IL-13R α 2 adjuvanted vaccines. Lung ILC2 were gated as CD45⁺ FSC^{low} SSC^{low} lineage⁻ IL-33R/ST2⁺ cells. The histogram plots in each panel show cell surface expression of IL-13R α 2 (**a**), IL-13R α 1 (**b**), IL-4R α (**c**), and γ C chain (**d**) on lung ILC2 [WT BALB/c mice given unadjuvanted FPV-HIV (blue lines) or FPV-HIV-IL-13R α 2 adjuvanted (purple lines), and IL-13^{-/-} mice given unadjuvanted FPV-HIV (grey lines)]. Graphs represent the mean fluorescence intensity of each receptor. The error bars represent the mean and standard deviation (s.d.). The p-values were calculated using GraphPad Prism software (version 6.05 for Windows).

* = p<0.05, ** = p<0.01, *** = p<0.001, **** = p<0.0001. For each group experiments were repeated minimum three times.

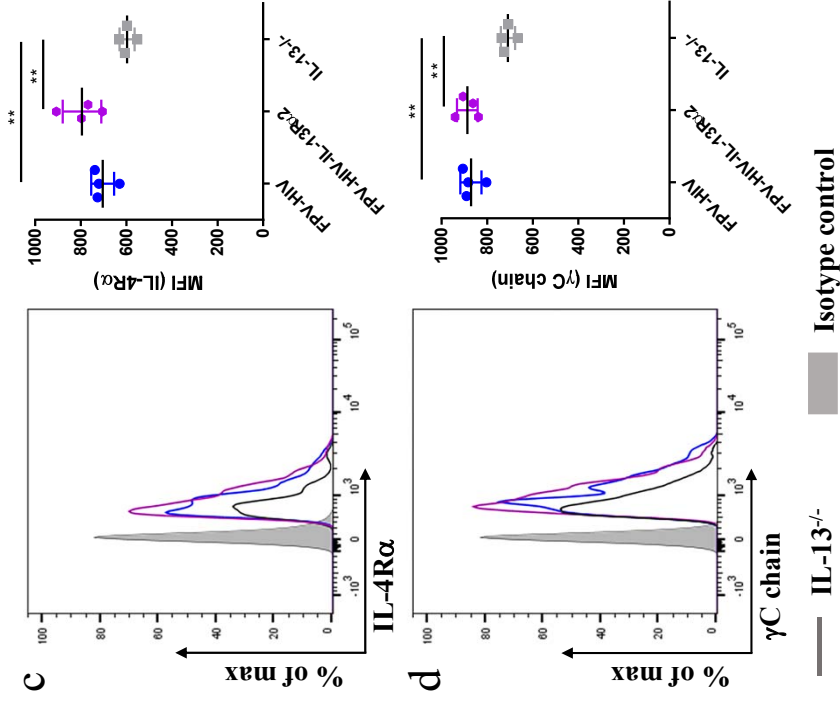
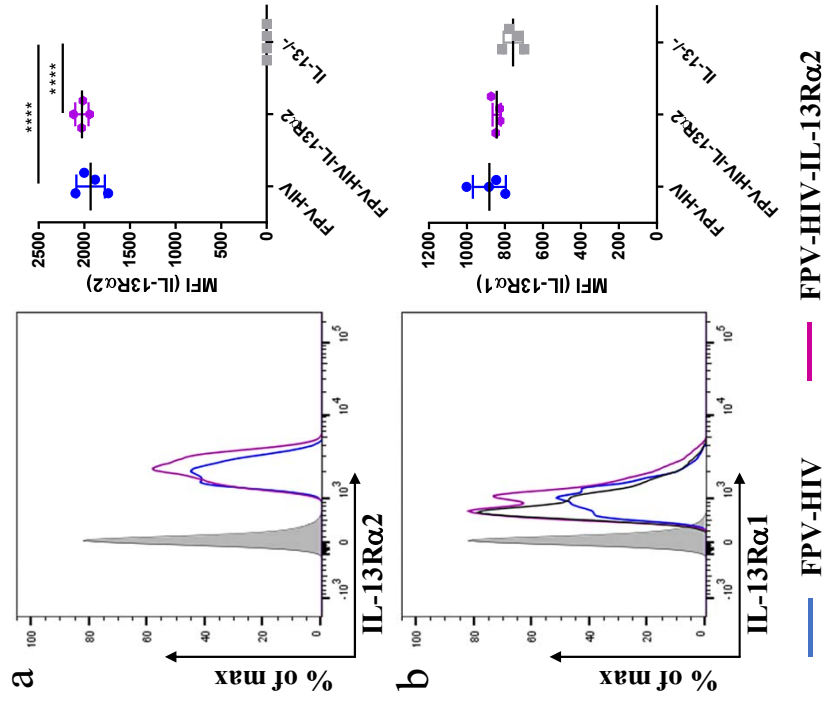
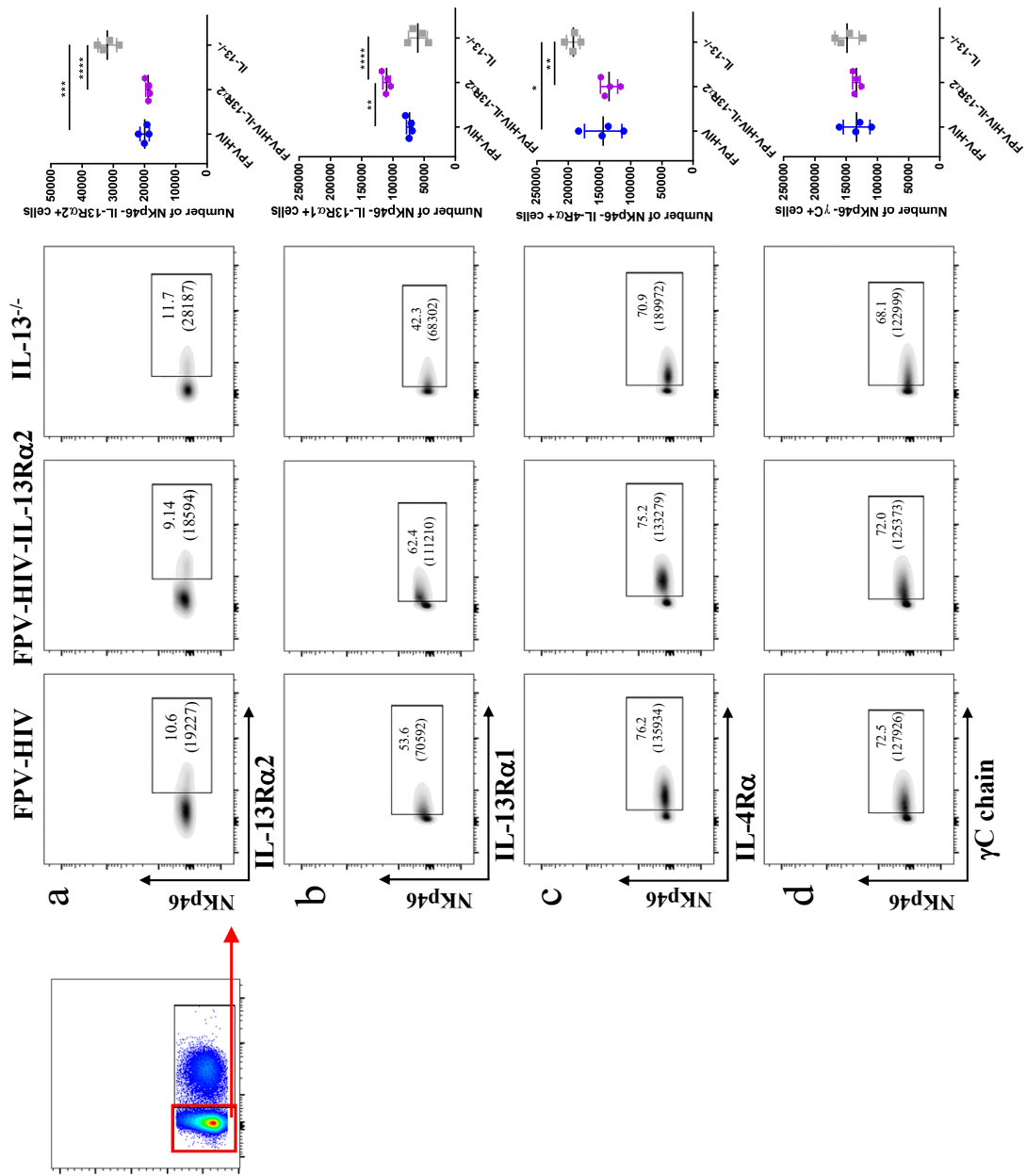


Fig. 6.9. Evaluation of number of lung lineage⁻ IL-33R/ST2⁻ NKp46⁻ ILC1/ILC3 expressing IL-13R α 2, IL-13R α 1, IL-4R α , and γ C - (permanent vs transient inhibition of IL-13).

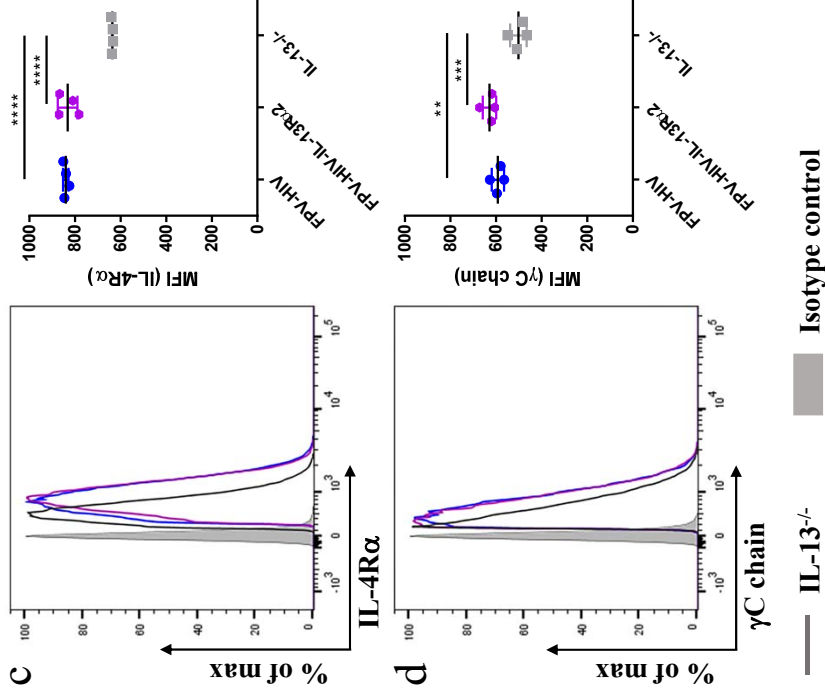
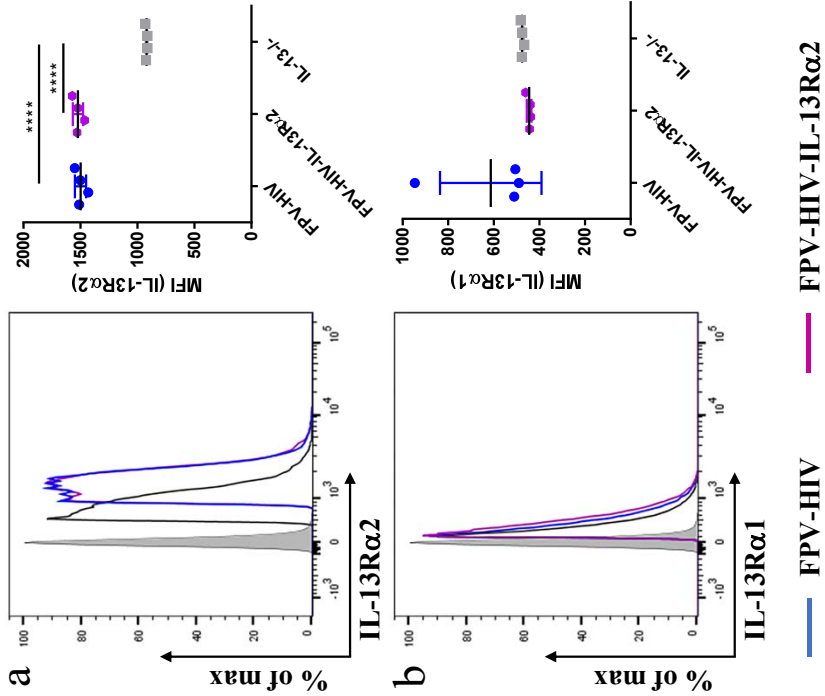
WT BALB/c and IL-13^{-/-} mice (each group n = 4) were immunized intranasally with unadjuvanted FPV-HIV or FPV-HIV-IL-13R α 2 adjuvanted vaccines. Lung NKp46⁻ ILC1/ILC3 were gated as CD45⁺ FSC^{low} SSC^{low} lineage⁻ IL-33R/ST2⁻ NKp46⁻ cells. The FACS plots in each panel indicate the percentage of NKp46⁻ ILC1/ILC3 expressing IL-13R α 2 **(a)**, IL-13R α 1 **(b)**, IL-4R α **(c)**, and γ C chain **(d)** on NKp46⁻ ILC1/ILC3. The bracket below the cell percentage indicates the number of cells in each gate. Graph in each panel represents number of NKp46⁻ ILC1/ILC3 expressing the different receptors back calculated to CD45⁺ population as described in materials and methods (24 h post vaccination). The error bars represent the mean and standard deviation (s.d.). The p-values were calculated using GraphPad Prism software (version 6.05 for Windows). * = p<0.05, ** = p<0.01, *** = p<0.001, **** = p<0.0001. For each group experiments were repeated minimum three times.



vaccine. In the transient versus permanent IL-13 inhibitory conditions, IL-13R α 2, IL-4R α , γ C, but not IL-13R α 1 densities were differentially regulated on NKp46⁺ ILC1/ILC3 (Fig. 6.10).

6.4.3 Following transient or permanent inhibition of IL-4/IL-13, IL-13R α 2 were not regulated on NKp46⁺ ILC1/ILC3 unlike NKp46⁺ ILC1/ILC3.

When IL-4/IL-13 receptors on NKp46⁺ ILC1/ILC3 were accessed under transient versus permanent inhibition vaccine conditions, surprisingly there were no significant differences in the number of NKp46⁺ ILC1/ILC3 expressing IL-13R α 2 in all vaccine groups tested (Fig. 6.11a). In contrast, the number of NKp46⁺ ILC1/ILC3 expressing γ C, IL-4R α , and IL-13R α 1 (Fig. 6.11b - c) were found to be significantly lower under permanent STAT6 or IL-13 inhibition (KO mice) compared to transient inhibition. Interestingly, both transient blockage of STAT6 (FPV-HIV-IL-4R antagonist) and IL-13 (FPV-HIV-IL-13R α 2) showed significantly elevated number of NKp46⁺ ILC1/ILC3 expressing γ C, IL-4R α , and IL-13R α 1 compared to BALB/c mice given the unadjuvanted FPV-HIV vaccine (Fig. 6.11b - c). Under permanent blockage of STAT6 and IL-13 (KO mice), significant down-regulation of not only γ C/IL-4R α but also IL-13R α 2 densities were detected on NKp46⁺ ILC1/ILC3 following vaccination, but not IL-13R α 1 (Fig. 6.12).



Isotype control

FPV-HIV-IL-13Rα2

FPV-HIV

Fig. 6.10. IL-13R α 2, IL-13R α 1, IL-4R α , and γ C receptor densities on lineage⁻ IL-33R/ST2⁻ NKp46⁻ ILC1/ILC3 following unadjuvanted and IL-13R α 2 adjuvanted vaccination.

WT BALB/c mice and IL-13^{-/-} mice (each group n = 4) were immunized intranasally with unadjuvanted FPV-HIV or FPV-HIV-IL-13R α 2 adjuvanted vaccines. Lung NKp46⁻ ILC1/ILC3 were gated as CD45⁺ FSC^{low} SSC^{low} lineage⁻ IL-33R/ST2⁻ NKp46⁻ cells. The histogram plots in each panel show cell surface expression of IL-13R α 2 (**a**), IL-13R α 1 (**b**), IL-4R α (**c**), and γ C chain (**d**), on lung NKp46⁻ ILC1 [WT BALB/c mice given unadjuvanted FPV-HIV (blue lines) or FPV-HIV-IL-13R α 2 adjuvanted (purple line) IL-13^{-/-} mice given unadjuvanted FPV-HIV (grey lines)]. Graph represents the mean fluorescence intensity (MFI) of each receptor. The error bars represent the mean and standard deviation (s.d.). The p-values were calculated using GraphPad Prism software (version 6.05 for Windows). * = p<0.05, ** = p<0.01, *** = p<0.001, **** = p<0.0001. For each group experiments were repeated minimum three times.

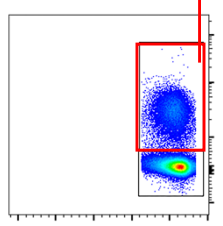
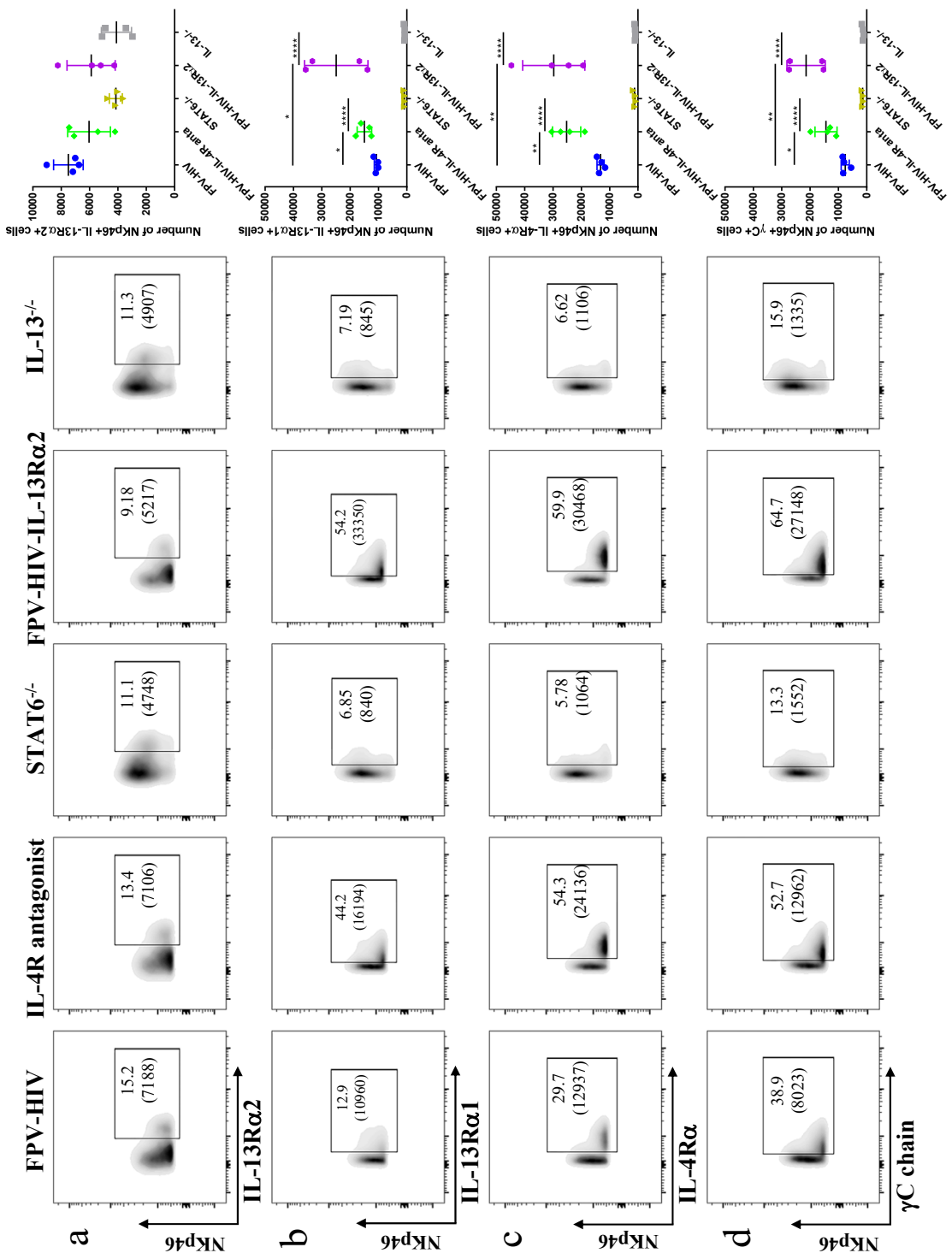


Fig. 6.11. Evaluation of number of lung lineage⁻ IL-33R/ST2⁻ NKp46⁺ ILC1/ILC3 expressing IL-13R α 2, IL-13R α 1, IL-4R α , and γ C receptors following rFPV vaccination.

WT BALB/c, STAT6^{-/-}, and IL-13^{-/-} mice (each group n = 4) were immunized intranasally with unadjuvanted FPV-HIV, FPV-HIV-IL-4R antagonist or FPV-HIV-IL-13R α 2 adjuvanted vaccines. Lung NKp46⁺ ILC1/ILC3 were gated as CD45⁺ FSC^{low} SSC^{low} lineage⁻ IL-33R/ST2⁻ NKp46⁺ cells. The FACS plots in each panel indicate the percentage of NKp46⁺ ILC1/ILC3 expressing IL-13R α 2 (**a**), IL-13R α 1 (**b**), IL-4R α (**c**), and γ C chain (**d**) on Lung NKp46⁺ ILC1/ILC3. The bracket below the cell percentage indicates the number of cells in each gate. Graph in each panel represents number of NKp46⁻ ILC1/ILC3 expressing the different receptors back calculated to CD45⁺ population as described in materials and methods (24 h post vaccination). The error bars represent the mean and standard deviation (s.d.). The p-values were calculated using GraphPad Prism software (version 6.05 for Windows). * = p<0.05, ** = p<0.01, *** = p<0.001, **** = p<0.0001. For each group experiments were repeated minimum three times.

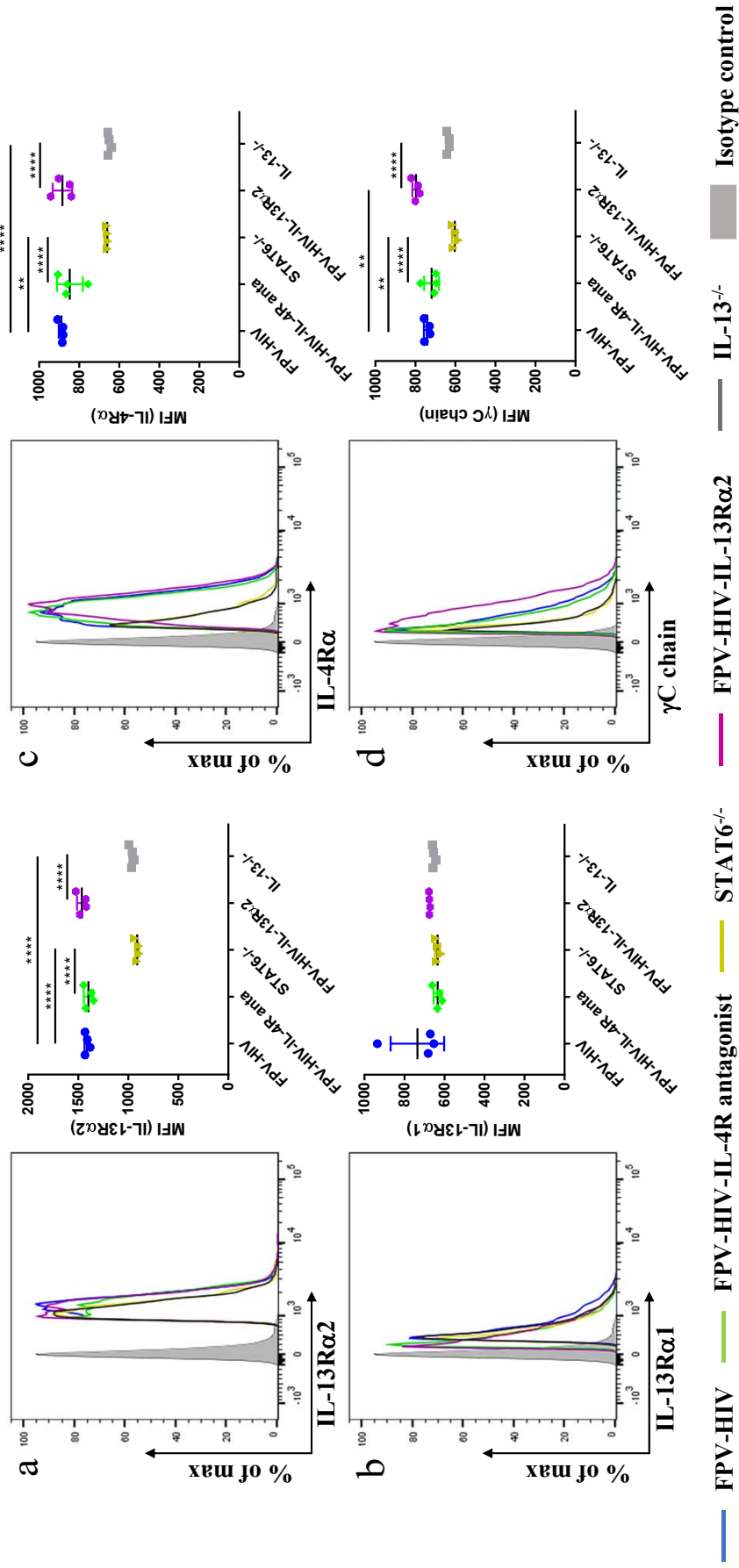


Fig. 6.12. IL-13R α 2, IL-13R α 1, IL-4R α , and γ C receptor densities on lineage IL-33R/ST2- NKp46⁺ ILC1/ILC3 following unadjuvanted, IL-4R antagonist, and IL-13R α 2 adjuvanted vaccination.

WT BALB/c, STAT6^{-/-}, and IL-13^{-/-} mice (each group n = 4) were immunized intranasally with unadjuvanted FPV-HIV, FPV-HIV-IL-4R antagonist or FPV-HIV-IL-13R α 2 adjuvanted vaccines. NKp46⁺ ILC1/ILC3 were gated as CD45⁺ FSC^{low} SSC^{low} lineage IL-33R/ST2- NKp46⁺ cells. The histogram plots in each panel show cell surface expression of IL-13R α 2 **(a)**, IL-13R α 1 **(b)**, IL-4R α **(c)**, and γ C chain **(d)** from WT BALB/c mice given unadjuvanted FPV-HIV (blue lines), FPV-HIV-IL-4R antagonist (green lines), or FPV-HIV-IL-13R α 2 adjuvanted (purple lines), and STAT6^{-/-} (yellow lines) or IL-13^{-/-} mice (grey lines) given unadjuvanted FPV-HIV. Graphs represent the mean fluorescence intensity of each receptor. The error bars represent the mean and standard deviation (s.d.).

The p-values were calculated using GraphPad Prism software (version 6.05 for Windows). * = p<0.05, ** = p<0.01, *** = p<0.001, **** = p<0.0001. For each group experiments were repeated minimum three times.

6.5 Discussion

This study demonstrated that the expression of type I ($\gamma\text{C}/\text{IL-4R}\alpha$) and type II ($\text{IL-4R}\alpha/\text{IL-13R}\alpha 1$) IL-4 receptor complexes and $\text{IL-13R}\alpha 2$ on ILC subsets were differentially regulated 24 h post intranasal rFPV vaccination, specifically under permanent and transient inhibition of cytokine IL-13 and STAT6 signalling. Data revealed that although there was a correlation between the IL-4/IL-13 receptor regulation between $\text{ST2}/\text{IL-33R}^+$ ILC2 and NKp46^- ILC1/ILC3, the receptor regulation on NKp46^+ ILC1/ILC3 were vastly different. Specifically, disruption of STAT6 signalling significantly impacted the $\text{IL-13R}\alpha 2$ expression on both $\text{ST2}/\text{IL-33R}^+$ ILC2 and NKp46^- ILC1/ILC3, unlike IL-13 inhibition, indicating that STAT6 independent IL-13 signalling can activate $\text{IL-13R}\alpha 2$ signalling. Hamid *et al* have recently reported the activation of this pathway under STAT6 inhibition in the context of B cell differentiation²⁸⁴.

Specifically, FPV-HIV-IL-4R antagonist vaccination has shown to induce reduced expression of IL-13 by $\text{ST2}/\text{IL-33R}^+$ ILC2 (Chapter 3). Interestingly, in this current study, elevated number of $\text{ST2}/\text{IL-33R}^+$ ILC2 were found to express $\text{IL-13R}\alpha 2$. The FPV-HIV-IL-4R antagonist vaccination has shown to induce IgG1 and IgG2a antibody differentiation most likely associated with IL-13 signalling via the not well-defined $\text{IL-13R}\alpha 2$ pathway²⁸⁴. Moreover, dendritic cells studies in our laboratory have further established that following viral vector-based vaccination (specifically rFPV), low IL-13 in the milieu (pM conditions) can promote $\text{IL-13R}\alpha 2$ signalling (Roy *et al*, Liu *et al* manuscript in preparation). Therefore, up-regulation of $\text{IL-13R}\alpha 2$ on $\text{ST2}/\text{IL-33R}^+$ ILC2 may suggest that under FPV-HIV-IL-4R antagonist vaccination condition (low IL-13), IL-13 may signal via $\text{IL-13R}\alpha 2$ pathway. In contrast, in STAT6 KO mice given

the unadjuvanted vaccine elevated IL-13 expression by ST2/IL-33R⁺ ILC2 was detected (Chapter 5), and no expression of IL-13R α 2 was observed (**Table 6.1**). Roy, Liu *et al* have recently shown that IL-13R α 2 gets activated on DC under low (pM) IL-13 concentrations, following viral vector vaccination (Roy, Liu *et al* in preparation). Collectively, these findings may explain the vastly different ILC2 IL-13R α 2 expression profiles observed under low (FPV-HIV-IL-4R antagonist adjuvanted vaccination) vs high (STAT6 KO FPV-HIV vaccination) IL-13 conditions. Findings may suggest an autocrine regulation of ILC2-derived-IL-13 via the IL-13R α 2 under certain conditions (FPV-HIV-IL-4R antagonist adjuvanted vaccination).

In the context of FPV-HIV-IL-4R antagonist vaccination, elevated expression of IFN- γ by NKp46⁻ ILC1/ILC3 was observed (Chapter 3). Interestingly, in this study, elevated expression of IL-13R α 2 was detected on these cells. In contrast, STAT6^{-/-} mice given the unadjuvanted vaccination showed reduced IFN- γ expression by NKp46⁻ ILC1/ILC3 (Chapter 5) and reduce expression of IL-13R α 2 on these cells compared to FPV-HIV-IL-4R antagonist vaccination. Recent studies in our laboratory have shown that ST2/IL-33R⁺ ILC2 also express elevated IFN- γ R (Jaeson *et al* in preparation). Taken together the i) ILC2-driven IL-13 and NKp46⁻ ILC1/ILC3-driven IFN- γ expression profiles, and ii) the expression profile of IL-13R α 2 on ST2/IL-33R⁺ ILC2 and NKp46⁻ ILC1/ILC3 under STAT6 inhibitory conditions, plus iii) the ability of ILC2 to express elevated IFN- γ R following vaccination (Jaeson *et al* in preparation), data support the notion that there is a co-regulation of ST2/IL-33R⁺ ILC2 and NKp46⁻ ILC1/ILC3, and the balance of IL-13 and IFN- γ at the vaccination site plays an important role in this process.

Table. 6.1 Comparison of ILC receptor and cytokine expression under different IL-4/IL-13 signaling conditions.

Condition	IL-13 level (by ILC2)	IL-13R α 2 (ILC2)	IL-13R α 2 (NKp46 ⁻ ILC)	IL-13R α 2 (NKp46 ⁺ ILC)	STAT6 signalling	IFN- γ level (NKp46 ⁻ ILC)	IFN- γ level (NKp46 ⁺ ILC)	Antibody differentiation
Control	+++	+++	+++	+++	√	+++	+++	+
IL-4R antagonist	±	+++++	+++++	+++	×	+++++	+++	++++
STAT6 ^{-/-}	+++++	-	+++	+++	×	+	+	++++
IL-13R α 2 vaccine	±	+++	+++	+++	√	+	+	±
IL-13 ^{-/-}	-	-	+++++	+++	√	++	+++	+

- absent, ± weak, + low, +++ medium, +++++ high, ++++++ very high

Unlike IL-13, no IL-4 expression by ST2/IL-33R⁺ ILC2 was detected in any vaccine groups tested. Thus, the down-regulation of the type I receptor complex on STAT6^{-/-} lung ST2/IL-33R⁺ ILC2 following the unadjuvanted vaccination compared to BLAB/c mice given the FPV-HIV-IL-4R antagonist or the unadjuvanted vaccines could be an inherent mechanism by which STAT6^{-/-} mice regulate these receptors on ILC2 to regulate cytokine balance. Furthermore, reduced number of NKp46⁻ ILC1/ILC3 were found to express both γ C and IL-4R α in FPV-HIV-IL-4R antagonist scenario. Knowing that IL-13R α 2 acts as an inhibitor of IL-4R α ¹¹⁹ and γ C pairs with IL-4R α to form type I complex⁹³, the down-regulation of these two receptors on NKp46⁻ ILC1/ILC3 could be associated with the elevated expression of IL-13R α 2 inhibiting type I (γ C/IL-4R α) complex formation, and IL-13 signalling via this pathway.

The regulation of IL-4/IL-13 receptor expression on ILC were significantly different under STAT6 compared to IL-13 inhibition conditions. Following FPV-HIV-IL-13R α 2 adjuvanted and unadjuvanted vaccination, both IL-13R α 1 and IL-13R α 2 on ST2/IL-33R⁺ ILC2 were not regulated, unlike the type I (γ C/IL-4R α) IL-4 receptor complex. No expression IL-13R α 2 and low expression of type I (γ C/IL-4R α) or type II (IL-4R α /IL-13R α 1) receptor complexes were detected on IL-13^{-/-} ST2/IL-33R⁺ ILC2 following unadjuvanted vaccination. In this scenario, although IL-4 expression by ST2/IL-33R⁺ ILC2 was not observed 24 h post vaccination, other cells in the milieu have high potential to express IL-4 to compensate for IL-13. Thus, the down-regulation of type I IL-4 receptor complex on IL-13^{-/-} ILC2 could be an inherent mechanism by which ILC2 regulated IL-4 function. Furthermore, FPV-HIV-IL-13R α 2 induce low IFN- γ expression by NKp46⁻ ILC1/ILC3 compared to BALB/c and IL-13^{-/-} mice given unadjuvanted vaccine. (The hierarchy of this IFN- γ expression was, BALB/c

unadjuvanted > IL-13^{-/-} unadjuvanted > BALB/c IL-13Rα2 adjuvanted (**Table 6.1**)). IFN-γ was significantly down-regulated and differentially regulated when IL-13 was sequestered from the vaccination site in WT BALB/c mice. The above findings further corroborate our notion that IL-13 is the master regulator of ILC2 and NKp46⁺ ILC1/ILC3 activity/function.

The IL-13Rα2, IL-13Rα1, IL-4Rα and γC receptor expression profiles on NKp46⁺ ILC1/ILC3 were found to be regulated in a vastly different manner compared to the other two ILC subsets. This suggested that this subset could have a different role in immune regulation following vaccination. Interestingly, no regulation of IL-13Rα2 on NKp46⁺ ILC1/ILC3 were detected under any of the IL-13 or STAT6 inhibitory conditions including BALB/C mice given the unadjuvanted vaccine. However interestingly, expression of γC, IL-4Rα, and IL-13Rα1 on NKp46⁺ ILC1/ILC3 were elevated following FPV-HIV-IL-4R antagonist and FPV-HIV-IL-13Rα2 adjuvanted vaccination scenarios unlike STAT6^{-/-} or IL-13^{-/-} mice given the unadjuvanted FPV-HIV vaccine. The expression of type I (γC/IL-4Rα) and type II (IL-4Rα/IL-13Rα2) IL-4 receptor complexes on NKp46⁺ ILC1/ILC3 not IL-13Rα2, suggested that these cells most likely are not responsive to ILC2-driven IL-13. Furthermore, the low IFN-γ expression by these cells following vaccination, and no regulation of IL-13Rα2 on these cells, suggest that NKp46⁺ ILC1/ILC3 most likely may not be involved in the regulation of ILC2 balance during viral vector vaccination.

Collectively, our findings indicated an autocrine regulation of IL-13 at the ILC2 level via IL-13Rα2 signalling, and co-regulation of ILC2-driven IL-13 and NKp46⁺ ILC1/ILC3-driven by IFN-γR and IL-13Rα2 receptors respectively, 24 h post viral

vector vaccination. IL-13 is the master regulator of both ILC2 and NKp46⁻ ILC1/ILC3 (not NKp46⁺ ILC1/ILC3) responsible for shaping the downstream adaptive outcomes following viral vector vaccination. Specifically, this IFN- γ R and IL-13R α 2 receptor regulation process at the ILC level may play an important role in regulation of B cell immunity.

Chapter 7.

General discussion.

7.1 General discussion.

This thesis for the first time demonstrated that 24 h following viral vector vaccination (rFPV) ILC activity were significantly modulated in a route dependent manner and ILC2-derived IL-13 at the vaccination site was a master regulator of the downstream T and B cell immune outcomes observed previously in the laboratory^{74, 75, 77, 113, 122, 123}. By dissecting the cytokine expression profiles and regulation of IL-4/IL-13 receptor complexes on ILC under permanent (gene knockout) versus transient inhibition of IL-13/IL-4, and STAT6, data revealed that ILC2-derived IL-13 at the vaccination site was most likely regulated by IL-13 signalling via the IL-13R α 2 pathway (under low IL-13 conditions), following viral vector vaccination. At the ILC2 level there was an autocrine regulation of IL-13, and it also regulated ILC1/ILC3-driven IFN- γ via a STAT6 independent mechanism, most likely IL-13R α 2 pathway (Chapter 5 & 6). Jaeson *et al.* have recently found elevated expression of IFN- γ R on ILC2 24 h post viral vector vaccination (Jaeson *et al* in preparation). These findings proposed the exciting notion that the balance of ILC2-driven IL-13 and ILC1/ILC3-driven IFN- γ are co-regulated (**Fig. 7.1**) and this STAT6 independent regulation is associated with maintaining the balance of IL-13 and IFN- γ at the vaccinations site, shaping the downstream antibody immunity²⁸⁴.

Intranasal versus intramuscular vaccination induced different ILC2 phenotypes (IL-33R⁺ vs IL-25R⁺) associated with different NKp46^{+/-} ILC1/ILC3 profiles, suggesting IL-13 and IFN- γ played different roles in ILC development in muscle and lung. Interestingly, the disruption of IL-25 at the lung mucosae, unlike IL-33 led to the generation of lineage⁻ ST2/IL-33R⁻ IL-25R⁺, lineage⁻ ST2/IL-33R⁻ TSLPR⁺ ILC2, and a unique lineage⁻ ST2/IL-33R⁻ IL-25R⁻ TSLPR⁻ ILC2 with vastly different IL-4/IL-13 expression profiles, suggesting that IL-25 could be a key regulator of ILC2. Moreover,

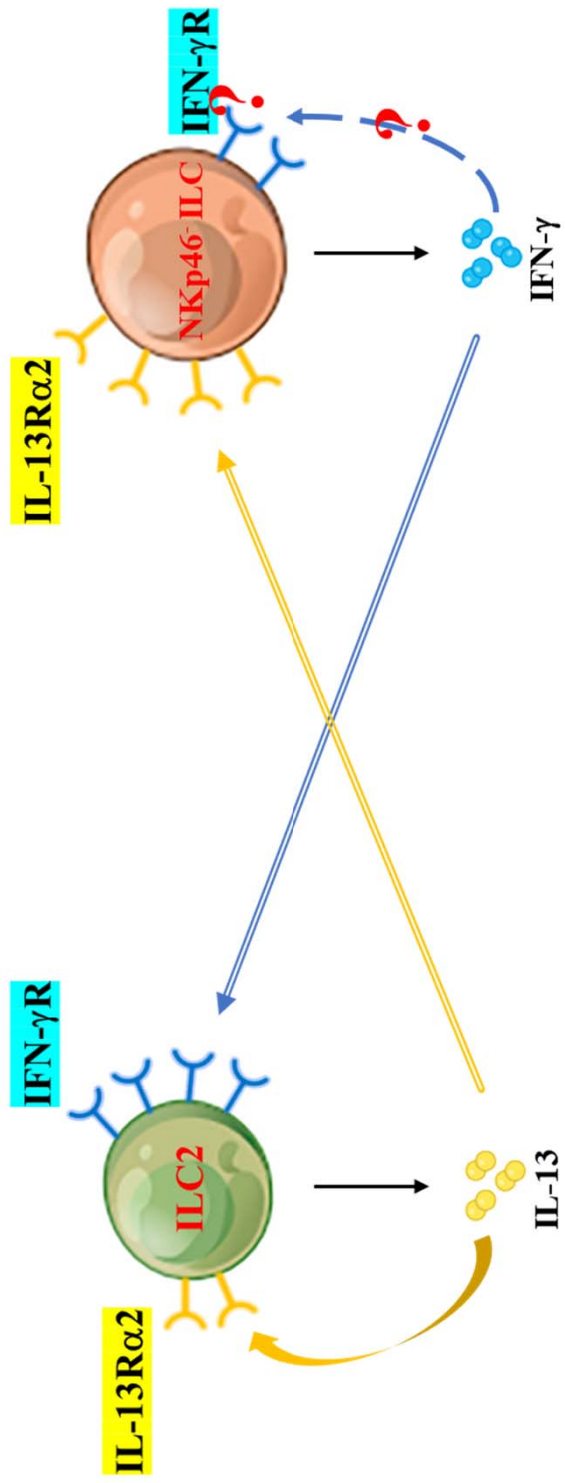


Fig. 7.1.1. Co-regulation of ILC2 and NKp46- ILC via IL-13Rα2 pathway

sequestration of IL-25 also induced elevated expression of IL-17A and altered the IFN- γ expression by NKp46^{+/-} ILC1/ILC3. Furthermore, knowing that i.m. IL-25BP vaccination also yielded vastly different outcomes, and i.m. IL-33BP vaccination also did not alter ILC development or activity (Ranasinghe *et al* in preparation) compared to intranasal vaccination, these findings clearly indicated that IL-25 regulated not only ILC2 but also ILC1/ILC3 differentiation, suggesting that IL-25 could be the master regulator of ILC development (at the precursor cell level). In contrast, IL-33 may play a role in ILC2 homing²⁵⁵ to the lung mucosae. Taken together the findings in this thesis, data support the notion that at the ILC level there is a hierarchy of cytokines IL-25 compared to IL-13, where former regulates the fundamental development of all ILCs and the latter is involved in maintaining the balance of ILC2-driven IL-13 and ILC1/ILC3-driven IFN- γ and the resulting downstream immune outcomes. Knowing the high plasticity of ILC^{109, 163, 166, 208, 209, 210, 211} (**Fig. 1.17**), this is not entirely surprising as at the precursor level all ILC could be IL-25R⁺ and under different stimulation conditions, they could develop into different ILC phenotypes. Moreover, as TSLPR⁺ ILC2 were found to express IL-4 and IL-13 following i.n. FPV-HIV-IL-25BP vaccination, it would also be of interest to study the impact of inhibition or sequestration of TSLP at the vaccination site, and this warrants further investigation.

Unlike chronic inflammatory conditions, viral vector vaccination induced uniquely different ILC subsets, indicating that ILCs are highly sensitive to different environmental conditions and they most likely are the gatekeepers of the immune system. Specifically, data revealed that under different infection conditions ILC-derived cytokines are differentially regulated most likely to prevent overdrive of the resulting immune outcomes, which was also substantiated by the data observed with permanent

vs transient inhibition of IL-13, IL-25 and STAT6 signalling. The various compensatory mechanisms in gene knockout animal models, highlight the caveats of using KO models in infection studies. Compensatory and/or redundancy mechanisms have been reported previously in the context of certain genetic diseases (gene mutations or deletions)^{285, 286, 287}. Thus, in the context of understanding the functional differences of ILC following viral vector vaccination, studies using reporter mice would also be of more benefit^{288, 289, 290}. The current findings once again stress the importance of understanding the molecular mechanisms associated with i) route of vaccine delivery, ii) cytokine milieu and iii) vaccine vectors/adjuvants, when designing vaccines against chronic pathogens, as all these factors can significantly alter the ILC function/activity, resulting in vastly different adaptive immune outcomes.

In conclusion, findings in this thesis demonstrated that different routes of vaccine delivery and different adjuvants can significantly modulate ILC function/activity at the vaccination site, as early as 24h post vaccination. ILC2-derived IL-13 and NKp46⁻ ILC1/ILC3-derived IFN- γ balance, plays an important role in this process and is likely regulated via IL-13Ra2 in a STAT6 independent manner. Specifically, now knowing that the cytokine environment induced by ILC can significantly alter the DC recruitment and the downstream adaptive immune responses^{113, 122, 123} (**Fig. 7.2**), when designing vaccines against chronic pathogens, clear understanding of the ILC induced, could help design better vaccines in the future. Collectively, the data suggest that, ILC most likely are the gatekeepers of the immune system following viral vector vaccination, and the level of ILC2-derived IL-13 and NKp46⁻ ILC1/ILC3-derived IFN- γ balance induced could be used as a predictor of the resulting downstream adaptive immune outcomes in the future.

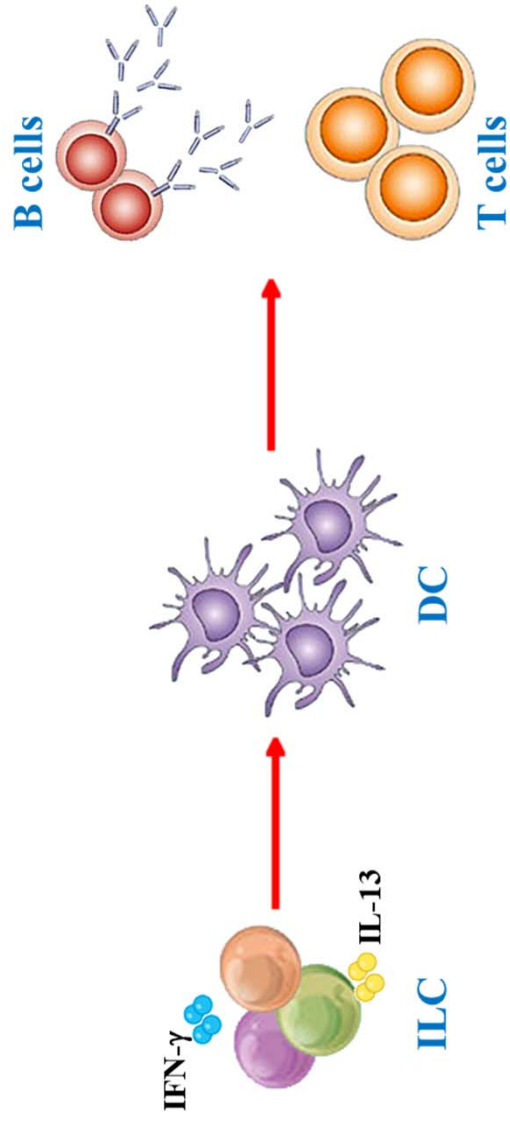


Fig. 7.2. ILC can manipulate downstream immunity.

7.2 Future directions.

- Current data demonstrated that ILC subsets and their functions were significantly manipulated following different routes of rFPV vaccination (i.n. vs i.m.). Therefore, it would be of great interest to evaluate ILC function/activity i) following different routes of vaccine delivery, specifically intradermal, intrarectal and intravaginal vaccination and also ii) following different viral vector-based vaccination (for example recombinant MVA, VV Adenovirus vectors, including DNA-based vaccines).
- This study for the first time demonstrated that ILC2 are the predominant source of IL-13 at the vaccination site and IL-13 is the master regulator of both ILC2 and NKp46⁻ ILC1/ILC3 responsible for shaping the downstream adaptive immune outcomes following viral vector vaccination. Also knowing that permanent vs transient inhibition of cytokines induced uniquely different immune outcomes, it would be of interest to transfer ILC2 from WT BALB/c mice into IL-13^{-/-} mice (adaptive transfer studies), vaccinate mice with different routes and viral vectors and evaluate the innate and adaptive immune responses to further understand the role of IL-13 in ILC activity.
- Also, using the different reporter mice systems associated with ILC may also help in gaining a better understanding of ILC activity. For example, IL-13 reporter mice have been used intensively in ILC studies^{136, 291, 292, 293}. Thus, it would be of interest to use BALB/c background IL-13 reporter mice during vaccination to track ILC2 activation. Moreover, Id2 and PLZF are two crucial genes involved in ILC development^{288, 289, 294, 295, 296}, reporter mice of these two genes could also be used together with transcription factor fluorescence staining

to obtain better understanding of ILC development and activation process during IL-13R α 2, IL-4R antagonist and IL-25BP adjuvanted vs unadjuvanted vaccination.

- To better understand the role of ILC development, following sequestration of IL-25 (IL-17E) compared to unadjuvanted vaccine conditions, evaluation of the IL-17/IL-25 receptor complexes may be of benefit. Furthermore, similar to recent studies in the laboratory (Jaeson et al in preparation), following IL-25BP and IL-33BP vaccination analyzing range of IL-17, IL-25 and also IL-13 related bio-markers (cytokines, receptors, transcription factors) on ILC at a single cell level using Fluidigm 48:48 arrays may help gain more knowledge of ILC development, specifically following viral vector vaccination.
- Chapter 6 data suggested an autocrine regulation of IL-13 at the ILC2 level and ILC2-driven IL-13 regulating NKp46⁻ ILC1/ILC3-driven IFN- γ via IL-13R α 2 signalling. As we postulate a co-regulation of IL-13 and IFN- γ at the ILC level (**Fig. 7.1**), it would be of interest to assess i) the IFN- γ R expression on ILC2 and NKp46⁻ ILC1/ILC3 24 h post vaccination using FACS analysis and ii) also the role of NKp46⁺ ILC1/ILC3 during vaccination.
- Moreover, data in this thesis have shown that IL-13R α 2 play an important role in the co-regulation of ILC2-driven IL-13 and ILC1/ILC3-driven IFN- γ . However, the exact mechanism by which this signalling occurs is still unclear. Therefore, evaluating the IL-13R α 2 signalling pathway and the possible downstream regulation would be of significant importance.

References

1. Chaplin, D.D. Overview of the immune response. *The Journal of allergy and clinical immunology* **125**, S3-23 (2010).
2. Turvey, S.E. & Broide, D.H. Innate immunity. *The Journal of allergy and clinical immunology* **125**, S24-32 (2010).
3. Ponda, P.P. & Mayer, L. Mucosal epithelium in health and disease. *Current molecular medicine* **5**, 549-556 (2005).
4. Linden, S.K., Sutton, P., Karlsson, N.G., Korolik, V. & McGuckin, M.A. Mucins in the mucosal barrier to infection. *Mucosal immunology* **1**, 183 (2008).
5. Thursby, E. & Juge, N. Introduction to the human gut microbiota. *Biochemical Journal* **474**, 1823-1836 (2017).
6. Guinane, C.M. & Cotter, P.D. Role of the gut microbiota in health and chronic gastrointestinal disease: understanding a hidden metabolic organ. *Therapeutic Advances in Gastroenterology* **6**, 295-308 (2013).
7. Janeway, C.A., Jr. & Medzhitov, R. Innate immune recognition. *Annual review of immunology* **20**, 197-216 (2002).
8. Xi, Y., Day, S.L., Jackson, R.J. & Ranasinghe, C. Role of novel type I interferon epsilon in viral infection and mucosal immunity. *Mucosal Immunol* **5**, 610-622 (2012).
9. Day, S.L., Ramshaw, I.A., Ramsay, A.J. & Ranasinghe, C. Differential effects of the type I interferons alpha4, beta, and epsilon on antiviral activity and vaccine efficacy. *Journal of immunology (Baltimore, Md. : 1950)* **180**, 7158-7166 (2008).

10. Robertsen, B. The role of type I interferons in innate and adaptive immunity against viruses in Atlantic salmon. *Developmental & Comparative Immunology* **80**, 41-52 (2018).
11. Parkin, J. & Cohen, B. An overview of the immune system. *Lancet (London, England)* **357**, 1777-1789 (2001).
12. Beutler, B. Innate immunity: an overview. *Molecular immunology* **40**, 845-859 (2004).
13. Tosi, M.F. Innate immune responses to infection. *The Journal of allergy and clinical immunology* **116**, 241-249; quiz 250 (2005).
14. Jonsson, A.H. & Yokoyama, W.M. Natural killer cell tolerance licensing and other mechanisms. *Advances in immunology* **101**, 27-79 (2009).
15. Stockwin, L.H., McGonagle, D., Martin, I.G. & Blair, G.E. Dendritic cells: Immunological sentinels with a central role in health and disease. *Immunology And Cell Biology* **78**, 91 (2000).
16. Sanos, S.L. & Diefenbach, A. Innate lymphoid cells: from border protection to the initiation of inflammatory diseases. *Immunol Cell Biol* **91**, 215-224 (2013).
17. Cooper, M.D. & Alder, M.N. The evolution of adaptive immune systems. *Cell* **124**, 815-822 (2006).
18. Nemazee, D. Receptor selection in B and T lymphocytes. *Annual review of immunology* **18**, 19-51 (2000).
19. Lauritsen, J.P., Haks, M.C., Lefebvre, J.M., Kappes, D.J. & Wiest, D.L. Recent insights into the signals that control alphabeta/gammadelta-lineage fate. *Immunological reviews* **209**, 176-190 (2006).
20. Blom, B. & Spits, H. Development of human lymphoid cells. *Annual review of immunology* **24**, 287-320 (2006).

21. Hedrick, S.M. Thymus lineage commitment: a single switch. *Immunity* **28**, 297-299 (2008).
22. Jenkinson, E.J., Jenkinson, W.E., Rossi, S.W. & Anderson, G. The thymus and T-cell commitment: the right niche for Notch? *Nature reviews. Immunology* **6**, 551-555 (2006).
23. Spits, H. & Di Santo, J.P. The expanding family of innate lymphoid cells: regulators and effectors of immunity and tissue remodeling. *Nat Immunol* **12**, 21-27 (2011).
24. Bonilla, F.A. & Oettgen, H.C. Adaptive immunity. *The Journal of allergy and clinical immunology* **125**, S33-40 (2010).
25. Larosa, D.F. & Orange, J.S. 1. Lymphocytes. *The Journal of allergy and clinical immunology* **121**, S364-369; quiz S412 (2008).
26. Alam, R. & Gorska, M. 3. Lymphocytes. *The Journal of allergy and clinical immunology* **111**, S476-485 (2003).
27. Dustin, M.L. The cellular context of T cell signaling. *Immunity* **30**, 482-492 (2009).
28. Wang, H. *et al.* IRF8 regulates B-cell lineage specification, commitment, and differentiation. *Blood* **112**, 4028-4038 (2008).
29. McGhee, J.R. & Fujihashi, K. Inside the mucosal immune system. *PLoS biology* **10**, e1001397 (2012).
30. Pelaseyed, T. *et al.* The mucus and mucins of the goblet cells and enterocytes provide the first defense line of the gastrointestinal tract and interact with the immune system. *Immunological reviews* **260**, 8-20 (2014).
31. Nagler-Anderson, C. Man the barrier! Strategic defences in the intestinal mucosa. *Nature reviews. Immunology* **1**, 59-67 (2001).

32. Salzman, N.H. *et al.* Enteric defensins are essential regulators of intestinal microbial ecology. *Nature immunology* **11**, 76-83 (2010).
33. Kiyono, H. & Azegami, T. The mucosal immune system: From dentistry to vaccine development. *Proceedings of the Japan Academy. Series B, Physical and biological sciences* **91**, 423-439 (2015).
34. Cesta, M.F. Normal structure, function, and histology of mucosa-associated lymphoid tissue. *Toxicologic pathology* **34**, 599-608 (2006).
35. Lorenz, R.G. & Newberry, R.D. Isolated lymphoid follicles can function as sites for induction of mucosal immune responses. *Annals of the New York Academy of Sciences* **1029**, 44-57 (2004).
36. Pabst, O. *et al.* Cryptopatches and isolated lymphoid follicles: dynamic lymphoid tissues dispensable for the generation of intraepithelial lymphocytes. *European journal of immunology* **35**, 98-107 (2005).
37. Mabbott, N.A., Donaldson, D.S., Ohno, H., Williams, I.R. & Mahajan, A. Microfold (M) cells: important immunosurveillance posts in the intestinal epithelium. *Mucosal immunology* **6**, 666-677 (2013).
38. Lugton, I.W. Mucosa-associated lymphoid tissues as sites for uptake, carriage and excretion of tubercle bacilli and other pathogenic mycobacteria. *Immunology And Cell Biology* **77**, 364 (1999).
39. Gallo, R.C. & Montagnier, L. The Discovery of HIV as the Cause of AIDS. *New England Journal of Medicine* **349**, 2283-2285 (2003).
40. Stephens, L.L., Swanepoel, C.C., Van Rooyen, B.A. & Abayomi, E.A. The human immunodeficiency virus, (HIV-1), pandemic: cellular therapies, stem cells and biobanking. *Transfusion and apheresis science : official journal of the World Apheresis Association : official journal of the European Society for Haemapheresis* **49**, 9-11 (2013).

41. Veazey, R.S. *et al.* Gastrointestinal tract as a major site of CD4+ T cell depletion and viral replication in SIV infection. *Science (New York, N.Y.)* **280**, 427-431 (1998).
42. Barouch, D.H. Challenges in the Development of an HIV-1 Vaccine. *Nature* **455**, 613-619 (2008).
43. Ensoli, B., Cafaro, A., Monini, P., Marcotullio, S. & Ensoli, F. Challenges in HIV Vaccine Research for Treatment and Prevention. *Frontiers in immunology* **5**, 417 (2014).
44. Burgers, W.A. & Williamson, C. The challenges of HIV vaccine development and testing. *Best Practice & Research Clinical Obstetrics & Gynaecology* **19**, 277-291 (2005).
45. De Rose, R., Kent, S.J. & Ranasinghe, C. Chapter 12 - Prime-Boost Vaccination: Impact on the HIV-1 Vaccine Field. *Novel Approaches and Strategies for Biologics, Vaccines and Cancer Therapies*. Academic Press: San Diego, 2015, pp 289-313.
46. Pantophlet, R. & Burton, D.R. GP120: target for neutralizing HIV-1 antibodies. *Annual review of immunology* **24**, 739-769 (2006).
47. O'Connell, R.J., Kim, J.H., Corey, L. & Michael, N.L. Human immunodeficiency virus vaccine trials. *Cold Spring Harbor perspectives in medicine* **2**, a007351 (2012).
48. Harro, C.D. *et al.* Recruitment and baseline epidemiologic profile of participants in the first phase 3 HIV vaccine efficacy trial. *Journal of acquired immune deficiency syndromes (1999)* **37**, 1385-1392 (2004).
49. Flynn, N.M. *et al.* Placebo-controlled phase 3 trial of a recombinant glycoprotein 120 vaccine to prevent HIV-1 infection. *The Journal of infectious diseases* **191**, 654-665 (2005).

50. Gilbert, P.B. *et al.* Correlation between immunologic responses to a recombinant glycoprotein 120 vaccine and incidence of HIV-1 infection in a phase 3 HIV-1 preventive vaccine trial. *The Journal of infectious diseases* **191**, 666-677 (2005).
51. Pitisuttithum, P. *et al.* Randomized, double-blind, placebo-controlled efficacy trial of a bivalent recombinant glycoprotein 120 HIV-1 vaccine among injection drug users in Bangkok, Thailand. *The Journal of infectious diseases* **194**, 1661-1671 (2006).
52. Pitisuttithum, P. HIV vaccine research in Thailand: lessons learned. *Expert review of vaccines* **7**, 311-317 (2008).
53. Buchbinder, S.P. *et al.* Efficacy assessment of a cell-mediated immunity HIV-1 vaccine (the Step Study): a double-blind, randomised, placebo-controlled, test-of-concept trial. *Lancet (London, England)* **372**, 1881-1893 (2008).
54. Gray, G.E. *et al.* Safety and efficacy of the HVTN 503/Phambili study of a clade-B-based HIV-1 vaccine in South Africa: a double-blind, randomised, placebo-controlled test-of-concept phase 2b study. *The Lancet. Infectious diseases* **11**, 507-515 (2011).
55. Rerks-Ngarm, S. *et al.* Vaccination with ALVAC and AIDSVAX to prevent HIV-1 infection in Thailand. *The New England journal of medicine* **361**, 2209-2220 (2009).
56. Haynes, B.F. *et al.* Immune-correlates analysis of an HIV-1 vaccine efficacy trial. *The New England journal of medicine* **366**, 1275-1286 (2012).
57. Tomaras, G.D. & Haynes, B.F. Advancing Toward HIV-1 Vaccine Efficacy through the Intersections of Immune Correlates. *Vaccines* **2**, 15-35 (2014).
58. Lycke, N. Recent progress in mucosal vaccine development: potential and limitations. *Nature reviews. Immunology* **12**, 592-605 (2012).

59. Belyakov, I.M. & Ahlers, J.D. What role does the route of immunization play in the generation of protective immunity against mucosal pathogens? *Journal of immunology (Baltimore, Md. : 1950)* **183**, 6883-6892 (2009).
60. Ranasinghe, C. *et al.* A comparative analysis of HIV-specific mucosal/systemic T cell immunity and avidity following rDNA/rFPV and poxvirus-poxvirus prime boost immunisations. *Vaccine* **29**, 3008-3020 (2011).
61. Belyakov, I.M., Isakov, D., Zhu, Q., Dzutsev, A. & Berzofsky, J.A. A novel functional CTL avidity/activity compartmentalization to the site of mucosal immunization contributes to protection of macaques against simian/human immunodeficiency viral depletion of mucosal CD4+ T cells. *Journal of immunology (Baltimore, Md. : 1950)* **178**, 7211-7221 (2007).
62. O'Hagan, D.T. & Lavelle, E. Novel adjuvants and delivery systems for HIV vaccines. *AIDS (London, England)* **16 Suppl 4**, S115-124 (2002).
63. Goulder, P.J. *et al.* Substantial differences in specificity of HIV-specific cytotoxic T cells in acute and chronic HIV infection. *The Journal of experimental medicine* **193**, 181-194 (2001).
64. Nabel, G.J. Challenges and opportunities for development of an AIDS vaccine. *Nature* **410**, 1002-1007 (2001).
65. Kent, S.J. *et al.* Mucosally-administered human-simian immunodeficiency virus DNA and fowlpoxvirus-based recombinant vaccines reduce acute phase viral replication in macaques following vaginal challenge with CCR5-tropic SHIVSF162P3. *Vaccine* **23**, 5009-5021 (2005).
66. Amara, R.R. *et al.* Control of a mucosal challenge and prevention of AIDS by a multiprotein DNA/MVA vaccine. *Science (New York, N.Y.)* **292**, 69-74 (2001).
67. Kent, S.J. *et al.* Enhanced T-cell immunogenicity and protective efficacy of a human immunodeficiency virus type 1 vaccine regimen consisting of

- consecutive priming with DNA and boosting with recombinant fowlpox virus. *Journal of virology* **72**, 10180-10188 (1998).
68. Robert-Guroff, M. Replicating and non-replicating viral vectors for vaccine development. *Current opinion in biotechnology* **18**, 546-556 (2007).
69. Gherardi, M.M. *et al.* Prime-boost immunization schedules based on influenza virus and vaccinia virus vectors potentiate cellular immune responses against human immunodeficiency virus Env protein systemically and in the genitoretal draining lymph nodes. *Journal of virology* **77**, 7048-7057 (2003).
70. Shiver, J.W. *et al.* Replication-incompetent adenoviral vaccine vector elicits effective anti-immunodeficiency-virus immunity. *Nature* **415**, 331-335 (2002).
71. Xu, R. *et al.* Characterization of immune responses elicited in macaques immunized sequentially with chimeric VEE/SIN alphavirus replicon particles expressing SIVGag and/or HIVEnv and with recombinant HIVgp140Env protein. *AIDS research and human retroviruses* **22**, 1022-1030 (2006).
72. Hill, A.V.S., Biswas, S., Draper, S., Rampling, T. & Reyes-Sandoval, A. Towards a multi-antigen multi-stage malaria vaccine. *Malaria Journal* **13**, O31 (2014).
73. Belyakov, I.M. & Ahlers, J.D. Comment on "trafficking of antigen-specific CD8+ T lymphocytes to mucosal surfaces following intramuscular vaccination". *Journal of immunology (Baltimore, Md. : 1950)* **182**, 1779; author reply 1779-1780 (2009).
74. Ranasinghe, C. *et al.* Evaluation of fowlpox-vaccinia virus prime-boost vaccine strategies for high-level mucosal and systemic immunity against HIV-1. *Vaccine* **24**, 5881-5895 (2006).

75. Ranasinghe, C. *et al.* Mucosal HIV-1 pox virus prime-boost immunization induces high-avidity CD8+ T cells with regime-dependent cytokine/granzyme B profiles. *Journal of immunology (Baltimore, Md. : 1950)* **178**, 2370-2379 (2007).
76. Quah, B.J., Wijesundara, D.K., Ranasinghe, C. & Parish, C.R. Fluorescent target array T helper assay: a multiplex flow cytometry assay to measure antigen-specific CD4+ T cell-mediated B cell help in vivo. *Journal of immunological methods* **387**, 181-190 (2013).
77. Ranasinghe, C. & Ramshaw, I.A. Immunisation route-dependent expression of IL-4/IL-13 can modulate HIV-specific CD8(+) CTL avidity. *European journal of immunology* **39**, 1819-1830 (2009).
78. Wijesundara, D.K., Jackson, R.J., Tschärke, D.C. & Ranasinghe, C. IL-4 and IL-13 mediated down-regulation of CD8 expression levels can dampen anti-viral CD8(+) T cell avidity following HIV-1 recombinant pox viral vaccination. *Vaccine* **31**, 4548-4555 (2013).
79. Wijesundara, D.K., Tschärke, D.C., Jackson, R.J. & Ranasinghe, C. Reduced interleukin-4 receptor alpha expression on CD8+ T cells correlates with higher quality anti-viral immunity. *PLoS One* **8**, e55788 (2013).
80. Bao, K. & Reinhardt, R.L. The differential expression of IL-4 and IL-13 and its impact on type-2 immunity. *Cytokine* **75**, 25-37 (2015).
81. Catley, M.C., Coote, J., Bari, M. & Tomlinson, K.L. Monoclonal antibodies for the treatment of asthma. *Pharmacology & therapeutics* **132**, 333-351 (2011).
82. Paul, W.E. & Zhu, J. How are T(H)2-type immune responses initiated and amplified? *Nature reviews. Immunology* **10**, 225-235 (2010).
83. Liang, H.E. *et al.* Divergent expression patterns of IL-4 and IL-13 define unique functions in allergic immunity. *Nature immunology* **13**, 58-66 (2011).

84. Kelso, A. & Groves, P. A single peripheral CD8⁺ T cell can give rise to progeny expressing type 1 and/or type 2 cytokine genes and can retain its multipotentiality through many cell divisions. *Proceedings of the National Academy of Sciences of the United States of America* **94**, 8070-8075 (1997).
85. Apte, S.H., Baz, A., Groves, P., Kelso, A. & Kienzle, N. Interferon-gamma and interleukin-4 reciprocally regulate CD8 expression in CD8⁺ T cells. *Proceedings of the National Academy of Sciences of the United States of America* **105**, 17475-17480 (2008).
86. Harland, K.L. *et al.* Epigenetic plasticity of Cd8a locus during CD8(+) T-cell development and effector differentiation and reprogramming. *Nature communications* **5**, 3547 (2014).
87. Kim, M., Lim, S.J., Oidovsambuu, S. & Nho, C.W. Gnetin H isolated from *Paeonia anomala* inhibits FcεpsilonRI-mediated mast cell signaling and degranulation. *Journal of ethnopharmacology* **154**, 798-806 (2014).
88. Caubet, J.C., Masilamani, M., Rivers, N.A., Mayer, L. & Sampson, H.A. Potential non-T cells source of interleukin-4 in food allergy. *Pediatric allergy and immunology : official publication of the European Society of Pediatric Allergy and Immunology* **25**, 243-249 (2014).
89. Motomura, Y. *et al.* Basophil-derived interleukin-4 controls the function of natural helper cells, a member of ILC2s, in lung inflammation. *Immunity* **40**, 758-771 (2014).
90. McKenzie, A.N., Spits, H. & Eberl, G. Innate lymphoid cells in inflammation and immunity. *Immunity* **41**, 366-374 (2014).
91. Hams, E. & Fallon, P.G. Innate type 2 cells and asthma. *Current opinion in pharmacology* **12**, 503-509 (2012).

92. Tabata, Y. & Khurana Hershey, G.K. IL-13 receptor isoforms: breaking through the complexity. *Current allergy and asthma reports* **7**, 338-345 (2007).
93. McCormick, S.M. & Heller, N.M. Commentary: IL-4 and IL-13 receptors and signaling. *Cytokine* **75**, 38-50 (2015).
94. Junttila, I.S. *et al.* Redirecting cell-type specific cytokine responses with engineered interleukin-4 superkines. *Nature chemical biology* **8**, 990-998 (2012).
95. Munitz, A., Brandt, E.B., Mingler, M., Finkelman, F.D. & Rothenberg, M.E. Distinct roles for IL-13 and IL-4 via IL-13 receptor alpha1 and the type II IL-4 receptor in asthma pathogenesis. *Proceedings of the National Academy of Sciences of the United States of America* **105**, 7240-7245 (2008).
96. Murata, T., Taguchi, J. & Puri, R.K. Interleukin-13 receptor alpha' but not alpha chain: a functional component of interleukin-4 receptors. *Blood* **91**, 3884-3891 (1998).
97. Murata, T., Noguchi, P.D. & Puri, R.K. IL-13 induces phosphorylation and activation of JAK2 Janus kinase in human colon carcinoma cell lines: similarities between IL-4 and IL-13 signaling. *Journal of immunology (Baltimore, Md. : 1950)* **156**, 2972-2978 (1996).
98. Murata, T., Husain, S.R., Mohri, H. & Puri, R.K. Two different IL-13 receptor chains are expressed in normal human skin fibroblasts, and IL-4 and IL-13 mediate signal transduction through a common pathway. *International immunology* **10**, 1103-1110 (1998).
99. Hershey, G.K. IL-13 receptors and signaling pathways: an evolving web. *The Journal of allergy and clinical immunology* **111**, 677-690; quiz 691 (2003).
100. Kelly-Welch, A., Hanson, E.M. & Keegan, A.D. Interleukin-4 (IL-4) pathway. *Science's STKE : signal transduction knowledge environment* **2005**, cm9 (2005).

101. Luzina, I.G. *et al.* Regulation of inflammation by interleukin-4: a review of "alternatives". *Journal of leukocyte biology* **92**, 753-764 (2012).
102. Murata, T. & Puri, R.K. Comparison of IL-13- and IL-4-induced signaling in EBV-immortalized human B cells. *Cellular immunology* **175**, 33-40 (1997).
103. Sun, X.J. *et al.* Role of IRS-2 in insulin and cytokine signalling. *Nature* **377**, 173-177 (1995).
104. Dhand, R. *et al.* PI 3-kinase is a dual specificity enzyme: autoregulation by an intrinsic protein-serine kinase activity. *The EMBO journal* **13**, 522-533 (1994).
105. Ruckerl, D. *et al.* Induction of IL-4Ralpha-dependent microRNAs identifies PI3K/Akt signaling as essential for IL-4-driven murine macrophage proliferation in vivo. *Blood* **120**, 2307-2316 (2012).
106. Heller, N.M., Qi, X., Gesbert, F. & Keegan, A.D. The extracellular and transmembrane domains of the gammaC and interleukin (IL)-13 receptor alpha chains, not their cytoplasmic domains, dictate the nature of signaling responses to IL-4 and IL-13. *The Journal of biological chemistry* **287**, 31948-31961 (2012).
107. Karlsson, H.K. & Zierath, J.R. Insulin signaling and glucose transport in insulin resistant human skeletal muscle. *Cell biochemistry and biophysics* **48**, 103-113 (2007).
108. Landis, J. & Shaw, L.M. Insulin receptor substrate 2-mediated phosphatidylinositol 3-kinase signaling selectively inhibits glycogen synthase kinase 3beta to regulate aerobic glycolysis. *The Journal of biological chemistry* **289**, 18603-18613 (2014).
109. Russo, S.J. *et al.* IRS2-Akt pathway in midbrain dopamine neurons regulates behavioral and cellular responses to opiates. *Nature neuroscience* **10**, 93-99 (2007).

110. Hallett, M.A., Venmar, K.T. & Fingleton, B. Cytokine stimulation of epithelial cancer cells: the similar and divergent functions of IL-4 and IL-13. *Cancer research* **72**, 6338-6343 (2012).
111. Jenkins, S.J. *et al.* IL-4 directly signals tissue-resident macrophages to proliferate beyond homeostatic levels controlled by CSF-1. *The Journal of experimental medicine* **210**, 2477-2491 (2013).
112. Lupardus, P.J., Birnbaum, M.E. & Garcia, K.C. Molecular basis for shared cytokine recognition revealed in the structure of an unusually high affinity complex between IL-13 and IL-13Ralpha2. *Structure (London, England : 1993)* **18**, 332-342 (2010).
113. Jackson, R.J., Worley, M., Trivedi, S. & Ranasinghe, C. Novel HIV IL-4R antagonist vaccine strategy can induce both high avidity CD8 T and B cell immunity with greater protective efficacy. *Vaccine* **32**, 5703-5714 (2014).
114. Daines, M.O. *et al.* Level of expression of IL-13R alpha 2 impacts receptor distribution and IL-13 signaling. *Journal of immunology (Baltimore, Md. : 1950)* **176**, 7495-7501 (2006).
115. Sivaprasad, U. *et al.* IL-13Ralpha2 has a protective role in a mouse model of cutaneous inflammation. *Journal of immunology (Baltimore, Md. : 1950)* **185**, 6802-6808 (2010).
116. O'Toole, M., Legault, H., Ramsey, R., Wynn, T.A. & Kasaian, M.T. A novel and sensitive ELISA reveals that the soluble form of IL-13R-alpha2 is not expressed in plasma of healthy or asthmatic subjects. *Clinical and experimental allergy : journal of the British Society for Allergy and Clinical Immunology* **38**, 594-601 (2008).

117. Murata, T., Obiri, N.I. & Puri, R.K. Human ovarian-carcinoma cell lines express IL-4 and IL-13 receptors: comparison between IL-4- and IL-13-induced signal transduction. *International journal of cancer* **70**, 230-240 (1997).
118. Wood, N. *et al.* Enhanced interleukin (IL)-13 responses in mice lacking IL-13 receptor alpha 2. *The Journal of experimental medicine* **197**, 703-709 (2003).
119. Rahaman, S.O. *et al.* IL-13R(alpha)2, a decoy receptor for IL-13 acts as an inhibitor of IL-4-dependent signal transduction in glioblastoma cells. *Cancer research* **62**, 1103-1109 (2002).
120. Rahaman, S.O., Vogelbaum, M.A. & Haque, S.J. Aberrant Stat3 signaling by interleukin-4 in malignant glioma cells: involvement of IL-13Ralpha2. *Cancer research* **65**, 2956-2963 (2005).
121. Ko, C.W. *et al.* Lack of interleukin-4 receptor alpha chain-dependent signalling promotes azoxymethane-induced colorectal aberrant crypt focus formation in Balb/c mice. *The Journal of pathology* **214**, 603-609 (2008).
122. Ranasinghe, C., Trivedi, S., Stambas, J. & Jackson, R.J. Unique IL-13Ralpha2-based HIV-1 vaccine strategy to enhance mucosal immunity, CD8(+) T-cell avidity and protective immunity. *Mucosal Immunol* **6**, 1068-1080 (2013).
123. Trivedi, S., Jackson, R.J. & Ranasinghe, C. Different HIV pox viral vector-based vaccines and adjuvants can induce unique antigen presenting cells that modulate CD8 T cell avidity. *Virology* **468-470**, 479-489 (2014).
124. Betts, M.R. *et al.* HIV nonprogressors preferentially maintain highly functional HIV-specific CD8+ T cells. *Blood* **107**, 4781-4789 (2006).
125. Berger, C.T. *et al.* High-functional-avidity cytotoxic T lymphocyte responses to HLA-B-restricted Gag-derived epitopes associated with relative HIV control. *Journal of virology* **85**, 9334-9345 (2011).

126. French, M.A. *et al.* Isotype-switched immunoglobulin G antibodies to HIV Gag proteins may provide alternative or additional immune responses to 'protective' human leukocyte antigen-B alleles in HIV controllers. *AIDS (London, England)* **27**, 519-528 (2013).
127. Cella, M., Miller, H. & Song, C. Beyond NK cells: the expanding universe of innate lymphoid cells. *Frontiers in immunology* **5**, 282 (2014).
128. Cortez, V.S., Robinette, M.L. & Colonna, M. Innate lymphoid cells: new insights into function and development. *Current opinion in immunology* **32**, 71-77 (2015).
129. Diefenbach, A., Colonna, M. & Koyasu, S. Development, differentiation, and diversity of innate lymphoid cells. *Immunity* **41**, 354-365 (2014).
130. Artis, D. & Spits, H. The biology of innate lymphoid cells. *Nature* **517**, 293 (2015).
131. Hwang, Y.Y. & McKenzie, A.N. Innate lymphoid cells in immunity and disease. *Advances in experimental medicine and biology* **785**, 9-26 (2013).
132. Spits, H. *et al.* Innate lymphoid cells--a proposal for uniform nomenclature. *Nature reviews. Immunology* **13**, 145-149 (2013).
133. Eberl, G. Development and evolution of ROR γ mat⁺ cells in a microbe's world. *Immunological reviews* **245**, 177-188 (2012).
134. Moro, K. *et al.* Innate production of T(H)2 cytokines by adipose tissue-associated c-Kit(+)/Sca-1(+) lymphoid cells. *Nature* **463**, 540-544 (2010).
135. Neill, D.R. *et al.* Nuocytes represent a new innate effector leukocyte that mediates type-2 immunity. *Nature* **464**, 1367-1370 (2010).
136. Price, A.E. *et al.* Systemically dispersed innate IL-13-expressing cells in type 2 immunity. *Proceedings of the National Academy of Sciences of the United States of America* **107**, 11489-11494 (2010).

137. Eberl, G. *et al.* An essential function for the nuclear receptor RORgamma(t) in the generation of fetal lymphoid tissue inducer cells. *Nature immunology* **5**, 64-73 (2004).
138. Nowarski, R., Gagliani, N., Huber, S. & Flavell, R.A. Innate immune cells in inflammation and cancer. *Cancer immunology research* **1**, 77-84 (2013).
139. Yagi, R. *et al.* The transcription factor GATA3 is critical for the development of all IL-7Ralpha-expressing innate lymphoid cells. *Immunity* **40**, 378-388 (2014).
140. Klose, C.S. *et al.* Differentiation of type 1 ILCs from a common progenitor to all helper-like innate lymphoid cell lineages. *Cell* **157**, 340-356 (2014).
141. Constantinides, M.G., McDonald, B.D., Verhoef, P.A. & Bendelac, A. A committed precursor to innate lymphoid cells. *Nature* **508**, 397-401 (2014).
142. Walker, J.A., Barlow, J.L. & McKenzie, A.N. Innate lymphoid cells--how did we miss them? *Nature reviews. Immunology* **13**, 75-87 (2013).
143. Saenz, S.A. *et al.* IL25 elicits a multipotent progenitor cell population that promotes T(H)2 cytokine responses. *Nature* **464**, 1362-1366 (2010).
144. Halim, T.Y., Krauss, R.H., Sun, A.C. & Takei, F. Lung natural helper cells are a critical source of Th2 cell-type cytokines in protease allergen-induced airway inflammation. *Immunity* **36**, 451-463 (2012).
145. Mjosberg, J. *et al.* The transcription factor GATA3 is essential for the function of human type 2 innate lymphoid cells. *Immunity* **37**, 649-659 (2012).
146. Monticelli, L.A. *et al.* Innate lymphoid cells promote lung-tissue homeostasis after infection with influenza virus. *Nature immunology* **12**, 1045-1054 (2011).
147. Mjosberg, J.M. *et al.* Human IL-25- and IL-33-responsive type 2 innate lymphoid cells are defined by expression of CRTH2 and CD161. *Nature immunology* **12**, 1055-1062 (2011).

148. Kabata, H., Moro, K., Koyasu, S. & Asano, K. Group 2 innate lymphoid cells and asthma. *Allergology international : official journal of the Japanese Society of Allergology* **64**, 227-234 (2015).
149. Hoyler, T. *et al.* The transcription factor GATA-3 controls cell fate and maintenance of type 2 innate lymphoid cells. *Immunity* **37**, 634-648 (2012).
150. Gasteiger, G., Fan, X., Dikiy, S., Lee, S.Y. & Rudensky, A.Y. Tissue residency of innate lymphoid cells in lymphoid and nonlymphoid organs. *Science (New York, N.Y.)* **350**, 981-985 (2015).
151. Koyasu, S. & Moro, K. Role of innate lymphocytes in infection and inflammation. *Frontiers in immunology* **3**, 101 (2012).
152. Wilhelm, C. *et al.* An IL-9 fate reporter demonstrates the induction of an innate IL-9 response in lung inflammation. *Nature immunology* **12**, 1071-1077 (2011).
153. Sojka, D.K., Tian, Z. & Yokoyama, W.M. Tissue-resident natural killer cells and their potential diversity. *Seminars in immunology* **26**, 127-131 (2014).
154. Vivier, E. *et al.* Innate or adaptive immunity? The example of natural killer cells. *Science (New York, N.Y.)* **331**, 44-49 (2011).
155. Bernink, J.H. *et al.* Human type 1 innate lymphoid cells accumulate in inflamed mucosal tissues. *Nature immunology* **14**, 221-229 (2013).
156. Fuchs, A. *et al.* Intraepithelial type 1 innate lymphoid cells are a unique subset of IL-12- and IL-15-responsive IFN-gamma-producing cells. *Immunity* **38**, 769-781 (2013).
157. Cortez, V.S., Fuchs, A., Cella, M., Gilfillan, S. & Colonna, M. Cutting edge: Salivary gland NK cells develop independently of Nfil3 in steady-state. *Journal of immunology (Baltimore, Md. : 1950)* **192**, 4487-4491 (2014).

158. Crotta, S. *et al.* The transcription factor E4BP4 is not required for extramedullary pathways of NK cell development. *Journal of immunology (Baltimore, Md. : 1950)* **192**, 2677-2688 (2014).
159. Daussy, C. *et al.* T-bet and Eomes instruct the development of two distinct natural killer cell lineages in the liver and in the bone marrow. *The Journal of experimental medicine* **211**, 563-577 (2014).
160. Gonzaga, R., Matzinger, P. & Perez-Diez, A. Resident peritoneal NK cells. *Journal of immunology (Baltimore, Md. : 1950)* **187**, 6235-6242 (2011).
161. Seillet, C. *et al.* Differential requirement for Nfil3 during NK cell development. *Journal of immunology (Baltimore, Md. : 1950)* **192**, 2667-2676 (2014).
162. Sojka, D.K. *et al.* Tissue-resident natural killer (NK) cells are cell lineages distinct from thymic and conventional splenic NK cells. *eLife* **3**, e01659 (2014).
163. Vonarbourg, C. *et al.* Regulated expression of nuclear receptor RORgammat confers distinct functional fates to NK cell receptor-expressing RORgammat(+) innate lymphocytes. *Immunity* **33**, 736-751 (2010).
164. Cella, M. *et al.* A human natural killer cell subset provides an innate source of IL-22 for mucosal immunity. *Nature* **457**, 722-725 (2009).
165. Colonna, M. Interleukin-22-producing natural killer cells and lymphoid tissue inducer-like cells in mucosal immunity. *Immunity* **31**, 15-23 (2009).
166. Tait Wojno, E.D. & Artis, D. Innate lymphoid cells: balancing immunity, inflammation, and tissue repair in the intestine. *Cell host & microbe* **12**, 445-457 (2012).
167. Cupedo, T. *et al.* Human fetal lymphoid tissue-inducer cells are interleukin 17-producing precursors to RORC+ CD127+ natural killer-like cells. *Nature immunology* **10**, 66-74 (2009).

168. Satoh-Takayama, N. *et al.* Microbial flora drives interleukin 22 production in intestinal NKp46+ cells that provide innate mucosal immune defense. *Immunity* **29**, 958-970 (2008).
169. Sonnenberg, G.F., Monticelli, L.A., Elloso, M.M., Fouser, L.A. & Artis, D. CD4(+) lymphoid tissue-inducer cells promote innate immunity in the gut. *Immunity* **34**, 122-134 (2011).
170. Buonocore, S. *et al.* Innate lymphoid cells drive interleukin-23-dependent innate intestinal pathology. *Nature* **464**, 1371-1375 (2010).
171. Ichii, M. *et al.* Functional diversity of stem and progenitor cells with B-lymphopoietic potential. *Immunological reviews* **237**, 10-21 (2010).
172. Yang, Q., Jeremiah Bell, J. & Bhandoola, A. T-cell lineage determination. *Immunological reviews* **238**, 12-22 (2010).
173. Yu, X. *et al.* The basic leucine zipper transcription factor NFIL3 directs the development of a common innate lymphoid cell precursor. *eLife* **3** (2014).
174. Takatori, H. *et al.* Lymphoid tissue inducer-like cells are an innate source of IL-17 and IL-22. *The Journal of experimental medicine* **206**, 35-41 (2009).
175. Bouskra, D. *et al.* Lymphoid tissue genesis induced by commensals through NOD1 regulates intestinal homeostasis. *Nature* **456**, 507-510 (2008).
176. Scandella, E. *et al.* Restoration of lymphoid organ integrity through the interaction of lymphoid tissue-inducer cells with stroma of the T cell zone. *Nature immunology* **9**, 667-675 (2008).
177. Ouyang, W., Kolls, J.K. & Zheng, Y. The biological functions of T helper 17 cell effector cytokines in inflammation. *Immunity* **28**, 454-467 (2008).
178. Cherrier, M., Sawa, S. & Eberl, G. Notch, Id2, and ROR γ sequentially orchestrate the fetal development of lymphoid tissue inducer cells. *The Journal of experimental medicine* **209**, 729-740 (2012).

179. Possot, C. *et al.* Notch signaling is necessary for adult, but not fetal, development of ROR γ mat(+) innate lymphoid cells. *Nature immunology* **12**, 949-958 (2011).
180. Satoh-Takayama, N. *et al.* IL-7 and IL-15 independently program the differentiation of intestinal CD3⁺NKp46⁺ cell subsets from Id2-dependent precursors. *The Journal of experimental medicine* **207**, 273-280 (2010).
181. Carotta, S., Pang, S.H., Nutt, S.L. & Belz, G.T. Identification of the earliest NK-cell precursor in the mouse BM. *Blood* **117**, 5449-5452 (2011).
182. Constantinides, M.G. *et al.* PLZF expression maps the early stages of ILC1 lineage development. *Proceedings of the National Academy of Sciences of the United States of America* **112**, 5123-5128 (2015).
183. Kovalovsky, D. *et al.* The BTB-zinc finger transcriptional regulator PLZF controls the development of invariant natural killer T cell effector functions. *Nature immunology* **9**, 1055-1064 (2008).
184. Savage, A.K. *et al.* The transcription factor PLZF directs the effector program of the NKT cell lineage. *Immunity* **29**, 391-403 (2008).
185. Klein Wolterink, R.G. *et al.* Essential, dose-dependent role for the transcription factor Gata3 in the development of IL-5⁺ and IL-13⁺ type 2 innate lymphoid cells. *Proceedings of the National Academy of Sciences of the United States of America* **110**, 10240-10245 (2013).
186. Wong, S.H. *et al.* Transcription factor ROR α is critical for nuocyte development. *Nature immunology* **13**, 229-236 (2012).
187. Montaldo, E., Juelke, K. & Romagnani, C. Group 3 innate lymphoid cells (ILC3s): Origin, differentiation, and plasticity in humans and mice. *European journal of immunology* **45**, 2171-2182 (2015).

188. Spooner, C.J. *et al.* Specification of type 2 innate lymphocytes by the transcriptional determinant Gfi1. *Nature immunology* **14**, 1229-1236 (2013).
189. Meylan, F. *et al.* The TNF-family cytokine TL1A promotes allergic immunopathology through group 2 innate lymphoid cells. *Mucosal immunology* **7**, 958-968 (2014).
190. Yu, X. *et al.* TNF superfamily member TL1A elicits type 2 innate lymphoid cells at mucosal barriers. *Mucosal immunology* **7**, 730-740 (2014).
191. Chang, Y.J. *et al.* Innate lymphoid cells mediate influenza-induced airway hyper-reactivity independently of adaptive immunity. *Nat Immunol* **12**, 631-638 (2011).
192. Barnig, C. *et al.* Lipoxin A4 regulates natural killer cell and type 2 innate lymphoid cell activation in asthma. *Science translational medicine* **5**, 174ra126 (2013).
193. Doherty, T.A. *et al.* Lung type 2 innate lymphoid cells express cysteinyl leukotriene receptor 1, which regulates TH2 cytokine production. *The Journal of allergy and clinical immunology* **132**, 205-213 (2013).
194. Salimi, M. *et al.* A role for IL-25 and IL-33-driven type-2 innate lymphoid cells in atopic dermatitis. *The Journal of experimental medicine* **210**, 2939-2950 (2013).
195. Kim, B.S. *et al.* TSLP elicits IL-33-independent innate lymphoid cell responses to promote skin inflammation. *Science translational medicine* **5**, 170ra116 (2013).
196. Drake, L.Y., Iijima, K. & Kita, H. Group 2 innate lymphoid cells and CD4⁺ T cells cooperate to mediate type 2 immune response in mice. *Allergy* **69**, 1300-1307 (2014).

197. Halim, T.Y. *et al.* Group 2 innate lymphoid cells are critical for the initiation of adaptive T helper 2 cell-mediated allergic lung inflammation. *Immunity* **40**, 425-435 (2014).
198. Powell, N. *et al.* The transcription factor T-bet regulates intestinal inflammation mediated by interleukin-7 receptor+ innate lymphoid cells. *Immunity* **37**, 674-684 (2012).
199. Sawa, S. *et al.* RORgammat+ innate lymphoid cells regulate intestinal homeostasis by integrating negative signals from the symbiotic microbiota. *Nature immunology* **12**, 320-326 (2011).
200. Pulendran, B. & Artis, D. New paradigms in type 2 immunity. *Science (New York, N.Y.)* **337**, 431-435 (2012).
201. Besnard, A.G. *et al.* IL-33-mediated protection against experimental cerebral malaria is linked to induction of type 2 innate lymphoid cells, M2 macrophages and regulatory T cells. *PLoS pathogens* **11**, e1004607 (2015).
202. Boyd, A., Killoran, K., Mitre, E. & Nutman, T.B. Pleural cavity type 2 innate lymphoid cells precede Th2 expansion in murine *Litomosoides sigmodontis* infection. *Experimental parasitology* **159**, 118-126 (2015).
203. Ajendra, J. *et al.* ST2 deficiency does not impair type 2 immune responses during chronic filarial infection but leads to an increased microfilaremia due to an impaired splenic microfilarial clearance. *PloS one* **9**, e93072 (2014).
204. Dunay, I.R. & Diefenbach, A. Group 1 innate lymphoid cells in *Toxoplasma gondii* infection. *Parasite immunology* **40** (2018).
205. Jackson, D.J. *et al.* IL-33-dependent type 2 inflammation during rhinovirus-induced asthma exacerbations in vivo. *American journal of respiratory and critical care medicine* **190**, 1373-1382 (2014).

206. Kløverpris, H.N. *et al.* Innate Lymphoid Cells Are Depleted Irreversibly during Acute HIV-1 Infection in the Absence of Viral Suppression. *Immunity* **44**, 391-405.
207. Li, H. *et al.* Hypercytotoxicity and rapid loss of NKp44+ innate lymphoid cells during acute SIV infection. *PLoS pathogens* **10**, e1004551 (2014).
208. Cella, M., Otero, K. & Colonna, M. Expansion of human NK-22 cells with IL-7, IL-2, and IL-1beta reveals intrinsic functional plasticity. *Proceedings of the National Academy of Sciences of the United States of America* **107**, 10961-10966 (2010).
209. Bernink, J.H. *et al.* Interleukin-12 and -23 Control Plasticity of CD127(+) Group 1 and Group 3 Innate Lymphoid Cells in the Intestinal Lamina Propria. *Immunity* **43**, 146-160 (2015).
210. Rankin, L.C. *et al.* The transcription factor T-bet is essential for the development of NKp46+ innate lymphocytes via the Notch pathway. *Nature immunology* **14**, 389-395 (2013).
211. Ohne, Y. *et al.* IL-1 is a critical regulator of group 2 innate lymphoid cell function and plasticity. *Nature immunology* **17**, 646-655 (2016).
212. Silver, J.S. *et al.* Inflammatory triggers associated with exacerbations of COPD orchestrate plasticity of group 2 innate lymphoid cells in the lungs. *Nature immunology* **17**, 626-635 (2016).
213. Huang, Y. *et al.* IL-25-responsive, lineage-negative KLRG1(hi) cells are multipotential 'inflammatory' type 2 innate lymphoid cells. *Nature immunology* **16**, 161-169 (2015).
214. Artis, D. & Spits, H. The biology of innate lymphoid cells. *Nature* **517**, 293-301 (2015).

215. Licona-Limon, P., Kim, L.K., Palm, N.W. & Flavell, R.A. TH2, allergy and group 2 innate lymphoid cells. *Nat Immunol* **14**, 536-542 (2013).
216. Oliphant, C.J. *et al.* MHCII-mediated dialog between group 2 innate lymphoid cells and CD4(+) T cells potentiates type 2 immunity and promotes parasitic helminth expulsion. *Immunity* **41**, 283-295 (2014).
217. Eberl, G., Colonna, M., Di Santo, J.P. & McKenzie, A.N. Innate lymphoid cells. Innate lymphoid cells: a new paradigm in immunology. *Science (New York, N.Y.)* **348**, aaa6566 (2015).
218. Serafini, N., Vosshenrich, C.A. & Di Santo, J.P. Transcriptional regulation of innate lymphoid cell fate. *Nature reviews. Immunology* **15**, 415-428 (2015).
219. Lim, A.I. *et al.* IL-12 drives functional plasticity of human group 2 innate lymphoid cells. *The Journal of experimental medicine* **213**, 569-583 (2016).
220. Klooverpris, H.N. *et al.* Innate Lymphoid Cells Are Depleted Irreversibly during Acute HIV-1 Infection in the Absence of Viral Suppression. *Immunity* **44**, 391-405 (2016).
221. Kim, J.H., Excler, J.L. & Michael, N.L. Lessons from the RV144 Thai phase III HIV-1 vaccine trial and the search for correlates of protection. *Annual review of medicine* **66**, 423-437 (2015).
222. Delaloye, J. *et al.* Innate immune sensing of modified vaccinia virus Ankara (MVA) is mediated by TLR2-TLR6, MDA-5 and the NALP3 inflammasome. *PLoS Pathog* **5**, e1000480 (2009).
223. Halim, T.Y. *et al.* Group 2 innate lymphoid cells license dendritic cells to potentiate memory TH2 cell responses. *Nat Immunol* **17**, 57-64 (2016).
224. Almeida, J.R. *et al.* Superior control of HIV-1 replication by CD8+ T cells is reflected by their avidity, polyfunctionality, and clonal turnover. *The Journal of experimental medicine* **204**, 2473-2485 (2007).

225. Lichterfeld, M. *et al.* Selective depletion of high-avidity human immunodeficiency virus type 1 (HIV-1)-specific CD8⁺ T cells after early HIV-1 infection. *J Virol* **81**, 4199-4214 (2007).
226. Ravichandran, J., Jackson, R.J., Trivedi, S. & Ranasinghe, C. IL-17A expression in HIV-specific CD8 T cells is regulated by IL-4/IL-13 following HIV-1 prime-boost immunization. *Journal of interferon & cytokine research : the official journal of the International Society for Interferon and Cytokine Research* **35**, 176-185 (2015).
227. Holmes, C. & Stanford, W.L. Concise review: stem cell antigen-1: expression, function, and enigma. *Stem cells (Dayton, Ohio)* **25**, 1339-1347 (2007).
228. Spits, H. & Cupedo, T. Innate lymphoid cells: emerging insights in development, lineage relationships, and function. *Annual review of immunology* **30**, 647-675 (2012).
229. Sanos, S.L. *et al.* ROR γ and commensal microflora are required for the differentiation of mucosal interleukin 22-producing NKp46⁺ cells. *Nat Immunol* **10**, 83-91 (2009).
230. Killig, M., Glatzer, T. & Romagnani, C. Recognition strategies of group 3 innate lymphoid cells. *Frontiers in immunology* **5**, 142 (2014).
231. Robinette, M.L. *et al.* IL-15 sustains IL-7R-independent ILC2 and ILC3 development. *Nature communications* **8**, 14601 (2017).
232. Walker, J.A. & McKenzie, A.N. Development and function of group 2 innate lymphoid cells. *Current opinion in immunology* **25**, 148-155 (2013).
233. Kruse, S., Braun, S. & Deichmann, K.A. Distinct signal transduction processes by IL-4 and IL-13 and influences from the Q551R variant of the human IL-4 receptor alpha chain. *Respiratory research* **3**, 24 (2002).

234. Jiang, H., Harris, M.B. & Rothman, P. IL-4/IL-13 signaling beyond JAK/STAT. *The Journal of allergy and clinical immunology* **105**, 1063-1070 (2000).
235. Kelly-Welch, A.E., Hanson, E.M., Boothby, M.R. & Keegan, A.D. Interleukin-4 and interleukin-13 signaling connections maps. *Science (New York, N.Y.)* **300**, 1527-1528 (2003).
236. Andrews, A.L. *et al.* The association of the cytoplasmic domains of interleukin 4 receptor alpha and interleukin 13 receptor alpha 2 regulates interleukin 4 signaling. *Molecular bioSystems* **9**, 3009-3014 (2013).
237. Fichtner-Feigl, S. *et al.* IL-13 signaling via IL-13R alpha2 induces major downstream fibrogenic factors mediating fibrosis in chronic TNBS colitis. *Gastroenterology* **135**, 2003-2013, 2013 e2001-2007 (2008).
238. Belz, G.T. ILC2s masquerade as ILC1s to drive chronic disease. *Nat Immunol* **17**, 611-612 (2016).
239. Daines, M.O. & Hershey, G.K. A novel mechanism by which interferon-gamma can regulate interleukin (IL)-13 responses. Evidence for intracellular stores of IL-13 receptor alpha -2 and their rapid mobilization by interferon-gamma. *The Journal of biological chemistry* **277**, 10387-10393 (2002).
240. Moro, K. *et al.* Interferon and IL-27 antagonize the function of group 2 innate lymphoid cells and type 2 innate immune responses. *Nat Immunol* **17**, 76-86 (2016).
241. Kudo, F. *et al.* Interferon-gamma constrains cytokine production of group 2 innate lymphoid cells. *Immunology* **147**, 21-29 (2016).
242. Duerr, C.U. *et al.* Type I interferon restricts type 2 immunopathology through the regulation of group 2 innate lymphoid cells. *Nat Immunol* **17**, 65-+ (2016).
243. Crellin, N.K., Trifari, S., Kaplan, C.D., Cupedo, T. & Spits, H. Human NKp44+IL-22+ cells and LTI-like cells constitute a stable RORC+ lineage

- distinct from conventional natural killer cells. *The Journal of experimental medicine* **207**, 281-290 (2010).
244. Fort, M.M. *et al.* IL-25 induces IL-4, IL-5, and IL-13 and Th2-associated pathologies in vivo. *Immunity* **15**, 985-995 (2001).
245. Barlow, J.L. *et al.* IL-33 is more potent than IL-25 in provoking IL-13-producing nuocytes (type 2 innate lymphoid cells) and airway contraction. *The Journal of allergy and clinical immunology* **132**, 933-941 (2013).
246. Bergot, A.S. *et al.* HPV16 E7 expression in skin induces TSLP secretion, type 2 ILC infiltration and atopic dermatitis-like lesions. *Immunology and cell biology* **93**, 540-547 (2015).
247. Roediger, B. *et al.* Cutaneous immunosurveillance and regulation of inflammation by group 2 innate lymphoid cells. *Nature immunology* **14**, 564-573 (2013).
248. Camelo, A. *et al.* IL-33, IL-25, and TSLP induce a distinct phenotypic and activation profile in human type 2 innate lymphoid cells. *Blood Advances* **1**, 577-589 (2017).
249. Klose, C.S.N. & Artis, D. Innate lymphoid cells as regulators of immunity, inflammation and tissue homeostasis. *Nature immunology* **17**, 765-774 (2016).
250. Chen, C.-C., Iijima, K., Kobayashi, T. & Kita, H. Differential regulation of type 2 innate lymphoid cells by IL-25 and IL-33 (P6254). *The Journal of Immunology* **190**, 115.123-115.123 (2013).
251. Huang, Q. *et al.* IL-25 Elicits Innate Lymphoid Cells and Multipotent Progenitor Type 2 Cells That Reduce Renal Ischemic/Reperfusion Injury. *Journal of the American Society of Nephrology : JASN* **26**, 2199-2211 (2015).
252. Gu, C., Wu, L. & Li, X. IL-17 family: cytokines, receptors and signaling. *Cytokine* **64**, 477-485 (2013).

253. Qian, Y., Kang, Z., Liu, C. & Li, X. IL-17 signaling in host defense and inflammatory diseases. *Cellular And Molecular Immunology* **7**, 328 (2010).
254. Camelo, A. *et al.* IL-33, IL-25, and TSLP induce a distinct phenotypic and activation profile in human type 2 innate lymphoid cells. *Blood Adv* **1**, 577-589 (2017).
255. Stier, M.T. *et al.* IL-33 promotes the egress of group 2 innate lymphoid cells from the bone marrow. *The Journal of experimental medicine* **215**, 263-281 (2018).
256. Hurdayal, R. & Brombacher, F. The role of IL-4 and IL-13 in cutaneous Leishmaniasis. *Immunology letters* **161**, 179-183 (2014).
257. Maizels, R.M., Hewitson, J.P. & Smith, K.A. Susceptibility and immunity to helminth parasites. *Current opinion in immunology* **24**, 459-466 (2012).
258. Jiang, S. & Dong, C. A complex issue on CD4(+) T-cell subsets. *Immunological reviews* **252**, 5-11 (2013).
259. Finkelman, F.D., Katona, I.M., Mosmann, T.R. & Coffman, R.L. IFN-gamma regulates the isotypes of Ig secreted during in vivo humoral immune responses. *Journal of immunology (Baltimore, Md. : 1950)* **140**, 1022-1027 (1988).
260. Coutelier, J.P., Coulie, P.G., Wauters, P., Heremans, H. & van der Logt, J.T. In vivo polyclonal B-lymphocyte activation elicited by murine viruses. *Journal of virology* **64**, 5383-5388 (1990).
261. Graham, M.B. *et al.* Response to influenza infection in mice with a targeted disruption in the interferon gamma gene. *The Journal of experimental medicine* **178**, 1725-1732 (1993).
262. van den Broek, M.F., Muller, U., Huang, S., Aguet, M. & Zinkernagel, R.M. Antiviral defense in mice lacking both alpha/beta and gamma interferon receptors. *Journal of virology* **69**, 4792-4796 (1995).

263. Maloy, K.J., Odermatt, B., Hengartner, H. & Zinkernagel, R.M. Interferon gamma-producing gammadelta T cell-dependent antibody isotype switching in the absence of germinal center formation during virus infection. *Proceedings of the National Academy of Sciences of the United States of America* **95**, 1160-1165 (1998).
264. Bian, F. *et al.* Altered balance of interleukin-13/interferon-gamma contributes to lacrimal gland destruction and secretory dysfunction in CD25 knockout model of Sjogren's syndrome. *Arthritis research & therapy* **17**, 53 (2015).
265. Albanesi, C. *et al.* IL-4 and IL-13 negatively regulate TNF-alpha- and IFN-gamma-induced beta-defensin expression through STAT-6, suppressor of cytokine signaling (SOCS)-1, and SOCS-3. *Journal of immunology (Baltimore, Md. : 1950)* **179**, 984-992 (2007).
266. Xiao, T. *et al.* Both IL-4 and IL-13 inhibit the TNF-alpha and IFN-gamma enhanced MDC production in a human keratinocyte cell line, HaCaT cells. *Journal of dermatological science* **31**, 111-117 (2003).
267. Ford, J.G. *et al.* Il-13 and IFN-gamma: interactions in lung inflammation. *Journal of immunology (Baltimore, Md. : 1950)* **167**, 1769-1777 (2001).
268. Ito, Y. & Mason, R.J. The effect of interleukin-13 (IL-13) and interferon- γ (IFN- γ) on expression of surfactant proteins in adult human alveolar type II cells in vitro. *Respiratory Research* **11**, 157 (2010).
269. Molofsky, A.B. *et al.* Interleukin-33 and Interferon-gamma Counter-Regulate Group 2 Innate Lymphoid Cell Activation during Immune Perturbation. *Immunity* **43**, 161-174 (2015).
270. Umeshita-Suyama, R. *et al.* Characterization of IL-4 and IL-13 signals dependent on the human IL-13 receptor alpha chain 1: redundancy of

- requirement of tyrosine residue for STAT3 activation. *International immunology* **12**, 1499-1509 (2000).
271. Metwali, A., Blum, A., Elliott, D.E. & Weinstock, J.V. Interleukin-4 receptor alpha chain and STAT6 signaling inhibit gamma interferon but not Th2 cytokine expression within schistosome granulomas. *Infection and immunity* **70**, 5651-5658 (2002).
272. Fichtner-Feigl, S., Strober, W., Kawakami, K., Puri, R.K. & Kitani, A. IL-13 signaling through the IL-13alpha2 receptor is involved in induction of TGF-beta1 production and fibrosis. *Nature medicine* **12**, 99-106 (2006).
273. Brunner, S.M. *et al.* IL-13 signaling via IL-13R α 2 triggers TGF- β 1-dependent allograft fibrosis. *Transplantation Research* **2**, 16 (2013).
274. Takeuchi, M., Alard, P. & Streilein, J.W. TGF-beta promotes immune deviation by altering accessory signals of antigen-presenting cells. *Journal of immunology (Baltimore, Md. : 1950)* **160**, 1589-1597 (1998).
275. Garcia, B. *et al.* Differential effects of transforming growth factor-beta 1 on IgA vs. IgG2b production by lipopolysaccharide-stimulated lymph node B cells: a comparative study with spleen B cells. *European journal of immunology* **26**, 2364-2370 (1996).
276. Arteaga, C.L. *et al.* Anti-transforming growth factor (TGF)-beta antibodies inhibit breast cancer cell tumorigenicity and increase mouse spleen natural killer cell activity. Implications for a possible role of tumor cell/host TGF-beta interactions in human breast cancer progression. *Journal of Clinical Investigation* **92**, 2569-2576 (1993).
277. Metwali, A. *et al.* The granulomatous response in murine Schistosomiasis mansoni does not switch to Th1 in IL-4-deficient C57BL/6 mice. *Journal of immunology (Baltimore, Md. : 1950)* **157**, 4546-4553 (1996).

278. Chiaramonte, M.G., Donaldson, D.D., Cheever, A.W. & Wynn, T.A. An IL-13 inhibitor blocks the development of hepatic fibrosis during a T-helper type 2-dominated inflammatory response. *The Journal of clinical investigation* **104**, 777-785 (1999).
279. Romeo, M.J., Agrawal, R., Pomes, A. & Woodfolk, J.A. A molecular perspective on TH2-promoting cytokine receptors in patients with allergic disease. *The Journal of allergy and clinical immunology* **133**, 952-960 (2014).
280. Nakashima, H., Terabe, M., Berzofsky, J.A., Husain, S.R. & Puri, R.K. A Novel Combination Immunotherapy for Cancer by IL-13R α 2-Targeted DNA Vaccine and Immunotoxin in Murine Tumor Models. *Journal of immunology (Baltimore, Md. : 1950)* **187**, 4935-4946 (2011).
281. Fujisawa, T., Joshi, B.H. & Puri, R.K. IL-13 regulates cancer invasion and metastasis through IL-13R α 2 via ERK/AP-1 pathway in mouse model of human ovarian cancer. *International journal of cancer* **131**, 344-356 (2012).
282. Papageorgis, P. *et al.* Targeting IL13R α 2 activates STAT6-TP63 pathway to suppress breast cancer lung metastasis. *Breast cancer research : BCR* **17**, 98 (2015).
283. Bartolome, R.A. *et al.* IL13 Receptor α 2 Signaling Requires a Scaffold Protein, FAM120A, to Activate the FAK and PI3K Pathways in Colon Cancer Metastasis. *Cancer research* **75**, 2434-2444 (2015).
284. Hamid, M.A., Jackson, R.J., Roy, S., Khanna, M. & Ransinghe, C. Unexpected involvement of IL-13 signalling via a STAT6 independent mechanism during murine IgG2a development following viral vaccination. *European Journal of Immunology* **48**, 1153-1163 (2018).

285. Zahler, A.M., Tuttle, J.D. & Chisholm, A.D. Genetic suppression of intronic +1G mutations by compensatory U1 snRNA changes in *Caenorhabditis elegans*. *Genetics* **167**, 1689-1696 (2004).
286. Kreiner, G. Compensatory mechanisms in genetic models of neurodegeneration: are the mice better than humans? *Frontiers in cellular neuroscience* **9**, 56 (2015).
287. Bondi, M.W., Houston, W.S., Eyler, L.T. & Brown, G.G. fMRI evidence of compensatory mechanisms in older adults at genetic risk for Alzheimer disease. *Neurology* **64**, 501-508 (2005).
288. Harly, C., Cam, M., Kaye, J. & Bhandoola, A. Development and differentiation of early innate lymphoid progenitors. *The Journal of Experimental Medicine* (2017).
289. Seehus, C.R. *et al.* Innate lymphoid cell development requires TOX-dependent generation of a common ILC progenitor. *Nature immunology* **16**, 599-608 (2015).
290. Cortez, V.S., Robinette, M.L. & Colonna, M. Innate lymphoid cells: new insights into function and development. *Current opinion in immunology* **32**, 71-77 (2015).
291. Lambrecht, B.N. & Hammad, H. Innate immune cells to the help. *Immunity* **40**, 313-314 (2014).
292. Hams, E., Locksley, R.M., McKenzie, A.N. & Fallon, P.G. Cutting edge: IL-25 elicits innate lymphoid type 2 and type II NKT cells that regulate obesity in mice. *Journal of immunology (Baltimore, Md. : 1950)* **191**, 5349-5353 (2013).
293. Roediger, B. *et al.* IL-2 is a critical regulator of group 2 innate lymphoid cell function during pulmonary inflammation. *The Journal of allergy and clinical immunology* **136**, 1653-1663.e1657 (2015).

294. Klose, Christoph S.N. *et al.* Differentiation of Type 1 ILCs from a Common Progenitor to All Helper-like Innate Lymphoid Cell Lineages. *Cell* **157**, 340-356 (2014).
295. Van Acker, A. *et al.* A Murine Intestinal Intraepithelial NKp46-Negative Innate Lymphoid Cell Population Characterized by Group 1 Properties. *Cell reports* **19**, 1431-1443 (2017).
296. Seillet, C. *et al.* Deciphering the Innate Lymphoid Cell Transcriptional Program. *Cell reports* **17**, 436-447 (2016).